Non-canonical RAS signaling pathways in the maintenance of hepatic stellate cell quiescence

Inaugural-Dissertation

zur Erlangung des Doktorgrades
der Mathematisch-Naturwissenschaftlichen Fakultät
der Heinrich-Heine-Universität Düsseldorf

vorgelegt von

Silke Pudewell
aus Düsseldorf

Düsseldorf, September 2022

aus dem Institut für Biochemie und Molekularbiologie II
der Heinrich-Heine-Universität Düsseldorf

Gedruckt mit der Genehmigung der
Mathematisch-Naturwissenschaftlichen Fakultät der
Heinrich-Heine-Universität Düsseldorf

Berichterstatter:

1. Prof. Dr. Reza Ahmadian

2. Prof. Dr. Lutz Schmitt

Tag der mündlichen Prüfung: 01.02.2023

ZUSAMMENFASSUNG

Das RAS Signalnetzwerk ist eine zentrale Komponente für das Überleben, die Proliferation, die Migration und viele weitere essenzielle Prozesse von Zellen. Es umfasst neben den gut untersuchten kanonischen Signalwegen, die extrazelluläre Stimuli über die RAF-MEK-ERK- und PI3K-AKT-Kaskade weiterleiten, auch mehrere weniger bekannte, nicht-kanonische Signalwege. In dieser Arbeit konnte ein neuer nicht-kanonischer Bindungspartner des embryonalen in Stammzellen exprimierten RAS (ERAS), die Arginase 1 (ARG1), in hepatischen Sternzellen (HSZs) identifiziert werden. Die Ureohydrolase, welche vorwiegend im Urea Zyklus bekannt ist, interagiert direkt und ist zudem Co-lokalisiert mit ERAS in ruhenden HSZs. Darüber hinaus konnten wir die Bedeutung von ARG1, und seiner nachgeschalteten Produktion von Polyaminen, für die Aufrechterhaltung undifferenzierter, ruhender HSZ durch den Einsatz verschiedener Inhibitoren während des Aktivierungsprozesses aufdecken. Die Auswirkungen der direkten ERAS-ARG1-Interaktion müssen noch weiter erforscht werden, könnten aber auf der spezifischen Translokalisierung beider Proteine in derselben Mikrodomäne beruhen. Ein weiterer eher ungewöhnlicher RAS-Binder ist das Stress-activated MAP kinase-interacting protein 1 (SIN1), ein unverzichtbares Mitglied des mTORC2-Komplexes, der für die Phosphorylierung verschiedener AGC-Kinasen wie AKT benötigt wird. Obwohl über die Interaktion von RAS mit der RAS-Bindungsdomäne (RBD) von SIN1 bereits vor 15 Jahren berichtet wurde, ist die Funktion dieser Interaktion noch weitgehend ungeklärt. In unserer Studie konnten wir die Bindung von SIN1 an alle klassischen RAS-Proteine (HRAS, KRAS4A, KRAS4B und NRAS), sowie RIT1 und ERAS bestätigen und zusätzlich wichtige Aminosäuren für ihre Interaktion identifizieren. Darüber hinaus konnten wir die autoinhibitorische Beziehung zwischen der RBD- und der PH (Pleckstrin-Homologie)-Domäne von SIN1 nachweisen und zeigten zum ersten Mal, dass die Interaktion der PH-Domäne mit Liposomen durch die Anwesenheit von RAS reduziert wird. Diese Ergebnisse deuten darauf hin, dass die Interaktion von RAS und SIN1 möglicherweise nicht fördernd, sondern inaktivierend wirkt und eine negative Rückkopplungsschleife der aktivierten kanonischen RAS-Signalwege unterstützt. In diesem Zusammenhang haben wir uns auch auf die Modulatoren des RAS-MAPK-Signalwegs, die akzessorischen Proteine, konzentriert und ihre Rolle in der Signalkaskade, aber auch ihre Beteiligung an der Krankheitsentstehung und -progression in einem ausführlichen Artikel beschrieben. Schließlich beinhaltet diese Arbeit eine detaillierte Studie über das akzessorische Protein IQGAP, das im Mittelpunkt einer kontroversen Debatte über die entscheidende Bindungsstelle mit der RHO-GTPase CDC42 steht. Hier konnten wir durch ein breites Spektrum an Mutationsanalysen verschiedene IQGAP-Domänen ein- und ausschließen und Diskrepanzen zu anderen Publikationen aufklären, indem wir den Unterschied zwischen der konstitutiv aktiven Mutante $CDC42^{Q61L}$ und dem Wildtyp-Protein hinsichtlich ihres Bindungsverhaltens aufzeigen.

SUMMARY

The RAS signaling network is a central component for cell survival, proliferation, migration and many other cellular processes. Besides the well-studied canonical pathways, which transmit extracellular stimuli *via* the prominent RAF-MEK-ERK and PI3K-AKT cascades, it further comprises several less known, non-canonical signaling pathways. In this thesis, arginase 1 (ARG1) was identified in hepatic stellate cells (HSCs) as a novel non-canonical binding partner of the embryonic stem cell expressed RAS (ERAS). ARG1, a key enzyme of the urea cycle, was demonstrated to directly interact and co-localizes with ERAS in quiescent HSCs. Furthermore, the importance of ARG1 and its downstream production of polyamines for the maintenance of undifferentiated, quiescent HSCs was pointed out by using a variety of inhibitors during the activation process. The impact of direct ERAS-ARG1 interaction still requires a more detailed examination, but could be based on the specific translocalization of both proteins in the same microdomain of the plasma membrane. Another rather unusual RAS binder is the stress-activated MAP kinase-interacting protein 1 (SIN1), an indispensable member of the mTORC2 complex, which is needed for the phosphorylation of several AGC-kinases, such as AKT. Even though the interaction of RAS with the RAS binding domain (RBD) of SIN1 was already reported 15 years ago, the consequence of their interaction remains largely unanswered. In our study, we confirmed the binding of SIN1 to all classical RAS proteins (HRAS, KRAS4A, KRAS4B, and NRAS), as well as to RIT1, and ERAS and additionally pinpointed critical residues for their interaction. We further investigated the auto-inhibitory relationship of the RBD and PH (Pleckstrin homology) domain of SIN1 and demonstrated for the first time that the interaction of the PH domain with liposomes is reduced due to the presence of RAS. These results suggest that the interaction of RAS and SIN1 may be inactivating rather than promoting, supporting a negative feedback loop of the activated canonical RAS signaling pathways. Accordingly, we also focused on the modulators of the RAS-MAPK pathway, collectively referred to as accessory proteins, and described not only their role in the signaling cascade but also their involvement in the development and progression of diseases in a detailed overview. Finally, this thesis includes an in-depth study of the accessory protein IQGAP, which is the center of a controversial debate about the decisive binding site with the RHO GTPase CDC42. Here, we could in- and exclude different IQGAP domains by a broad range of mutational analyses and clarify discrepancies with other publications by demonstrating the difference between the constitutively active mutant $CDC42^{Q61L}$ and the wild type protein regarding their binding behavior.

TABLE OF CONTENTS

LIST OF ABBREVIATION

4EBP1	Eukaryotic translation initiation factor 4E (eIF4E)-binding protein 1
aa	Amino acid
ACL	ATP-citrate lyase
AGC	Protein kinases A/PKG/PKC
aHSC	Activated HSC
AKT	Proteinkinase B
aRBD	Alternative RBD
ARF	ADP ribosylation factor
ARG1	Arginase 1
ATG13	Autophagy-related protein 13
ATG3	Autophagy-related protein 3
ATG5	Autophagy protein 5
CAA	Cationic amino acid
CAT	Cationic amino acid transporter
CBL	Casitas B-lineage lymphoma proto-oncogene
CD	C-terminal domain
CD133	Prominin-1
CDC42	Cell division control protein 42 homolog
c-FOS	Cellular oncogene fos
CNK1	Connector enhancer of kinase suppressor of RAS1
CRIM	Conserved region in the middle
DFMO	α-difluoromethylornithine
DOK1	Docking protein 1
ECM	Extracellular matrix
EGFR	Epidermal growth factor receptor
eIF2α	Eukaryotic translation initiation factor 2 alpha
eIF5A	Eukaryotic transcription initiation factor 5A
ELK1	ETS Like-1 protein
eNOS	Endothelial nitric oxide synthase
ERAS	Embryonic stem cell expressed RAS
ERK	Extracellular-signal regulated kinases
FAT	Frap, ATM, TRRAP
FL	Full length
FLOT1	Flotillin-1
FOXO	Forkhead box protein O
FRB	FKBP12 rapamycin binding
GAB1	GRB2-associated-binding protein
GAL3	Galectin-3
GAP	GTPase activating protein
GCN2	General control nonderepressible 2
GDI	Guanine nucleotide dissociation inhibitor
GDP	Guanosin-Di-phosphate
GEF	Guanine-nucleotide exchange factor
GFAP	Glial fibrillary acid protein
GRB2	Growth factor receptor-bound protein 2
GSK3β	Glycogen synthase kinase-3 beta
GTP	Guanosin-Tri-phosphate
HEAT	Huntington, EF3A, ATM, TOR
HGF	Hepatocyte growth factor
HRAS	Harvey Rat sarcoma virus
HSC	Hepatic stellate cell
HVR	Hypervariable region
IDRs	Intrinsically disordered regions
iNOS	Inducible nitric oxide synthase
IQGAP1	IQ motif containing GTPase activating protein 1
Iso	Isoform
KD	Kinase domain
kDa	Kilo dalton
KRAS	Kirsten rat sarcoma virus
KSR1	Kinase suppressor of RAS-1
LB	Lysogeny broth
LC3	Microtubule-associated proteins 1A/1B light chain 3
LDs	Leucine-rich sequence motifs
MEK	Mitogen-activated protein
mLST8	Mammalian lethal with SEC13 protein 8
mRNA	Messenger ribonucleic acid
MSC	Mesenchymal stem cell
mTOR	Mammalian target of rapamycin
mTORC	Mammalian target of rapamycin complex
NFκB	Nuclear factor 'kappa-light-chain-enhancer' of activated B-cells
nNOS	Neural nitric oxide synthase
NO	Nitric oxide

NOHA	N(omega)-hydroxy-nor-l-arginine
NRAS	Neuroblastoma RAS
NTD	N-terminal domain
OAT	Ornithine aminotransferase
ODC1	Ornithine decarboxylase 1
PDK1	3-phosphoinositide-dependent protein kinase-1
PH	Pleckstrin homology
PHB	Prohibitin homologues
PI3K	Phosphoinositide 3-kinases
PIP	Phosphatidylinositolphosphate
PKC	Protein kinase C
PM	Plasma membrane
PTB	Phosphotyrosine binding
PTM	Posttranslational modification
qHSC	Quiescent HSC
RAB	Ras related in brain
RAC1	Ras-related C3 botulinum toxin substrate 1
RAD	RAS association domain
RAF	Rapidly growing fibrosarcoma
RALGDS	Ral guanine nucleotide dissociation stimulator
RAN	Ras-related nuclear
RAS	Rat sarcoma
RASSF	Ras association domain family
RBD	RAS binding domain
RGS14	Regulator of G-protein signaling 14
RHEB	Ras homolog enriched in brain
RHO	Ras Homolog
RHOA	Ras homolog family member A
rHSC	Reverted HSC
RICTOR	Rapamycin-insensitive companion of mTOR
RLIP76	Ral interacting protein of 76 kDa
ROS	Reactive oxygen species
RRMs	RNA recognition motifs
RSK	90 kDa ribosomal S6 kinase
RTK	Receptor tyrosine kinase
S6K	S6 kinase
SEC	Sinusoidal endothelial cell
SGK	Serum- and glucocorticoid-induced protein kinase
SH	Src homology
SHP2	SH2 domain-containing tyrosine phosphatase 2
SIN1	Stress-activated MAP kinase-interacting protein 1
SOS1	Son of Sevenless 1
SPRED1	Sprouty-related, EVH1 domain-containing protein 1
TIAM1	T-cell lymphoma invasion and metastasis-inducing protein 1
TM	Transmembrane
TSC1/2	Tuberous sclerosis 1/2 protein
α-SMA	α-smooth muscle actin

LIST OF AMINO ACIDS

Amino acid	3-Letter code	1-Letter code
Alanine	Ala	A
Arginine	Arg	R
Asparagine	Asn	N
Aspartic Acid	Asp	D
Cysteine	Cys	C
Glutamic acid	Glu	E
Glutamine	Gln	Q
Glycine	Gly	G
Histidine	His	H
Isoleucine	Ile	I
Leucine	Leu	L
Lysine	Lys	K
Methionine	Met	M
Phenylalanine	Phe	F
Proline	Pro	P
Serine	Ser	S
Threonine	Thr	T
Tryptophan	Trp	W
Tyrosine	Tyr	Y
Valine	Val	V

1. INTRODUCTION

In order to act on upcoming stimuli from the environment, extracellular signals need to be transferred into the cell to consequently trigger downstream signaling cascades and cellular responses. Direct cell-cell communication, as well as autocrine, paracrine, and endocrine signaling is needed to sustain cell homeostasis and a healthy organism. Conserved signaling pathways assure fast and specific cellular responses that control proliferation, survival, and metabolism but also cell differentiation, quiescence, and many more. This thesis will focus on the role of non-canonical RAS interaction partners on a mechanistic, biochemical and functional basis, including the cellular context of hepatic stellate cells (HSCs) and the maintenance of their quiescent state.

1.1 RAS SUPERFAMILY

The RAS (Rat sarcoma) superfamily of GTPases describes small guanine nucleotide-binding proteins and comprises more than 150 members that can be grouped into at least 5 subclasses: RAS, RHO (Ras homologous), RAB (Ras-related in brain), ARF (ADP-ribosylation factor) and RAN (Ras-related nuclear protein) [1,2]. Small GTPases are molecular switches that share conserved regions called G-domains, which are responsible for nucleotide binding and effector interaction [3]. Most GTPases of the RAS superfamily cycle between an active GTP- and an inactive GDP-bound state and are regulated by GEFs (Guanine-nucleotide exchange factors) and GAPs (GTPase activating proteins). Additionally, RHO GTPases are regulated by GDIs (Guanine nucleotide dissociation inhibitors), which can control their subcellular localization by trafficking them from the membrane to the cytosol.

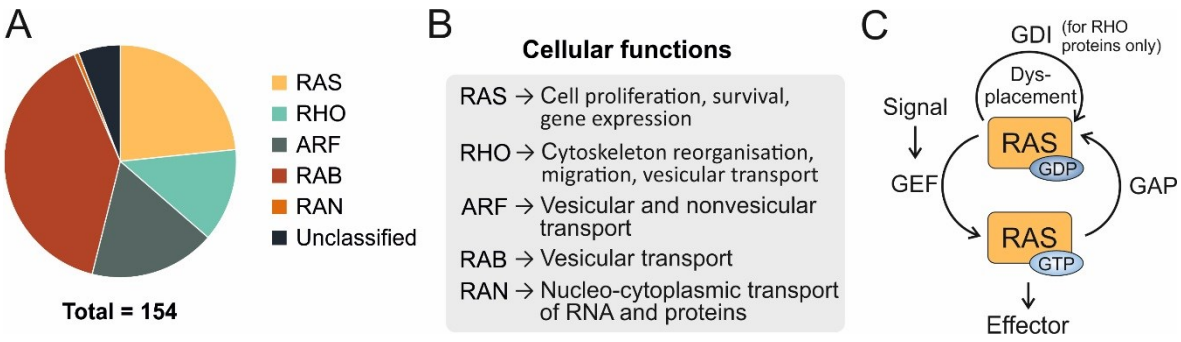

FIGURE 1. RAS superfamily, functions and regulation. The RAS superfamily consists of 154 members in 5 subfamilies with distinct functions: RAS (36) – regulate cell proliferation, survival and transcription; RHO (20) – mainly regulate cytoskeleton reorganization and migration; ARF (27) – important for vesicular and nonvesicular transport; RAB (61) – regulate vesicular transport, and RAN (1) – regulates the nucleo-cytoplasmic transport of RNA and proteins. Seven more proteins do not belong to any of these five subfamilies and are unclassified. The regulation of RAS superfamily GTPases is dependent on their nucleotide loading and catalyzed by guanine-nucleotide exchange factors and GTPase activating proteins. RHO GTPases are further regulated by guanine nucleotide dissociation inhibitors that translocate these proteins from the membrane to the cytosol.

Within the RAS subfamily, HRAS (Harvey Rat sarcoma virus), NRAS (Neuroblastoma RAS) and the isoforms KRAS (Kirsten rat sarcoma virus) 4A and 4B are collectively called the classical RAS proteins. Excluding their hypervariable region (HVR), the sequence homology of these 4 proteins is over 90%, but still allows specific functions and interaction partners of

each paralogue. The HVR comprises the last 24 amino acids and is highly variable among the proteins. All classical RAS proteins contain a CAAX-box at their C-terminus, consisting of a cysteine (c), followed by two aliphatic (aa) and one final (x) amino acid. This motif gets recognized by farnesyl- or geranylgeranyl-transferases, which transfer an isoprenyl moiety to the protein at the cysteine of the CAAX-box. The x residue of the motif determines the type of prenylation, in this case methionine, serine, glutamine, alanine and cysteine indicate a farnesylation, whereas leucine and glutamate enable geranylgeranylation [4]. In the case of RAS proteins, all classical RAS proteins are getting farnesylated. In contrast, the typical RHO proteins CDC42 (Cell division control protein 42 homolog), RHOA (Ras homolog family member A) and RAC1 (Ras-related C3 botulinum toxin substrate 1) are all geranylgeranylated. Additionally to this isoprenylation, KRAS4A, NRAS (one time each) and HRAS (two times) get palmitoylated, a reversible lipid modification which is central for the association in lipid rafts and clustering events [5]. KRAS4B, for instance, does not get further post-translationally modified but includes a lysine rich domain, which is likely to associate with the membrane due to its positive charge [6]. The differences in the HVR and the post-translational processing of the classical RAS proteins determine their very own special function in signaling and localization. A more uncommon member of the RAS subfamily is ERAS (embryonic stem cell expressed RAS). ERAS contains a unique N-terminal extension of 38 amino acids and shares around 40% sequence homology of the conserved G-domains with HRAS. Due to a serine instead of a glycine on position 50 (corresponding to a G12S mutation in HRAS), ERAS is GAP insensitive and therefore, constitutively active [7,8]. Furthermore, ERAS gets post-translationally modified by farnesylation and is likely to get palmitoylated similar to HRAS (marked as yellow background in Figure 2) [8]. Still, the function of ERAS seems to differ strongly from those of the classical RAS proteins, mainly signaling *via* PI3K (Phosphoinositide 3-kinases) and is expressed specifically in embryonic stem cells, hepatic stellate cells and some tumor types [7,9,10].

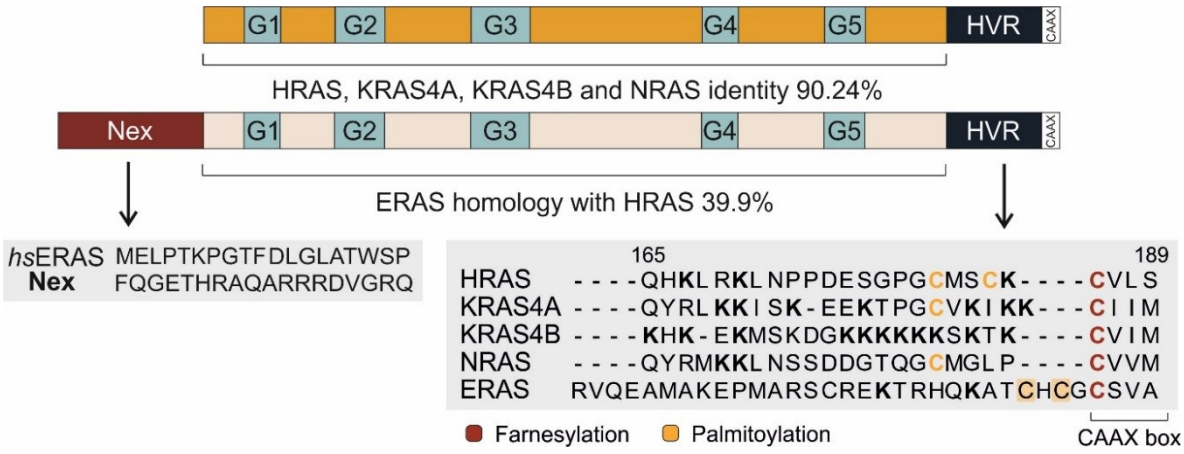

FIGURE 2. Domain organization of classical RAS proteins and ERAS. RAS proteins contain five conserved G-domains (G1-5), which determine nucleotide recognition, nucleotide binding and effector interaction. The classical RAS proteins HRAS, KRAS4A, KRAS4B and NRAS share 90.24% sequence homology in these conserved domains. In contrast, the more uncommon RAS GTPase ERAS shares 39.9% homology but includes furthermore a unique N-terminal extension of 38 amino acids. The alignment of the hypervariable region (HVR) displays a highly diverse sequence upon the proteins, but a collectively shared CAAX-box motif for cysteine farnesylation (red). Other post-translational modifications (palmitoylation) are indicated in yellow. For ERAS, palmitoylation is predicted on yellow highlighted cysteines, but not proven yet.

1.2 RAS SIGNALING PATHWAYS

RAS proteins are molecular switches for some of the most important signaling pathways. Their effectors got studied extensively during the past 40 years, in which the RAS signaling cascades were roughly divided into canonical and non-canonical processes. The canonical RAS signaling pathway acts *via* RAF (rapidly growing fibrosarcoma) -MEK (MAPK, mitogen-activated protein) -ERK (extracellular-signal regulated kinases) and PI3K-AKT (Proteinkinase B). ERK and/or AKT phosphorylation induce cell proliferation, survival and growth and are main players in cell homeostasis. As a proto-oncogene, RAS is often mutated in cancer and constitutively activates the canonical RAS signaling pathways contributing to cancer formation and progression. The non-canonical RAS signaling pathways comprise, among others, TIAM1 (T-cell lymphoma invasion and metastasis-inducing protein 1), RALGDS (Ral guanine nucleotide dissociation stimulator) and RLIP76 (Ral interacting protein of 76 kDa), which can be mostly connected to cytoskeleton reorganization, endocytosis and cell migration [11]. Besides those proteins, multiple other RAS interactors could be included in the list of non-canonical signaling effectors, like the Stress-activated MAP kinase-interacting protein 1 (SIN1, also: MAPKAP1) or the so-called liver arginase 1 (ARG1), which will be discussed and highlighted in this thesis.

1.2.1 THE CANONICAL RAS SIGNALING PATHWAY

The RTK-RAS-MAPK and RAS-PI3K pathways are highly conserved signaling cascades and fundamental for cell proliferation and survival. A rough outline of the signaling pathways is illustrated in Figure 3.

The function of the signaling pathways is to integrate extracellular stimuli to an intracellular cell response. Upon ligand binding to receptor tyrosine kinases (RTKs), like the epidermal growth factor receptor (EGFR), most RTKs dimerize and autophosphorylate their catalytic domains [12,13]. In the next step, direct effectors, adaptor or docking proteins can bind to the phosphorylated residues mostly *via* SH2 (Src homology) or PTB (Phosphotyrosine binding) domains [14,15]. One of the most extensively studied adaptor proteins is GRB2 (Growth factor receptor-bound protein 2), a 25 kDa protein consisting of one SH2 and two SH3 domains [16,17]. GRB2 can activate SOS1 (Son of Sevenless 1), a RAS GEF that exchanges RAS•GDP to RAS•GTP and activates RAS downstream signaling effectors like the RAF kinase [18,19]. RAF gets activated in a multi-step mechanism starting with the (i) recruitment of RAF to the membrane and binding to active RAS, (ii) homo- or heterodimerization of RAF isoforms (ARAF, BRAF, CRAF), (iii) kinase domain transphosphorylation and finally (iv) stabilization of the activated state and downstream signaling [20,21]. Activated RAF can transmit the signal towards MEK1/2 and subsequently to ERK1/2 [22]. ERK phosphorylation triggers nuclear as well as cytosolic responses by activation of for example ELK1 (ETS Like-1 protein), c-FOS (Cellular oncogene fos), MYC and NFκB (nuclear factor 'kappa-light-chain-enhancer' of activated B-cells) or RSK (90 kDa ribosomal S6 kinase) respectively, which results in cell responses to sustain cell proliferation and survival [23–26].

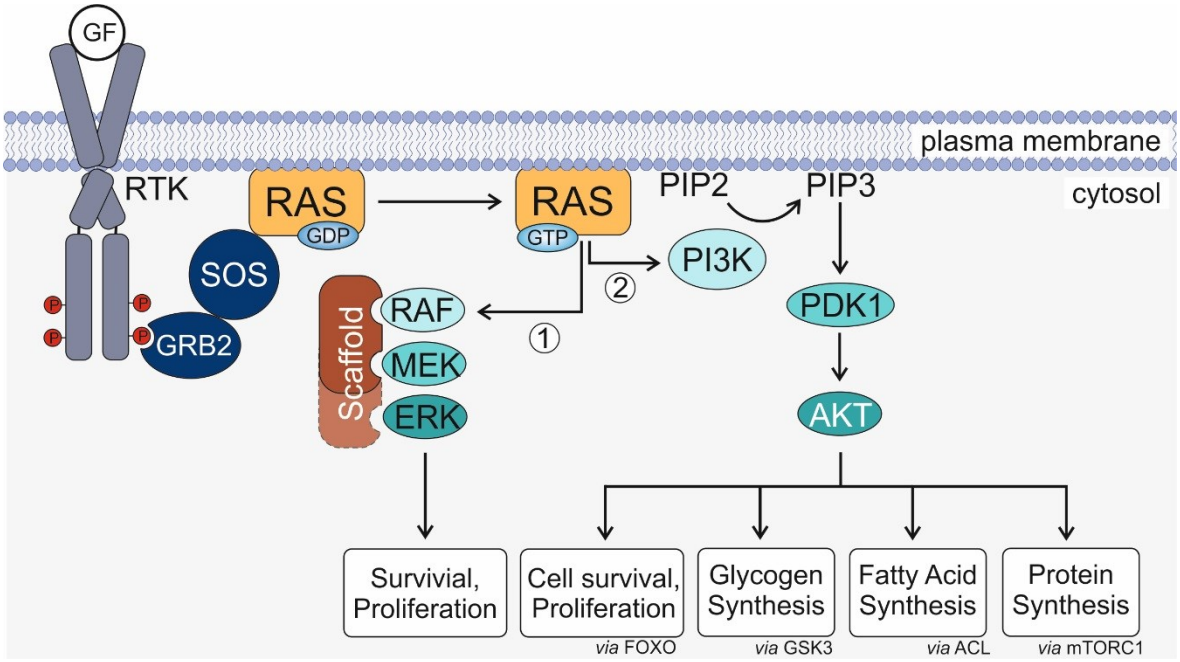

FIGURE 3. Classical RAS Signaling Pathways. The RAS-MAPK (1) and RAS-PI3K (2) pathways are the two most common canonical RAS signaling cascades. Receptor tyrosine kinases get activated by growth factors or hormones and subsequently intrinsically auto-phosphorylated. The signal gets transmitted directly *via* adaptor proteins like GRB2 to guanine-nucleotide exchange factors like SOS1. SOS1 exchanges GDP to GTP and therefore activates RAS. GTP-bound RAS can signal down the RAF-MEK-ERK axis, triggering cell survival and proliferation and additionally directly activate PI3K, which catalyzes the phosphorylation of PIP_2 to PIP_3 and finally phosphorylates AKT *via* PDK1. AKT effectors induce, among others, proliferation, glycogen and fatty acid synthesis and translation.

The second important signaling cascade acts through the phosphatidylinositol 3-kinase (PI3K), a protein consisting of two subunits. The regulatory domain p85 incorporates two SH2 domains and can directly associate with a phosphorylated RTK. The catalytic domain p110 phosphorylates phosphatidylinositol-4,5-bis-phosphate (PIP_2) to phosphatidylinositol-3,4,5-tris-phosphate (PIP_3). This modified lipid can trigger various associations of for example the pleckstrin homology (PH) domain of AKT [27]. The direct activation of p110 subunit can also be carried out by G-protein coupled receptors or activated RAS, which makes PI3K one of the most important effectors and downstream signaling cascades of the RAS signaling pathway [28]. The recruitment of AKT to the membrane by the second messenger PIP_3 is the rate limiting step in AKT activation. AKT can be phosphorylated on two sites: threonine 308 and serine 473. Thr308 is mainly phosphorylated by 3-phosphoinositide-dependent protein kinase-1 (PDK1), a PH domain containing protein that binds to PIP_3 as well [29]. The full activation of AKT is obtained by additional phosphorylation on Ser473, which is mainly carried out by the mTORC2 (mammalian target of rapamycin complex 2) complex that will be discussed below. The main downstream effects of AKT cover cell survival and proliferation *via* FOXO (Forkhead box protein O) [30], glucose metabolism by the inhibition of GSK3β (Glycogen synthase kinase-3 beta) [31], fatty acid synthesis *via* direct ACL (ATP-citrate lyase) phosphorylation [32], and translational control *via* the mTORC1 (mammalian target of rapamycin complex 1) complex [33].

1.2.2 ACCESSORY PROTEINS OF THE RAS-MAPK SIGNALING PATHWAY

Many processes of the RAS-MAPK pathways are not only regulated by phosphorylation and activation events but get furthermore modulated and fine-tuned in a spatiotemporal manner by accessory proteins [15]. Accessory proteins are defined as non-constituent members of the signaling pathway and can be divided into four subgroups. **Scaffold proteins** connect two or more proteins and organize them in a functional unit. Those proteins usually contain many domains and might be found in several complexes, also enabling crosstalk between different signaling cascades.

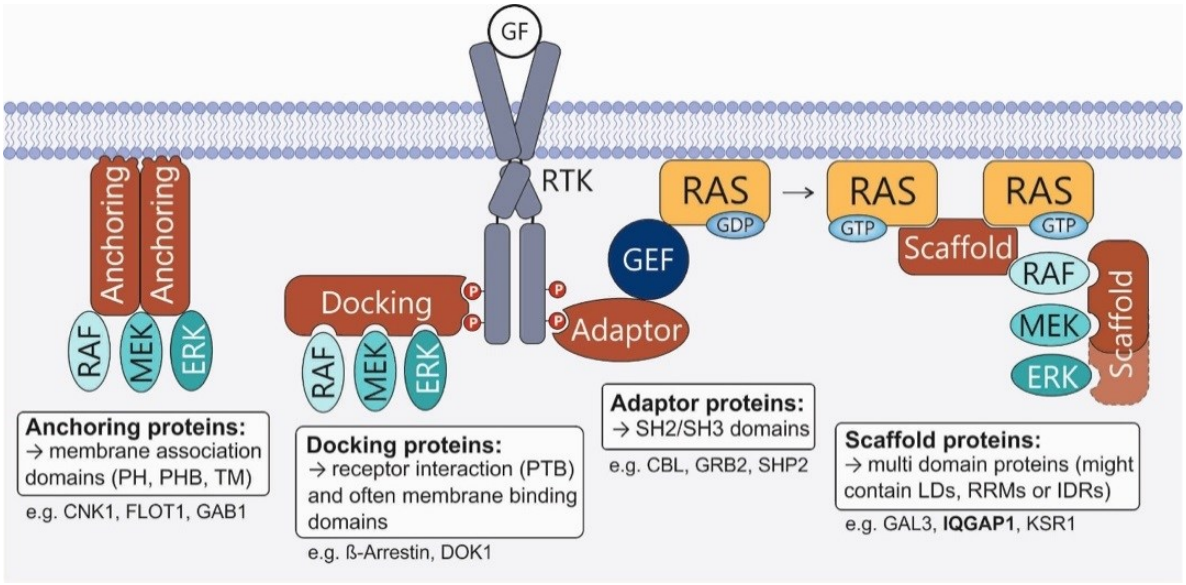

FIGURE 4. Accessory proteins in RAS-MAPK pathway. Accessory proteins can be categorized into four subgroups: (1) Anchoring proteins, (2) docking proteins, (3) adaptor proteins and (4) scaffold proteins. Anchoring proteins contain domains that associate with membranes, like pleckstrin homology (PH) prohibitin homologues (PHB) and transmembrane (TM) domains. Examples are the connector enhancer of kinase suppressor of RAS1 (CNK1), Flotillin-1 (FLOT1) or GRB2-associated-binding protein (GAB1). Docking proteins usually contain a phosphotyrosine-binding domain (PTB), like β-arrestin or the docking protein 1 (DOK1). Adaptor proteins like casitas B-lineage lymphoma proto-oncogene (CBL), growth factor receptor binding protein 2 (GRB2) or SH2 domain-containing tyrosine phosphatase 2 (SHP2) all contain SRC homology 2 (SH2) and mostly SH3 domains. Scaffold proteins do need to contain specific domains but frequently include leucine-rich sequence motifs (LDs) or other repeats, RNA recognition motifs (RRMs) and intrinsically disordered regions (IDRs). Scaffold proteins are for example galectin-3 (GAL3), IQ motif containing GTPase activating protein 1 (IQGAP1) or kinase suppressor of RAS-1 (KSR1).

An example for a scaffold protein is the IQ motif containing GTPase activating protein 1 (IQGAP1), a 189 kDa multi-domain protein with over 100 binding partners [34]. Besides its scaffolding function in the RAS-MAPK pathway, which is performed by direct interaction with RAF, MEK and ERK [35], IQGAP1 is further involved in the direct binding and stimulation of PI3K and AKT [36,37], as well as the association of RHO GTPases like RAC1 and CDC42 [38]. The number of interaction partners and the size of the protein makes it easy to believe in the multitude of functions IQGAP1 is involved in, which spread from cytoskeleton organization, cell adhesion, protein trafficking to transcription and many more [39,40]. To understand the role of IQGAP1 in distinct signaling pathways, the identification of binding sites and the mechanisms of binding selectivity are important fields to cover and analyze in detail [41].

The second group of accessory proteins are **adaptor proteins**. These proteins often contain SH2 and SH3 domains and simply connect two proteins to bring them in a close distance and orientation to each other. An example here is the already mentioned linker GRB2. The third group are so called **anchoring proteins**, which not only bind components of the signaling cascade, but also intracellular membranes. Therefore, these proteins localize the signaling machinery to a very specific site of action and can further sequester proteins from diffusion into other cytoplasmic areas. The last group of accessory proteins are named **docking proteins**. These proteins assemble activated receptors like RTKs and G-protein coupled receptors with signaling components at the membrane. They usually contain phosphotyrosine-binding (PTB) domains, as well as membrane associating domains to increase the residence time at the site of action. Reducing the dimensionality of protein-protein interactions by binding multiple components and structures is one main functions of accessory proteins. Their interaction with the constituent members of signaling cascades is highly important to modulate and sustain the fine-tuned signaling machinery within the cell [15,42].

1.2.3 The non-canonical RAS signaling pathway

The interaction and activation of RAS with other downstream effectors than PI3K and RAF are less prominent and here collectively called the non-canonical signaling pathways. These pathways are connected to a broad variety of cell responses that are not necessarily involved in cell survival and proliferation like the canonical signaling pathways. TIAM1 for instance, a specific GEF for RAC1, gets activated by RAS and therefore stimulates the cytoskeleton reorganization and regulates cell migration [43]. The interaction of RAS and the RALGDS was already discovered in 1998 and results in the activation of RAL and its downstream cascades, also leading to cell migration and the regulation of gene expression and vesical trafficking [44,45].

Many approaches were done to identify new RAS interaction partners. By searching for domains that directly associate (RAs) or bind (RBs) to RAS, 39 RA and 14 RB domain containing proteins were found in the human proteome [46]. Among these proteins were familiar faces like RAF, PI3K and TIAM1, but also accessory proteins like RGS14 (Regulator of G-protein signaling 14) and other hotspot binding partners like RASSF (Ras association domain family) proteins, increasing the number of RAS signaling cascades drastically. Lately, a study by Béganton *et al.* in 2020 determined over 800 high confidence proximal interactors of HRAS, KRAS4B and NRAS using the proximity-dependent biotin identification technology [47]. Although not all mentioned proteins are direct interactors, this study gives a great impression of how big the RAS interaction, clustering, microdomain formation and crosstalk network really is or can be.

1.2.3.1 THE MTORC2 SIGNALING PATHWAY

One of the more unknown RAS binding domain (RBD) containing proteins is the stress-activated MAP kinase-interacting protein 1 (SIN1, mSIN1 also: MAPKAP1), a subunit of the mTORC2 complex. The mTORC2 complex consists of four distinct members. First, the mammalian or mechanistic target of rapamycin (mTOR), which was discovered 31 years ago in yeast [48] and carries out the kinase activity of the complex, and second, the mammalian lethal with SEC13 protein 8 (mLST8). Those two proteins form a heterodimer and are also part of the mTORC1 complex [49]. The presence of mLST8 seems to be dispensable for mTORC1 but essential for mTORC2 complex integrity and function [50,51]. The second half of mTORC2 consists of RICTOR (Rapamycin-insensitive companion of mTOR), another large scaffolding protein of the complex, and SIN1.

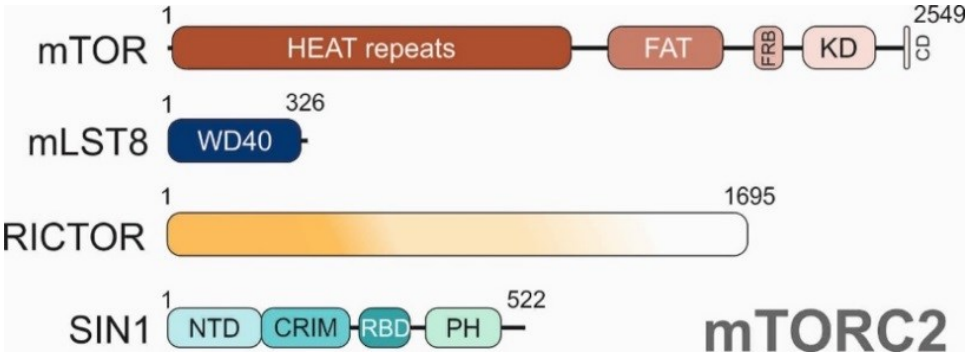

Figure 5. Members and domain organization of the mTORC2 complex. The mTORC2 complex consists of four irreplaceable members: mTOR, mLST8, RICTOR, and SIN1. mTOR comprises five domains. The HEAT repeats (Huntington, EF3A, ATM, TOR repeats) cover the N-terminal side of mTOR, followed by the FAT (Frap, ATM, TRRAP) and FRB (FKBP12 rapamycin binding) domains. The C-terminal part consists of the kinase domain (KD) and the CD (C-terminal domain). mLST8 is a 326 aa protein and is built up from WD40 repeats. The domain organization of RICTOR is still not clearly defined but incorporates Armadillo and HEAT repeats on the N-terminal side, a disordered region, which can get phosphorylated and a folded C-terminal domain in the other half. SIN1 is built up out of the N-terminal domain (NTD), the conserved region in the middle (CRIM), a RAS-binding domain (RBD) and a pleckstrin homology (PH) domain in the C-terminus. All four members are needed to assemble a functional mTORC2 complex and carry out substrate phosphorylation.

STRESS-ACTIVATED MAPK INTERACTING PROTEIN 1 (SIN1)

SIN1 is one of the core proteins and an irreplaceable member of the mTORC2 complex. Its knock out leads to an impaired kinase activity and therefore decreased AKT phosphorylation, which is embryonically lethal [52,53]. The protein can be divided into four domains (see Figure 5). The N-terminal domain (NTD, aa 1-137) integrates into RICTOR and is needed for its connection with the mTORC2 complex. Several interaction sites of the NTD with RICTOR were identified, and the deletion or the extension of this domain disrupts the mTORC2 complex [54,55]. The conserved region in the middle (CRIM, aa 137-266) directly interacts with effectors and is responsible for effector recognition and complex specificity. Mutations in the CRIM domain lead as well to impaired kinase activity [56,57]. The RAS binding domain (RBD, aa 279-353) is followed by a PH domain (aa 376-486). Those two domains could not be structurally characterized within the mTORC2 complex as they obtain a flexible, wobbly structure [54]. The crystallization of the SIN1-PH domain alone

was solved by Pan and Matsuura in 2012 (PDB: 3VOQ) [58] and indicates the typical features that are also found in for example the PH domain of AKT. Functionally, the AKT-PH domain can be exchanged with the SIN1-PH domain without affecting the phosphorylation level of AKT, implementing a similar localization of SIN1 and AKT within the cell, as well as the ability to bind phosphoinositide-tri-phosphate (PI(3,4,5)P) [59]. Interestingly, an additional binding site of the PH domain with mTOR was observed, generating the idea of an inactive closed conformation of the mTORC2 substrate binding pocket whenever SIN1-PH connects with mTOR and an open "active" conformation while associating with the membrane [60,61]. In 2021, Castel *et al.* were able to structurally solve the conformation of SIN1-RBD (PDB: 7LC2) and RBD-PH domain (PDB: 7LC1) bound to $KRAS^{Q61R}$ (1-169) [62]. In this paper, an additional "alternative RBD" (aRBD) of SIN1 was introduced, located between the RBD and PH domain that specifically interacts with the HVR of KRAS4A but no other classical RAS proteins. Zheng *et al.* disproved this hypothesis in 2022 by publishing another structure of direct HRAS-SIN1-RBD interaction and showed direct binding of SIN1-RBD with all classical RAS G-domains [63]. The binding of the earlier defined RBD to the switch I and II region of RAS, which was introduced by Schroder *et al.* in 2007, could further be confirmed by both groups [62,64]. The function of the RBD in SIN1 still remains unsolved. The stimulation of mTORC2 activity upon RAS activation as well as the inhibition of the RAS-MAPK pathway *via* SIN1 interaction were both intensively discussed [64,65]. Still, the meaning of the interaction of SIN1 and RAS needs to be elucidated in the future.

For SIN1, six isoforms are known, which are displayed in the table below. Isoform 1 is encoding for the longest protein and is referred to as the full length (FL) protein, including 12 of the 13 exons of the gene (exon 8 is not included in any of the transcript variants). Besides isoform 4, which lacks the NTD and can therefore not associate with RICTOR, all other isoforms could be found as part of the mTORC2 complex. Interestingly, isoform 6, which contains an additional exon 9a right after the RBD, but misses the PH domain, was suggested to play a unique role outside of the mTORC2 complex, associating with the basal body [66]. The certain roles of the different SIN1 isoforms are not yet defined, but the fact that isoform 3 specifically lacks the recently defined aRBD and that isoform 2 only misses the second part of the RBD, makes it tempting to speculate about the role of RAS binding in SIN1.

TABLE 1: SIN1 ISOFORMS

Iso-form	Amino acids	Sequence alteration	Comment	Uniprot ID
1	522	-	Includes all domains (NTD-CRIM-RBD-PH)	Q9BPZ7-1
2	486	321-356 missing	Lacks second half of the RBD	Q9BPZ7-2
3	475	357-403 missing	Lacks the aRBD between RBD and PH	Q9BPZ7-3
4	330	1-192 missing	NTD and first half of the CRIM are missing → Not part of mTORC2 complex	Q9BPZ7-4
5	323	321-438 and 442-522 missing	Lacks almost the whole C-terminus from the second half of the RBD (no PH domain)	Q9BPZ7-5
6	372	373-522 missing Alternative exon 9a	Lacks the PH domain and has an alternative ending of the RBD which differs to the aRBD	Q9BPZ7-6

Regulation of the mTORC2 complex

Compared to the mTORC1 complex, which is mainly regulated *via* nutrients, growth factors, and stress [67], the mTORC2 activation is less extensively studied but shifted a lot more into the focus of researchers lately. For a long time, the received opinion of mTORC2 activation cycled around growth factor dependent signaling, mainly *via* the PI3K activation [60]. The readout of most studies is the phosphorylation of AKT at serine 473 [68]. Generally, the mTORC2 complex targets AGC (protein kinases A/PKG/PKC) kinases, which include AKT, PKC (protein kinase C) and SGK (serum- and glucocorticoid-induced protein kinase) [57,69,70]. The downstream effects of the AGC kinases cover a wide variety of cell responses, like the regulation of ion channels *via* SGK or the reorganization of the cytoskeleton by activation of RHO GTPases *via* PKC [71,72].

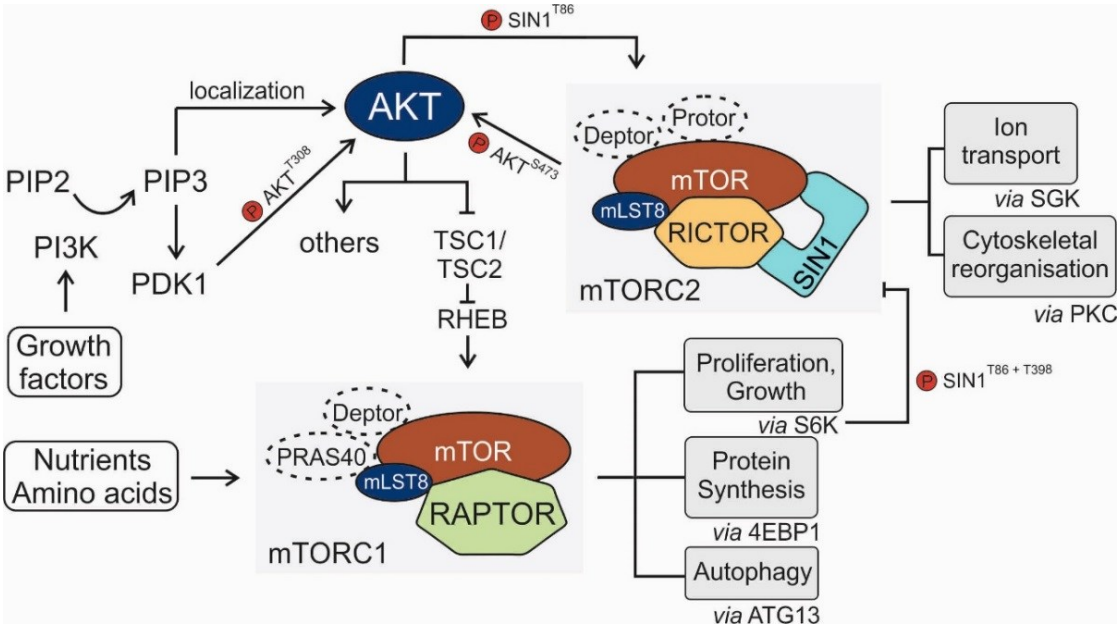

Figure 6. Regulation of mTORC1 and mTORC2 complex. Nutrient and amino acid levels are common mTORC1 upstream regulators, whereas growth factors activate the mTORC2 complex *via* the PI3K axis. PI3K activity leads to AKT phosphorylation by trans-localization of AKT and PDK1 to the membrane, where the mTORC2 complex can phosphorylate AKT at serine 473. If this pathway is also directly affecting mTORC2 upstream needs to be clarified in the future. Downstream targets of mTORC2, like SGK and PKC, lead to ion transport and cytoskeleton regulation respectively. AKT signaling pathway leads to a variety of cell responses but can furthermore positively regulate mTORC1 complex by inhibiting TSC1/TSC2 (Tuberous sclerosis 1/2 protein) and therefore activate RHEB (Ras homolog enriched in brain) which in turn activates mTORC1. Downstream effectors of mTORC1 are ATG13 (Autophagy-related protein 13), which controls autophagy, 4EBP1 (Eukaryotic translation initiation factor 4E (eIF4E)-binding protein 1), a regulator in protein synthesis and S6K (S6 kinase), which induces cell proliferation and growth and further phosphorylate SIN1 at threonine 86 and 356, which negatively regulates the mTORC2 complex integrity.

A new study identified different pools of mTORC2 within the cell, using a novel reporter called LocaTOR2 [73]. This work, among others, implements that the subcellular localization of mTORC2 is fundamental for its regulation and activity towards AKT and other downstream effectors. Growth factor induced mTORC2 activation is achieved by PI3K activity and subsequent recruitment of AKT and PDK1 to the membrane. Studies showed that the mTORC2 complex can be recruited to the plasma membrane (PM) as well, but

might also have a stimulation independent pool at the PM that acts upon effector availability [60,73]. Another process of growth factor response is the activation of RAC1, which itself binds to mTOR in a nucleotide independent manner and activates mTORC2 by translocating it to a specific subcellular membrane [74]. The activation of mTORC2 on ribosomes was shown in a PI3K dependent manner and can phosphorylate AKT during translation at T450 to increase its stability [75–77]. Besides those pools, the mTORC2 complex could be found on the outer mitochondrial membrane, early and late endosomes, lysosomes and in the nucleus [73,78]. Another direct way to regulate mTORC2 activity is the phosphorylation of SIN1 at T86 and T398. Single phosphorylation of SIN1 increases mTORC2 activity and can be executed by $pAKT^{T308/S473}$ in a positive feedback loop. The order of the phosphorylation events is not determined yet [79]. On the contrary, the double phosphorylation of SIN1 at T86 and T398 dissociates the protein from the complex and disrupts mTORC2 integrity [80,81]. The ribosomal protein S6 kinase (S6K) is, besides from the eukaryotic translation initiation factor 4E-binding protein 1 (4EBP1) and the autophagy-related protein 13 (ATG13), one of the main effectors of the mTORC1 complex and can positively but also negatively connect mTORC1 and mTORC2 signaling to each other by phosphorylation of SIN1 [82,83]. The localization of mTORC2, the phosphorylation, and pathway cross talks play a critical role in mTORC2 activity. How SIN1 is involved in those events and especially in the membrane association needs extensive studies and will be discussed in this thesis.

1.2.3.2 ARG1 SIGNALING PATHWAY

Another quite unusual interaction partner of RAS (specifically ERAS) is arginase 1 (ARG1), the so called liver arginase, that was just discovered by our study in 2022 [84]. Its connection with the RAS signaling pathway still needs a lot more research, as ARG1 is predominantly known for its role in the urea cycle by catalyzing the last step, converting L-arginine into L-ornithine and urea [85,86]. The urea cycle mainly takes place in the liver, more precisely in the hepatocytes. The process to detoxify the cells from ammonia is performed by five enzymes and located in the mitochondria and the cytosol. The major role of ARG1 can also be estimated by the cell type specific expression, which is extremely high in hepatocytes compared to other cell types (see Table 2). Still, the decent expression of ARG1 in red blood cells, Kupffer cells (liver resident macrophages), hepatic stellate cells, cholangiocytes (epithelial cells of the bile duct), B-cells, T-cells, and endothelial cells, which all lack a complete urea cycle, suggests another role of ARG1 activity in those liver resident cells. Noticeably, a low ARG1 expression could also be found in a variety of other cell types like macrophages, spermatids, or astrocytes, covering a wide expression profile in organs from bone marrow, spleen, to skeletal muscle and brain (for Ref. see Table 2, adapted from The Human Protein Atlas [87]).

TABLE 2: CELL TYPE SPECIFIC ARG1 EXPRESSION

Cell type	nTPM	Liver	Bone marrow	Lymph node	Spleen	Adipose tissue	Breast	Colon	Endo-metrium	Placenta	Skeletal muscle	Testis	Brain
Hepatocytes	991.4	X											
Erythroid cells	43.6	X	X										
Kupffer cells	27.6	X											
Hepatic stellate cells	23.2	X											
Cholangiocytes	17.2	X											
B-cells	2.7	X	X	X	X								
T-cells	2.1	X	X	X	X	X	X	X	X				
Endothelial cells	1.5	X					X			X	X		
Macrophages	0.9		X			X					X	X	
Late spermatids	0.6											X	
Excitatory neurons	0.5												X
Astrocytes	0.3												X
Early spermatids	0.3											X	
Reference		[88]	[89]	[89]	[89]	[90]	[91]	[92]	[93]	[94]	[95]	[96]	[97]

nTPM = normalized transcripts per million

Besides its detoxification function, arginase fulfills two more important tasks, which are (i) the production of ornithine to produce proline and polyamines, and (ii) antagonizing nitric oxide synthase (NOS) activity, which consumes the same substrate L-arginine and converts it to L-citrulline and nitric oxide (NO) [98]. Proline is a non-essential amino acid and is crucial for collagen synthesis [99]. It is synthesized by the ornithine aminotransferase (OAT) from L-ornithine, while the latter can also be consumed by the ornithine decarboxylase 1 (ODC1), the rate limiting enzyme in polyamine production. Polyamines comprise the three molecules putrescine, spermine, and spermidine, which can all be transformed into each other and are involved in many cellular processes like autophagy, immune cell regulation, protection from oxidative damage, and are best known for their promoting effect on cell proliferation and gene expression [100–104]. The counteraction of ARG1 and NOS depends on the isoform expression, cell type and catalytic activity of the proteins. NOS exists in three isoforms: nNOS (NOS1) is the neuronal isoform and strongly expressed in brain, iNOS (NOS2) is the inducible isoform that is occasionally regulated on transcriptional levels mainly via NFκB [105] and eNOS (NOS3) the endothelial NOS, which is essential for the maintenance of the blood pressure and therefore critical for vascular health and disease [98,106,107]. The arginine paradox describes the misbalance of the substrate affinity (K_m), the maximal enzymatic velocity (V_m) of arginase and NOS and the extra- and intracellular L-arginine concentration. NO synthases have a much lower K_m (higher affinity) for L-arginine than arginase (2-20 µM vs. 2-20 mM respectively) [106,108] and should therefore not be able to compete with each other. However, NO synthases possess a much lower enzymatic capacity than arginase (1 µmol/min/mg vs. 1400 µmol/min/mg respectively) and could therefore lose the advantage of better affinity [106,109]. In addition, the intracellular concentration of L-arginine of around 100-800 µM is high enough to completely saturate NOS but not arginase enzyme activity, still, extracellular changes of L-arginine concentration are altering the NO production, suggesting the consumption of extracellular L-arginine by arginase and/or NO synthases is needed for their activity [110,111]. As this paradox, as well as the counteraction of ARG1 and NOS, are not completely understood

yet, cell type and context specific investigations are highly needed to answer open questions about their regulation and function.

Interestingly, erythrocytes contain both ARG1 and eNOS [112]. In animal studies, postischemic recovery could be improved by arginase inhibition *via* NO production, suggesting a competitive relationship in which ARG1 steals away L-arginine from eNOS [113]. *In vivo* knock out models of endothelial cell eNOS and/or red blood cell eNOS could independently show effects on blood pressure homeostasis, giving an insight into the function of the high ARG1 levels in erythroid cells (Table 2) [114]. An intensively studied field is the role of arginase and NOS in macrophages. The immune cells shift from the M1 "kill/fight" mode to M2 "healing/fixing" mode and change from NOS to arginase expression respectively. In M1 state, NO production is needed for immune response and inflammation reactions, whereas the M2 state is important for wound healing by collagen production from proline and increased proliferation *via* polyamines as well as anti-inflammatory events [115]. NOS and arginase pathways crosstalk and negatively regulate each other for example *via* the intermediate of NOS reaction NOHA (N(omega)-hydroxy-nor-l-arginine), a potent inhibitor of arginase, or the S-nitrolysation and the resulting inhibition of ODC1 by NO [116,117]. Arginase, on the other hand, can inhibit the nuclear localization of NFκB by spermine and therefore inhibit specifically iNOS and also its cationic amino acid (CAA) transporter (CAT) CAT2B expression [118]. Another example of arginase/NOS regulation and counteraction can be found in astrocytes, where iNOS and ARG1 expression are directly regulated by each other. The eIF2α (eukaryotic translation initiation factor 2 alpha) kinase GCN2 (general control nonderepressible 2), can sense amino acid concentrations and phosphorylate its substrate eIF2α upon low L-arginine concentrations, which could be lowered by high arginase activity. eIF2α is needed for iNOS mRNA translation and drastically lowered upon ARG1 expression. On the other hand, ARG1 depletion led again to high iNOS expression [119]. This effect could also be observed in hepatic stellate cells during activation in our study [84]. As astrocytes and hepatic stellate cells have several things in common [120], the regulating system of ARG1 and iNOS could only be one of them and might also be true for several other cell types that have not been investigated yet.

1.3 HEPATIC STELLATE CELLS

1.3.1 THE LIVER IN HEALTH AND DISEASE

The liver is a central organ for the body's metabolism and detoxification. It is involved in protein synthesis, balancing of hormonal levels, and storage of minerals and vitamins. Anatomically, the liver can roughly be divided into the left and the right liver lobe. The latter additionally contains the caudate and quadrate lobe. The portal vein enters the liver from the bottom, bringing in nutrient loaded blood from the intestines, while the hepatic artery is supplying the liver with fresh blood from the heart. Both blood vessels branch out within the liver into sinusoids and combine again into the central or hepatic vein, leaving the liver towards the heart. Associated with the liver is the gall bladder, which collects, stores, and concentrates bile acid and releases it towards the small intestine.

Histologically, the liver is composed of around 500.000 smaller units, called the liver lobules. A lobule has a hexagonal shape, containing a portal triad (hepatic artery, portal vein and bile duct) at each corner. The blood from the hepatic artery and portal vein combines in the sinusoid and exits the lobule through the central vein in the middle of the lobule [121]. The

sinusoid is lined with sinusoidal endothelial cells (SECs), which represent around 10% of the total liver cells [122]. The major cell type is represented by the hepatocytes with around 70%. Hepatocytes execute the main functions of the liver. They produce bile and directly secrete it into the bile canaliculus, a capillary system that flows into the bile duct. Bile is needed to metabolize lipids, but also to get out components like bilirubin and toxins like drugs or alcohol, that have been metabolized by the hepatocytes into less harmful products and can be excreted through the kidneys. Furthermore, hepatocytes produce a vast amount of blood plasma proteins and store glycogen, the fat soluble vitamins B12 and D, and minerals like iron and copper. Another vitamin that is stored predominantly in the liver is vitamin A. Vitamin A is converted into retinol and is stored in hepatic stellate cells (HSCs), also called fat-storing cells or Ito cells, which are located in the space of Disse between hepatocytes and SECs. The function of these cells will be discussed in the next chapter in detail. Kupffer cells display around 7% of the total liver cells and represent the last of the four major cell types abundant in the liver. The function of these liver resident macrophages is to safeguard the body from bacterial infiltration mainly coming from the intestine, and clear the blood from endotoxins and phagocytose debris [123,124].

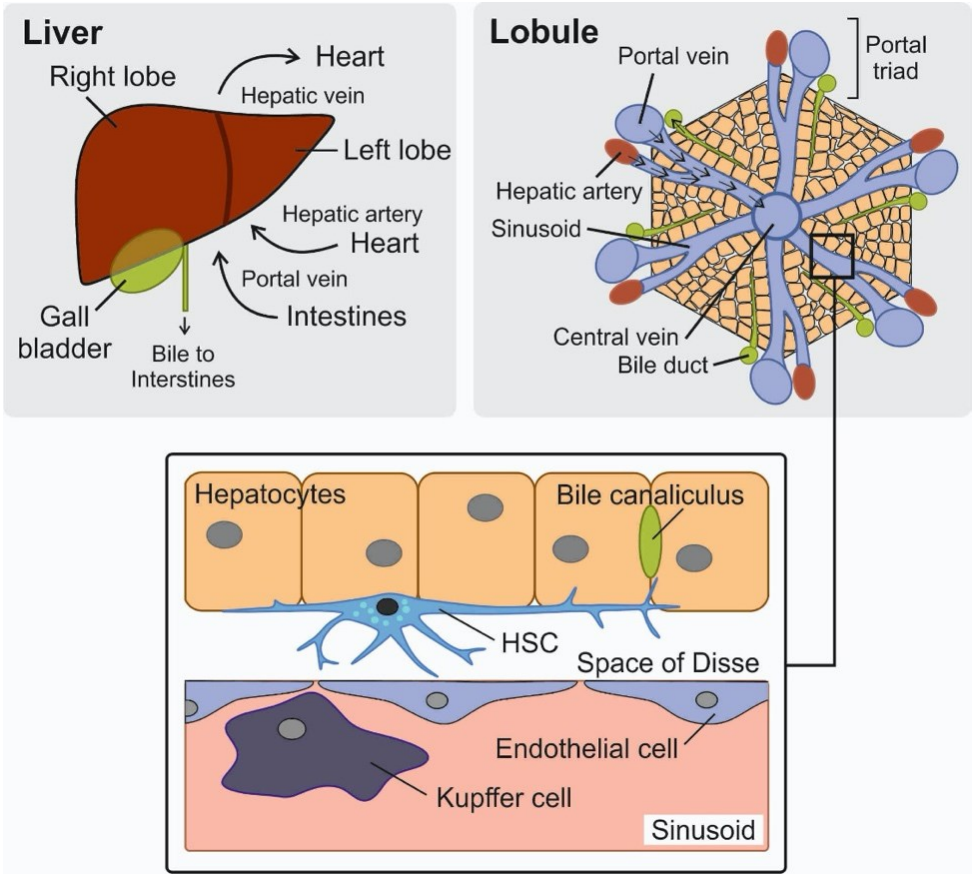

Figure 7. Anatomy and microanatomy of the liver. The liver consists of four liver lobes which are all built up out of liver lobules, the smaller functional units of the organ. Nutrients, metabolites, and other substances from the intestines enter the liver from the portal vein and combine with oxygen loaded blood from the hepatic artery within the liver lobule. Together with the bile duct, which collects the bile from the hepatocytes and sends it towards the gall bladder, these three vessels form the portal triad. The blood passes through the sinusoid, safeguarded by Kupffer cells, and leaves the lobule by the central vein. The sinusoid is built from sinusoidal endothelial cells, followed by the space of Disse, where hepatic stellate cells are located, and hepatocytes. The blood exits the liver by the hepatic vein towards the heart.

The liver has a great regeneration potential as after the exposure or consumption of toxins (*e.g.,* poisonous plants), the self-healing of the certain organ was evolutionarily advantageous. It is striking that the liver is the only organ that can re-grow up to 2/3 of its total mass within 1-2 weeks. This process is mainly covered by a fast proliferation of hepatocytes and can be investigated after partial hepatectomy [125]. Upon chronic liver damage, ongoing inflammation is leading to liver fibrosis and ultimately to cirrhosis. Reasons for these states are often chronic hepatitis B and C infections or long-term alcohol abuse [126,127]. Liver fibrosis is predominantly driven by activated HSCs that produce high amounts of extracellular matrix proteins as well as pro-inflammatory and fibrogenic cytokines [128].

1.3.2 Characteristics of quiescent and activated hepatic stellate cells

Hepatic stellate cells make up about 5-8% of the total liver cells [122] and run under several different names: perisinusoidal cells, Ito-cells, lipocytes, fat-storing cells or liver resident mesenchymal stem cells. The cells were first described by Kupffer in 1876 [129] as star-shaped cells and further characterized by Ito and Wake almost a century later. [130,131] Today, much more research has been done to elucidate the function, characteristics, and signaling pathways of HSCs in health and disease.

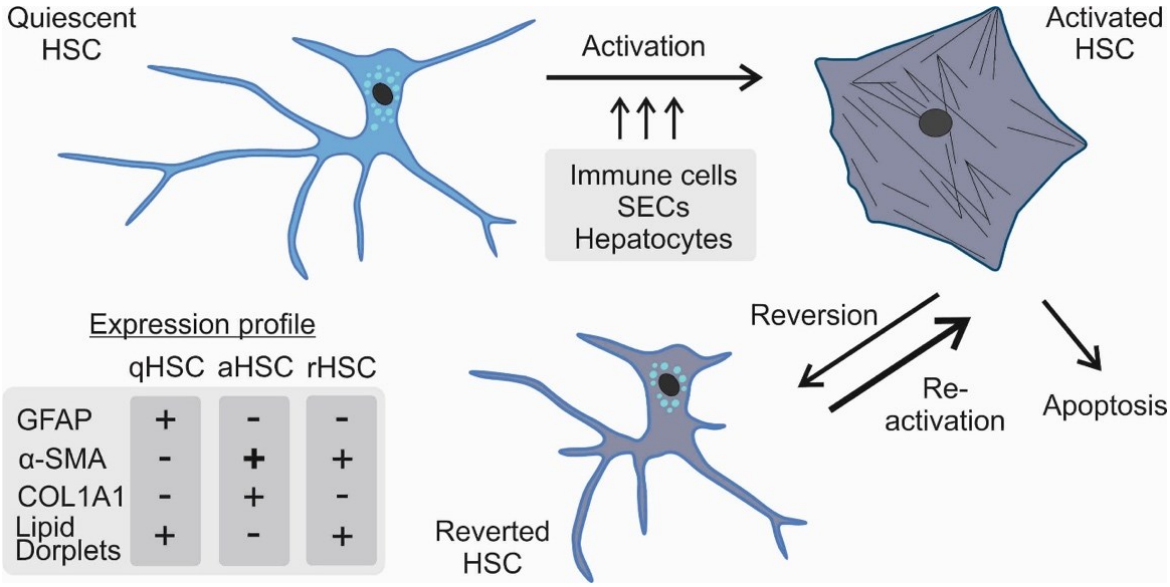

FIGURE 8. Quiescence, activation and reversion of hepatic stellate cells. Quiescent HSCs (qHSCs) activate upon liver damage and extracellular triggers that can be sent out by surrounding cells like hepatocytes, SECs and immune cells. Activated HSCs (aHSCs) display a myofibroblast-like phenotype and get reprogrammed in their protein expression profile, as well as their function. Upon liver recovery, aHSCs can undergo apoptosis or get reverted into quiescent-like HSCs which are called reversed HSCs (rHSCs). The phenotype resembles the qHSC, still, the gene expression is not completely recovered which results in a much faster and stronger reactivation if liver damage reoccurs. The quiescence marker GFAP can only be found in qHSCs, the activation marker α-SMA is strongly expressed in aHSCs and decently expressed in rHSCs. COL1A1 (collagen type 1 alpha 1) is only expressed in aHSCs and gets downregulated after reversion. Loss of lipid droplets can also be an indicator for aHSCs *in vitro* and reappear in rHSCs.

In a healthy liver, HSCs exist in a non-proliferating quiescent state (qHSCs) and activate upon liver injury into contractile myofibroblast-like cells (aHSCs). The main functions of quiescent HSCs comprise (i) storage of vitamin A, (ii) regulation of the sinusoidal blood flow, (iii) production and degradation of extracellular matrix (ECM) proteins and (iv) auto-, endo- and paracrine communication to maintain tissue homeostasis [128]. qHSCs can easily be recognized by their stellate cell shape and the high amount of lipid droplets in their cytosol. These fat globules store around 80% of the body's vitamin A as retinyl esters, which also play a role in gene expression, proliferation, immune signaling, and tissue homeostasis [132,133]. Furthermore, qHSCs express a specific set of proteins, including GFAP (glial fibrillary acid protein), CD133 (prominin-1), nestin, the hepatocyte growth factor (HGF), and ERAS which hint toward the developmental potential of HSCs [8,134–136]. Indeed, HSCs are mesenchymal stem cells and can differentiate for example into osteocytes, adipocytes or chondrocytes and show similarities with the protein expression profile of bone marrow MSCs [137,138]. qHSCs get activated *via* a vast number of extracellular stimuli including hormones, cytokines, growth factors, chemokines, reactive oxygen species (ROS) and pro-inflammatory and fibrogenic signals from surrounding cells like hepatocytes, endothelial cells, platelets, and a big range of immune cells [139]. Furthermore, HSCs are activated by changes in ECM composition, epithelial cell injury and intestinal dysbiosis [139]. The characteristics of activated HSCs differ strongly from quiescent cells. Within the cell, many signaling and metabolizing pathways are reprogrammed during trans-differentiation, including autophagy regulation, retinol metabolism, ECM production and more. The expression of α-smooth muscle actin (α-SMA) is one of the distinct activation markers of HSCs [140]. Additionally, the phenotype of the cells changes during activation, as it can be observed while *in vitro* cultivation of primary HSCs, which differentiate upon isolation and cultivation on uncoated plastic dishes. The cell shape and size increase to a myofibroblast-like appearance exhibiting a high density of stress fibers. During this process, the rodent HSCs lose their lipid droplets, even though, this observation cannot completely be confirmed by *in vivo* fibrosis models. A fibrotic liver, which is mainly driven by activated HSCs, can recover and go back into a normal state if the disease is not fairly advanced (cirrhosis). Most of the aHSCs undergo apoptosis, still, a smaller amount gets reverted into a quiescent-like state and can be called reverted HSCs (rHSCs). Their genetic program does not recover completely, resulting in a much faster and more intensive activation of rHSCs after a recurrence of fibrotic initiators [141,142].

In order to understand the activation processes of HSCs, by pinpointing crucial signaling pathways, HSC trans-differentiation could be medically treated before liver fibrosis is strongly advanced. More research in this area will allow new and alternative therapeutic possibilities in the future.

2. AIMS AND OBJECTIVES

Especially the classical RAS proteins and their downstream effectors attract the attention of the research community due to their role as gatekeepers in cell signaling, but also their involvement in a great deal of cancer types and RASopathies, during the past decades. Basic research is much needed to understand not only the preferred canonical but also the more uncommon non-canonical RAS-signaling pathways. Non-canonical signaling pathways might be cell type-specific, only occur under certain conditions, for example cell differentiation, or might even be related to the emergence and progression of diseases.

Hepatic stellate cells (HSCs) are liver resident stem cells that switch from a quiescent to an activated state during liver fibrosis. Here, they are the main drivers of extracellular matrix production and contribute significantly to disease progression. Understanding the signaling cascades central to maintaining the quiescent state of HSCs and the proteins important for reprogramming cell signaling, will help expand our understanding of liver fibrosis and develop new therapeutic approaches.

This thesis aimed to investigate RAS-connected signaling pathways in the maintenance of hepatic stellate cell quiescence. This included: (i) analyzing the interaction of ERAS and its novel binding partner ARG1 by biophysical, biochemical, and cell biological approaches, as well as (ii) exploring the function of the ERAS-ARG1 axis for the quiescent state of HSCs. Furthermore, this thesis focused on (iii) the basic understanding of RAS-SIN1 interaction that was previously observed for ERAS and SIN1 in quiescent HSCs. In addition, part of this work was (vi) to extend the picture of accessory proteins, the modulators of the RAS-signaling pathway, and to move these proteins from the side line to the center of attention regarding new therapeutic approaches and, (v) investigate the binding site of the accessory protein IQGAP in a complex with CDC42 in detail.

Taken together, this thesis should improve the understanding of the RAS signaling network by focusing on less prominent members of the RAS family and providing insights into modulators, non-canonical interactors, specific binding modes, and new feedback mechanisms.

3. ACCESSORY PROTEINS OF THE RAS-MAPK PATHWAY: MOVING FROM THE SIDE LINE TO THE FRONT LINE

Perspective

Silke Pudewell, Christoph Wittich, Neda S. Kazemein Jasemi, Farhad Bazgir & Mohammad R. Ahmadian

doi: 10.1038/s42003-021-02149-3

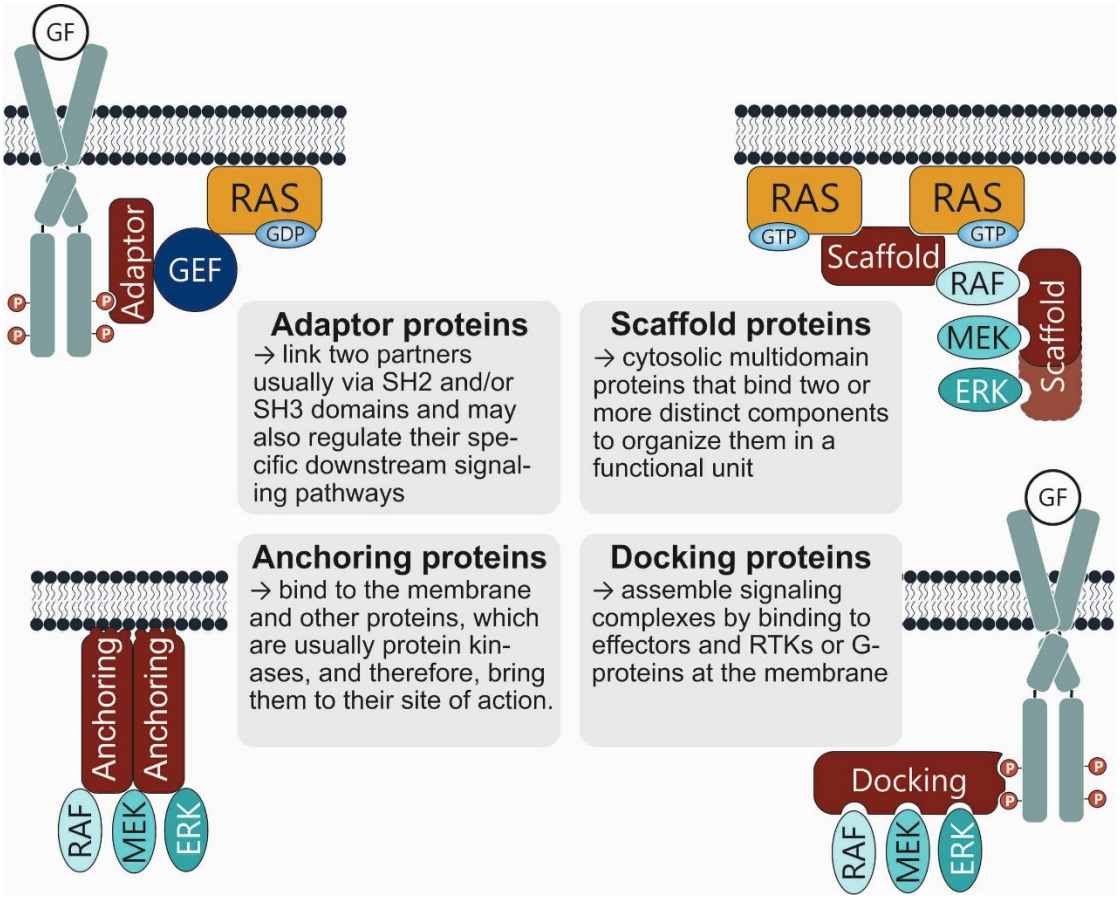

Journal: Communications Biology, Volume 4, Article number: 696 (2021)

Published: 08 June 2021

Impact factor: 6.548

Own contribution: 60%

Concept and preparation of the manuscript, illustration of figure 2 and 3, literature research, reference management, discussion

communications biology

PERSPECTIVE

https://doi.org/10.1038/s42003-021-02149-3 OPEN

Accessory proteins of the RAS-MAPK pathway: moving from the side line to the front line

Silke Pudewell[1], Christoph Wittich[1], Neda S. Kazemein Jasemi[1], Farhad Bazgir[1] & Mohammad R. Ahmadian[1]✉

Health and disease are directly related to the RTK-RAS-MAPK signalling cascade. After more than three decades of intensive research, understanding its spatiotemporal features is afflicted with major conceptual shortcomings. Here we consider how the compilation of a vast array of accessory proteins may resolve some parts of the puzzles in this field, as they safeguard the strength, efficiency and specificity of signal transduction. Targeting such modulators, rather than the constituent components of the RTK-RAS-MAPK signalling cascade may attenuate rather than inhibit disease-relevant signalling pathways.

Nature has evolved sophisticated, cell type-specific mechanisms to sense, amplify and integrate diverse external signals, and ultimately generate the appropriate cellular response. Signals are processed by evolutionarily conserved signalling cassettes that comprise specific constituent components acting as receptors, mediators, effectors and regulatory proteins. Activated receptor tyrosine kinases (RTKs), for instance, link the RAS activator SOS1 to RAS paralogs, e.g., the proto-oncogene KRAS4B, which in turn regulate various signalling pathways, including the mitogen-activated protein kinase (MAPK) pathway[1]. This pathway contains a three-tiered kinase cascade comprising the serine/threonine kinases ARAF/BRAF/CRAF, the dual specificity kinase MEK1/2 and the serine/threonine kinases ERK1/2[1,2]. The RTK-RAS-MAPK axis is a highly conserved, intracellular signalling pathway that has an essential role throughout mammalian development, from embryogenesis to tissue-specific cellular homoeostasis in the adult[3]. Dysregulation of components or regulators of this cascade is frequently associated with tumour growth and a distinct subset of developmental disorders called the RAS-MAPK syndromes or RASopathies[4–6]. This signalling cascade has rapidly taken centre stage in cancer and RASopathy therapies (see below).

However, the strength, efficiency, specificity and accuracy of signal transduction are controlled by mechanisms that increase the connectivity of the signalling molecules and thus increase their local concentration and reduce their dimensionality. This state can be achieved by liquid–liquid phase separation (LLPS), a mechanism in which two separate liquid phases with different protein compositions emerge from one mixed solution[7]. A large number of proteins, hereafter, collectively designated as the 'accessory proteins', fulfil the requirements to drive LLPS and have been reported to act as adaptor, anchoring, docking or scaffold proteins. Accessory proteins link constituent components of individual signal transduction pathways by forming physical complexes. What the functions of the accessory proteins are, why are they crucial for signal transduction, and whether they represent better therapeutic targets for different human diseases are questions that will be addressed in this article in the context of the RTK-RAS-MAPK signalling pathway.

Structural and functional variety of accessory proteins. Rapidly emerging reports on signalling networks support the idea that various signalling molecules operate together in functional protein complexes. For example, activated protein nanoclusters in specialised membrane

[1] Institute of Biochemistry and Molecular Biology II, Medical Faculty of the Heinrich-Heine University, Düsseldorf, Germany. ✉email: reza.ahmadian@hhu.de

microdomains selectively connect with and subsequently activate cytosolic signalling components or complexes[8,9]. RAS nanoclusters form and locally increase the concentration of RAS paralogs in membrane microdomains[10].

Membrane-resident signalling proteins, such as transmembrane (TM) and membrane-associated proteins, are predominantly trafficked to the plasma membrane via the secretory pathways[11]. But how are the cytosolic proteins trafficked to their cognate membrane nanoclusters? Mounting evidence has emerged recently that a large number of membraneless compartments (also called non-membrane-bound organelles or biomacromolecular condensates) are assembled via LLPS[12]. The formation of cytosolic signalling condensates is based on two processes. First multivalent molecules undergo phase separation, whereas in a second step other proteins are able to diffuse into the phase without considerably contributing to the stability of the phase. This process can increase local concentrations of molecules by several folds. One example is the enrichment of kinases in membrane-associated liquid droplets around T-cell receptors while phosphatases are excluded[13].

An essential group of proteins that are themselves not constituent components of signal transduction but allow assembly and spatiotemporal organisation of a signalling cascade are accessory proteins. These proteins have the features to interact with and assemble other biomolecules, ranging from lipids, over proteins to nucleic acids. They mostly lack enzymatic activity but are equipped with different types of protein–protein interaction domains, motifs and intrinsically disordered regions (IDRs). Thus, accessory proteins dictate the local formation of macromolecular protein complexes through modular multivalent interactions, and thereby organise and facilitate signal transduction.

Accessory proteins bind and connect at least two constituent components to orchestrate their spatiotemporal localisation and enhance their assembly by reducing the dimensionality of interactions and/or increasing local concentrations of interacting proteins[14–16]. They can be categorised in four distinct groups based on their structure and mode of action: (1) scaffold proteins are cytosolic multidomain proteins that bind two or more distinct components to organise them in a functional unit and modulate their function. (2) Adaptor proteins link two partners usually via SH2 and/or SH3 domains and may also regulate their specific downstream signalling pathways. (3) Anchoring proteins bind to the membrane and other proteins, which are usually protein kinases, and therefore, bring them to their site of action. (4) Docking proteins assemble signalling complexes by binding to effectors and RTKs or G-proteins at the membrane.

Accessory proteins of the RTK-RAS-MAPK pathway. New discoveries and concepts regarding the receptor-driven RAS-MAPK signal transduction have emerged during the last three decades: novel pathway components, structure elucidation, biophysical principles, biomimetic strategies and clinical drug candidates. By focusing particularly on the signalling process itself, the emphasis of this article is on the implementation of the accessory proteins, which bind molecular components and orchestrate their assembly and eventually activity in a context-dependent manner. We believe that the spatial arrangements of such biophysical features over time determine specificity, efficiency, fidelity of signal transduction and safeguard against any deleterious effects.

A multitude of accessory proteins, which largely vary in size and domain architecture (Fig. 1), are involved in orchestrating RTK-RAS-MAPK signal transduction. The high variability of scaffold proteins is—due to their high interaction specificity—comprehensible. Certain domains or repeats frequently exist in individual proteins, for example, LDs (repeated leucine-rich sequence) in Paxillin, WDs (WD-repeat) in MORG1, RRMs (RNA recognition motif) in nucleolin and LIMs in FHL1/2. Furthermore, IDRs are found in several proteins, which may fold upon interaction with their binding partner. IDRs are also involved in oligomerization for example in galectin-3[17]. Anchoring proteins contain membrane-binding domains, such as the PH domain in CNK1 and GAB1/2, and TM segment, e.g., in LAT, NTAL and SEF1. PAQR10/11 contain 7 TM segments and anchor RAS to the Golgi apparatus via their N-terminal cytoplasmic tail[18]. The PHB domain of FLOT1 has been reported to be a membrane association domain as it is post-translationally modified by palmitoylation[19]. This leads to FLOT1 association with lipid rafts of phagosomes and the plasma membrane. Docking proteins frequently possess both PH domains, which increase their residence time at the membrane, and PTB domains, which enable them to interact specifically with activated RTKs. Adaptor proteins are specialised in linking activated RTKs via SH2 domains with their downstream signalling molecules, in most cases, via SH3 domains.

Linking TM receptors to RAS. GRB2 links activated RTKs or anchoring proteins, such as LAT, with SOS1/2 to activate RAS paralogs (Fig. 2a)[20]. The adaptor protein function of GRB2 is accomplished by a central SH2 domain that binds to the tyrosine-phosphorylated RTK and two flanking SH3 domains, which bind to the C-terminal proline-rich domain of SOS1 and translocate it to the plasma membrane[21,22]. Activated SOS1, in turn, stimulates, as a RASGEF, the GDP/GTP exchange of RAS paralogs and thereby activates amongst others the MAPK cascade[23].

Furthermore, direct GRB2 association with activated RTKs leads to the recruitment of GAB1 and CBL. GAB1 provides a docking platform for several signalling molecules, e.g., SHP2, PLCγ and PI3K, thereby cross-linking different signalling pathways[24]. CBL was originally described to act as an adaptor protein as it contains several domains and motifs for protein–protein interactions (Fig. 1). Later, it was identified as a RING-dependent E3-ubiquitin-protein-ligase that transfers the ubiquitin to RTKs for endocytic internalisation, and recycling or degradation[25]. It also regulates signalling processes of the non-RTKs SYK, ZAP70 and SRC[26]. CBL constitutively interacts with GRB2, mediating hematopoietic cell proliferation[27], and T-cell and B-cell receptor and cytokine receptor signalling via interaction with CRKL SH2 domain[28]. As CBL and SOS1 bind to the same region of GRB2, the overexpression of CBL inhibits complex formation between SOS1 and GRB2 underlining the fine-tuning mechanism of accessory proteins by binding other pathway modulators[29].

Engagement of GRB2 is versatile and leads to different outcomes depending on the cellular context. GRB2 can bind indirectly to RTKs via interaction with the tyrosine-phosphorylated adaptor proteins SHC and FRS2. SHC links activated TRKA receptors to GRB2 in PC12nnr5 cells[21,22,30], which can recruit SOS to the PM and control the extent of RAS activation[23]. Upon activation of the B-cell antigen receptor (BCR) in B-lymphocytes, the tyrosine kinase SYK phosphorylates SHC which leads to translocation of GRB2-SOS1 and activation of membrane-associated RAS signalling[31]. The SHC–GRB2 complex, downstream of cytokine receptors, also activates the PI3K pathway to control cell survival and/or proliferation[32]. A similar mechanism of GRB2-SOS-RAS activation is operated via FRS2, which acts downstream of TRKA in neurons[21], and FGFR in embryonic stem cells[33,34]. FRS2 has multiple tyrosine phosphorylation sites to activate, in response to a wide range of agonists, PI3K and RAS-MAPK pathways in various cell types via binding

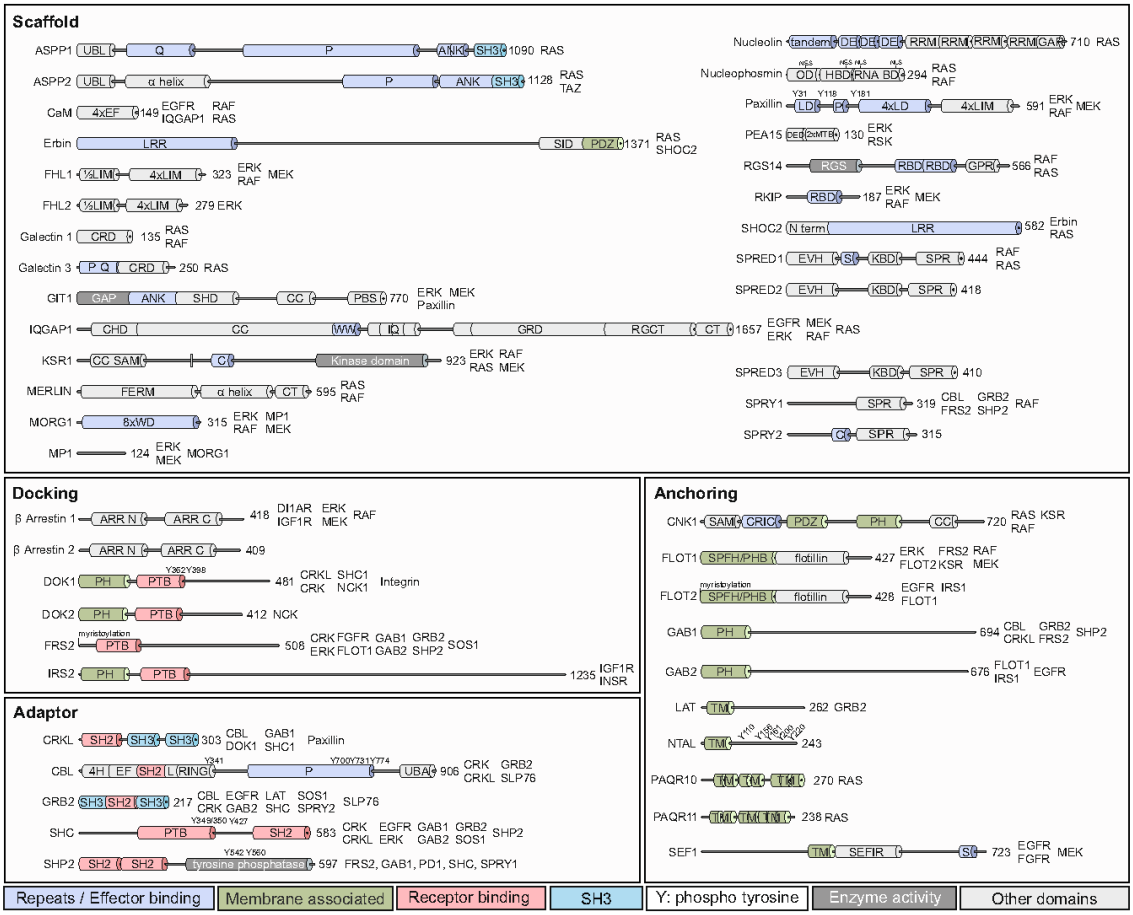

Fig. 1 Domain organisation and crucial interactions of RTK-RAS-MAPK accessory proteins. Schematic representation of relevant domains in scaffold, docking, adaptor and anchoring proteins. Direct binding partners, which are part of the RTK-RAS-MAPK pathway, are mentioned next to the amino-acid numbers at the right side of the proteins. Please check the list of abbreviations in the supplemental table for more details. Abbreviations are summarised in Supplementary Table 1.

to GRB2 and SHP2, respectively[35–39]. The binding of the ubiquitous protein tyrosine phosphatase SHP2 to GRB2, induces recruitment by the FRS2-SHP2 complex, which controls retinal precursor proliferation and lens development[40].

Modulating the RAS cycle. The RAS cycle between an inactive, GDP-bound state and an active, GTP-bound state is strictly controlled by multidomain regulatory proteins[41–44]. Unlike the well-understood cellular process of RAS activation by RASGEFs, such as SOS1 little is known about the recruitment and activation of RASGAPs. The first evidence has emerged that the RASGAPs neurofibromin and p120 are recruited to the plasma membrane and RAS•GTP by two distinct scaffold proteins, SPRED1 and merlin (Fig. 2b). The EVH domain of SPRED1, a member of the sprouty family, binds the GAP domain of neurofibromin without interfering with its GAP function[45,46]. SPRED1 appears to directly contact BRAF and thus to interfere with KRAS signalling[47]. Merlin, a member of the ERM family, directly binds to, on the one hand, p120 and RAS (probably KRAS4B), a mechanism that potentiates RAS inactivation in Schwann cells, and on the other hand, CRAF and blocks its interaction with RAS[48,49]. p120 modulates many regulators and signalling proteins via its N-terminal protein interaction domains, apparently independent of its GAP function[50,51].

RAS-RAF connection. Lipidation and clustering of the RAS paralogs are critical steps for a tight control of signal transduction through the MAPK pathway. This process connects two distinct macromolecular clusters, plasma membrane-associated RAS-containing clusters[9] and cytosolic RAF/MEK/ERK-containing clusters[52].

The scaffold proteins galectin 1 and 3 are carbohydrate-binding proteins that are involved in many physiological functions. While galectin 1 homodimer binds to HRAS-RAF complex and stabilises HRAS•GTP at the plasma membrane[10,53], galectin 3 selectively binds and clusters KRAS4B•GTP (Fig. 2c)[54]. The nucleolar phosphoproteins nucleophosmin and nucleolin shuttle between nucleus and PM and are different types of RAS scaffold proteins, which have been reported to stabilise KRAS4B levels in a nucleotide-independent manner at the plasma membrane. Nucleophosmin also increases the KRAS4B•GTP clusters and enhances MAPK signal transduction[55].

Another type of clustering is performed by the scaffold protein SHOC2 (also known as SUR8), which connects activated RAS with the RAF kinases (Fig. 2d). SHOC2 is an integral element of a heterotrimeric holoenzyme complex with PP1 and MRAS, which

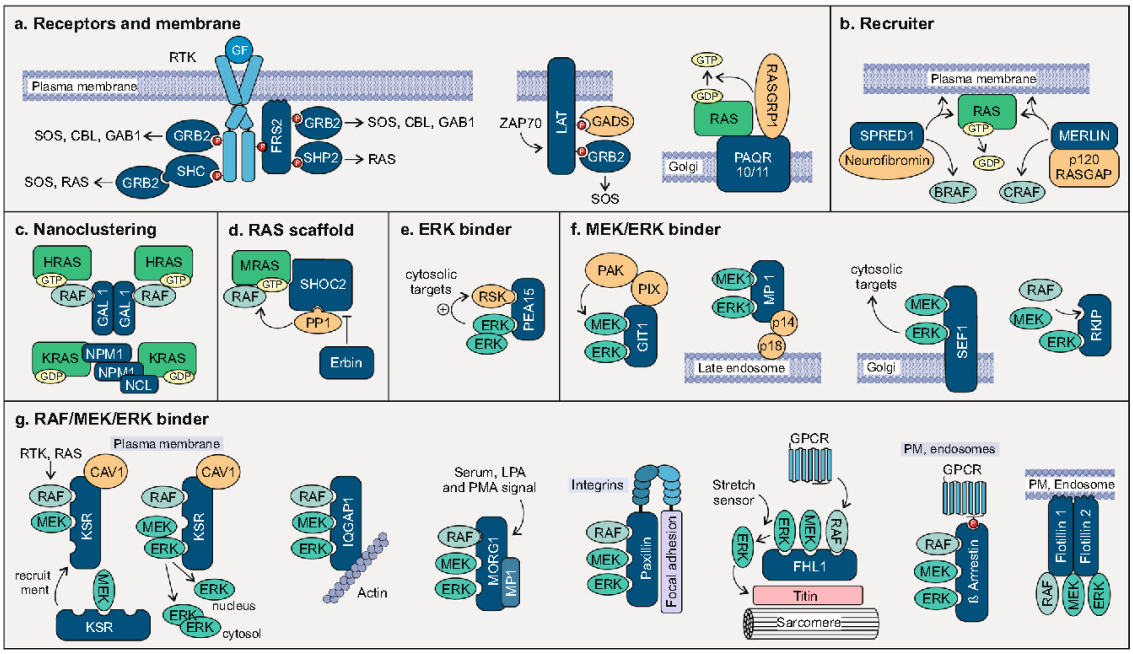

Fig. 2 Involvement of RTK-RAS-MAPK accessory proteins in signal transduction. Accessory proteins are involved in every step of the RTK-RAS-MAPK pathway and increase the connectivity between signalling components. Adaptor proteins and docking proteins interact with phosphorylated receptors, in contrast to anchoring proteins, which are directly associated with the membrane (**a**). Recruiter translocate binding partner towards the site of action, e.g., a GTPase activating protein to activated RAS at the plasma membrane (**b**). Scaffold proteins that induce nanoclustering, increase the local concentration of their binding partner in lipid rafts (**c**). RAS scaffold proteins bind RAS and other components of the RTK-RAS-MAPK pathway (**d**), whereas ERK binder (**e**), MEK/ERK binder (**f**) and RAF/MEK/ERK binder (**g**) can connect one, two, or all three members of the MAPKs, bringing them close together, regulate their activity and determine their localisation. See text for more details.

dephosphorylates and releases RAF from its inhibited state[56,57], and subsequently activates the MAPK pathway[58]. The scaffold protein Erbin interferes with this process[59]. It binds and sequesters SHOC2 from its RAS/RAF complex, and inhibits ERK activation[60]. Erbin is a large scaffold protein (Fig. 1). As such, it links different pathways by binding, besides SHOC2, also various other accessory proteins, including GRB2[61], CBL[62], Merlin[63] and KSR1[2,64].

RAF/MEK/ERK cascade. RAF kinase translocation to the plasma membrane and activation by direct interaction with RAS•GTP is well described[2,65–67]. Activated BRAF/CRAF heterodimer phosphorylates MEK1/2, which in turn phosphorylates ERK1/2 at the TEY motif in the activation loop[68,69]. Activated ERK1/2 are ultimately recruited to their substrates in various subcellular compartments[70,71]. The assembly of macromolecular complexes of the MAPK components and their connection with RAS nanoclusters at the membrane, which constitutes the RAS–ERK axis, is arranged by homo- and heterodimerization of the members of this pathway[68]. To achieve signal diversity, specificity and fine-tuning, the spatiotemporal flux through the pathway is organised by various distinct accessory proteins, which bind either ERK, MEK/ERK, or RAF/MEK/ERK[1,70,72].

PEA15 modulates ERK activity towards its cytosolic substrates, including RSK2. It enhances ERK-dependent phosphorylation of RSK2 by binding both of them independently (Fig. 2e)[73]. PEA15 phosphorylation by PKC, AKT, or CaMKII inhibits this process. In addition, PEA15 steers subcellular localisation of ERK by facilitating its nucleocytoplasmic export[74].

The MEK/ERK accessory proteins are illustrated in Fig. 2f. GIT1 binds MEK1 and ERK1 in response to integrin, RTK and GPCR activation. Its activity is directly regulated by different downstream effectors, such as PIX/PAK complex[75]. MP1 binds and translocates MEK1 and ERK1 to late endosomes by associating with p14 and p18[76,77]. The anchoring protein SEF binds activated MEK on the Golgi apparatus, and subsequently binds ERK, leading to activation of ERK and finally its cytosolic substrates such as RSK2[78]. The latter phosphorylates SEF and induces its translocation to the plasma membrane, where it directly inhibits FGFRs, and enhances EGFR signalling instead[79]. RKIP acts as a competitive inhibitor of MEK phosphorylation. It binds ERK and mutually exclusively RAF or MEK, and thus, dissociates active RAF/MEK complexes[80]. The phosphorylation of RKIP by PKC results in the release of RAF1 and enables the activation of the MAPK pathway[81].

The scaffolding of RAF/MEK/ERK is dependent on several factors, including the tissue specificity, cellular localisation of the signalling complexes and the type of upstream signals (Fig. 2g). KSR1 is one of the best-studied scaffolds that binds to all three members of the RAF/MEK/ERK cascade[72]. KSR1 translocates, upon RTK-RAS activation, in a complex with MEK to CAV1-rich microdomains in the plasma membrane to bind activated RAF and modulate MEK and ERK activation. Feedback phosphorylation of KSR1 and BRAF by ERK promotes their dissociation and results in the release of KSR1/MEK from the plasma membrane[82]. In this way, MEK is sequestered from upstream signals and cannot itself regulate ERK activation.

The multidomain protein IQGAP1 scaffolds and activates the RAF/MEK/ERK kinases by directly associating with the EGF

receptor[83,84]. With over 100 binding partners, the localisation and effect of IQGAP1 interaction reach from actin cytoskeleton reorganisation in the context of neurite outgrowth, migration or vascular barrier integrity to insulin secretion via exocytosis or cell proliferation and differentiation via ERK signalling. The extensive interactions of IQGAP1 vary according to cell types and environmental conditions[85]. In contrast, MORG1, FHL1, paxillin and β-arrestin act EGF-independent (Fig. 2g). MORG1 exists in a complex with MP1 and facilitates ERK1/2 activation in response to LPA and PMA, and GPCR activation[86]. The focal adhesion protein paxillin modulates the activation of the RAF/MEK/ERK complex through the binding of other proteins, controlling the remodelling of the actin cytoskeleton[87]. FHL1 scaffolds RAF/MEK/ERK on the N2B domain of the giant protein titin at the sarcomere of the mammalian muscle cells[88]. β-arrestin stimulates ERK signalling in response to activation of GPCR or other receptors on the plasma membrane but also on endosomes. FLOT1/2 are membrane raft-associated proteins that form heterodimers. They are not only involved in the EGF receptor clustering and activation, but also directly bind CRAF, MEK and ERK enhancing their activity upon stimulation[89]. CNK1 physically interacts with RAF facilitating its activation by assisting RAF membrane localisation and oligomerization upon RAS activation[90], whereas being able to interact with RAS as well via the N-terminal regions[91].

Accessory proteins as in human disease. Even if dysregulated constituent components of the RTK-RAS-MAPK pathway are among the most intensively studied target structures for disease treatment, new emphasis should be laid on accessory proteins (Fig. 3). Their loss-of-function or gain-of-function mutations are mostly and frequently associated with the initiation and progression of human diseases and disorders. The hyperactivation of the RTK-RAS-MAPK pathway is a known cause of many diseases, like cancer and developmental disorders, including RASopathies.

Cancer. The upregulation of activating proteins or the downregulation of inhibiting proteins leads to gain-of-function of the RTK-RAS-MAPK pathway in almost all types of cancer (Fig. 3a). The expression of accessory proteins is tightly controlled and often dysregulated in tumours. Paxillin is a scaffold protein, which is involved in focal adhesion. A gain-of-function mutation in *Paxillin* has been found in 9% of all non-small cell lung cancers (NSCLC) (1)[92]. Furthermore, genomic amplification of *Paxillin* in lung cancer promotes tumour growth, invasion and migration[93]. SPRED1/2, negative modulators of RAS signalling, are downregulated in 84% of patients with hepatocellular carcinoma (2)[94]. The scaffold protein IQGAP1 promotes tumour formation,

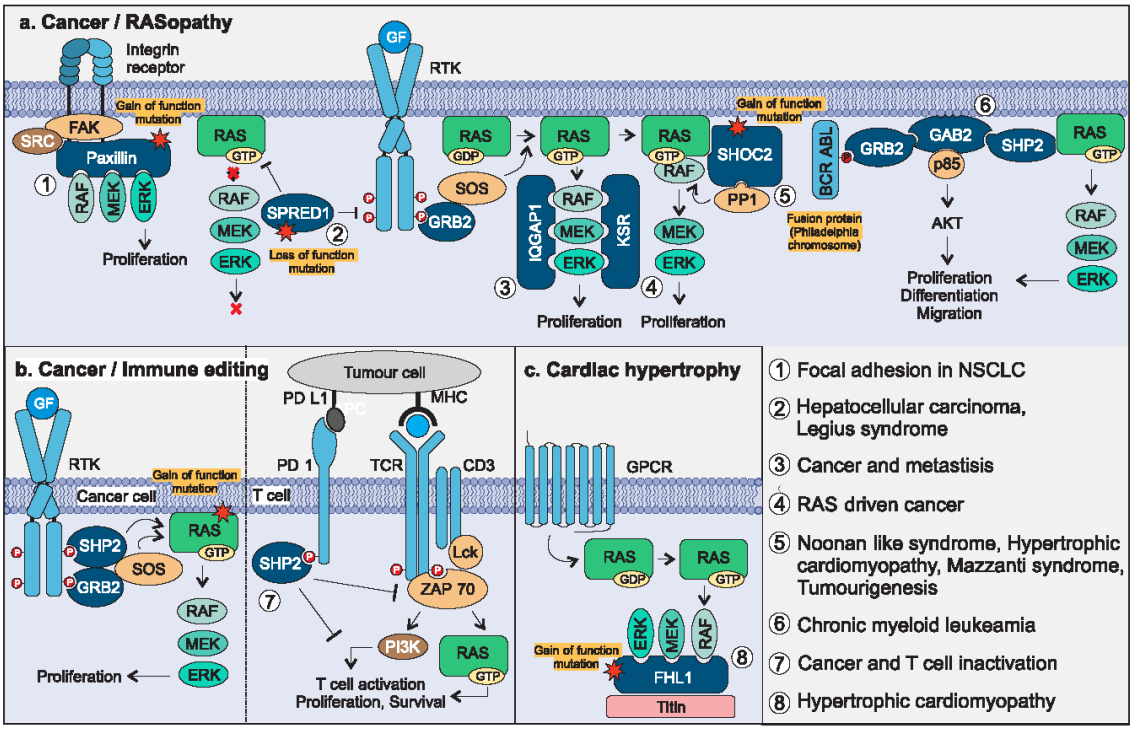

Fig. 3 Involvement of accessory proteins in diseases. The canonical RAS/MAPK pathway is tightly regulated by many proteins, attenuators and negative feedback mechanisms. Mutations in regulators like accessory proteins can lead to a dysregulated RAS/MAPK pathway and therefore to a variety of diseases as cancer and RASopathies (**a**). The genomic amplification of Paxillin is found in many NSCLC patients and activates the focal adhesion complex downstream of integrins (1). Loss-of-function mutations of SPRED1 activate the RAS-MAPK pathway and lead to Legius syndrome (germline) and hepatocellular carcinoma (somatic) (2). IQGAP1 mutations are often associated with tumour formation and metastasis (3), whereas KSR is a central player in KRAS-driven cancers, inducing proliferation and survival (4). Mild gain-of-function mutations of SHOC2 lead to Noonan-like syndrome with loose anagen hair or Mazzanti syndrome, other somatic mutations can lead to hypertrophic cardiomyopathy or tumourigenesis (5). The signalling of BCR-ABL-positive cells in chronic myeloid leukaemia is also dependent on GAB2 activation, cross-linking AKT and RAS pathway (6). The adaptor protein SHP2 is not only part of hyperactive RAS signalling in cancer cells, but is of major importance in the inactivation of T cells, inhibiting the TCR signal in response to ligand binding to PD-1 (**b**). FHL1 is involved in the development of cardiac hypertrophy, which is caused by a gain-of-function mutation, leading to increased ERK signalling (**c**).

transformation, invasion and metastasis in various cancer types (3)[95]. A study of a KSR$^{-/-}$ mouse model proves the resistance against RAS-dependent tumour formation[96], highlighting the pro-oncogenic function of KSR in RAS-driven cancers (4). SHOC2 mediates tumourigenesis and metastasis in different cancer types via tethering RAS and CRAF proteins in close proximity and thus promoting RAS-mediated CRAF activation[97,98]. Knockout models of SHOC2 in KRAS mutated lung adenocarcinoma in mice have revealed a significant reduction of tumour growth, as well as a prolonged survival, accentuating the scaffold protein as a potential therapeutic target (5)[99]. GAB2 has been implicated as a central modulator for oncogenic BCR-ABL signalling[100]. GAB2-deficient mice have exhibited resistance against cancer cell transformation of myeloid progenitors in the presence of BCR-ABL, which is found in 90% of patients with chronic myeloid leukemia (6)[100,101]. SHP2 is not only associated with a large number of cancers but plays a central role in PD-L1/PD-1 singling that inhibits the TCR-activated pathways, including RAS-MAPK, in T cells (Fig. 3b (7))[102]. This leads to an inactivation of the T cells, guarding the tumour cells against the immune system. Thus, SHP2 inhibitors have a dual role as a possible therapeutic target by reducing RAS signalling and inducing the body's immune response.

RASopathies. RASopathies or RAS-MAPK syndromes are defined as a group of developmental disorders that are caused by mild gain-of-function germline mutations in genes related to not only the constituent members of the RTK-RAS-MAPK pathway[103] but also various accessory proteins, including CBL, SHP2, SPRED1 and SHOC2 (Fig. 3a)[103].

Germline *CBL* mutations exhibit a wide phenotypic variability related to Noonan syndrome, which is characterised by a relatively high frequency of neurological features, predisposition to juvenile myelomonocytic leukaemia and low prevalence of cardiac defects, reduced growth and cryptorchidism[104]. The mutations are mainly located in the central region of CBL, which is known to abolish the ubiquitination of RTKs by impairing CBLs E3 ligase activity[104]. Legius syndrome-associated mutations in *SPRED1*, mostly result in loss-of-function of the scaffold protein, and gain-of-function of the RAS-MAPK pathway[105,106]. In contrast, mutations in genes encoding SHP2 and SHOC2 lead to a gain-of-function and contribute to MAPK signalling upregulation that causes diverse developmental phenotypes[56,59,107]. A recurrent activating mutation at the very N-terminus of SHOC2 (Ser-2 to Gly) leads to N-myristoylation of SHOC2, confers continuous membrane association and consequently causes Mazzanti syndrome, a RASopathy characterised by features resembling Noonan syndrome[107,108]. Another RASopathy-causing *SHOC2* mutation (Gln-269 to His and His-270 to Tyr) has been recently identified to be associated with prenatal-onset hypertrophic cardiomyopathy[107]. This mutation changes the relative orientation of the two leucine-rich repeat domains of SHOC2 and enhances its binding to MRAS and PPP1CB, two other RASopathy genes[109], and thus, increased signalling through the MAPK cascade[107].

Other diseases. Moyamoya angiopathy is characterised by progressive stenosis of the terminal portion of the internal carotid arteries and the development of a network of abnormal collateral vessels. This is a rare condition that can be caused by de novo *CBL* mutations even in the absence of obvious signs of RASopathy[110]. Evidence linking CNK1 dysfunction to autosomal recessive intellectual disability in patients emphasises the importance of this anchoring protein in the orchestration of the RTK-RAS-MAPK signalling in brain development and cognition[111]. The scaffold proteins FHL1/2 link RAS-MAPK signalling to the sarcomere and is a critical component of the hypertrophy signalling in cardiac cells (Fig. 3c)[88]. FHL1/2 mutations are associated with cardiac diseases[112]. FLOT1 has been implicated in the development of Alzheimer and type 2 diabetes and could be a promising proteomic biomarker[113,114].

Accessory proteins as therapeutic targets. Direct targeting of constituent members of the RTK-RAS-MAPK axis in the context of disease treatment, such as cancer, is a big challenge. Therapies for KRAS mutated cancers remain a major clinical need, despite allele-specific inhibitors that trap and inactivate mutant KRAS (G12C)[115,116]. Three decades of research led to significant advances in tumour treatment[117]. However, the side-effects can still be severe and more-specific treatments could ease patient suffering. Unfortunately, many of the expectations for RAS pathway-targeted drugs have not been fulfilled. High toxicity and resistance acquisition have hampered many of the drugs developed to date[117,118]. An alternative therapeutic strategy to treat KRAS mutant cancers aims at protein degradation via proteolysis targeting chimeras (PROTACs)[119]. The ablation of CRAF in advanced tumours driven by KRAS oncogene leads to significant tumour regression with no detectable appearance of resistance mechanisms and limited toxicities[120]. In this context, a recent study has reported first progress to develop degrader molecules that target KRAS oncogene in NSCLC[121].

Emerging evidence suggests that constituent signalling proteins assemble into macromolecular complexes and co-operate in clusters at specific sites of the cell. Therefore, it is important to note that the stoichiometric imbalance of each subunit of a complex—either by gene overexpression on the one side, and depletion, knockout or targeted protein degradation on the other—perturbs the equilibrium, and interferes at some level with the function of the protein or its complex[122]. With accessory proteins being of immense relevance for the whole signalling machinery and operating particularly from the side line, we propose that functional interference with a defined site of accessory proteins may attenuate rather than inhibit the signalling of hyperactivated RTK-RAS-MAPK axis.

The knockout or knockdown of accessory proteins in cell-based or animal models could already show the importance of these modulators in cancer signalling. The scaffold protein SHOC2 has an important role in embryogenesis, therefore, loss-of-SHOC2 is embryonically lethal. In contrast, the systemic knockout in adult mice as well as in human cell lines is quite well tolerated and leads to growth inhibition of RAS-mutated NSCLC cell lines[99]. Furthermore, the depletion of SHOC2 leads to a sensitisation towards MEK inhibitor treatment, by interfering with the feedback-loop of MEK inhibition via BRAF/CRAF dimerisation, which is SHOC2 dependent[99]. Therefore, dual targeting of SHOC2 and MEK appears as a promising treatment strategy in RAS-mutated cancers. Another approach deals with the scaffold protein GIT1. The knockdown of GIT1 in human osteosarcoma cells has shown in vivo and in vitro reduced tumour cell growth, invasion and angiogenesis, which could make GIT1 a potential target in gene therapy[123].

There is a number of approaches to target specific functions of accessory proteins (Table 1). The CNK1 inhibitor PHT-7.3 binds to its PH domain and prevents the colocalisation with prenylated KRAS4B on the plasma membrane[124]. PHT-7.3 successfully inhibits the growth of tumour cells induced by mutated but not wild type KRAS4B. The interference of GRB2 mRNA by liposome-incorporated nuclease-resistant antisense oligodeoxynucleotides in BCR-ABL fusion protein-positive cancer cells, leads to reduced tumour growth in Xenograft models[125]. It

Table 1 Accessory proteins as attractive therapeutic targets.

Accessory protein	Disease	Drug	State of art	Comment	Ref.
CNK1	Cancers with KRAS mutations	PHT-7.3	Cell-based model	PHT-7.3 binds selectively to CNK1 PH domain, interferes its colocalisation with KRAS4B on the plasma membrane and diminishes RAF/MEK/ERK signalling	124
GRB2	BCR-ABL-positive leukaemia	Anti-miDNA L-GRB2	Xenograft model	L-GRB2 selectively targets GRB2 mRNA and inhibits its translation	125
IQGAP1	Cancers with KRAS mutations	WW competitive peptide	Mouse model	WW competitive peptide antagonist of IQGAP1 interferes with its scaffolding ERK interaction; it is applied in combination with the BRAF inhibitor vemurafenib (PLX-4032) against KRAS4B oncogene	126
KSR	Cancers with KRAS mutations	APS-2-79	Cell-based model	APS-2-79 binds and stabilises KSR in its inactive state, interferes with KSR/RAF heterodimerization and inhibit oncogenic KRAS4B signalling	128,129
SHP2	Cancers	SHP099	Xenograft model	SHP099 binds SHP2 as an allosteric inhibitor, stabilises its autoinhibited state and inhibit oncogenic Ras signalling	130–133

interferes with the RAS/MAPK pathway and the cross-talk towards AKT pathway via GAB2. A WW-peptide of IQGAP1 binds ERK and competes with endogenous IQGAP1, which leads to attenuation of ERK activation[126]. This treatment together with the BRAF inhibitor vemurafenib (PLX-4032), was very successful in tumour mouse models[126]. It has later been shown that not the WW-domain but the IQ domain is necessary to bind ERK[127]. The effects on the tumour growth suppression may stem from the interference with another yet unknown binding partner of IQGAP1 as an integral element of its complex scaffolding function. Another interesting example of accessory proteins as a therapeutic target is the small molecule APS-2-79, which binds KSR in its inactive state and interferes with RAF binding and thus blocks MEK phosphorylation[128]. The cell-based experiments with APS-2-79 have shown not only reduced ERK activation and growth inhibition in combination with the MEK inhibitor trametinib, but also antagonising its resistance mechanism[129]. Besides active site inhibitors, an allosteric inhibitor of SHP2 SHP099 stabilises the autoinhibited state and interferes with the enzymatic activity as well as its adaptor protein function to bind, for example, the GRB2-SOS complex[130]. A combination of SHP099 with a MEK inhibitor has been shown to interfere with the feedback mechanism via SHP2 and to block the resistance initiation observed in KRAS4B-driven cancer therapy[130–132]. In addition, SHP2 inhibition by SHP099 has been shown to have a positive effect on anti-tumour immunity in colon cancer xenograft models, especially in a co-treatment with an anti-PD-1 antibody[133].

Given that the majority of accessory proteins are now emerging as attractive therapeutic targets, still a very small number of accessory inhibitors have been discovered yet.

Concluding remarks and outlook

Accessory proteins tightly control signal transduction by fine-tuning spatiotemporal organisation of signalling components and maintaining specificity and function of the pathway on a cell type and even subcellular level. They operate from the side line, from which they specifically leverage their multivalent domains on the formation of macromolecular clusters, as highlighted in this article. Even though interest in accessory proteins has grown in the past few years, the possibilities to practically visualise them, track their pathway and experimentally and selectively affect their functions in human cells are keys to address questions about their cell type specificities, subcellular distribution and physical interactions in a context-dependent manner. To investigate the impact of an accessory protein in the context of RAS-MAPK signalling, we suggest the following approach: (i) It is necessary to first determine a cell line that expresses the gene related to the accessory protein of interest using quantitative real-time PCR. (ii) It is crucial to investigate the accessory protein at the endogenous levels. The overexpression studies cause in spite of their experimental advantages various difficulties[122]. A prominent example is KSR overexpression that has been erroneously identified as a suppressor of RAS signalling. (iii) The major challenges faced and likely to be faced in near future are the difficult task of the direct use of antibodies post-purchase without careful validation[134]. It is of major importance to validate the antibody specificity by immunoblotting purified protein or protein fragments, and cell lysates overexpressing gene or gene fragments encoding the accessory protein. (iv) Cell fractionation and confocal imaging under-stimulated and non-stimulated conditions will prove if the proteins pre-assemble in complexes with their binding partners (as predicted for KSR-MEK) and where they are located within the cell; as we expect the accessory proteins to orchestrate the RTK-RAS-MAPK signalling in specific subcellular compartments (e.g., plasma membrane, early endosomes, lysosomes, Golgi or ER). (v) Gene knockout cell lines, generated by CRISPR/Cas9 technology, will allow measuring the impact of the accessory proteins as positive or negative modulators of the RAS-MAPK pathway, by determining the p-ERK/ERK ratio. Moreover, this approach will give an idea about possible feedback or compensation mechanisms of accessory proteins among each other. Thus, exploring these concepts in greater detail will provide the framework for future research that will fill existing gaps in our knowledge and expand our understanding of more effective therapies.

Received: 12 February 2021; Accepted: 23 April 2021;
Published online: 08 June 2021

References

1. McKay, M. M. & Morrison, D. K. Integrating signals from RTKs to ERK/MAPK. *Oncogene* **26**, 3113–3121 (2007).
2. Lavoie, H. & Therrien, M. Regulation of RAF protein kinases in ERK signalling. *Nat. Rev. Mol. Cell Biol.* **16**, 281–298 (2015).
3. Nakhaei-Rad, S. et al. Structural fingerprints, interactions, and signaling networks of RAS family proteins beyond RAS isoforms. *Crit. Rev. Biochem. Mol. Biol.* **53**, 130–156 (2018).
4. Tartaglia, M. & Gelb, B. D. Disorders of dysregulated signal traffic through the RAS-MAPK pathway: phenotypic spectrum and molecular mechanisms. *Ann. N. Y. Acad. Sci.* **1214**, 99–121 (2010).
5. Dhillon, A. S., Hagan, S., Rath, O. & Kolch, W. MAP kinase signalling pathways in cancer. *Oncogene* **26**, 3279–3290 (2007).

6. Castel, P., Rauen, K. A. & McCormick, F. The duality of human oncoproteins: drivers of cancer and congenital disorders. *Nat. Rev. Cancer* **20**, 383–397 (2020).
7. Lyon, A. S., Peeples, W. B. & Rosen, M. K. A framework for understanding the functions of biomolecular condensates across scales. *Nat. Rev. Mol. Cell Biol.* **18**, 285–298 (2020).
8. Kholodenko, B. N., Hancock, J. F. & Kolch, W. Signalling ballet in space and time. *Nat. Rev. Mol. Cell Biol.* **11**, 414–426 (2010).
9. Zhou, Y., Prakash, P., Gorfe, A. A. & Hancock, J. F. Ras and the plasma membrane: a complicated relationship. *Cold Spring Harb. Perspect. Med.* **8**, a031831 (2018).
10. Blaževitš, O. et al. Galectin-1 dimers can scaffold Raf-effectors to increase H-ras nanoclustering. *Sci. Rep.* **6**, 24165 (2016).
11. Omerovic, J. & Prior, I. A. Compartmentalized signalling: ras proteins and signalling nanoclusters. *FEBS J.* **276**, 1817–1825 (2009).
12. Banani, S. F., Lee, H. O., Hyman, A. A. & Rosen, M. K. Biomolecular condensates: organizers of cellular biochemistry. *Nat. Rev. Mol. Cell Biol.* **18**, 285–298 (2017).
13. Su, X. et al. Phase separation of signaling molecules promotes T cell receptor signal transduction. *Science* **352**, 595–599 (2016).
14. Hunter, T. Signaling - 2000 and beyond. *Cell* **100**, 113–127 (2000) .
15. Tian, T. et al. Plasma membrane nanoswitches generate high-fidelity Ras signal transduction. *Nat. Cell Biol.* **9**, 905–914 (2007).
16. Ivakhno, S. & Armstrong, J. D. Non-linear dimensionality reduction of signaling networks. *BMC Syst. Biol.* **1**, 1–17 (2007).
17. Lin, Y. H. et al. The intrinsically disordered N-terminal domain of galectin-3 dynamically mediates multisite self-association of the protein through fuzzy interactions. *J. Biol. Chem.* **292**, 17845–17856 (2017).
18. Jin, T. et al. PAQR10 and PAQR11 mediate Ras signaling in the Golgi apparatus. *Cell Res.* **22**, 661–676 (2012).
19. Morrow, I. C. et al. Flotillin-1/reggie-2 traffics to surface raft domains via a novel Golgi-independent pathway. Identification of a novel membrane targeting domain and a role for palmitoylation. *J. Biol. Chem.* **277**, 48834–48841 (2002).
20. Huang, W. Y. C. et al. A molecular assembly phase transition and kinetic proofreading modulate Ras activation by SOS. *Science* **363**, 1098–1103 (2019) .
21. MacDonald, J. I. S., Gryz, E. A., Kubu, C. J., Verdi, J. M. & Meakin, S. O. Direct binding of the signaling adapter protein Grb2 to the activation loop tyrosines on the nerve growth factor receptor tyrosine kinase, TrkA. *J. Biol. Chem.* **275**, 18225–18233 (2000).
22. Biernat, W. Epidermal growth factor receptor in glioblastoma. *Folia Neuropathol.* **43**, 123–132 (2005).
23. Ravichandran, K. S., Lorenz, U., Shoelson, S. E. & Burakoff, S. J. Interaction of Shc with Grb2 regulates association of Grb2 with mSOS. *Mol. Cell. Biol.* **15**, 593–600 (1995).
24. Wöhrle, F. U., Daly, R. J. & Brummer, T. Function, regulation and pathological roles of the Gab/DOS docking proteins. *Cell Commun. Signal.* **7**, 22 (2009).
25. Joazeiro, C. A. P. et al. The tyrosine kinase negative regulator c-Cbl as a RING-type, E2- dependent ubiquitin-protein ligase. *Science* **286**, 309–312 (1999).
26. Sanjay, A., Horne, W. C. & Baron, R. The Cbl family: ubiquitin ligases regulating signaling by tyrosine kinases. *Sci. Signal.* **2001**, pe40–pe40 (2001).
27. Brizzi, M. F. et al. Discrete protein interactions with the Grb2/c-Cbl complex in SCF- and TPO-mediated myeloid cell proliferation. *Oncogene* **13**, 2067–2076 (1996).
28. Elly, C. et al. Tyrosine phosphorylation and complex formation of Cbl-b upon T cell receptor stimulation. *Oncogene* **18**, 1147–1156 (1999).
29. Wong, A., Lamothe, B., Lee, A., Schlessinger, J. & Lax, I. FRS2α attenuates FGF receptor signaling by Grb2-mediated recruitment of the ubiquitin ligase Cbl. *Proc. Natl Acad. Sci. USA* **99**, 6684–6689 (2002).
30. Stephens, R. M. et al. Trk receptors use redundant signal transduction pathways involving SHC and PLC-gamma 1 to mediate NGF responses | TSpace Repository. *Neuron* **3**, 691–705 (1994).
31. Harmer, S. L. & DeFranco, A. L. Shc contains two Grb2 binding sites needed for efficient formation of complexes with SOS in B lymphocytes. *Mol. Cell. Biol.* **17**, 4087–4095 (1997).
32. Gu, H. et al. New role for Shc in activation of the phosphatidylinositol 3-kinase/Akt pathway. *Mol. Cell. Biol.* **20**, 7109–7120 (2000).
33. Kouhara, H. et al. A lipid-anchored Grb2-binding protein that links FGF-receptor activation to the Ras/MAPK signaling pathway. *Cell* **89**, 693–702 (1997).
34. Murohashi, M. et al. An FGF4-FRS2α-Cdx2 axis in trophoblast stem cells induces Bmp4 to regulate proper growth of early mouse embryos. *Stem Cells* **28**, 113–121 (2010).
35. Zhang, S. Q. et al. Shp2 regulates Src family kinase activity and Ras/Erk activation by controlling Csk recruitment. *Mol. Cell* **13**, 341–355 (2004).
36. Hadari, Y. R., Kouhara, H., Lax, I. & Schlessinger, J. Binding of Shp2 tyrosine phosphatase to FRS2 is essential for fibroblast growth factor-induced PC12 cell differentiation. *Mol. Cell. Biol.* **18**, 3966–3973 (1998).
37. Dance, M., Montagner, A., Salles, J. P., Yart, A. & Raynal, P. The molecular functions of Shp2 in the Ras/mitogen-activated protein kinase (ERK1/2) pathway. *Cell. Signal.* **20**, 453–459 (2008).
38. Tajan, M., de Rocca Serra, A., Valet, P., Edouard, T. & Yart, A. SHP2 sails from physiology to pathology. *Eur. J. Med. Genet.* **58**, 509–525 (2015).
39. Chen, P. Y. & Friesel, R. FGFR1 forms an FRS2-dependent complex with mTOR to regulate smooth muscle marker gene expression. *Biochem. Biophys. Res. Commun.* **382**, 424–429 (2009).
40. Gotoh, N. et al. Tyrosine phosphorylation sites on FRS2α responsible for Shp2 recruitment are critical for induction of lens and retina. *Proc. Natl Acad. Sci. USA* **101**, 17144–17149 (2004).
41. Quilliam, L. A., Rebhun, J. F. & Castro, A. F. A growing family of guanine nucleotide exchange factors is responsible for activation of ras-family GTPases. *Prog. Nucleic Acid Res. Mol. Biol.* **71**, 391–444 (2002).
42. Scheffzek, K. & Shivalingaiah, G. Ras-specific gtpase-activating proteins—structures, mechanisms, and interactions. *Cold Spring Harb. Perspect. Med.* **9**, a031500 (2019).
43. Simanshu, D. K., Nissley, D. V. & McCormick, F. RAS proteins and their regulators in human disease. *Cell* **170**, 17–33 (2017).
44. Haghighi, F. et al. bFGF-mediated pluripotency maintenance in human induced pluripotent stem cells is associated with NRAS-MAPK signaling. *Cell Commun. Signal.* **16**, 96 (2018).
45. Stowe, I. B. et al. A shared molecular mechanism underlies the human rasopathies Legius syndrome and Neurofibromatosis-1. *Genes Dev.* **26**, 1421–1426 (2012).
46. Dunzendorfer-Matt, T., Mercado, E. L., Maly, K., McCormick, F. & Scheffzek, K. The neurofibromin recruitment factor Spred1 binds to the GAP related domain without affecting Ras inactivation. *Proc. Natl Acad. Sci. USA* **113**, 7497–7502 (2016).
47. Siljamäki, E. & Abankwa, D. SPRED1 interferes with K-ras but Not H-ras membrane anchorage and signaling. *Mol. Cell. Biol.* **36**, 2612–2625 (2016).
48. Cui, Y. et al. The NF2 tumor suppressor merlin interacts with Ras and RasGAP, which may modulate Ras signaling. *Oncogene* **38**, 6370–6381 (2019).
49. Cui, Y. et al. Merlin cooperates with neurofibromin and Spred1 to suppress the Ras–Erk pathway. *Hum. Mol. Genet.* **29**, 3793–3806 (2020).
50. Pamonsinlapatham, P. et al. P120-Ras GTPase activating protein (RasGAP): a multi-interacting protein in downstream signaling. *Biochimie* **91**, 320–328 (2009).
51. Jaiswal, M. et al. Functional cross-talk between ras and rho pathways: a ras-specific gtpase-activating protein (p120RasGAP) competitively inhibits the rhogap activity of deleted in liver cancer (DLC) tumor suppressor by masking the catalytic arginine finger. *J. Biol. Chem.* **289**, 6839–6849 (2014).
52. An, S. et al. Raf-interactome in tuning the complexity and diversity of Raf function. *FEBS J.* **282**, 32–53 (2015).
53. Belanis, L., Plowman, S. J., Rotblat, B., Hancock, J. F. & Kloog, Y. Galectin-1 is a novel structural component and a major regulator of H-Ras nanoclusters. *Mol. Biol. Cell* **19**, 1404–1414 (2008).
54. Shalom-Feuerstein, R. et al. K-Ras nanoclustering is subverted by overexpression of the scaffold protein galectin-3. *Cancer Res.* **68**, 6608–6616 (2008).
55. Inder, K. L. et al. Nucleophosmin and nucleolin regulate K-ras plasma membrane interactions and MAPK signal transduction. *J. Biol. Chem.* **284**, 28410–28419 (2009).
56. Young, L. C. et al. SHOC2-MRAS-PP1 complex positively regulates RAF activity and contributes to Noonan syndrome pathogenesis. *Proc. Natl Acad. Sci. USA* **115**, E10576–E10585 (2018).
57. Rodriguez-Viciana, P., Oses-Prieto, J., Burlingame, A., Fried, M. & McCormick, F. A phosphatase holoenzyme comprised of Shoc2/Sur8 and the catalytic subunit of PP1 functions as an M-Ras effector to modulate Raf activity. *Mol. Cell* **22**, 217–230 (2006) .
58. del Río, I. B. et al. SHOC2 complex-driven RAF dimerization selectively contributes to ERK pathway dynamics. *Proc. Natl Acad. Sci. USA* **116**, 13330–13339 (2019).
59. Jang, H., Stevens, P., Gao, T. & Galperin, E. The leucine-rich repeat signaling scaffolds Shoc2 and Erbin: cellular mechanism and role in disease. *FEBS J.* **288**, 721–739 (2020).
60. Dai, P., Xiong, W. C. & Mei, L. Erbin inhibits RAF activation by disrupting the Sur-8-Ras-Raf complex. *J. Biol. Chem.* **281**, 927–933 (2006).
61. Zheng, Z. et al. miR-183-5p inhibits occurrence and progression of acute myeloid leukemia via targeting erbin. *Mol. Ther.* **27**, 542–558 (2019).
62. Yao, S. et al. Erbin interacts with c-Cbl and promotes tumourigenesis and tumour growth in colorectal cancer by preventing c-Cbl-mediated ubiquitination and down-regulation of EGFR. *J. Pathol.* **236**, 65–77 (2015).

63. Wilkes, M. C. et al. Erbin and the NF2 tumor suppressor merlin cooperatively regulate cell-type-specific activation of PAK2 by TGF-β. *Dev. Cell* **16**, 433–444 (2009).
64. Stevens, P. D. et al. Erbin suppresses KSR1-mediated RaS/RAF signaling and tumorigenesis in colorectal cancer. *Cancer Res.* **78**, 4839–4852 (2018).
65. Matallanas, D. et al. Raf family kinases: old dogs have learned new tricks. *Genes Cancer* **2**, 232–60 (2011).
66. Rezaei Adariani, S. et al. Structural snapshots of RAF kinase interactions. *Biochem. Soc. Trans.* **46**, 1393–1406 (2018).
67. Terrell, E. M. & Morrison, D. K. Ras-mediated activation of the Raf family kinases. *Cold Spring Harb. Perspect. Med.* **9**, a033746 (2019).
68. Santos, E. & Crespo, P. The RAS-ERK pathway: a route for couples. *Sci. Signal.* **11**, eaav0917 (2018).
69. Roskoski, R. ERK1/2 MAP kinases: structure, function, and regulation. *Pharmacol. Res.* **66**, 105–143 (2012).
70. Wortzel, I. & Seger, R. The ERK cascade: distinct functions within various subcellular organelles. *Genes Cancer* **2**, 195–209 (2011).
71. Kolch, W. Meaningful relationships: The regulation of the Ras/Raf/MEK/ERK pathway by protein interactions. *Biochem. J.* **351**, 289–305 (2000).
72. Kolch, W. Coordinating ERK/MAPK signalling through scaffolds and inhibitors. *Nat. Rev. Mol. Cell Biol.* **6**, 827–837 (2005).
73. Vaidyanathan, H. et al. ERK MAP kinase is targeted to RSK2 by the phosphoprotein PEA-15. *Proc. Natl Acad. Sci. USA* **104**, 19837–19842 (2007).
74. Formstecher, E. et al. PEA-15 mediates cytoplasmic sequestration of ERK MAP kinase. *Dev. Cell* **1**, 239–250 (2001).
75. Zhang, N. et al. GIT1 is a novel MEK1-ERK1/2 scaffold that localizes to focal adhesions. *Cell Biol. Int.* **34**, 41–47 (2009).
76. Teis, D., Wunderlich, W. & Huber, L. A. Localization of the MP1-MAPK scaffold complex to endosomes is mediated by p14 and required for signal transduction. *Dev. Cell* **3**, 803–814 (2002).
77. Nada, S. et al. The novel lipid raft adaptor p18 controls endosome dynamics by anchoring the MEK-ERK pathway to late endosomes. *EMBO J.* **28**, 477–489 (2009).
78. Kovalenko, D., Yang, X., Nadeau, R. J., Harkins, L. K. & Friesel, R. Sef inhibits fibroblast growth factor signaling by inhibiting FGFR1 tyrosine phosphorylation and subsequent ERK activation. *J. Biol. Chem.* **278**, 14087–14091 (2003).
79. Ren, Y. et al. Tyrosine 330 in hSef is critical for the localization and the inhibitory effect on FGF signaling. *Biochem. Biophys. Res. Commun.* **354**, 741–746 (2007).
80. Yeung, K. et al. Suppression of Raf-1 kinase activity and MAP kinase signalling by RKIP. *Nature* **401**, 173–177 (1999).
81. Keller, E. T., Fu, Z. & Brennan, M. The role of Raf kinase inhibitor protein (RKIP) in health and disease. *Biochem. Pharmacol.* **68**, 1049–1053 (2004).
82. McKay, M. M., Ritt, D. A. & Morrison, D. K. Signaling dynamics of the KSR1 scaffold complex. *Proc. Natl Acad. Sci. USA* **106**, 11022–11027 (2009).
83. McNulty, D. E., Li, Z., White, C. D., Sacks, D. B. & Annan, R. S. MAPK scaffold IQGAP1 binds the EGF receptor and modulates its activation. *J. Biol. Chem.* **286**, 15010–15021 (2011).
84. Bañón-Rodríguez, I. et al. EGFR controls IQGAP basolateral membrane localization and mitotic spindle orientation during epithelial morphogenesis. *EMBO J.* **33**, 129–145 (2014).
85. Hedman, A. C., Smith, J. M. & Sacks, D. B. The biology of IQGAP proteins: beyond the cytoskeleton. *EMBO Rep.* **16**, 427–446 (2015).
86. Vomastek, T. et al. Modular construction of a signaling scaffold: MORG1 interacts with components of the ERK cascade and links ERK signaling to specific agonists. *Proc. Natl Acad. Sci. USA* **101**, 6981–6986 (2004).
87. Turner, C. E. Paxillin and focal adhesion signalling. *Nat. Cell Biol.* **2**, E231–E236 (2000).
88. Sheikh, F. et al. An FHL1-containing complex within the cardiomyocyte sarcomere mediates hypertrophic biomechanical stress responses in mice. *J. Clin. Invest.* **118**, 3870–3880 (2008).
89. Amaddii, M. et al. Flotillin-1/Reggie-2 protein plays dual role in activation of receptor-tyrosine kinase/mitogen-activated protein kinase signaling. *J. Biol. Chem.* **287**, 7265–7278 (2012).
90. Therrien, M., Wong, A. M. & Rubin, G. M. CNK, a RAF-binding multidomain protein required for RAS signaling. *Cell* **95**, 343–353 (1998).
91. Therrien, M., Wong, A. M., Kwan, E. & Rubin, G. M. Functional analysis of CNK in RAS signaling. *Proc. Natl Acad. Sci. USA* **96**, 13259–13263 (1999).
92. Mackinnon, A. C. et al. Paxillin expression and amplification in early lung lesions of high-risk patients, lung adenocarcinoma and metastatic disease. *J. Clin. Pathol.* **64**, 16–24 (2011).
93. Jagadeeswaran, R. et al. Paxillin is a target for somatic mutations in lung cancer: implications for cell growth and invasion. *Cancer Res* **68**, 132–142 (2008).
94. Yoshida, T. et al. Spreds, inhibitors of the Ras/ERK signal transduction, are dysregulated in human hepatocellular carcinoma and linked to the malignant phenotype of tumors. *Oncogene* **25**, 6056–6066 (2006).
95. White, C. D., Brown, M. D. & Sacks, D. B. IQGAPs in cancer: a family of scaffold proteins underlying tumorigenesis. *FEBS Lett.* **583**, 1817–1824 (2009).
96. Nguyen, A. et al. Kinase suppressor of Ras (KSR) is a scaffold which facilitates mitogen-activated protein kinase activation in vivo. *Mol. Cell. Biol.* **22**, 3035–3045 (2002).
97. Kaduwal, S. et al. Sur8/Shoc2 promotes cell motility and metastasis through activation of Ras-PI3K signaling. *Oncotarget* **6**, 33091–33105 (2015).
98. Lee, Y. M. et al. Sur8 mediates tumorigenesis and metastasis in colorectal cancer. *Exp. Mol. Med.* **48**, e249 (2016).
99. Jones, G. G. et al. SHOC2 phosphatase-dependent RAF dimerization mediates resistance to MEK inhibition in RAS-mutant cancers. *Nat. Commun.* **10**, 2532 (2019).
100. Gu, S. et al. Distinct GAB2 signaling pathways are essential for myeloid and lymphoid transformation and leukemogenesis by BCR-ABL1. *Blood* **127**, 1803–1813 (2016).
101. Shtivelman, E., Lifshitz, B., Gale, R. P. & Canaani, E. Fused transcript of abl and bcr genes in chronic myelogenous leukaemia. *Nature* **315**, 550–554 (1985).
102. Patsoukis, N. et al. Selective effects of PD-1 on Akt and ras pathways regulate molecular components of the cell cycle and inhibit T cell proliferation. *Sci. Signal.* **5**, ra46 (2012).
103. Tajan, M., Paccoud, R., Branka, S., Edouard, T. & Yart, A. The RASopathy family: consequences of germline activation of the RAS/MAPK pathway. *Endocr. Rev.* **39**, 676–700 (2018).
104. Martinelli, S. et al. Molecular diversity and associated phenotypic spectrum of germline CBL mutations. *Hum. Mutat.* **36**, 787–796 (2015).
105. Brems, H. & Legius, E. Legius syndrome, an update. molecular pathology of mutations in SPRED1. *Keio J. Med.* **62**, 107–112 (2013).
106. Yan, W. et al. Structural Insights into the SPRED1-Neurofibromin-KRAS Complex and Disruption of SPRED1-Neurofibromin Interaction by Oncogenic EGFR. *Cell Rep.* **32**, 107909 (2020).
107. Motta, M. et al. Clinical and functional characterization of a novel RASopathy-causing *SHOC2* mutation associated with prenatal-onset hypertrophic cardiomyopathy. *Hum. Mutat.* **40**, 23767 (2019).
108. Cordeddu, V. et al. Mutation of SHOC2 promotes aberrant protein N-myristoylation and causes Noonan-like syndrome with loose anagen hair. *Nat. Genet.* **41**, 1022–1026 (2009).
109. Motta, M. et al. Activating MRAS mutations cause Noonan syndrome associated with hypertrophic cardiomyopathy. *Hum. Mol. Genet.* **29**, 1772–1783 (2019).
110. Guey, S. et al. De novo mutations in CBL causing early-onset paediatric moyamoya angiopathy. *J. Med. Genet.* **54**, 550–557 (2017).
111. Kazeminasab, S. et al. CNKSR1 gene defect can cause syndromic autosomal recessive intellectual disability. *Am. J. Med. Genet. Part B Neuropsychiatr. Genet.* **177**, 691–699 (2018).
112. Liang, Y., Bradford, W. H., Zhang, J. & Sheikh, F. Four and a half LIM domain protein signaling and cardiomyopathy. *Biophys. Rev.* **10**, 1073–1085 (2018).
113. Angelopoulou, E., Paudel, Y. N., Shaikh, M. F. & Piperi, C. Flotillin: a promising biomarker for alzheimer's disease. *J. Pers. Med.* **10**, 20 (2020).
114. Galazis, N., Afxentiou, T., Xenophontos, M., Diamanti-Kandarakis, E. & Atiomo, W. Proteomic biomarkers of type 2 diabetes mellitus risk in women with polycystic ovary syndrome. *Eur. J. Endocrinol.* **168**, R33–R43 (2013).
115. Moore, A. R., Rosenberg, S. C., McCormick, F. & Malek, S. RAS-targeted therapies: is the undruggable drugged? *Nat. Rev. Drug Discov.* **19**, 533–552 (2020).
116. Ostrem, J. M., Peters, U., Sos, M. L., Wells, J. A. & Shokat, K. M. K-Ras(G12C) inhibitors allosterically control GTP affinity and effector interactions. *Nature* **503**, 548–551 (2013).
117. Matallanas, D. & Crespo, P. New druggable targets in the Ras pathway? *Curr. Opin. Mol. Ther.* **12**, 674–683 (2010).
118. Vasan, N., Baselga, J. & Hyman, D. M. A view on drug resistance in cancer. *Nature* **575**, 299–309 (2019).
119. Khan, S. et al. PROteolysis TArgeting Chimeras (PROTACs) as emerging anticancer therapeutics. *Oncogene* **39**, 4909–4924 (2020).
120. Sanclemente, M. et al. c-RAF ablation induces regression of advanced Kras/Trp53 mutant lung adenocarcinomas by a mechanism independent of MAPK signaling. *Cancer Cell* **33**, 217–228.e4 (2018).
121. Zeng, M. et al. Exploring targeted degradation strategy for oncogenic KRASG12C. *Cell Chem. Biol.* **27**, 19–31.e6 (2020).
122. Prelich, G. Gene overexpression: uses, mechanisms, and interpretation. *Genetics* **190**, 841–854 (2012).
123. Zhang, Z., Hu, P., Xiong, J. & Wang, S. Inhibiting GIT1 reduces the growth, invasion and angiogenesis of osteosarcoma. *Cancer Manag. Res.* **10**, 6445–6455 (2018).
124. Indarte, M. et al. An inhibitor of the pleckstrin homology domain of CNK1 selectively blocks the growth of mutant KRAS cells and tumors. *Cancer Res.* **79**, 3100–3111 (2019).

125. Tari, A. M. et al. Liposome-incorporated Grb2 antisense oligodeoxynucleotide increases the survival of mice bearing bcr-abl-positive leukemia xenografts. *Int. J. Oncol.* **31**, 1243–1250 (2007).
126. Jameson, K. L. et al. IQGAP1 scaffold-kinase interaction blockade selectively targets RAS-MAP kinase-driven tumors. *Nat. Med.* **19**, 626–630 (2013).
127. Bardwell, A. J., Lagunes, L., Zebarjedi, R. & Bardwell, L. TheWWdomain of the scaffolding protein IQGAP1 is neither necessary nor sufficient for binding to the MAPKs ERK1 and ERK2. *J. Biol. Chem.* **292**, 8750–8761 (2017).
128. Dhawan, N. S., Scopton, A. P. & Dar, A. C. Small molecule stabilization of the KSR inactive state antagonizes oncogenic Ras signalling. *Nature* **537**, 112–116 (2016).
129. Neilsen, B. K., Frodyma, D. E., Lewis, R. E. & Fisher, K. W. KSR as a therapeutic target for Ras-dependent cancers. *Expert Opin. Ther. Targets* **21**, 499–509 (2017).
130. Xie, J. et al. Allosteric inhibitors of SHP2 with therapeutic potential for cancer treatment. *J. Med. Chem.* **60**, 10205–10219 (2017).
131. Mainardi, S. et al. SHP2 is required for growth of KRAS-mutant non-small-cell lung cancer in vivo letter. *Nat. Med.* **24**, 961–967 (2018).
132. Ruess, D. A. et al. Mutant KRAS-driven cancers depend on PTPN11/SHP2 phosphatase. *Nat. Med.* **24**, 954–960 (2018).
133. Zhao, M. et al. SHP2 inhibition triggers anti-tumor immunity and synergizes with PD-1 blockade. *Acta Pharm. Sin. B* **9**, 304–315 (2019).
134. Acharya, P., Quinlan, A. & Neumeister, V. The ABCs of finding a good antibody: how to find a good antibody, validate it, and publish meaningful data. *F1000Res.* **6**, 851 (2017).

Acknowledgements

We are grateful to our colleagues Ehsan Amin, Ion C. Cirstea, Oliver Krumbach, Niloufar Mosaddeghzadeh, Saeideh Nakhaei-Rad and K. Nouri, for stimulating discussion. This study was supported by the Research Committee of the Medical Faculty of the Heinrich Heine University Düsseldorf (grant number: 2020-70/9772617), the German Research Foundation (Deutsche Forschungsgemeinschaft or DFG; grant number: AH 92/8-1), the German Research Foundation (Deutsche Forschungsgemeinschaft or DFG) through the International Research Training Group 'Intra- and interorgan communication of the cardiovascular system' (grant number: IRTG 1902-p6), the European Network on Noonan Syndrome and Related Disorders (NSEuroNet; grant number: 01GM1621B); the German Federal Ministry of Education and Research (BMBF)—German Network of RASopathy Research (GeNeRARe; gant numbers: 01GM1902C).

Author contributions

S.P., N.S.K.J., F.B. and C.W. systematically searched and read the literature using the PubMed database; C.W. generated Fig. 1, and S.P. generated Figures 2 and 3. All authors, including M.R.A. designed, wrote and approved the final version of the manuscript.

Competing interests

The authors declare no competing interests.

Additional information

Supplementary information The online version contains supplementary material available at https://doi.org/10.1038/s42003-021-02149-3.

Correspondence and requests for materials should be addressed to M.R.A.

Reprints and permission information is available at http://www.nature.com/reprints

Publisher's note Springer Nature remains neutral with regard to jurisdictional claims in published maps and institutional affiliations.

4. Spotlight on Accessory Proteins: RTK-RAS-MAPK Modulators as New Therapeutic Targets

Commentary

Silke Pudewell and Mohammad Reza Ahmadian

doi: 10.3390/biom11060895

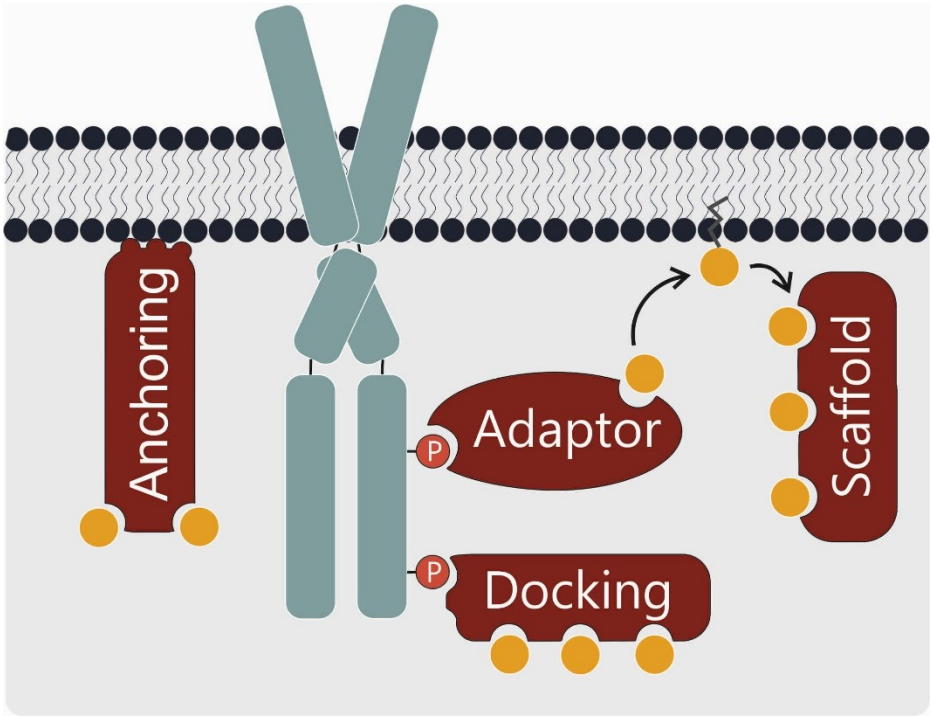

Journal: Biomolecules, Volume 11, Article number: 895 (2021)

Published: 16 June 2021

Impact factor: 6.064

Own contribution: 90%

Concept and preparation of the manuscript, figure illustration, reference management, discussion and conclusions

biomolecules

MDPI

Commentary

Spotlight on Accessory Proteins: RTK-RAS-MAPK Modulators as New Therapeutic Targets

Silke Pudewell and Mohammad Reza Ahmadian *

Institute of Biochemistry and Molecular Biology II, Medical Faculty, Heinrich-Heine University, 40225 Düsseldorf, Germany; sipud101@uni-duesseldorf.de
* Correspondence: reza.ahmadian@hhu.de

Abstract: The RTK-RAS-MAPK axis is one of the most extensively studied signaling cascades and is related to the development of both cancers and RASopathies. In the last 30 years, many ideas and approaches have emerged for directly targeting constituent members of this cascade, predominantly in the context of cancer treatment. These approaches are still insufficient due to undesirable drug toxicity, resistance, and low efficacy. Significant advances have been made in understanding the spatiotemporal features of the constituent members of the RTK-RAS-MAPK axis, which are linked and modulated by many accessory proteins. Given that the majority of such modulators are now emerging as attractive therapeutic targets, a very small number of accessory inhibitors have yet to be discovered.

Keywords: adaptor proteins; anchoring proteins; docking proteins; KRAS; scaffold proteins; RAF kinase; RTK; MEK; ERK

Citation: Pudewell, S.; Ahmadian, M.R. Spotlight on Accessory Proteins: RTK-RAS-MAPK Modulators as New Therapeutic Targets. *Biomolecules* **2021**, *11*, 895. https://doi.org/10.3390/biom11060895

Academic Editor: Daniel Abankwa

Received: 10 May 2021
Accepted: 15 June 2021
Published: 16 June 2021

External signals are sensed, integrated, and amplified by conserved signaling cassettes. The activation of the RTK-RAS-MAPK signaling cascade is regulated by several different extracellular signals and intracellular proteins. Growth factors activate receptor tyrosine kinases (RTKs) at the plasma membrane, which in turn activate RAS via the GDP/GTP exchange reaction. These reactions are catalyzed by guanosine exchange factors (GEFs), such as SOS1 (son of sevenless 1). GTP-bound RAS initiates RAF dimerization and induces the phosphorylation cascade towards MEK and ERK [1]. Aberrant regulation or hyperactivation of the pathway leads to cancer and a group of developmental disorders with a mild gain-of-function of the RAS-MAPK pathway, which are collectively called RASopathies [2,3].

Targeting the constituent components of the RTK-RAS-MAPK signaling cascade often leads to high toxicity and activation of backup mechanisms, lowering the treatment efficacy and increasing the burden of the therapy. In this context, we have to consider that RASopathies are caused by germline mutations, therefore, most patients are children.

Here, we highlight a group of proteins named "accessory proteins", which are emerging as new potential therapeutic targets for the treatment of RAS-MAPK-related diseases. These proteins orchestrate the assembly and spatiotemporal localization of the constituent members of the cascade, without being part of the signaling pathway themselves [4]. Accessory proteins can be categorized into four distinct subgroups (see Figure 1): (1) anchoring proteins that bind to the membrane and other effectors (mostly kinases); (2) docking proteins that bind to receptors (e.g., RTKs and GPCRs) and more than one effector; (3) adaptor proteins that simply link two signaling components (e.g., receptor and GEF); and (4) scaffold proteins that bind two or more partners and provide a signaling platform.

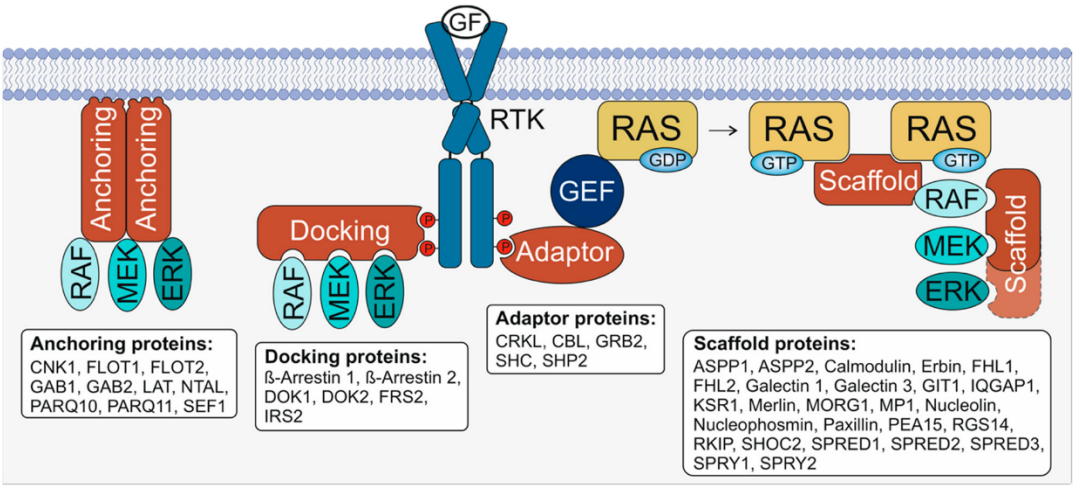

Figure 1. Accessory proteins can be divided into at least four subgroups: anchoring, docking, adaptor, and scaffold proteins. All groups include several different binders of the RTK-RAS-MAPK signaling pathway, such as RAF, MEK, and/or ERK, and often share common domains. Anchoring proteins include membrane-associated domains, such as pleckstrin homology (PH) and transmembrane (TM) domains or a posttranslational modification, (e.g., myristoylation in FLOT2) to determine a special subcellular localization and increase the dwell time of the proteins at the membrane. Docking proteins connect receptors with downstream effectors and feature receptor binding domains, such as PTBs (phosphotyrosine binding domains). FRS2, for example, interacts with the FGFR (fibroblast growth factor receptor) and links activated RTKs (receptor tyrosine kinases) with adaptor proteins such as GRB2 and SHC, and with other effectors, such as SOS1. Adaptor proteins can simply connect two proteins and often exhibit SH (SRC homology) 2 and SH3 domains. GRB2 is a well-known adaptor protein of RTKs and SOS1 but can also, as mentioned before, bind to other accessory proteins and RTKs and fine-tune the signaling machinery and the cross-talk of different pathways. Scaffold proteins can simultaneously bind several signaling components. They can contribute to clustering events by oligomerization via special domains or intrinsically disordered regions (such as galectin 1 and 3), recruit proteins to the site of action (such as SPRED1), or determine RAS signaling at a specific subcellular localization (such as MP1, which binds MEK1 and ERK1 on late endosomes). Scaffold proteins are also able to bind other accessory proteins and allow tight control of the RAS-MAPK pathway.

As modulators of the RTK-RAS-MAPK axis, accessory proteins are multidomain proteins that bind several interaction partners and connect them as a functional unit. Accordingly, they contribute to liquid–liquid phase separation (LLPS) events, which are crucial for a directed assembly of the respective signaling machinery [5,6]. Furthermore, they can fine-tune the crosstalk between signaling pathways, increase the dwell time of proteins on the membrane, induce nanoclustering, sequester effectors, and shield them from activation, or determine the cell type specificity and subcellular localization of signaling cassettes [7]. These modulating abilities turn accessory proteins into incredibly flexible and important proteins within a very specific context. In fact, it is easy to understand why the dysregulation of accessory proteins not only leads to cancer development and cancer progression in RAS-mutant tumors but also contributes to RASopathies.

The last 30 years of research have led to significant discoveries and improvements in cancer treatment, but new therapeutic approaches are still needed, especially for cancers with KRAS mutations. Several accessory proteins have been suggested to be promising targets in RAS-mutant cancer treatment, but a very limited number of inhibitors have yet to be discovered. The major advantage of targeting modulators rather than main players is that the hyperactive signaling mechanism is attenuated and reduced to a physiological level, but not abolished, through robust inhibition. For example, the knockout of KSR in mice does not abolish ERK phosphorylation completely, furthermore, it is quite well tolerated while mouse development and is resistant against RAS-driven tumor formation [8]. This

can lead to less toxicity, particularly regarding side effects (including feedback mechanisms) and decrease the burden of the treatment [9]. An example of the advantage of targeting modulators is the case of the scaffold protein SHOC2; depletion of this protein leads to a better response with MEK inhibitor treatment by interfering with the feedback mechanism towards RAF [10]. SHOC2 binds PP1 and MRAS in a holoenzyme complex, which enables RAF dimerization by dephosphorylation and the release of RAF from its autoinhibited state. The knockout of SHOC2 in mice is embryonic lethal but quite well tolerated in adult animals and human cell lines, and the knockout of SHOC2 leads to growth inhibition of RAS-mutant cell lines [10]. In addition to cancer involvement of SHOC2, mutations of this protein were also detected in Mazzanti syndrome (a RASopathy) and in prenatal-onset hypertrophic cardiomyopathy [11,12]. The mutations cause continuous membrane localization or enhanced binding of MRAS and PPP1CB, respectively, and highlight the fine-tuned signaling modulation of the scaffold protein. Another example is the anchoring protein CNK1. It localizes at the membrane via a pleckstrin homology (PH) domain and binds RAF and RAS with different C- and N-terminal domains, facilitating RAF activation and MAPK signaling [13]. The PH-domain inhibitor PHT-7.3 effectively prevents the colocalization of CNK1 with membrane-localized RAS and inhibits cell growth of KRAS-mutant cancer cell lines but not KRAS wild-type cell lines [14].

These two examples highlight the importance of a tightly controlled spatiotemporal organization of signaling components through accessory proteins and are just small insights into the large group of these modulators [4]. More research can pave the way for new therapeutic strategies involving single and cotreatment approaches that directly target the specific scaffold, adaptor, docking, or anchoring function of accessory proteins.

Funding: This study was supported by the Research Committee of the Medical Faculty of the Heinrich Heine University Düsseldorf (Grant number: 2020-70/9772617), the German Research Foundation (Deutsche Forschungsgemeinschaft or DFG; Grant number: AH 92/8-1), the German Research Foundation (Deutsche Forschungsgemeinschaft or DFG) through the International Research Training Group "Intra- and interorgan communication of the cardiovascular system" (Grant number: IRTG 1902-p6), the European Network on Noonan Syndrome and Related Disorders (NSEuroNet; Grant number: 01GM1621B); the German Federal Ministry of Education and Research (BMBF)–German Network of RASopathy Research (GeNeRARe; Grant numbers: 01GM1902C).

Acknowledgments: We are grateful to our colleagues Farhad Bazgir, Neda Sadat Kazemein Jasemi, Niloufar Mosaddeghzadeh, and Christoph Wittich for stimulating discussion.

Conflicts of Interest: The authors declare no competing interests.

References

1. McKay, M.M.; Morrison, D.K. Integrating signals from RTKs to ERK/MAPK. *Oncogene* **2007**, *26*, 3113–3121. [CrossRef] [PubMed]
2. Castel, P.; Rauen, K.A.; McCormick, F. The duality of human oncoproteins: Drivers of cancer and congenital disorders. *Nat. Rev. Cancer* **2020**, *20*, 383–397. [CrossRef] [PubMed]
3. Tartaglia, M.; Gelb, B.D. Disorders of dysregulated signal traffic through the RAS-MAPK pathway: Phenotypic spectrum and molecular mechanisms. *Ann. N. Y. Acad. Sci.* **2010**, *1214*, 99–121. [CrossRef] [PubMed]
4. Pudewell, S.; Wittich, C.; Kazemein Jasemi, N.S.; Bazgir, F.; Ahmadian, M.R. Accessory proteins of the RAS-MAPK pathway: Moving from the side line to the front line. *Commun. Biol.* **2021**, *4*, 696. [CrossRef] [PubMed]
5. Lyon, A.S.; Peeples, W.B.; Rosen, M.K. A framework for understanding the functions of biomolecular condensates across scales. *Nat. Rev. Mol. Cell Biol.* **2020**. [CrossRef]
6. Banani, S.F.; Lee, H.O.; Hyman, A.A.; Rosen, M.K. Biomolecular condensates: Organizers of cellular biochemistry. *Nat. Rev. Mol. Cell Biol.* **2017**, *18*, 285–298. [CrossRef] [PubMed]
7. Kolch, W. Coordinating ERK/MAPK signalling through scaffolds and inhibitors. *Nat. Rev. Mol. Cell Biol.* **2005**, *6*, 827–837. [CrossRef] [PubMed]
8. Nguyen, A.; Burack, W.R.; Stock, J.L.; Kortum, R.; Chaika, O.V.; Afkarian, M.; Muller, W.J.; Murphy, K.M.; Morrison, D.K.; Lewis, R.E.; et al. Kinase Suppressor of Ras (KSR) Is a Scaffold Which Facilitates Mitogen-Activated Protein Kinase Activation In Vivo. *Mol. Cell. Biol.* **2002**, *22*, 3035–3045. [CrossRef] [PubMed]
9. Matallanas, D.; Crespo, P. New druggable targets in the Ras pathway? *Curr. Opin. Mol. Ther.* **2010**, 674–683.

10. Jones, G.G.; Del Río, I.B.; Sari, S.; Sekerim, A.; Young, L.C.; Hartig, N.; Zubiaur, I.A.; El-Bahrawy, M.A.; Hynds, R.E.; Lei, W.; et al. SHOC2 phosphatase-dependent RAF dimerization mediates resistance to MEK inhibition in RAS-mutant cancers. *Nat. Commun.* **2019**, *10*, 1–16. [CrossRef] [PubMed]
11. Motta, M.; Giancotti, A.; Mastromoro, G.; Chandramouli, B.; Pinna, V.; Pantaleoni, F.; Di Giosaffatte, N.; Petrini, S.; Mazza, T.; D'Ambrosio, V.; et al. Clinical and functional characterization of a novel RASopathy-causing *SHOC2* mutation associated with prenatal-onset hypertrophic cardiomyopathy. *Hum. Mutat.* **2019**, *40*, 1046–1056. [CrossRef] [PubMed]
12. Cordeddu, V.; Di Schiavi, E.; Pennacchio, L.A.; Ma'ayan, A.; Sarkozy, A.; Fodale, V.; Cecchetti, S.; Cardinale, A.; Martin, J.; Schackwitz, W.; et al. Mutation of SHOC2 promotes aberrant protein N-myristoylation and causes Noonan-like syndrome with loose anagen hair. *Nat. Genet.* **2009**, *41*, 1022–1026. [CrossRef] [PubMed]
13. Therrien, M.; Wong, A.M.; Kwan, E.; Rubin, G.M. Functional analysis of CNK in RAS signaling. *Proc. Natl. Acad. Sci. USA* **1999**, *96*, 13259–13263. [CrossRef] [PubMed]
14. Indarte, M.; Puentes, R.; Maruggi, M.; Ihle, N.T.; Grandjean, G.; Scott, M.; Ahmed, Z.; Meuillet, E.J.; Zhang, S.; Lemos, R.; et al. An inhibitor of the pleckstrin homology domain of CNK1 selectively blocks the growth of mutant KRAS cells and tumors. *Cancer Res.* **2019**, *79*, 3100–3111. [CrossRef] [PubMed]

5. Physical Interaction between Embryonic Stem Cell-Expressed Ras (ERas) and Arginase-1 in Quiescent Hepatic Stellate Cells

Article

Silke Pudewell*, Jana Lissy*, Hossein Nakhaeizadeh*, Mohamed S. Taha, Mohammad Akbarzadeh, Soheila Rezaei Adariani, Saeideh Nakhaei-Rad, Junjie Li, Claus Kordes, Dieter Häussinger, Roland P. Piekorz, Miriam M. Cortese-Krott and Mohammad Reza Ahmadian

*These authors equally contributed to this study

doi: 10.3390/cells11030508

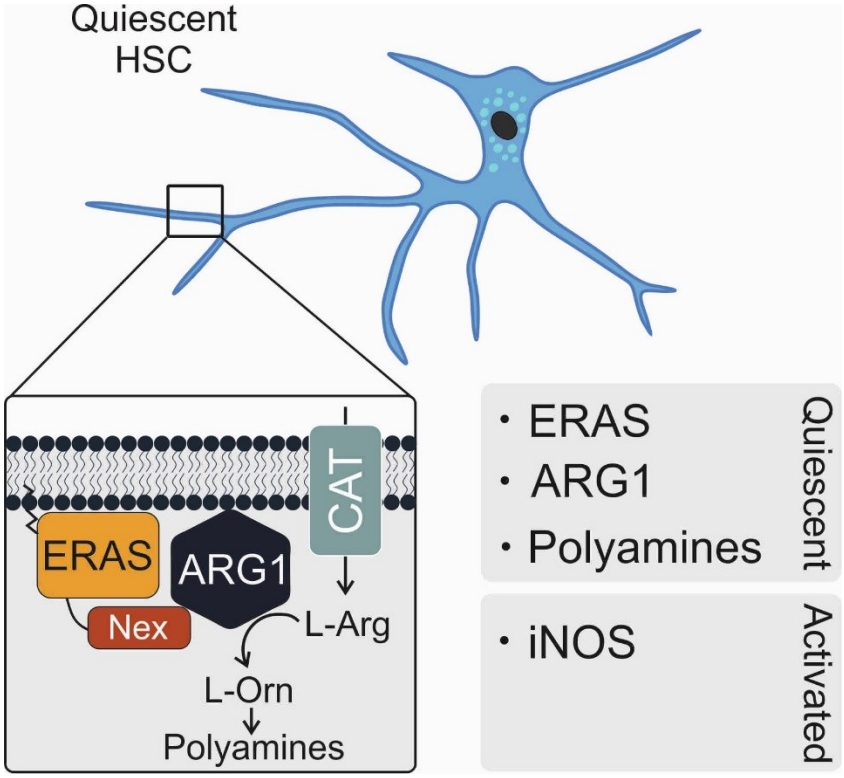

Journal: Cells, Volume 11, Article number: 508 (2022)

Published: 01 February 2022

Impact factor: 7.666

Own contribution: 35%

Hepatic stellate cell cultivation, urea assays, proliferations assay, oil red o staining and microscopy, confocal laser scanning microscopy, liposome sedimentation assay, qRT-PCR, pull down assay, western blotting, preparation of figures, writing the manuscript, reference management, discussion

cells

MDPI

Article

Physical Interaction between Embryonic Stem Cell-Expressed Ras (ERas) and Arginase-1 in Quiescent Hepatic Stellate Cells

Silke Pudewell [1,†], Jana Lissy [1,†], Hossein Nakhaeizadeh [1,†], Mohamed S. Taha [1,2], Mohammad Akbarzadeh [1,3], Soheila Rezaei Adariani [1,3], Saeideh Nakhaei-Rad [1,4], Junjie Li [5], Claus Kordes [6], Dieter Häussinger [6], Roland P. Piekorz [1], Miriam M. Cortese-Krott [5] and Mohammad Reza Ahmadian [1,*]

1 Institute of Biochemistry and Molecular Biology II, Medical Faculty and University Hospital Düsseldorf, Heinrich Heine University Düsseldorf, 40225 Düsseldorf, Germany; silke.pudewell@hhu.de (S.P.); Lissy.jana@gmail.com (J.L.); hossein.nakhaeizadeh@gmail.com (H.N.); ms_taha@yahoo.com (M.S.T.); mohammad.akbarzadeh@mpi-dortmund.mpg.de (M.A.); soheila.rezaei@mpi-dortmund.mpg.de (S.R.A.); s.nakhaeirad@um.ac.ir (S.N.-R.); Roland.Piekorz@hhu.de (R.P.P.)
2 Research on Children with Special Needs Department, Medical Research and Clinical Studies Institute, National Research Centre, 12622 Dokki, Cairo, Egypt
3 Department of Chemical Biology, Max-Planck Institute of Molecular Physiology, Otto-Hahn-Strasse 11, 44227 Dortmund, Germany
4 Stem Cell Biology and Regenerative Medicine Research Group, Institute of Biotechnology, Ferdowsi University of Mashhad, Mashhad 9177948974, Iran
5 Myocardial Infarction Research Laboratory, Department of Cardiology, Pulmonology, and Vascular Medicine, Medical Faculty and University Hospital Düsseldorf, Heinrich Heine University Düsseldorf, 40225 Düsseldorf, Germany; Junjie.Li@hhu.de (J.L.); miriam.cortese-krott@med.uni-duesseldorf.de (M.M.C.-K.)
6 Clinic of Gastroenterology, Hepatology and Infectious Diseases, Medical Faculty of the Heinrich-Heine University, 40225 Düsseldorf, Germany; Claus.Kordes@hhu.de (C.K.); haeussin@hhu.de (D.H.)
* Correspondence: reza.ahmadian@hhu.de; Tel.: +49-211-811-2384
† These authors equally contributed to this study.

Abstract: Embryonic stem cell-expressed Ras (ERas) is an atypical constitutively active member of the Ras family and controls distinct signaling pathways, which are critical, for instance, for the maintenance of quiescent hepatic stellate cells (HSCs). Unlike classical Ras paralogs, ERas has a unique N-terminal extension (Nex) with as yet unknown function. In this study, we employed affinity pull-down and quantitative liquid chromatography-tandem mass spectrometry (LC–MS/MS) analyses and identified 76 novel binding proteins for human and rat ERas Nex peptides, localized in different subcellular compartments and involved in various cellular processes. One of the identified Nex-binding proteins is the nonmitochondrial, cytosolic arginase 1 (ARG1), a key enzyme of the urea cycle and involved in the de novo synthesis of polyamines, such as spermidine and spermine. Here, we show, for the first time, a high-affinity interaction between ERas Nex and purified ARG1 as well as their subcellular colocalization. The inhibition of ARG1 activity strikingly accelerates the activation of HSCs ex vivo, suggesting a central role of ARG1 activity in the maintenance of HSC quiescence.

Keywords: arginase 1; ARG1; embryonic stem cell-expressed Ras; ERas; hepatic stellate cells; quiescence; iNOS; L-arginine; L-ornithine; polyamines; spermidine; spermine; urea cycle

check for updates

Citation: Pudewell, S.; Lissy, J.; Nakhaeizadeh, H.; Taha, M.S.; Akbarzadeh, M.; Rezaei Adariani, S.; Nakhaei-Rad, S.; Li, J.; Kordes, C.; Häussinger, D.; et al. Physical Interaction between Embryonic Stem Cell-Expressed Ras (ERas) and Arginase-1 in Quiescent Hepatic Stellate Cells. *Cells* **2022**, *11*, 508. https://doi.org/10.3390/cells11030508

Academic Editor: Giovanni Amabile

Received: 6 December 2021
Accepted: 27 January 2022
Published: 1 February 2022

1. Introduction

Embryonic stem cell expressed Ras (ERas) is a unique member of the Ras superfamily that was first identified in undifferentiated mouse embryonic stem cells (ESCs). ERas expression has also been reported in gastric cancer, breast cancer, and neuroblastoma cell lines [1–6] and has been proposed to be critical for growth and tumor-like properties in these cells [1,7]. We have already demonstrated that ERas is expressed in quiescent rat hepatic stellate cells (HSCs), where it controls HSC quiescence in the liver through distinct signaling pathways, including PI3K-AKT and MST-LATS-YAP [8]. HSCs are pericytes

that reside in close contact with sinusoidal endothelial cells in the space of Disse [9]. This unique space in liver sinusoids is bordered by endothelial cells and hepatocytes providing a niche that helps to sustain HSC quiescence [10]. Once activated, HSCs show typical characteristics and functions of mesenchymal stem cells and have therefore been classified as such [11]. A mechanism that has since been described for pericytes of other organ systems as well [12]. An intact stem cell niche is crucial for the maintenance of stemness, differentiation and developmental fate decisions of stem cells [10,13]. In a normal, healthy liver, HSCs represent 5–8% of the total liver cells and store about 85% of the body's vitamin A as retinyl palmitate in membrane-coated vesicles [9]. The expression of neural and mesodermal markers, i.e., glial fibrillary protein (GFAP) and desmin, are known to be displayed in a quiescent phenotype. Following liver injury, quiescent HSCs (qHSCs) activate and develop into proliferative and contractile myofibroblast-like cells (aHSCs), revealing profibrogenic transcriptional properties and accounting for extracellular matrix accumulation [14,15]. Activated HSCs show downregulation of GFAP and ERas, upregulation of α-smooth muscle actin (α-SMA) and collagen type I, as well as loss of lipid droplets [8,10].

Arginase (EC 3.5.3.1.) is a manganese-containing enzyme that catalyzes the hydrolysis of L-arginine to L-ornithine and urea. It is a key enzyme of the hepatic urea cycle but is also expressed in extrahepatic tissues lacking a complete urea cycle. There are two paralogs that differ in expression, regulation, and localization [16]. The nonmitochondrial, cytosolic enzyme, arginase 1 (ARG1), is the predominant paralog in the liver and red blood cells [17], whereas the mitochondrial arginase 2 is mainly expressed in extrahepatic tissues [16,18–20]. L-arginine is not only a substrate for arginase, but can alternatively be converted to nitric oxide (NO) and L-citrulline by nitric oxide synthases (NOS). Thus, one biological function of arginase in extra-hepatic organs lies in the regulation of NO synthesis, by competing with NOS for the common substrate L-arginine [21] and also participates in numerous inflammatory diseases by the downregulation of NOS activity, the induction of fibrosis and tissue regeneration [22]. Interestingly, the much higher K_m of the NO synthases (2–20 μM) [23] and the quite low V_{max} (1 μmol/min/mg) [23] in contrast to the low K_m (2–20 mM) [24] and high V_{max} (1400 μmol/min/mg) [25] of arginase together with a high extracellular and low intracellular L-arginine concentration, respectively, describes the arginine paradox, which might be solved by the consumption of different pools of L-arginine by these two competing enzymes.

The aim of this study was to identify the ERas interaction partners that play a role in the homeostasis of HSC quiescence. Using a proteomic approach, we identified numerous novel potential ERas Nex interactors, including ARG1, that are involved in diverse cellular processes. We characterized ERas-ARG1 interaction on protein and cellular levels. Furthermore, we demonstrate the L-arginine metabolism as a central mediator of HSC quiescence and propose that the ARG1-polyamine axis plays a role in hepatic stellate cell homeostasis.

2. Materials and Methods

2.1. Reagents

Dulbecco's modified Eagle medium (DMEM), fetal bovine serum (FBS) and penicillin/streptomycin were obtained from Gibco® Life Technologies. Primary and secondary antibodies for immunoblotting and immunocytochemistry are listed in the Supplementary Table S2. The nucleotides mant-GppNHp and Gpp(CH_2)p were obtained from Jena Bioscience GmbH. CellTiter-Blue® was purchased from Promega (Mannheim, Germany).

2.2. Constructs and Proteins

ARG1 (P05089; aa 1–322), human ERas FL (Q7Z444; aa 1–233), ΔC (aa1-201), Nex (aa 1–38), rat ERas FL (D3ZTE4; aa 1-227), Nex (aa 1–38), and ΔC (aa 1–201) were cloned into pMal-c5X-His or pGEX-4T1-N-TEV. Expression was carried out in *Escherichia coli*.

Proteins and peptides were prepared using glutathione and Ni-NTA-based affinity and size exclusion chromatography as described previously [26].

2.3. Cell Culture

HSC isolation was done as described previously [8]. HSCs were seeded and cultured for 4 or 8 days in DMEM supplemented with 10% FBS and 1% penicillin/streptomycin. HEK293 were cultured in DMEM supplemented with 10% FBS and 1% penicillin/streptomycin. The cells were cultured in an exponential growth phase at 37 °C, 5% CO_2, and 95% humidity. Transfection was performed by TurboFect™ Transfection Reagent (Thermo Fisher Scientific, Waltham, MA, USA) following the manufactures' protocol.

2.4. Affinity Pull-Down Assay

GST-fusion proteins were immobilized on GSH agarose beads and subsequently mixed with purified proteins or total cell lysates and incubated for 1 h, at 4 °C to pull down associating proteins. The beads were washed four times, boiled in SDS (sodium dodecyl sulfate) loading buffer at 95 °C for 5 min. Samples were separated using SDS polyacrylamide gels. The gels were either immunoblotted and stained with specific antibodies as described previously [8] or directly stained with Coomassie brilliant blue (CBB).

2.5. Immunoprecipitation

Immunoprecipitation was performed as described previously [8]. In brief, freshly isolated HSC cells or HEK293 cells were lysed in immunoprecipitation buffer (20 mM Tris-HCl, pH 7.4, 150 mM NaCl, 5 mM $MgCl_2$, 0.5% Nonidet P-40, 10 mM β-glycerolphosphate, 0.5 mM Na_3VO_4, 10% glycerol, EDTA-free protease inhibitor). Total cell lysates of HSCs were incubated with ERas antibody or IgG control respectively for 1 h, at 4 °C, followed by 1 h incubation at 4 °C with Protein G beads. TCL of HEK293 cells was incubated with GFP-coupled nanobeads (kindly provided by Manuel Franke) for 1 h, at 4 °C as described before [8]. Eluted proteins were finally denatured in SDS loading buffer at 95 °C and analyzed by immunoblotting as described previously [8].

2.6. Quantitative Real Time-Polymerase Chain Reaction

Cells were disrupted by QIAzol lysis reagent (Qiagen, Hilden, Germany) and total RNA was extracted via RNeasy plus kit (Qiagen) according to the manufacturer's protocol. The quality and quantity of isolated RNA samples were analyzed on 1% agarose gels and using a Nanodrop spectrophotometer (Thermo Fisher Scientific), respectively. Possible genomic DNA contaminations were removed using the DNA-free™ DNA Removal Kit (Ambion, Life Technologies, Carlsbad, CA, USA). DNase-treated RNA was transcribed into complementary DNA (cDNA) using the ImProm-II™ reverse transcription system (Promega, Madison, WI, USA). Quantitative real-time reverse transcriptase-polymerase chain reaction (qRT-PCR) was performed using SYBR Green reagent (Life Technologies). Primer sequences are listed in Supplementary Table S3. The $2^{-\Delta Ct}$ method was employed for estimating the relative mRNA expression levels. *Hprt1* was used as a housekeeping gene.

2.7. Arginase Activity Assay

Purified ARG1 from *E. coli* was activated by incubation with 10 mM $MnCl_2$, 50 mM Tris-HCl pH 7.5, at 55 °C for 10 min. ARG1 activity was determined by mixing 100 nM of ARG1 with increasing concentrations of L-arginine (250–2000 µM) at 37 °C. Samples were taken at various time points between 20 s and 5 min and denatured at 95 °C for 5 min. The L-arginine concentration was determined via HPLC (Beckman Coulter System Gold, LC118/LC116) in a reversed-phase Discovery C18 column (250 mm). As a mobile phase, 10% acetonitrile and 20 mM Na_2HPO_4 monohydrate with a final pH of 6 was used. The absorbance was measured at 210 nm with a flow rate of 1 mL/min at room

temperature. Michaelis–Menten kinetics were determined by plotting the reaction velocity (v) as a function of the L-arginine concentration using Grafit 5.0.13.

Higher concentrations of urea were determined by a colorimetric urea assay [27]. Cell lysates were mixed with increasing concentrations of L-arginine (1–50 mM) at incubated at 37 °C. Samples were taken at various time points and the reaction was stopped by adding 400 µL acidic mixture consisting of H_2SO_4, H_3PO_4 and H_2O (1:3:7). In cell culture supernatants, urea production was quantified by mixing 50 µL of the medium with 400 µL acidic mixture. Urea concentration was quantified by the addition of 25 µL 9% isonitrosopropiophenone (dissolved in 100% EtOH) and incubation for 45 min at 100 °C. The reaction was kept in the dark for 10 min at room temperature before measuring the absorbance at 540 nm in a TECAN Infinite M200 PRO reader. A urea standard was used to calculate exact concentrations.

2.8. Synthetic Liposomes and Liposome Sedimentation

Synthetic liposomes were generated by mixing and sonicating 500 µg total lipids: 20% (*w*/*w*) phosphatidylethanolamine (PE), 45% (*w*/*w*) Phosphatidylcholine (PC), 20% (*w*/*w*) Phosphatidylserine (PS), 10% (*w*/*w*) cholesterol, and 5% (*w*/*w*) phosphatidylinositol 4, 5-bisphosphate (PIP_2). Lipids were dried out using light nitrogen stream and obtained lipid film was hydrated in 300 µL buffer containing 20 mM HEPES (pH 7,5), 50 mM NaCl, 5 mM $MgCl_2$, and 3 mM DTT. The lipid suspension was sonicated once at low settings and extruded 21 times through a 0.2 µm pore size membrane filter.

For the liposome sedimentation assay, liposomes were mixed with an excess amount of purified ARG1 protein and incubated 30 min at 4 °C on a rotor. The mixture was centrifuged for 30 min at 20.000× *g* and 4 °C. The supernatant (which contains unbound proteins) was mixed with 5× SDS (20%) loading buffer and the liposome pellet (containing liposome bound proteins) were resuspended in an equal amount of 1× SDS loading buffer. The samples were analyzed via SDS gel electrophoresis and Coomassie staining or immunoblotting as described before [8].

2.9. Mass Spectroscopy and Data Analysis of ERas Nex-Binding Proteins

For mass spectrometric analysis of ERas Nex binding proteins, SDS gel fragments were cut from each lane of the affinity pull-down assay. The gel pieces were reduced, alkylated, and digested by trypsin. The resulting digest mixtures were analyzed by mass spectrometry as described in [28]. Peptides extracted with 0.1% trifluoroacetic acid were subjected to a liquid chromatography system (RSLC, Dionex/Thermo Scientific, Idstein, Germany) equipped with an Acclaim PepMap 100 C18 column (75 µm inner diameter, 50 cm length, 2 mm particle size from Dionex/Thermo Scientific, Idstein, Germany) coupled to an Orbitrap Elite mass spectrometer (Thermo Scientific, Bremen, Germany) essentially as described in [28]. For protein and peptide identification and quantification, raw files were further processed using the MaxQuant software suite version 1.3.0.5 (Max Planck Institute of Biochemistry, Planegg, Germany). Database searches were carried out against the UniProt database (release 06.2013) using standard parameters. Label-free quantification was done using the "match between runs" option with a time slot of 2 min. Peptides and proteins were accepted at a false discovery rate of 1% and proteins with quantitative information available for at least three analyzed samples were subjected to subsequent statistical analysis. Protein quantification was performed using the SAM algorithm [29] implemented in Perseus version 1.2.7.4 (Max Planck Institute of Biochemistry, Planegg, Germany) on log-transformed data (false discovery rate threshold: 0.01). Missing values were replaced by imputation (width: 0.3; downshift: 1.8).

2.10. Gene Ontology Analysis

Gene Ontology (GO) terms for the biological processes, molecular function, and cellular location of ERas Nex interacting proteins, including isoforms, paralogs, or related proteins were achieved using the PANTHER database [30].

2.11. Surface Plasmon Resonance (SPR)

For kinetic analysis of the interaction between ERas and ARG1, a Biacore X100 system was used together with CM5 sensor chips (GE Healthcare Life Sciences, Uppsala, Sweden). An anti-GST antibody (Supplementary Table S2) was immobilized to the dextran surface of a CM5 sensor chip using the GST capture kit (GE Healthcare Life Sciences). Afterwards, 10 µM of purified GST-*hs*Nex was introduced to the immobilized GST-antibody at 25 °C (30 µL/min). Increasing concentrations of MBP-ARG1 (contact time: 90 sec, 30 µL/min) were injected in a multicycle mode and dissociation was measured at the end of the injection of the final concentration for a period of 300 sec. The dissociation constants (K_d) were calculated using BIAevaluation (version 2.0.1) by the Langmuir 1:1 model and the GraFit 5 version. All SPR measurements were carried out at 25 °C in a buffer, containing 10 mM HEPES, pH 7.4, 150 mM NaCl, and 0.05 % (*v*/*v*) surfactant P20 (GE Healthcare Life Sciences, Uppsala, Sweden).

2.12. Detergent-Free Subcellular Fractionation of HSCs

Subcellular fractionation of HSCs (d0) was conducted by using a differential centrifugation method combined with detergent-free buffers and sucrose cushions as described previously [31].

2.13. Confocal Imaging

Confocal images were obtained using a LSM 880-microscope (Zeiss, Jena, Germany). Immunostaining was performed as described previously [32]. Primary antibodies and secondary antibodies are listed in the Supplementary Table S2.

2.14. Cell Viability Assay

To determine cell viability which directly correlates to cell number, 5000 cells/well were seeded in 96-well plates in 100 µL medium. On the desired day, 20 µL of CellTiter-Blue solution was added to each well and the fluorescence was determined at 590 nm using a TECAN Infinite M200 PRO reader. The cells were incubated under normal growth conditions and the fluorescence was measured again after one and two hours. The fluorescence was plotted against the time and the slope determined the relative number of viable cells.

2.15. Oil Red O Staining

For the ORO staining, HSCs were cultured in 24-well plates and washed 3 times with phosphate-buffered saline (PBS). Afterwards, the cells were fixed with 4% PFA for 10 min at room temperature, followed by a 20 min incubation with the 1x ORO working solution as described [33,34]. The cells were rinsed with 60% isopropanol and imaged with a bright field microscope.

2.16. Statistical Analysis

The data were evaluated using GraphPad Prism 6 software. For variance analysis, an ordinary one-way or two-way analysis of variance test was performed using Turkey's or Dunnett's multiple comparison test or paired or unpaired *t*-test as indicated. Results were considered significant with $p < 0.05$ (* $p < 0.05$, ** $p < 0.01$, *** $p < 0.001$, **** $p < 0.0001$).

3. Results

3.1. Novel Binding Partners of ERas Are Involved in Multiple Cellular Processes

In spite of sharing a conserved G domain, some members of the Ras family have additional features outside the G domain that may act as functional regulatory modules [35]. The role of the additional 38-amino acid N-terminal extension of ERas is unclear and shows a sequence identity of 42% between human and rat protein (Figure 1A). We have proposed in a mutational study that it may modulate ERas localization through interaction with potential adaptor or scaffold proteins [32]. To find out more about ERas Nex interaction partners, we investigated protein interaction properties of *hs*Nex and *rn*Nex by performing

affinity pull-down (n = 3) and MALDI-TOF mass spectrometry using total cell lysates and purified GST-*hs*Nex, GST-*rn*Nex and GST, respectively. Pulldown samples were run on SDS-PAGE and stained with Coomassie brilliant blue. Gel pieces were further processed and analyzed by mass spectrometry as described in Materials and Methods (Figure 1B, white boxes). The bands corresponding to GST-*hs*Nex, GST-*rn*Nex and GST were excluded from the analysis (Figure 1B, black boxes). All proteins interacting with GST-*hs*Nex, GST-*rn*Nex were detected and validated individually with a high degree of confidence based on the peptide sequences using specific databases and programs as described in Materials and Methods. The criteria for considering proteins being significant interactors of ERas Nex included their presence in all three independent pull-down experiments, their absence in the GST pull-down controls, removal of contaminant proteins arising from sample handling (such as keratin and bovine serum albumin). Collectively, we shortlisted a set of 76 ERas Nex potential interacting proteins, 35 of them were associated with *rn*Nex, 21 with *hs*Nex, and 20 proteins were found to bind to both Nex peptides (Figure 1C; Supplementary Table S1).

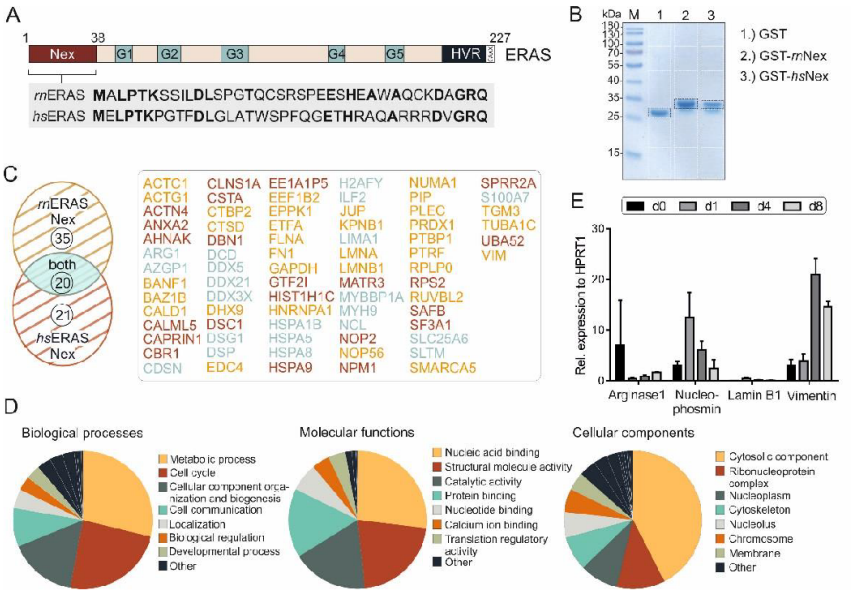

Figure 1. ERas N-terminal extension and its novel binding partners. (**A**) ERas contains, in addition to five motifs (G1-5) in its G domain, an N-terminal extension (Nex) and a C-terminal hypervariable region (HVR) ending with a consensus sequence known as CAAX. An alignment of ERas N-terminus of *Rattus norvegicus* (*rn*) and *Homo sapiens* (*hs*) shows a sequence identity (bold amino acids) of 42%. (**B**) Purified GST, GST-*rn*Nex or GST-*hs*Nex proteins were used for affinity pull-down experiments with GSH beads in total cell lysates, to identify ERas Nex binding partners. Bound proteins were resolved on a 10% SDS gel and stained with Coomassie brilliant blue. White boxes indicate different gel fragments excised for mass spectrometric (MS) analysis. Black boxes indicate GST, GST-*rn*Nex or GST-*hs*Nex and were excluded from MS analysis (n = 3). (**C**). Evaluation of MS analysis revealed in total 76 ERas Nex binding partners from which 35 preferentially interact with *rn*Nex (yellow), 21 with *hs*Nex (red) and 20 with both (blue) (for more detail see Table S1). (**D**) Gene Ontology analysis of identified ERas Nex interacting proteins categorized according to biological processes, molecular functions, and subcellular localizations. Biological processes (left panel) were predominantly classified into metabolic pathways (29%), cell cycle control (24%), and cellular components and organization (16%). Molecular functions (middle panel) included: nucleic acid (RNA/DNA) binding proteins (27%), catalytic activity (18%) and protein binding (16%). Cellular components comprised predominated the cytosolic fraction (43%). (**E**) mRNA expression data of ERas Nex binding partners: arginase 1, nucleophosmin, lamin B1, and vimentin on day 0, 1, 4, and 8 of HSC cultivation (n = 3). The error bars indicate S.D.

Identified proteins that interact with ERas Nex were classified into three ontologies: molecular function, biological process, and cellular component (Figure 1D). The vast majority of these proteins are involved in nucleic acid binding, molecular and catalytic activities and protein interactions. They are involved in the control of metabolic processes, cell cycle, and cell communication by localizing in different subcellular compartments, particularly in the cytosol.

Four proteins were selected and analyzed by qRT-PCR (Figure 1E). ARG1 expression was highest in quiescent day 0 HSCs (freshly isolated from rat liver), whereas nucleophosmin and lamin B1 had the highest expression at day 1 and vimentin at day 4 after isolation and initiation of their culture-dependent activation. As we are interested in proteins, that might be important for sustaining the quiescence in HSCs, proteins with a high expression in day 0 cells were of particular interest.

3.2. ERas-ARG1 Interaction in Quiescent HSCs

In proteomic analysis, we identified ARG1 as a potential binding partner of *hs*Nex and *rn*Nex (Supplementary Table S1), which is also upregulated in quiescent HSCs. Isolated rat HSCs activate during culture on plastic surfaces. Here, they switch from a quiescent state (qHSC) to an activated state (aHSC) (Figure 2A) as they do in response to, for example, chronic liver injury. Day 0 HSCs are considered as quiescent cells, expressing the marker proteins GFAP and desmin, whereas day 8 HSCs are activated and display the activation marker α-SMA. ERas was found to be exclusively expressed at day 0 and also ARG1 exhibited the highest expression at that day 0. The ARG1 expression decreases at day 1 and increases again at day 4 and 8 (Figure 2B). Interestingly, the inducible nitric oxide synthase (iNOS), which uses, like ARG1, L-arginine as substrate, was reciprocally expressed and could only be detected at day 1.

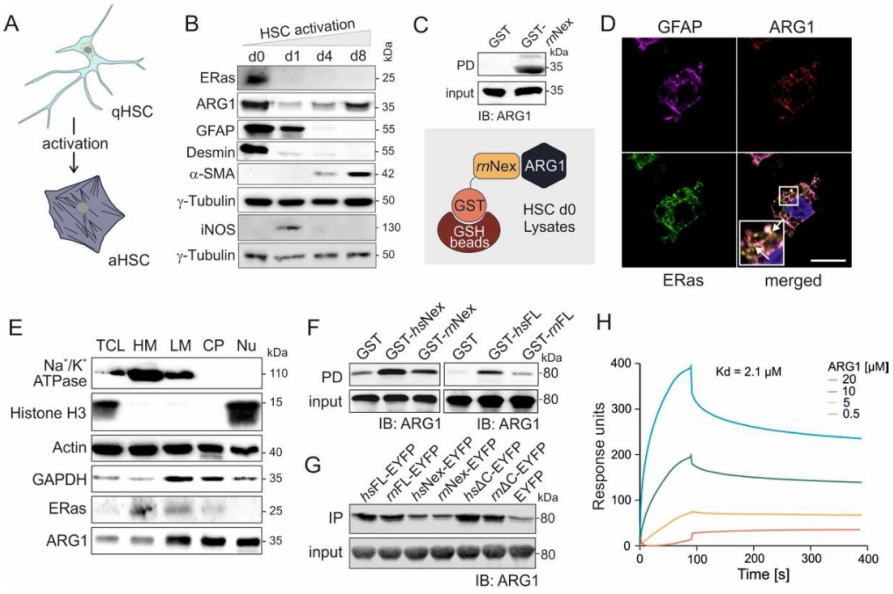

Figure 2. ERas and ARG1 expression, localization, and interaction in hepatic stellate cells. (**A**) Graphic illustration of quiescent (qHSCs) and activated hepatic stellate cells (aHSCs). During culture, the HSCs change in their cell shape and size, and reduce their lipid droplet content. (**B**) Immunoblot analysis of ERas and ARG1 from freshly isolated (d0) and activated HSCs maintained in monoculture for up to 8 days (d1, d4, d8). GFAP was used as a marker for quiescent HSCs (d0), and α-SMA was

used as a marker for activated HSCs (d8). γ-tubulin served as a loading control. (**C**) Pull-down assay of ARG1 and GST-*rn*Nex in freshly isolated HSC (d0) lysates. Input and output were immunoblotted and detected with anti-ARG1 antibody. (**D**) Confocal imaging of GFAP, ARG1 and ERas of freshly isolated HSCs after 6 h of culture at day 0 shows colocalization of ERas and ARG1 (white arrows). Scale bar: 10 µm. Six-fold magnification of the merged image. (**E**) Cell fractionation of HSCs d0 in five distinct fractions including: heavy membrane (HM; plasma membrane and rough endoplasmic reticulum), light membrane (LM; polysomes, Golgi apparatus, smooth endoplasmic reticulum), cytoplasm (CP; cytoplasm and lysosomes), nucleus (Nu) and total cell lysate (TCL). Immunoblot analysis was performed for Na^+/K^+-ATPase, Histone H3, Actin, GAPDH, ERas and ARG1. (**F**) Pull-down assay of purified ARG1 protein with GST-Nex or GST-FL of human and rat ERas. (**G**) Immunoprecipitation (IP) analysis of ARG1 with various ERas constructs overexpressed in HEK 293 cells (*hs*ERas FL, *rn*ERas FL, *hs*ERas Nex, *rn*ERas Nex, *hs*ERas$^{\Delta C}$, *rn*ERas$^{\Delta C}$, empty vector). IP was conducted using GFP-coupled nanobeads. Empty EYFP served as a control. Protein complexes retained on the beads were resolved by Laemmli buffer and processed for immunoblotting using a monoclonal antibody against ARG1. (**H**) Sensorgrams obtained from the binding of 0.5–20 µM ARG1 to immobilized GST-*hs*Nex on the surface of a CM5 sensor chip.

The interaction of ERas and ARG1 was verified by pull-down (Figure 2C) and IP experiments (Supplementary Figure S1), where ARG1 could be pulled down with purified GST-bound ERas *rn*Nex or coprecipitated by fishing with an ERas antibody in freshly isolated HSC d0 cell lysates, respectively. Next, confocal imaging revealed a strong colocalization of ERas and ARG1 in freshly isolated and 6 h cultivated HSCs (Figure 2D, white arrows, additional images in Supplementary Figure S2). The marker GFAP was stained as a quiescent HSC marker. The subcellular localization of ARG1 and ERas was further determined via cell fractionation (Figure 2E). Here, both proteins could be detected in heavy membrane (plasma membrane and rough endoplasmic reticulum), light membrane (polysomes, Golgi apparatus, smooth endoplasmic reticulum) and cytoplasmic fraction (cytoplasm and lysosomes). ARG1 could additionally be found in the nuclear fraction. Furthermore, ARG1 and the Na^+/K^+-ATPase colocalized in cLSM pictures as displayed in the Supplementary Figure S3.

3.3. Physical Interaction of ARG1 with ERas

Besides the investigation of protein expression and intracellular localization, we furthermore analyzed the direct interaction of ARG1 and ERas as well as their complex association in vitro. Association of purified ARG1 with different purified ERas variants, including *hs*Nex, *rn*Nex and the full-length ERas orthologs *hs*FL and *rn*FL, was first analyzed in a GST pull-down assay (Figure 2F). Purified GST was used as a control. Figure 2F shows that ARG1 bound much tighter to human than rat ERas proteins. Next, we analyzed the interaction of ARG1 with six human and rat ERas constructs: *hs*FL, *rn*FL, *hs*Nex, *rn*Nex, *hs*ΔC and *rn*ΔC (C-terminal truncated variants), in immunoprecipitation experiments using ERas overexpression in HEK293 cells. Notably, ERas FL and ΔC interaction with ARG1 appeared much stronger as compared to Nex, which indicates that ARG1 might be engaged via additional binding sites other than the N-terminal extension, which contribute to a higher affinity (Figure 2G). Therefore, a pull-down of purified ARG1 with overexpressed N-terminally truncated ERas (ΔN; aa 39-233) revealed that ERas ΔN is considerably impaired in binding ARG1 but still exhibited a weak binding as compared to ERas WT and EYFP, which was used as positive and negative controls (Supplementary Figure S4A). This result confirms Nex as a critical binding site of ERas for ARG1 but also confirms that other regions of ERas also contact ARG1. The pull-down of ARG1 with purified GST-ERas G-domain from *rn* and *hs* clearly showed that ERas possess with the G-domain of ERas a second binding site for ARG1 (Supplementary Figure S4B).

Subsequent kinetic of the ERas-ARG1 interaction was investigated using surface plasmon resonance. In this approach, we injected different concentrations of ARG1 (0.5, 5,

10, and 20 µM) to immobilized GST-*hs*Nex (10 µM) and measured their kinetic of interaction (Figure 2H). A dissociation constant (K_d) of 2.1 µM was determined for GST-*hs*Nex-ARG1 interaction using 1:1 binding Langmuir algorithm model, supporting the previous cell-based analysis of direct protein binding.

3.4. Inhibition of ARG1-Polyamine Axis Leads to Accelerated HSC Activation

In order to investigate the impact of ARG1 activity on HSC quiescence and activation, we chose three inhibitors of the L-arginine metabolism illustrated in Figure 3A. The NO synthase inhibitor N^5-(1-iminoethyl)-L-ornithine (L-NIO) inhibits the conversion of L-arginine to L-citrulline and NO. N^{ω}-hydroxy-L-arginine (nor-NOHA) inhibits the activity of arginase and DL-α-difluoromethylornithine (DFMO) blocks the ornithine decarboxylase I (ODC1), which is the first and rate-limiting enzyme in the polyamine synthesis that converts L-ornithine to putrescine.

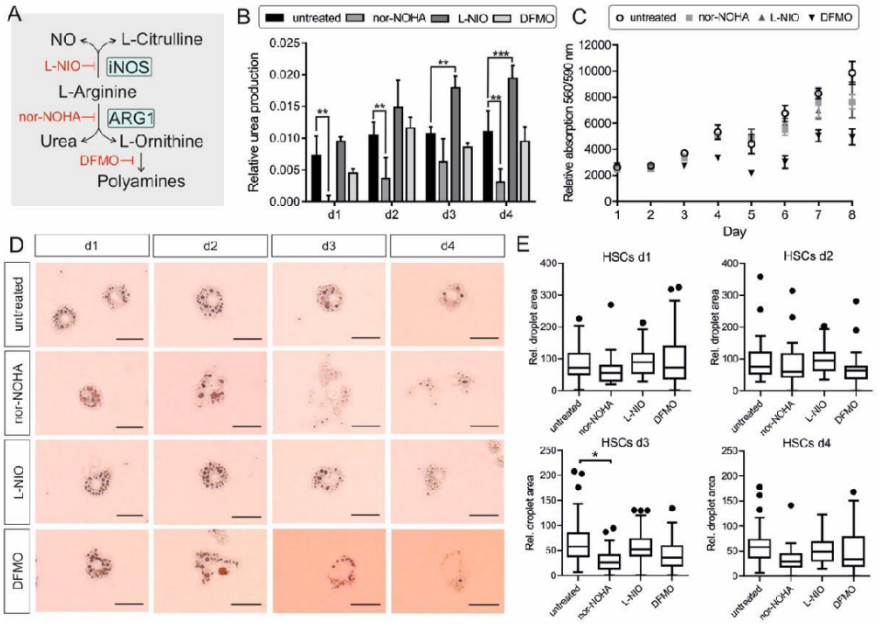

Figure 3. Impact of L-arginine metabolism manipulation on HSC activation. (**A**) Overview of L-arginine metabolism by ARG1 and iNOS and further conversion of L-ornithine to polyamines. Inhibitors of the pathway (iNOS: L-NIO; Arginase: nor-NOHA; ODC1: DFMO) are illustrated in red. (**B**) Urea production of HSCs day 1–4 via colorimetric urea assay in the cell culture supernatants relative to medium control. Significant differences were detected for: untreated—nor-NOHA d1: $p = 0.00315$; d2: $p = 0.00517$; d3: no sig.; d4: $p = 0.00192$/untreated—L-NIO d1: no. sig.; d2: no sig.; d3: $p = 0.00316$; d4: $p = 0.000934$/untreated—DFMO d1-4: no sig. (n = 3) (**C**) Cell viability of HSCs day 0–8 with and without inhibitor treatment via Cell titer blue assay relative to blank medium. The cell viability is correlating proportional with the cell number. (n = 3) (**D**) HSCs at day 1–4 in untreated, nor-NOHA, L-NIO, or DFMO treated conditions and stained with Oil Red O to highlight lipid droplets. The scale bar indicates 0.025 mm. (**E**) Quantitative analysis of ORO-stained droplet number and area (see **D**) of n = 5 cells for each day and condition. Pictures were analyzed by ImageJ and plotted via Prism. The difference between untreated control and nor-NOHA treatment at day 3 was significant ($p = 0.0308$). All statistics were obtained via multiple comparison unpaired *t*-test using Prism 6. The error bars indicate S.D.

HSCs were cultured with 0.5 mM L-NIO or nor-NOHA or 1 mM DFMO final concentrations for 4 days. Cell culture supernatant was taken from each condition every

day without medium change to determine urea production via a colorimetric urea assay (n = 3). The urea measurement showed a strong increase of urea production and release in the supernatant at day 1 of untreated cells. The urea levels on day 2, 3, and 4 were quite steady. The inhibitory effect of nor-NOHA on ARG1 activity and therefore urea production could be confirmed by almost no detectable urea concentration at day 1 and significantly reduced urea production at day 2 and 4. Interestingly, the NO synthase inhibitor L-NIO caused higher urea levels in the cells compared to all other conditions, most likely due to more substrate availability for arginase. DFMO treatment had no significant effect on the urea level compared to the untreated control (Figure 3B). To confirm that the increased or decreased urea concentrations were not based on a shift in total cell number, a cell viability assay was performed from day 0 to 8 (n = 3). The total cell number did not change up to day 3. At day 4 the cell number increased for untreated, nor-NOHA and L-NIO treated cells, but not DFMO-treated cells. Over the period of 8 days, DFMO-treated cells displayed a considerably lower cell proliferation rate compared to the other conditions, most likely caused by the reduced polyamine concentration in the cells. The addition of nor-NOHA did not change the cell viability and the corresponding cell number (Figure 4C).

To detect the activation state of the HSCs under the same conditions used earlier, one 24-well was used each day for Oil Red O (ORO) staining, which stains and highlights the lipid droplets within the cytoplasm that get smaller and reduced in number during HSC activation. The ORO staining of the HSCs displayed many big lipid droplets at day 1 for all conditions. The number and diameter of droplets decreased during activation of the untreated cells, still, the cell shape and the characteristic of the lipid droplets showed that the HSCs were not fully activated at day 4. L-NIO treated cells exhibited smaller and more stellate-shaped cell morphology and contained a comparable high amount of lipid droplets at day 4. Nor-NOHA treated cells showed a bulky cell shape from day 3 onwards and a notable loss of lipid droplets. DFMO treated cells exhibited a significant reduction in droplet diameter and a myofibroblast-like cell shape (Figure 4D). The lipid droplet area was used to quantify the state of HSC activation (Figure 4E). At day 1, the cells of all conditions displayed a similar phenotype. At day 3 the difference between untreated cells and arginase inhibited cells was significant ($p = 0.0308$). Due to the limitations of contrast in light microscopy, other factors like cell shape and total cell size could not be considered. An exemplary picture is shown in Supplementary Figure S5, displaying the variable cell morphology of the HSCs with different treatments. The cotreatment of HSCs with nor-NOHA and L-NIO exhibited the phenotype of nor-NOHA treated cells, rather than L-NIO mono-treatment (Supplementary Figure S6).

The results indicated an accelerated activation under nor-NOHA and DFMO treatment, which was absent when L-NIO was added to the HSCs. The data implied that ARG1 activity and the downstream polyamine synthesis impacted on the maintenance of quiescent HSCs, raising the question about the impact of the ERas interaction with ARG1 on its enzyme activity, in this context.

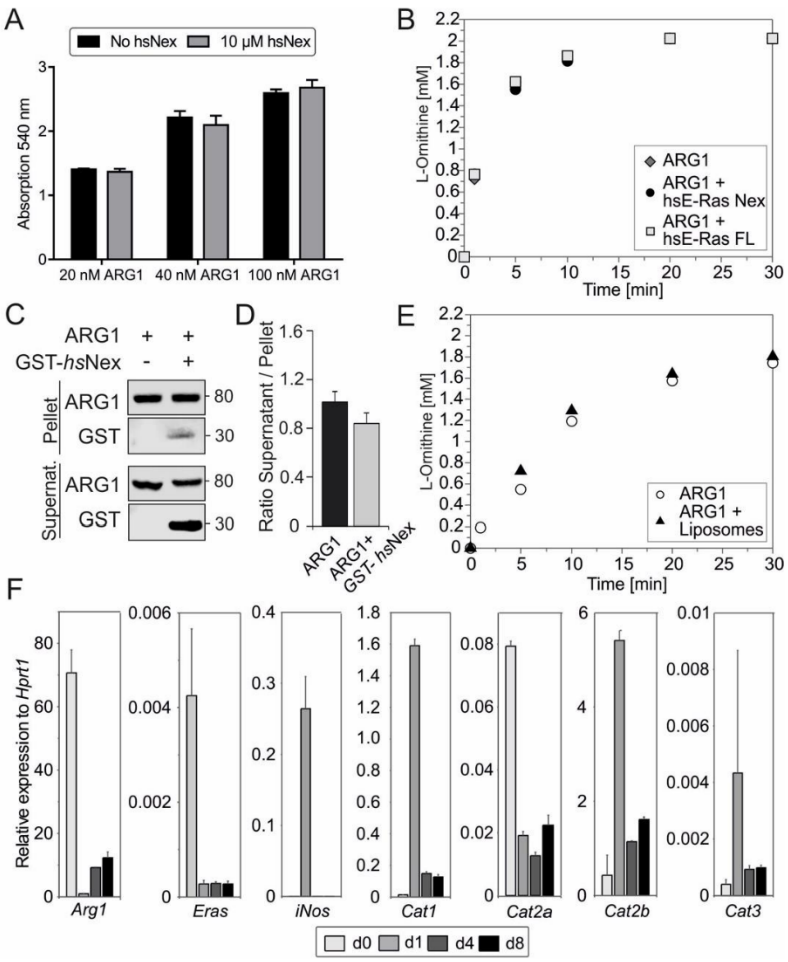

Figure 4. Functional analysis of ERas-ARG1 interaction. (**A**) Arginase activity assay of 20, 40 or 100 nM ARG1, with or without 10 µM *hs*Nex, measured via colorimetric urea assay (n = 3). (**B**) Arginase activity was measured with 2 mM L-arginine, 100 nM ARG1 and 500 nM ERas *hs*Nex or *hs*FL at pH = 9.0 by HPLC. (**C**) Liposome sedimentation assay of 0.2 µM ARG1, immobilized on liposomes together with GST-*hs*Nex and incubated for 30 min at room temperature (RT). After sedimentation with 20,000× *g* for 30 min, immunoblotting was used to show protein binding on liposomes and protein–protein interactions by using monoclonal antibodies against ARG1 and GST. (**D**) Ratio of supernatant to pellet from liposome assay indicating ARG1 binding to liposomes with and without the addition of GST–*hs*Nex. (E) Arginase activity measured with 2 mM L-arginine, 100 nM ARG1 without, or in the presence of liposomes at pH = 7.5 in HPLC. (**F**) qRT-PCR analysis of *Arg1, ERas, iNos, Cat1, Cat2a, Cat2b and Cat3* in HSCs at day 0, 1, 4, and 8. Gene expression was normalized to the expression of the housekeeping gene *Hprt1*. All error bars represent S.D.

3.5. Human ERas Has No Effect on ARG1 Enzymatic Activity

We next aimed to investigate the impact of ERas on ARG1 enzyme activity. Therefore, we measured the urea production with and without 10 µM ERas *hs*Nex at increasing concentrations of purified ARG1 after one hour (Figure 4A), as well as a full time-dependent cycle of L-arginine conversion into L-ornithine and urea with 100 nM ARG1, 2 mM L-arginine and five times excess ERas *hs*Nex or *hs*FL (0.5 µM) in HPLC at pH 9 (Figure 4B). In

both experiments, no change in the velocity of enzymatic ARG1 activity could be detected. Furthermore, we measured fixed ARG1 concentration with increasing concentrations of ERas *hs*FL and *hs*Nex (Supplementary Figure S7) and the Michaelis-Menten constant of the enzymatic reaction of ARG1 (6.5 ± 0.99 mM) and ARG1 + ERas *hs*Nex (7.79 ± 0.33 mM) with concentrations between 0.25 and 10 or 5 mM, respectively (Supplementary Figure S8), and could also not detect any differences. The arginase activity in HSCs was determined by colorimetric urea assay using TCL of HSCs at day 0, 1, 4 and 8 (Supplementary Figure S9). The ARG1 activity in cell lysates was highest in quiescent (d0) HSC lysates, following the protein expression data in Figure 2B.

3.6. ARG1 Binding to Liposomes Had No Effect on Its Enzymatic Activity

In a subsequent liposome sedimentation assay, we were able to show ARG1 binding to liposomes, even after applying high forces of 20,000× *g*. In addition, results from this liposome assay indicated the binding of GST-*hs*Nex to ARG1 as seen in immunoblotting with GST-antibody (Figure 4C). GST was used as a negative control (data not shown). The ratio of supernatant to the pellet of ARG1 binding with and without the presence of ERas *hs*Nex does not display significant changes (Figure 4D). In order to investigate a possible function of membrane binding towards the enzymatic activity of ARG1, a full enzymatic reaction of ARG1 and 2 mM L-arginine was performed in the presence of liposomes at pH 7.5 (Figure 4E). This experiment did not show any major differences as well. Taken together, the interaction of ERas and ARG1, but also the association of ARG1 with the membrane does not contribute to an enhanced enzymatic activity of ARG1.

3.7. Correlation of ERas, Arg1, and Cat2a mRNA Expression in qHSCs

In the next approach, we determined the expression of different L-arginine transporters in quiescent and activating HSCs (Figure 4F). Even though ERas interaction with ARG1 does not affect the enzymatic activity of the latter, the interaction between the two proteins might be important for the subcellular localization of ARG1 or the formation of a functional microdomain with, for example, L-arginine transporter at the plasma membrane. Therefore, mRNA levels were determined by qRT-PCR, showing the same pattern for mRNA and protein expression (Figures 2B and 4F) for *Arg1, Eras* and *iNos*. Interestingly, the cationic amino acid transporter (CATs) with the paralogs CAT1, CAT2A, CAT2B and CAT3 were regulated strongly during HSC activation. *Cat1* mRNA expression was highest at day 1, correlating with iNOS expression. *Cat2a* mRNA expression showed the highest expression in quiescent HSCs at day 0 and reduced expression in more activated states of HSCs, equivalent to *Arg1* and *ERas* regulation. The mRNA level of the CAT isoform 2B was upregulated at day 1 and was the highest among all paralogs. In contrast, *Cat3* mRNA expression was the lowest in comparison to the other paralogs and was slightly upregulated at day 1. The interaction or colocalization of ARG1, ERas and CAT2B could not be investigated yet due to the insufficient quality of the CAT2 antibody, but will provide an interesting research approach for the future.

4. Discussion

The aim of this study was to identify new interaction partners of ERas that are involved in the maintenance of HSC quiescence. Hepatic stellate cells are not only important to sense changes within their stem cell niche, but also to contribute to inflammatory events and communicate with neighboring cells. Their role in the pathological changes during liver fibrosis is well known and connected to the continuous activation of quiescent HSCs resulting in extracellular matrix-producing myofibroblast-like cells. Therefore, identification of signaling pathways and specific proteins that are essential for HSCs quiescence or activation is necessary to understand the molecular basis of liver fibrosis and development of therapeutic approaches for patients with chronic liver diseases.

In this study, we characterized the protein binding properties of the unique N-terminal extension of ERas, which is 42% identical between rat and human proteins. The MS analysis

identified 20 shared proteins, pulled down with the rat and human N-terminal region (Nex), as well as 35 proteins for *rn*Nex alone and 21 proteins for *hs*Nex. The molecular functions of ERas interaction partners are diverse and reach from nucleic acid binding, like the protein nucleophosmin, and structural molecule activity, like vimentin, to catalytic activities or translation regulation. Therefore, biological processes are widespread with a tendency of 29% of metabolic processes. This category includes ARG1 with its L-arginine-hydrolyzing enzymatic activity. The cellular localization of ERas binding partners are predominantly cytosolic, which coincides with the heavy and light membrane localization of ERas due to its post-translational modifications by farnesylation and palmitoylation [8,32]. We checked the mRNA expression of four representative proteins, that differ strongly in localization and function. ARG1 was expressed strongly at day 0 cells, which are considered as quiescent HSCs. The expression of ARG1 got downregulated during activation, which gave us a first hint of the involvement of ARG1 in the maintenance of HSC quiescence.

In cell biological experiments, we could confirm the coexpression, colocalization, and direct interaction of ERas and ARG1 in quiescent HSCs and also in cell-free experiments using purified proteins. Furthermore, we could confirm an active role of ARG1 when HSCs become myofibroblast-like cells, as the inhibition of arginase by nor-NOHA accelerated the activation of primary rat HSCs. Similar results were obtained after using the ODC1 inhibitor DFMO during HSC cultivation. These data suggest that not only the involvement of ARG1, but also the downstream production of polyamines are of major importance to maintain quiescence in HSCs. Polyamines can get synthesized downstream of L-ornithine by the ODC1 and further reversibly processed from putrescine to spermidine and spermine. The roles of polyamines in cells are broad and vary from cell proliferation to gene expression, ion channel regulation, and protection from oxidative damage to autophagy and regulatory aspects in immune cells [36–39]. Other studies using carbon tetrachloride (CCl_4) or ethanol for inducing liver injury demonstrated a protective effect of polyamines as well as a positive effect on hepatocyte proliferation [40,41]. Interestingly, it was also reported that polyamines support the self-renewal of embryonic stem cells (ESCs) [42,43]. ERas is highly expressed in ESCs, still ARG1 could neither be detected in the mRNA profile of embryonic stem cells, nor in mesenchymal stem cells (Supplementary Figure S10). However, polyamines can be transported from and to other cells via transporter systems and do not necessarily need to be produced and consumed in the same cell [44]. Even though the effect of polyamines on HSCs has not been described, it is tempting to speculate that the communication of HSCs and hepatocytes might include the production and exchange of polyamines to maintain liver homeostasis and regeneration after tissue injury. This hypothesis needs to be verified experimentally in future studies.

The interaction of ERas and ARG1 did not show any effects on ARG1 enzymatic activity in our experimental set-up. Therefore, the interaction of ERas and ARG1 may have other functional significance that can only be speculated about at this point. On the one hand, ARG1 and iNOS, which are reciprocally expressed during HSC activation, might each directly control the other's expression. The elevated expression of iNOS, one day after isolation and cultivation outside of their stem cell niche, is likely to be a stress response, driven by the transcription factor NFκB that regulates iNOS mRNA expression [45]. NFκB was furthermore described to play an essential role in both profibrogenic and antifibrogenic signaling pathways during liver diseases, and was also investigated in HSCs [46,47]. The expression level of iNOS is not only controlled by NFκB, but also by the translation initiation factor 2α (eIF2α), which is in turn regulated by L-arginine levels and therefore likely to be connected to ARG1 activity, also shown in astrocytes which have multiple similarities with HSCs [48–50]. On the other hand, the interaction of ERas and ARG1 could recruit ARG1 to a specific subcellular localization on lipid membranes to either increase ARG1 activity as it was shown in red blood cells, where the activity of arginase was approximately 100 times higher in membrane fractions compared to cytoplasmic fractions [51], or to source exogenous but not endogenous L-Arg, according to observations in other cells types, thereby solving "the arginine paradox" [52]. ERas-ARG1 interaction might recruit ARG1 to

the plasma membrane close to a cationic amino acid transporters (CATs) whose paralogs considerably differ in their affinity for L-arginine (CAT1: 0.10–0.16 mM; CAT2A 2–5 mM; CAT2B and CAT3: 0.25–0.70 mM) [53]. One hint might be the coexpression of ARG1 and CAT2A in quiescent HSCs that have a comparable low affinity for L-arginine and would match consumption and transportation affinity of L-arginine. For comparison, iNOS is coexpressed with the inducible CAT2B paralog in HSCs at day 1, which has also been reported for astrocytes [49,54]. In order to analyze the formation of an ARG1-ERas-CAT2A colocalization on the plasma membrane, future extensive studies and validated antibodies, which we do not currently have, are needed.

This study could successfully add arginase 1 to the list of interaction partners of ERas and to the proteins that are needed for the maintenance of quiescent HSCs. The alteration of the L-arginine metabolism *via* arginase and ODC1 inhibitors shows a strong picture towards an accelerated activation, whereas the iNOS inhibitor slows down the development of HSCs into myofibroblast-like cells. As HSCs are located in a tightly controlled stem cell niche in the space of Disse [10], we always have to consider the effect of amino acid/polyamine depletion and delivery, as well as the communication of HSCs as liver pericytes with surrounding cells and the vascular system.

Supplementary Materials: The following are available online at https://www.mdpi.com/article/10.3390/cells11030508/s1, Figure S1: Immunoprecipitation analysis of ARG1 and *rn*ERas, Figure S2: Confocal images of ERas, ARG1 and GFAP in quiescent HSCs., Figure S3: Confocal images of ERas—ARG1 and ARG1—Na^+/K^+-ATPase in quiescent HSCs., Figure S4: Pull-down experiments of ERas *hs*FL, *hs*ΔN and *rn*/*hs* G-domain with purified ARG1., Figure S5: Phase contrast microscopy of HSCs day 4., Figure S6: Oil Red O staining of HSCs day 1 to 4 with combination treatment of L-NIO and nor-NOHA., Figure S7. Urea assay with ARG1 and human ERas FL or Nex., Figure S8. ARG1 kinetic with and without ERas hsNex., Figure S9: Colorimetric arginase activity assay in HSC lysates., Figure S10: qRT-PCR analysis of ARG1 and OCT4 in HSCs, ESCs and MSCs., Table S1: Interaction partners of rat and human ERas Nex., Table S2. Primary and secondary antibodies. Table S3. qRT-PCR Primers.

Author Contributions: M.R.A. conceived and coordinated the study. S.P., J.L. (Jana Lissy) and M.R.A. designed and wrote the paper. S.P., J.L. (Jana Lissy), H.N., M.S.T., M.A., S.N.-R., J.L. (Junjie Li) and S.R.A. performed, and analyzed the experiments. M.M.C.-K., R.P.P., D.H. and C.K. provided reagents, cells, and expertise. All authors have read and agreed to the published version of the manuscript.

Funding: This study was funded by the German Research Foundation (Deutsche Forschungsgemeinschaft or DFG) through the Collaborative Research Center 974 (SFB 974 A03) "Communication and Systems Relevance during Liver Injury and Regeneration"; the German Research Foundation (Deutsche Forschungsgemeinschaft or DFG; grant number: AH 92/8-1); the European Network on Noonan Syndrome and Related Disorders (NSEuroNet; grant number: 01GM1621B); the German Federal Ministry of Education and Research (BMBF)—German Network of RASopathy Research (GeNeRARe; grant number:, 01GM1902C); and the Research Committee of the Medical Faculty of the Heinrich Heine University (grant number: 9772764 to MRA and MCK).

Institutional Review Board Statement: Not applicable.

Informed Consent Statement: Not applicable.

Data Availability Statement: This study includes no data deposited in external repositories.

Acknowledgments: We are grateful to Niloufar Mosaddeghzadeh for helpful discussions and Ilse Meyer, Claudia Rupprecht, Kotsene Loumonvi, Doreen Reichert, Fereshteh Haghighi and Julia Dahlmann for supporting the primary and stem cell preparation, and Boris Görg for providing a helpful hand with cLSM.

Conflicts of Interest: The authors declare no conflict of interest.

References

1. Takahashi, K.; Mitsui, K.; Yamanaka, S. Role of ERas in promoting tumour-like properties in mouse embryonic stem cells. *Nature* **2003**, *423*, 541–545. [CrossRef] [PubMed]
2. Aoyama, M.; Kataoka, H.; Kubota, E.; Tada, T.; Asai, K. Resistance to chemotherapeutic agents and promotion of transforming activity mediated by embryonic stem cell-expressed Ras (ERas) signal in neuroblastoma cells. *Int. J. Oncol.* **2010**, *37*, 1011–1016. [CrossRef] [PubMed]
3. Ikink, G.J.; Boer, M.; Bakker, E.R.M.; Vendel-Zwaagstra, A.; Klijn, C.; Ten Hoeve, J.; Jonkers, J.; Wessels, L.F.; Hilkens, J. Insertional mutagenesis in a HER2-positive breast cancer model reveals ERAS as a driver of cancer and therapy resistance. *Oncogene* **2018**, *37*, 1594–1609. [CrossRef] [PubMed]
4. Kubota, E.; Kataoka, H.; Aoyama, M.; Mizoshita, T.; Mori, Y.; Shimura, T.; Tanaka, M.; Sasaki, M.; Takahashi, S.; Asai, K.; et al. Role of ES cell-expressed Ras (ERas) in tumorigenicity of gastric cancer. *Am. J. Pathol.* **2010**, *177*, 955–963. [CrossRef]
5. Perna, D.; Karreth, F.A.; Rust, A.G.; Perez-Mancera, P.A.; Rashid, M.; Iorioc, F.; Alifrangis, C.; Arends, M.J.; Bosenberg, M.W.; Bollag, G.; et al. BRAF inhibitor resistance mediated by the AKT pathway in an oncogenic BRAF mouse melanoma model. *Proc. Natl. Acad. Sci. USA* **2015**, *112*, E536–E545. [CrossRef]
6. Yasuda, K.; Yashiro, M.; Sawada, T.; Ohira, M.; Hirakawa, K. ERas Oncogene Expression and Epigenetic Regulation by Histone Acetylation in Human Cancer Cells. *Anticancer Res.* **2007**, *27*, 4071–4075.
7. Tanaka, Y.; Ikeda, T.; Kishi, Y.; Masuda, S.; Shibata, H.; Takeuchi, K.; Komura, M.; Iwanaka, T.; Muramatsu, S.I.; Kondo, Y.; et al. ERas is expressed in primate embryonic stem cells but not related to tumorigenesis. *Cell Transplant.* **2009**, *18*, 381–389. [CrossRef]
8. Nakhaei-Rad, S.; Nakhaeizadeh, H.; Götze, S.; Kordes, C.; Sawitza, I.; Hoffmann, M.J.; Franke, M.; Schulz, W.A.; Scheller, J.; Piekorz, R.P.; et al. The Role of Embryonic Stem Cell-expressed RAS (ERAS) in the Maintenance of Quiescent Hepatic Stellate Cells. *J. Biol. Chem.* **2016**, *291*, 8399–8413. [CrossRef]
9. Friedman, S.L. Hepatic Stellate Cells: Protean, Multifunctional, and Enigmatic Cells of the Liver. *Physiol. Rev.* **2008**, *88*, 125–172. [CrossRef]
10. Kordes, C.; Häussinger, D. Hepatic stem cell niches. *J. Clin. Investig.* **2013**, *123*, 1874–1880. [CrossRef]
11. Kordes, C.; Sawitza, I.; Götze, S.; Häussinger, D. Hepatic Stellate Cells Support Hematopoiesis and are Liver-Resident Mesenchymal Stem Cells. *Cell. Physiol. Biochem.* **2013**, *31*, 290–304. [CrossRef] [PubMed]
12. Shaw, I.; Rider, S.; Mullins, J.; Hughes, J.; Péault, B. Pericytes in the renal vasculature: Roles in health and disease. *Nat. Rev. Nephrol.* **2018**, *14*, 521–534. [CrossRef] [PubMed]
13. Kordes, C.; Bock, H.H.; Reichert, D.; May, P.; Häussinger, D. Hepatic stellate cells: Current state and open questions. *Biol. Chem.* **2021**, *402*, 1021–1032. [CrossRef] [PubMed]
14. Wandzioch, E.; Kolterud, Å.; Jacobsson, M.; Friedman, S.L.; Carlsson, L. Lhx2-/- mice develop liver fibrosis. *Proc. Natl. Acad. Sci. USA* **2004**, *101*, 16549–16554. [CrossRef] [PubMed]
15. Canbay, A.; Taimr, P.; Torok, N.; Higuchi, H.; Friedman, S.; Gores, G.J. Apoptotic body engulfment by a human stellate cell line is profibrogenic. *Lab. Investig.* **2003**, *83*, 655–663. [CrossRef] [PubMed]
16. Cederbaum, S.D.; Yu, H.; Grody, W.W.; Kern, R.M.; Yoo, P.; Iyer, R.K. Arginases I and II: Do their functions overlap? *Mol. Genet. Metab.* **2004**, *81*, 38–44. [CrossRef]
17. Yang, J.; Gonon, A.T.; Sjöquist, P.O.; Lundberg, J.O.; Pernow, J. Arginase regulates red blood cell nitric oxide synthase and export of cardioprotective nitric oxide bioactivity. *Proc. Natl. Acad. Sci. USA* **2013**, *110*, 15049–15054. [CrossRef]
18. Lange, P.S.; Langley, B.; Lu, P.; Ratan, R.R. Novel roles for arginase in cell survival, regeneration, and translation in the central nervous system. *J. Nutr.* **2004**, *134*, 2812–2817. [CrossRef]
19. Jänne, J.; Alhonen, L.; Leinonen, P. Polyamines: From molecular biology to clinical applications. *Ann. Med.* **1991**, *23*, 241–259. [CrossRef]
20. Mezl, V.A.; Knox, W.E. Metabolism of arginine in lactating rat mammary gland. *Biochem. J.* **1977**, *166*, 105–113. [CrossRef]
21. Durante, W.; Johnson, F.K.; Johnson, R.A. Arginase: A critical regulator of nitric oxide synthesis and vascular function. *Clin. Exp. Pharmacol. Physiol.* **2007**, *34*, 906–911. [CrossRef] [PubMed]
22. Munder, M. Arginase: An emerging key player in the mammalian immune system: Review. *Br. J. Pharmacol.* **2009**, *158*, 638–651. [CrossRef] [PubMed]
23. Griffi, O.W.; Stueh, D.J. Nitric Oxide Synthases: Properties and Catalytic Mechanism. *Ann. Rev. Physiol.* **1995**, *57*, 707–736. [CrossRef]
24. Grody, W.W.; Dizikes, G.J.; Cederbaum, S.D. Human arginase isozymes. *Isozymes* **1987**, *13*, 181–214. [PubMed]
25. Reczkowski, R.S.; Ash, D.E. Rat liver arginase: Kinetic mechanism, alternate substrates, and inhibitors. *Arch. Biochem. Biophys.* **1994**, *312*, 31–37. [CrossRef]
26. Gremer, L.; Merbitz-Zahradnik, T.; Dvorsky, R.; Cirstea, I.C.; Kratz, C.P.; Zenker, M.; Wittinghofer, A.; Ahmadian, M.R. Germline KRAS mutations cause aberrant biochemical and physical properties leading to developmental disorders. *Hum. Mutat.* **2011**, *32*, 33–43. [CrossRef] [PubMed]
27. Corraliza, I.M.; Campo, M.L.; Soler, G.; Modolell, M. Determination of arginase activity in macrophages: A micromethod. *J. Immunol. Methods* **1994**, *174*, 231–235. [CrossRef]

28. Poschmann, G.; Seyfarth, K.; Besong Agbo, D.; Klafki, H.W.; Rozman, J.; Wurst, W.; Wiltfang, J.; Meyer, H.E.; Klingenspor, M.; Stühler, K. High-fat diet induced isoform changes of the Parkinson's disease protein DJ-1. *J. Proteome Res.* **2014**, *13*, 2339–2351. [CrossRef]
29. Tusher, V.G.; Tibshirani, R.; Chu, G. Significance analysis of microarrays applied to the ionizing radiation response. *Proc. Natl. Acad. Sci. USA* **2001**, *98*, 5116–5121. [CrossRef]
30. Mi, H.; Huang, X.; Muruganujan, A.; Tang, H.; Mills, C.; Kang, D.; Thomas, P.D. PANTHER version 11: Expanded annotation data from Gene Ontology and Reactome pathways, and data analysis tool enhancements. *Nucleic Acids Res.* **2017**, *45*, D183–D189. [CrossRef]
31. Taha, M.S.; Nouri, K.; Milroy, L.G.; Moll, J.M.; Herrmann, C.; Brunsveld, L.; Piekorz, R.P.; Ahmadian, M.R. Subcellular Fractionation and Localization Studies Reveal a Direct Interaction of the Fragile X Mental Retardation Protein (FMRP) with Nucleolin. *PLoS ONE* **2014**, *9*, e91465. [CrossRef] [PubMed]
32. Nakhaei-Rad, S.; Nakhaeizadeh, H.; Kordes, C.; Cirstea, I.C.; Schmick, M.; Dvorsky, R.; Bastiaens, P.I.H.; Häussinger, D.; Ahmadian, M.R. The function of embryonic stem cell-expressed RAS (E-RAS), a unique RAS family member, correlates with its additional motifs and its structural properties. *J. Biol. Chem.* **2015**, *290*, 15892–15903. [CrossRef] [PubMed]
33. Mehlem, A.; Hagberg, C.E.; Muhl, L.; Eriksson, U.; Falkevall, A. Imaging of neutral lipids by oil red O for analyzing the metabolic status in health and disease. *Nat. Protoc.* **2013**, *8*, 1149–1154. [CrossRef] [PubMed]
34. Jophlin, L.L.; Koutalos, Y.; Chen, C.; Shah, V.; Rockey, D.C. Hepatic stellate cells retain retinoid-laden lipid droplets after cellular transdifferentiation into activated myofibroblasts. *Am. J. Physiol. Gastrointest. Liver Physiol.* **2018**, *315*, G713–G721. [CrossRef]
35. Nakhaei-Rad, S.; Haghighi, F.; Nouri, P.; Rezaei Adariani, S.; Lissy, J.; Kazemein Jasemi, N.S.; Dvorsky, R.; Ahmadian, M.R. Structural fingerprints, interactions, and signaling networks of RAS family proteins beyond RAS isoforms. *Crit. Rev. Biochem. Mol. Biol.* **2018**, *53*, 130–156. [CrossRef]
36. Pegg, A.E. The function of spermine. *IUBMB Life* **2014**, *66*, 8–18. [CrossRef]
37. Hesterberg, R.; Cleveland, J.; Epling-Burnette, P. Role of Polyamines in Immune Cell Functions. *Med. Sci.* **2018**, *6*, 22. [CrossRef]
38. Madeo, F.; Eisenberg, T.; Büttner, S.; Ruckenstuhl, C.; Kroemer, G. Spermidine: A novel autophagy inducer and longevity elixir. *Autophagy* **2010**, *6*, 160–162. [CrossRef]
39. Ghosh, I.; Sankhe, R.; Mudgal, J.; Arora, D.; Nampoothiri, M. Spermidine, an autophagy inducer, as a therapeutic strategy in neurological disorders. *Neuropeptides* **2020**, *83*, 102083. [CrossRef]
40. Hyvönen, M.T.; Sinervirta, R.; Grigorenko, N.; Khomutov, A.R.; Vepsäläinen, J.; Keinänen, T.A.; Alhonen, L. α-Methylspermidine protects against carbon tetrachloride-induced hepatic and pancreatic damage. *Amino Acids* **2010**, *38*, 575–581. [CrossRef]
41. Do, T.H.T.; Gaboriau, F.; Morel, I.; Lepage, S.; Cannie, I.; Loréal, O.; Lescoat, G. Modulation of ethanol effect on hepatocyte proliferation by polyamines. *Amino Acids* **2013**, *44*, 869–877. [CrossRef] [PubMed]
42. Zhao, T.; Goh, K.J.; Ng, H.H.; Vardy, L.A. A role for polyamine regulators in ESC self-renewal. *Cell Cycle* **2012**, *11*, 4517–4523. [CrossRef] [PubMed]
43. James, C.; Zhao, T.Y.; Rahim, A.; Saxena, P.; Muthalif, N.A.; Uemura, T.; Tsuneyoshi, N.; Ong, S.; Igarashi, K.; Lim, C.Y.; et al. MINDY1 Is a Downstream Target of the Polyamines and Promotes Embryonic Stem Cell Self-Renewal. *Stem Cells* **2018**, *36*, 1170–1178. [CrossRef] [PubMed]
44. Uemura, T.; Gerner, E.W. Polyamine transport systems in mammalian cells and tissues. *Methods Mol. Biol.* **2011**, *720*, 339–348. [CrossRef] [PubMed]
45. Stachon, T.; Latta, L.; Seitz, B.; Szentmáry, N. Hypoxic stress increases NF-κB and iNOS mRNA expression in normal, but not in keratoconus corneal fibroblasts. *Graefe's Arch. Clin. Exp. Ophthalmol.* **2021**, *259*, 449–458. [CrossRef]
46. Sun, B.; Karin, M. NF-κB signaling, liver disease and hepatoprotective agents. *Oncogene* **2008**, *27*, 6228–6244. [CrossRef]
47. Luedde, T.; Schwabe, R.F. NF-κB in the liver—linking injury, fibrosis and hepatocellular carcinoma. *Nat. Rev. Gastroenterol. Hepatol.* **2011**, *8*, 108. [CrossRef]
48. Lee, J.; Ryu, H.; Ferrante, R.J.; Morris, S.M.; Ratan, R.R. Translational control of inducible nitric oxide synthase expression by arginine can explain the arginine paradox. *Proc. Natl. Acad. Sci. USA* **2003**, *100*, 4843–4848. [CrossRef]
49. Schachtrup, C.; Le Moan, N.; Passino, M.A.; Akassoglou, K. Hepatic stellate cells and astrocytes: Stars of scar formation and tissue repair. *Cell Cycle* **2011**, *10*, 1764–1771. [CrossRef]
50. Buniatian, G.H.; Hartmann, H.J.; Traub, P.; Weser, U.; Wiesinger, H.; Gebhardt, R. Acquisition of blood-tissue barrier-supporting features by hepatic stellate cells and astrocytes of myofibroblastic phenotype. Inverse dynamics of metallothionein and glial fibrillary acidic protein expression. *Neurochem. Int.* **2001**, *38*, 373–383. [CrossRef]
51. Jiang, M.; Ding, Y.; Su, Y.; Hu, X.; Li, J.; Zhang, Z. Arginase-flotillin interaction brings arginase to red blood cell membrane. *FEBS Lett.* **2006**, *580*, 6561–6564. [CrossRef] [PubMed]
52. Dioguardi, F.S. To Give or Not to Give? Lessons from the Arginine Paradox. *J. Nutrigenet. Nutrigenom.* **2011**, *4*, 90–98. [CrossRef] [PubMed]
53. Closs, E.I.; Simon, A.; Vékony, N.; Rotmann, A. Plasma membrane transporters for arginine. *J. Nutr.* **2004**, *134*, 2752S–2759S. [CrossRef] [PubMed]
54. Stevens, B.R.; Kakuda, D.K.; Yu, K.; Waters, M.; Vo, C.B.; Raizada, M.K. Induced nitric oxide synthesis is dependent on induced alternatively spliced CAT-2 encoding L-arginine transport in brain astrocytes. *J. Biol. Chem.* **1996**, *271*, 24017–24022. [CrossRef]

6. CDC42-IQGAP INTERACTIONS SCRUTINIZED: NEW INSIGHTS INTO THE BINDING PROPERTIES OF THE GAP-RELATED DOMAIN

Article

Niloufar Mosaddeghzadeh*, Silke Pudewell*, Farhad Bazgir, Neda S. Kazemein Jasemi, Oliver H.F. Krumbach, Lothar Gremer, Dieter Willbold, Radovan Dvorsky, Mohammad R. Ahmadian

*These authors equally contributed to this study

doi: 10.3390/ijms23168842

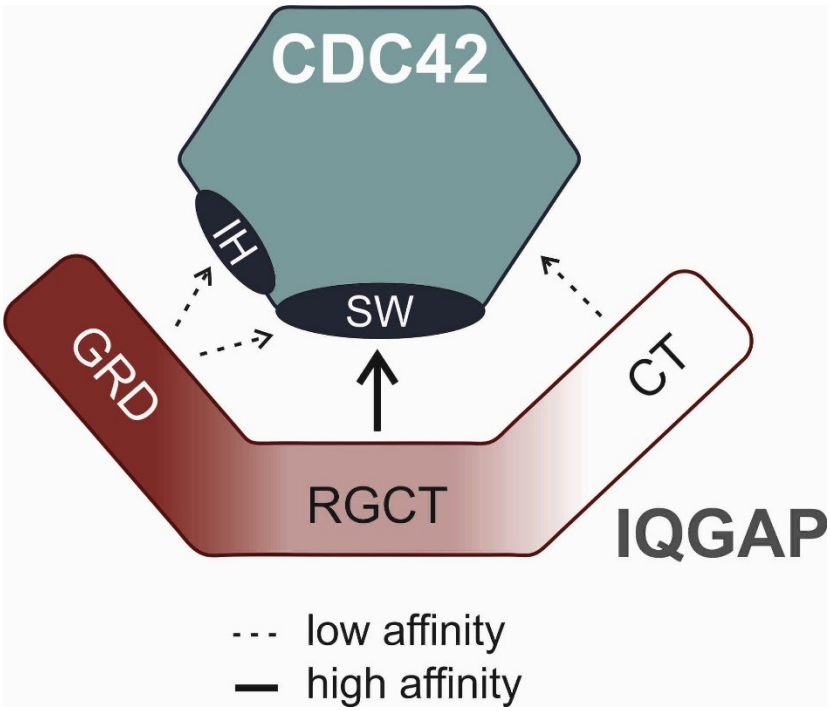

Journal: International journal of molecular science, Volume 23, Article number: 8842 (2022)

Published: 09 August 2022

Impact factor: 6.208

Own contribution: 20%

IQGAP protein expression, fluorescence polarization measurements, cell culture, pull down assays, western blotting, data evaluation, preparation of figures, writing the manuscript, reference management, discussion

International Journal of
Molecular Sciences

MDPI

Article

CDC42-IQGAP Interactions Scrutinized: New Insights into the Binding Properties of the GAP-Related Domain

Niloufar Mosaddeghzadeh [1,†], Silke Pudewell [1,†], Farhad Bazgir [1], Neda S. Kazemein Jasemi [1], Oliver H. F. Krumbach [1], Lothar Gremer [2,3], Dieter Willbold [2,3], Radovan Dvorsky [1,4] and Mohammad R. Ahmadian [1,*]

1 Institute of Biochemistry and Molecular Biology II, Medical Faculty and University Hospital Düsseldorf, Heinrich Heine University Düsseldorf, 40225 Düsseldorf, Germany
2 Institute of Physical Biology, Heinrich Heine University Düsseldorf, 40225 Düsseldorf, Germany
3 Institute of Biological Information Processing, Structural Biochemistry (IBI-7), Forschungszentrum Jülich, 52425 Jülich, Germany
4 Center for Interdisciplinary Biosciences, P. J. Šafárik University, Jesenná 5, 040 01 Košice, Slovakia
* Correspondence: reza.ahmadian@uni-duesseldorf.de; Tel.: +49-211-811-2384
† These authors contributed equally to this work.

Abstract: The IQ motif-containing GTPase-activating protein (IQGAP) family composes of three highly-related and evolutionarily conserved paralogs (IQGAP1, IQGAP2 and IQGAP3), which fine tune as scaffolding proteins numerous fundamental cellular processes. IQGAP1 is described as an effector of CDC42, although its effector function yet re-mains unclear. Biophysical, biochemical and molecular dynamic simulation studies have proposed that IQGAP RASGAP-related domains (GRDs) bind to the switch regions and the insert helix of CDC42 in a GTP-dependent manner. Our kinetic and equilibrium studies have shown that IQGAP1 GRD binds, in contrast to its C-terminal 794 amino acids (called C794), CDC42 in a nucleotide-independent manner indicating a binding outside the switch regions. To resolve this discrepancy and move beyond the one-sided view of GRD, we carried out affinity measurements and a systematic mutational analysis of the interfacing residues between GRD and CDC42 based on the crystal structure of the IQGAP2 GRD-CDC42^{Q61L} GTP complex. We determined a 100-fold lower affinity of the GRD1 of IQGAP1 and of GRD2 of IQGAP2 for CDC42 mGppNHp in comparison to C794/C795 proteins. Moreover, partial and major mutation of CDC42 switch regions substantially affected C794/C795 binding but only a little GRD1 and remarkably not at all the GRD2 binding. However, we clearly showed that GRD2 contributes to the overall affinity of C795 by using a 11 amino acid mutated GRD variant. Furthermore, the GRD1 binding to the CDC42 was abolished using specific point mutations within the insert helix of CDC42 clearly supporting the notion that CDC42 binding site(s) of IQGAP GRD lies outside the switch regions among others in the insert helix. Collectively, this study provides further evidence for a mechanistic framework model that is based on a multi-step binding process, in which IQGAP GRD might act as a 'scaffolding domain' by binding CDC42 irrespective of its nucleotide-bound forms, followed by other IQGAP domains downstream of GRD that act as an effector domain and is in charge for a GTP-dependent interaction with CDC42.

Keywords: CDC42; GAP; GAP-related domain; GRD; GTPase activating protein; IQGAP; nucleotide-independent binding; RASGAP; RHO GTPases; scaffold protein; scaffolding protein; switch regions

check for updates

Citation: Mosaddeghzadeh, N.; Pudewell, S.; Bazgir, F.; Kazemein Jasemi, N.S.; Krumbach, O.H.F.; Gremer, L.; Willbold, D.; Dvorsky, R.; Ahmadian, M.R. CDC42-IQGAP Interactions Scrutinized: New Insights into the Binding Properties of the GAP-Related Domain. *Int. J. Mol. Sci.* **2022**, *23*, 8842. https://doi.org/10.3390/ijms23168842

Academic Editor: Alexande Baykov

Received: 23 June 2022
Accepted: 6 August 2022
Published: 9 August 2022

1. Introduction

RHO GTPases act, with some exceptions [1], as molecular switches by cycling between an inactive (GDP-bound) and an active (GTP-bound) state. Their functions at the plasma membrane are usually controlled by three groups of regulatory proteins: guanine nucleotide dissociation inhibitors (GDIs), guanine nucleotide exchange factors (GEFs) and GTPases activating proteins (GAPs) [2]. The formation of the active GTP-bound state of

RHO GTPases, such as CDC42, is accompanied by a conformational change in two regions, known as switch I and II (encompassing amino acids or aa 29–42 and 62–68, respectively); these regions provide a platform for a GTP-dependent, high-affinity association of structurally and functionally diverse effector proteins, e.g., ACK, PAK1, WASP, ROCKI, DIA and IQGAP1, through their so-called GTPase-binding domains (GBDs) [3–13] (reviewed in [14]). GTPase-effector signaling activates further a wide variety of pathways in all eukaryotic cells [2].

A unique feature distinguishing the RHO family from other small GTPase families is the presence of a 12 amino-acid insertion (aa 124–135 in CDC42) that protrudes from the G domain structure by forming a short helix, the so-called insert helix (IH) [15]. This IH is highly charged and variable among the members of the RHO family [15]. The IH has been very recently shown to have larger conformational flexibility in the GDP-bound CDC42 than in the GTP-bound CDC42 [16]. IH is a binding site for RHOGDI1, p50GAP, DIA, FMNL2, PLD1 and IQGAP2 [10,12,17–21], and appears rather essential for downstream activation of RHO GTPases [21–23].

IQGAP1 is ubiquitously expressed and shares a similar domain structure with its human paralogs IQGAP2 and IQGAP3 (Figure 1A), including an N-terminal calponin homology domain (CHD), a coiled-coil repeat region (CC), a tryptophan-containing proline-rich motif-binding region (WW), four isoleucine/glutamine-containing motifs (IQ), a RASGAP-related domain (GRD), a RASGAP C-terminal domain (RGCT) and a very C-terminal domain (CT). IQGAPs interact with a large number of proteins and modulate the spatiotemporal distributions of distinct signal-transducing protein complexes [24–34]. As multidomain scaffold proteins, they safeguard the magnitude, efficiency and specificity of signal transduction [35]. They have been localized at multiple subcellular sites orchestrating different signaling pathways and thus controlling a variety of cellular functions [36–42]. Notably, IQGAP1 has been implicated as a drug target due to its vital regulatory roles in cancer development [42–49] although the molecular mechanism of its functions is unclear.

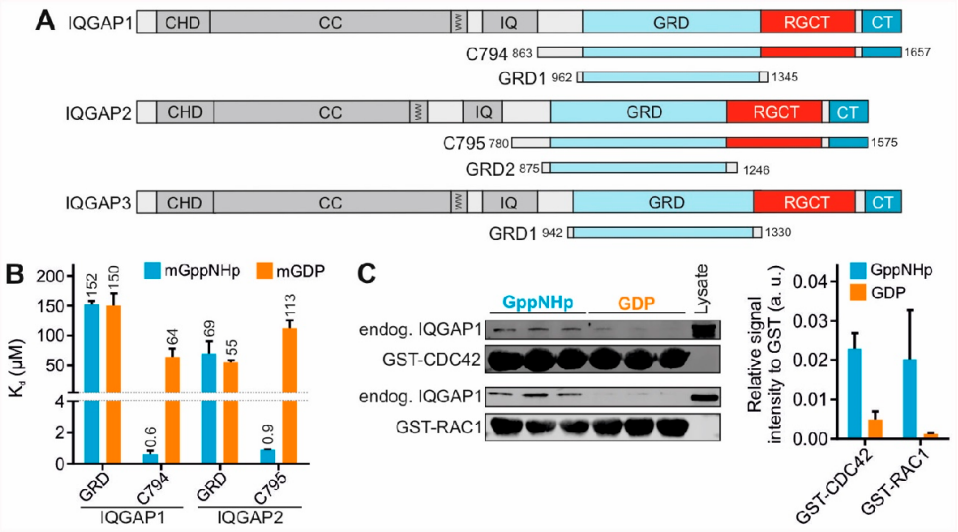

Figure 1. IQGAP GRD binding is nucleotide independent. (**A**) Domain organization of the IQGAP paralogs along with their GRDs and C-terminal fragments assessed in this study (see text for more details). (**B**) Fluorescence polarization analysis of IQGAP1 and IQGAP2 proteins with mGppNHp- and mGDP-bound CDC42. (**C**) Pull-down of endogenous IQGAP1 FL from HEK293 lysates with GppNHp- or GDP-bound GST-CDC42 and GST-RAC1, respectively. Densitometry evaluation of relative IQGAP1 binding to GST-CDC42 proteins (a. u., arbitrary unit) from a triplicate experiment is shown as bar charts.

Earlier studies analyzed the crucial role of IQGAP RGCT in high-affinity binding to the switch regions of the GTP-bound, active CDC42 and proposed it as an IQGAP 'effector domain' [5,50,51]. Accordingly, Swart-Mataraza et al. reported that the CDC42 GppNHp can still bind to IQGAP-ΔGRD (lacking aa 1122–1324) [52]. Moreover, Li et al. mapped the CDC42 and IQGAP binding regions and determined that switch I and surrounding regions (residues 29–55) together with the insert region (residues 122–134) are required for high affinity binding to IQGAP1 [53]. LeCour et al., however, solved a crystal structure of constitutively active CDC42(Q61L) in complex with the IQGAP2 GRD (GRD2) and proposed that CDC42 binds GRD2 from two different sites in a 4:2 stoichiometry [12,54]. One is the 'GAPex-mode binding site' (ex stands for 'extra' subdomains consisting of variable N- and C- terminal flanking regions) and the other is the 'RASGAP-mode binding site' very much resembling the RASGAP and CDC42GAP structures [18,55] with a conserved core domain (GAPc). Analyzing this structure, Ozdemir et al. proposed that CDC42 IH binding to the GAPex-domain induces GRD2 dimerization and changes the RASGAP site allosterically, which subsequently create another interaction interface for CDC42 binding (leading to a 2:1 stoichiometry of GRD2 and CDC42) [54].

A number of biophysical and biochemical studies have provided valuable insights into the structural and binding properties of the C-terminal domains of IQGAP1 (C794) and IQGAP2 (C795), encompassing the GRD, RGCT and CT domains, with CDC42 [12,50,52–54,56–63]. Evidently, all three domains bind with different affinities to CDC42 [5]. However, the mechanistic principles behind these interactions have remained unclear. Moreover, there are conflicting views regarding the assignment of a 'CDC42-specific GBD' for IQGAPs. One model proposes the GRD and its RASGAP-mode binding with the switch regions of CDC42 [12,54,56,58,64], whereas the other model excludes GRD and marks RGCT, located distal to the GRD, as crucial for high-affinity binding to CDC42 in a GTP-dependent manner [5,26,50–52]. Aiming to shed light on this discrepancy and to understand the molecular basis of CDC42-IQGAP interaction we comprehensively investigated the nature of the GRD interaction with CDC42 in this study and determined the role of the IH of CDC42 in contributing to GRD association. Furthermore, we studied the binding characteristics of C794 regarding the switch region and IH contact sites by mutational analysis, and verified the results in cell-based studies with endogenous IQGAP1. Collectively, our results consolidate and refine the importance of IQGAP RGCT as the true GBD in the recognition of CDC42 and its binding in a GTP-dependent manner. The GRD, although not a central effector domain, is evidently necessary for scaffolding CDC42 and facilitating its recruitment to preexisting cues.

2. Results and Discussion

IQGAP1 and IQGAP2 proteins were analyzed in this study to critically evaluate the function of the respective GRD domains. First, we determined the CDC42 binding properties of different IQGAP proteins, including IQGAP1 full-length (FL). Second, we examined the role of amino-acids crucial for the interplay between IQGAP2 and CDC42 using mutational IQGAPs and CDC42 variants. Third, we analyzed the impact of CDC42 IH as an IQGAP binding site. Fourth, we investigated the RASGAP activity of IQGAP1 GRD towards eight different members of the RAS family and examined the introduction of a catalytic arginine finger in the GRD.

2.1. GRD Is Not the Prominent Binding Domain for High IQGAP-CDC42 Affinity

2.1.1. GRD Binds to CDC42 with Very Low Affinity in a Nucleotide-Independent Manner

Different domains and fragments of the IQGAPs, including GRD1 and C794 of IQGAP1, as well as GRD2 and C795 of IQGAP2 (Figure 1A), were purified to determine their binding affinities for mGDP- and mGppNHp-bound CDC42 using fluorescence polarization. Obtained dissociation constants (K_d; Figure 1B) clearly show that all IQGAP constructs are able to bind CDC42 but with different affinities and preferences for the nucleotide-bound forms of CDC42. GRDs of both IQGAPs are low-affinity binders and do

not discriminate between the active and the inactive states of CDC42. Similar observations were made for GRD3 and the CT of IQGAP1 (Supplementary Figure S1). In contrast, C794 and C795, encompassing in addition to both GRD and CT also the central RGCT (Figure 1A), exhibited K_d values of 0.6 and 0.9 μM, respectively, indicating an around 100-fold higher affinity for the GTP-bound active CDC42 as compared to CDC42 GDP (Figure 1B). This result clearly suggests that RGCT but not GRD represents a 'CDC42-specific GBD' for at least IQGAP1 and IQGAP2, by directly associating with the switch regions of CDC42 GTP. Unfortunately, our efforts to obtain IQGAP1 RGCT (aa 1276–1575) and IQGAP3 C790 (aa 841–1631) for determining their binding affinities to the members of the RHO GTPase family, including CDC42, has been remaining unsuccessful [26,51]. Purified IQGAP1 RGCT tends to assemble into higher oligomeric or polymeric states, and, thus, is disabled in binding CDC42 [51].

Several lines of evidence support the crucial role of RGCT rather than GRD as the IQGAP effector domain for CDC42: (i) Here we can show that proteins containing RGCT bind with a more than 100-fold affinity to CDC42 mGppNHp as compared to isolated GRD or CT (Figure 1B and Figure S1), (ii) substitution of the Serine 1443 for glutamate (a phosphomimetic mutation) drastically impaired IQGAP1 binding to CDC42 mGppNHp [5,51]; (iii) an IQGAP1 protein, lacking the GRD (aa1122–1324), only binds CDC42 GppNHp, in contrast to IQGAP1 itself, that binds both GppNHp-bound and GDP-bound CDC42 [52]. The latter has been also demonstrated in other studies [63,64] and support our previous [26,51] and current findings that IQGAP domains, including GRD and CT, bind CDC42 GDP as strong as CDC42 GppNHp (Figure 1B).

2.1.2. Endogenous IQGAP1 also Binds CDC42 GDP

Serum-stimulated HEK293 cells, endogenously expressing IQGAP1 full-length (FL), were now used to carry out a pull-down assay with purified GST-fusion proteins of CDC42 and RAC1 in either GDP-bound or GppNHp-bound forms. IQGAP1 FL bound to these GTPases, regardless of their nucleotide status even though the binding to GDP-bound proteins was observed to be much weaker than the GppNHp-bound proteins (Figure 1C). This pattern corresponds to the binding behavior of C794 and not with the binding of GRD1 alone. Densitometric evaluation of three independent pull-down experiments showed that IQGAP1 FL binding to CDC42 GDP is much stronger than to RAC1 GDP (Figure 1C).

Altogether, our data suggest that IQGAP1 forms a complex with CDC42 through different sites in both nucleotide-dependent and nucleotide-independent manner.

2.2. Switch Regions of CDC42 Are Not the Main Binding Sites for the GRDs

Timpson's and our group have provided evidence that the IQGAP RGCT is essential for high affinity binding to the switch regions of the GTP-bound, active CDC42 and thus acts as an IQGAP 'effector domain' [5,50,51]. This critical issue has now been further expanded with additional experiments as described above (Figure 1), and confirms the crucial role of the RGCT as an IQGAP 'effector domain' that selectively associates with CDC42 GTP and carries out the high affinity association. Other groups have, in contrast, used the constitutive active CDC42(Q61L) in their structural and biochemical analysis and proposed that CDC42(Q61L) GTP GRD forms a GTPase-effector complex [12,54,56,57]. Such a role of the GRD in associating with CDC42 GTP is astonishing considering the afore mentioned studies on both GRD1-CT that binds CDC42 with a higher affinity as compared with GRD and an IQGAP1 variant, lacking the RASGAP domain (aa 1122–1324), which equally interacts with CDC42 as compared with IQGAP1 wild type [52]. To clarify this discrepancy, we have carefully examined 'the RASGAP-mode binding site' of CDC42 using mutational approaches coupled with kinetic and equilibrium measurements. Results of this examination are discussed in following subsections.

2.2.1. Mutations in CDC42 Switch Regions Only Mildly Affect GRD Binding

Proposed interacting mode of GRD with the switch regions of CDC42 (RASGAP mode binding) was deduced from the IQGAP2 GRD2 structure in complex $CDC42^{Q61L}$ GTP [12] and two CDC42 mutation variants within the switch I and II regions (2xSW and 8xSW) and a 11-residues mutant variant within the GRD of IQGAP2 C795 (11xGRD) were generated as illustrated in Figure 2A. Identical and highly conserved residues within the interacting interface highlighted in Figure 2B, were all replaced by alanine. All variants were stable in their purified forms and Far-UV CD spectroscopic measurements excluded any improper folding as compared to the wild-type proteins (Supplementary Figure S2).

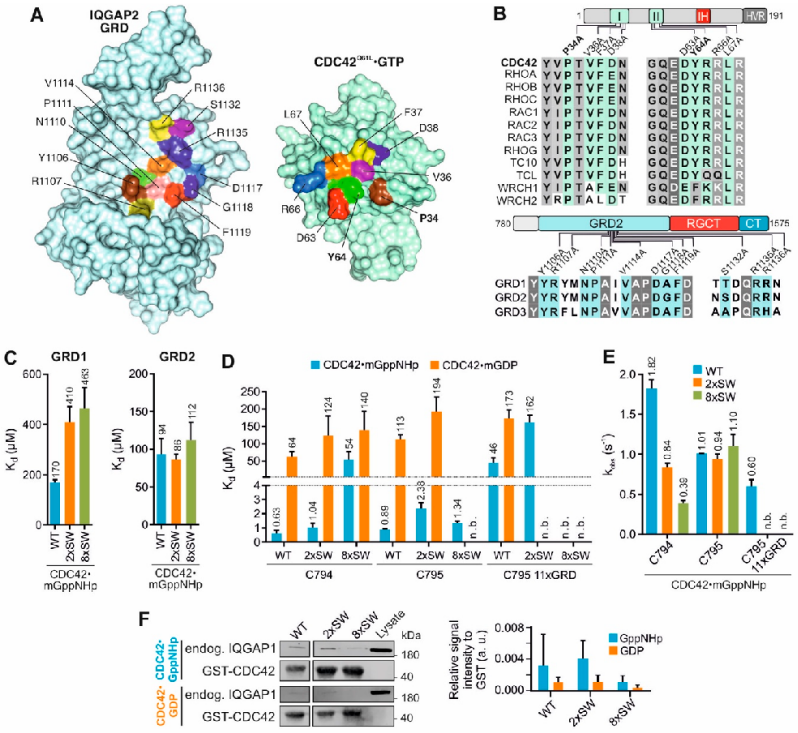

Figure 2. Analysis of CDC42 switch region and IQGAP1 GRD mutants. (**A**) The selection of GRD2 and CDC42 mutations is based on the GRD2/$CDC42^{Q61L}$ structure (PDB: 5CJP). Interacting residues colored on both proteins were selected for mutational analysis. For more details see also Table S1. (**B**) Multiple sequence alignments of switch regions of RHO GTPases and IQGAPs highlight identical or homologous interacting residues that have been replaced in this study by alanine for analyzing their impact on IQGAP binding. Conserved residues are shaded in grey. Mutations in CDC42 switch regions include 2xSW (bolded residues) and 8xSW (all eight residues, as indicated), and 11xGRD in IQGAP2 C795. (**C**) Fluorescence polarization measurements of mGppNHp-bound CDC42 WT, 2xSW and 8xSW with IQGAP1 GRD1 or IQGAP2 GRD2. (**D**) The K_d values for the interactions of IQGAP1 C794, IQGAP2 C795 and C795 11xGRD with the CDC42 variants in mGppNHp- and mGDP-bound form were determined using fluorescence polarization. n.b. stands for no binding observed. C794 and C795 CDC42 WT measurements are included from Figure 1B for simple comparison. (**E**) Observed rate constants (k_{obs}) for the IQGAPs association with mGppNHp-bound CDC42 WT, 2xSW and 8xSW were measured using stopped-flow fluorimetry. (**F**) Pull-down of endogenous IQGAP1 FL from HEK293 lysates with GST-CDC42 in GppNHp-bound or GDP-bound state. Cell lysate was used as an input control. Densitometry evaluation of relative IQGAP1 binding to GST-CDC42 proteins (a. u., arbitrary unit) from triplicate experiments is shown as bar charts.

We first determined the K_d values for the GRD1 and GRD2 interaction with the mGppNHp-bound CDC42 WT, 2xSW and 8xSW. Interestingly, we found a two to three-fold reduction in the binding affinity of GRD1 but no notable reduction for GRD2 with the CDC42 variants as compared to CDC42 WT (Figures 1B, 2C and S3). As the effect of 2x and 8x introduced mutations on the proposed crucial interaction sites of CDC42 and GRD2 did not result in a decrease of affinity, our data clearly indicates that the association of CDC42 switch regions with IQGAP must be through other sites rather than the GRD.

2.2.2. IQGAP C794/C795 Binding Is Impaired by Switch Region and GRD Mutations

Next, we measured the K_d values for the interaction of IQGAP1 C794 or IQGAP2 C795, containing the GRD, RGCT and CT domains, with mGDP-bound and mGppNHp-bound CDC42 variants. Data shown in Figure 2D (Supplementary Figure S4) indicate that the substitution of two amino acids in the switch regions was not sufficient to largely impair the CDC42-C794 interaction. However, mGppNHp-bound, but not mGDP-bound CDC42 8xSW exhibited a drastic reduction (86-fold) in its binding affinity for C794. For mGDP-bound CDC42, introduction of SW mutations only slightly decreased the affinity of C794. The IQGAP2 C795 binding to the CDC42 switch regions was not impaired by neither 2x nor 8x mutants of CDC42 in mGppNHp-bound state. Interestingly, IQGAP2 C795 showed a slightly decreased binding to the mGDP-bound CDC42 2xSW mutant but no binding to the 8xSW mutant, a much different result than obtained for GRD2 binding alone. The data from real-time stopped-flow fluorescence spectrometry (Figure 2E and Figure S5) showed both IQGAPs associated with similar k_{obs} values, as observed in Figure 2D.

The next question addressed was to what extent CDC42 binding of IQGAP1 FL was affected by the switch region mutations. Therefore, endogenous IQGAP1 was pulled down from HEK293 lysates using GDP-bound and GppNHp-bound GST-CDC42 WT, 2xSW and 8xSW. As shown in Figure 2F, IQGAP1 binding to CDC42 did not change with two amino acid substitution of the switch regions but was disrupted with the eight mutations. These experiments support our kinetic and equilibrium measurements and clearly indicate that the switch regions are significant for the IQGAP1 interaction with both GDP-bound and GppNHp-bound CDC42.

Taken together, the presented data suggest a slightly different binding behavior of IQGAP1 and IQGAP2 variants for CDC42. Our results do not support the interacting mode between IQGAP and CDC42 based on the crystal structure [12] and the central role of the GRD in it [54] since the introduction of SW mutations of CDC42 clearly affected C795/C794 binding but only little the GRD binding. We, in contrary, propose that the interactions sites on IQGAP for complex formation with CDC42 GTP are clearly within the RGCT and might be different between IQGAP1 and IQGAP2.

2.3. Insert Helix Contributes to the Binding Affinity of CDC42 for IQGAP1 GRD

The question arises as which regions on CDC42 could bind GRD if we can now exclude the switch regions. A region/site that has attracted our attention is the IH of CDC42 for valid reasons. We have shown that IQGAPs bind to RAC-like and CDC42-like proteins but not to the other members of the RHO family [26] and the IH consistently is a highly variable region among the RHO GTPases (Figure 3A) [15]. Several CDC42-binding proteins, including RHOGDI1, p50GAP, FMNL2 and IQGAP2 have been shown to contact the IH [10,12,17,18,20]. Thus, mutational analysis of the CDC42 IH was performed, using four different single residue mutations and a quadruple mutation (Figure 3A and Table S1). Note that variable residues were replaced in CDC42 by the corresponding residues of RAC1. Most remarkably and in sharp contrast to the SW mutations (Figure 2), all IH mutations abolished GRD1-CDC42 interaction irrespective of the nucleotide-bound states of CDC42 (Figures 3B and S6), which underlines the central role of CDC42 IH in GRD binding. The scenario was rather different for C794, which binds mGDP-bound CDC42 with 3-fold and mGppNHp-bound CDC42 with 20-fold lower affinities (Figure 3B). These

data are consistent with the recent observation by Nussinov and colleagues that the CDC42 IH reveals nucleotide-dependent conformational flexibility [16].

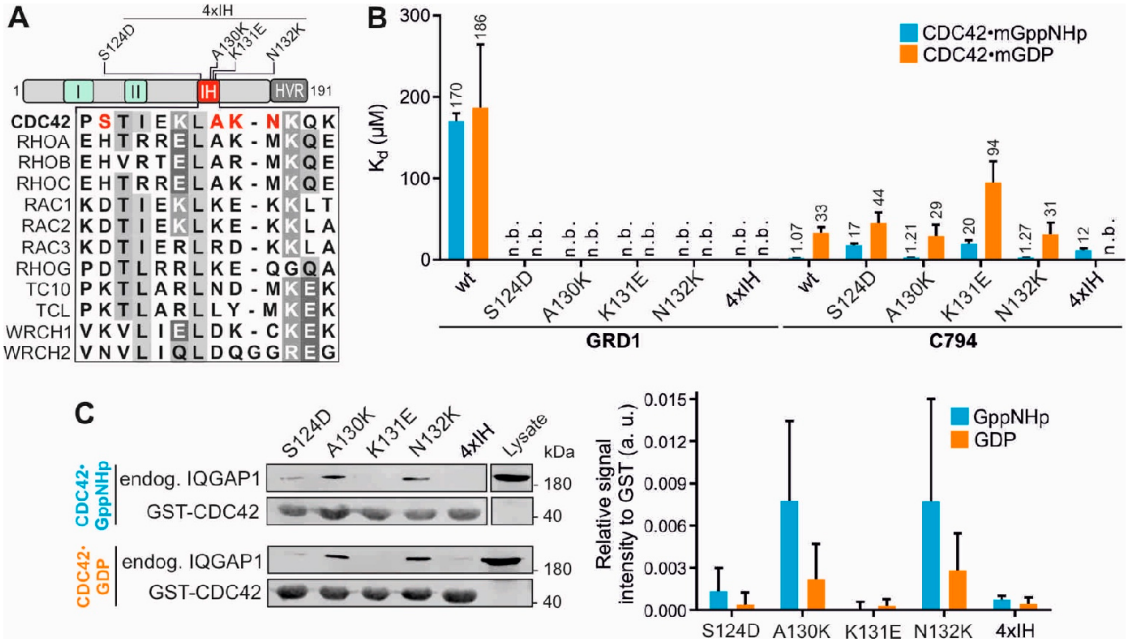

Figure 3. CDC42 IH mutations decrease binding affinity. (**A**) Amino acid alignment of the insert helix of selected members of the RHO GTPase family. CDC42 mutations (red) to RAC1 were introduced outside of the conserved regions (grey). (**B**) Fluorescence polarization data for the interaction of GRD1 and C794 with the CDC42 IH variants. (**C**) Pull-down of endogenous IQGAP1 FL from HEK293 lysates with GST-CDC42 IH variants in both GppNHp-bound and GDP-bound forms. Cell lysate was used as an input control. The pull-down data for GST-CDC42^{wt} is shown in Figure 2F as all pull-down experiments were conducted under the same conditions. Densitometry evaluation of relative IQGAP1 binding to GST-CDC42 proteins (a. u., arbitrary unit) from a triplicate experiment is shown as bar charts.

The data from fluorescence polarization could be verified via pull-down assay. The binding pattern of CDC42 IH mutants with endogenous IQGAP1 followed the same pattern, displaying no binding for A130K and 4xIH and very weak binding for S124D (Figure 3C). Generally, binding could be observed much stronger for GppNHp-bound than for GDP-bound CDC42 variants, supporting the pull-down data shown above (Figure 1C).

Several published studies have shown that mutations of the CDC42 IH impact their properties in binding IQGAPs. Li et al. (1999) have shown that IH deletion in CDC42 impairs its binding affinity for the effectors, in particular IQGAP1 C794 [53]. Owen et al. (2008) investigated the impact of the IH mutations in CDC42^{Q61L} on IQGAP1 C794 binding [56]. Consistent with our findings, they observed a slight decrease in C794 affinity for CDC42^{Q61L} with A130K or N132K. Moreover, Ozdemir et al. also applied the CDC42^{Q61L} variant and suggested the IH together with switch I region to be mainly responsible for its binding to the *ex*-domain of GRD (GRDex) of IQGAP2 [54].

2.4. Q61L Variant Is Not a Wildtype Equivalent for CDC42-IQGAP Interactions

An issue that still needs to be addressed is why are there several discrepancies between the studies regarding the GRD binding property for CDC42? A possible answer to this question is the use of different CDC42 mutants in these studies that are alike, but not equivalent, especially regarding this interaction.

In the GTP-bound CDC42, Q61 acts as a 'catalytic residue' that is involved in hydrogen bonding with a catalytic water molecule, an arginine finger of GAP and the γ-phosphate of GTP, initiating a nucleophilic attack that hydrolyzes GTP (Figure 4A) [18,65]. L61 does not, however, undergo these functionally critical hydrogen bonds but rather points towards protein surface without causing significant structural changes (Figure 4A). As a result, the substitution of Q61 by leucine drastically increases the binding affinity of IQGAPs for $CDC42^{Q61L}$ GTP by up to 15-fold as was clearly demonstrated previously [5,26,51]. Despite this fact, many groups use this CDC42 variant for the interaction analysis of effectors, such as IQGAPs [12,54,56,57]. Thus, we revisited this issue and have comparatively analyzed the interaction of IQGAP1 GRD with $CDC42^{Q61L}$ and $CDC42^{wt}$ using fluorescence polarization and size exclusion chromatography (SEC). Equilibrium measurements shown in Figure 4B clearly revealed that the Q61L mutation results in a strong enhancement of GRD1 and GRD2 binding with the mGppNHp-bound CDC42, but not with mGDP-bound CDC42. The binding affinity of mGppNHp-bound $CDC42^{Q61L}$ rises from a low affinity 186 μM/69 μM binding to a high 2.7 μM/2.5 μM binding for GRD1/GRD2, respectively (Figures 4B and S7). This is a change of 30–50-fold and might explain the huge differences of CDC42 interactions with GRD. Moreover, SEC analysis showed that GRD1 forms a 2:2 stoichiometry with $CDC42^{wt}$ GppNHp but 2:1 stoichiometry with $CDC42^{Q61L}$ GppNHp (Figure 4C–F).The latter is remarkably consistent with the previous reports on a high-affinity binding of IQGAP2 GRD2 with $CDC42^{Q61L}$ GTP and 4:2 and 2:1 stoichiometry, respectively [12,54]. These findings verified the clear difference between $CDC42^{wt}$ and $CDC42^{Q61L}$ and how replacement of Q61 by L changes the binding properties (affinity and stoichiometry) of CDC42 interaction with IQGAP GRDs.

Chen et al. have reported that the Q61L mutation strengthen hydrogen bond interactions between CDC42 and the γ-phosphate of GTP [66]. Analyzing the $Cdc42^{Q61L}$ GTP GRD2 structure, Ozdemir et al. proposed that CDC42 IH binding to the GAPex-domain induces allosteric changes in the RASGAP site, which in turn facilitate GRD dimerization, and enable the second $CDC42^{Q61L}$ to bind to this site (yielding a 2:1 stoichiometry) [54]. Collectively, we recapitulate that $CDC42^{Q61L}$ is not an ideal analog of $CDC42^{wt}$ especially in studying the interaction of the downstream effectors. G12V and Q61L mutations of CDC42 cause GAP insensitivity leading to sustained hyperactivation of CDC42 [16,18,55,65,66]. Thus, we suggest $CDC42^{wt}$ GppNHp and even $CDC42^{G12V}$ GTP variants as more suitable species for the investigation of CDC42-effector interaction rather than $CDC42^{Q61L}$ GTP.

2.5. GRD Lacks the Structural Fingerprints to Induce the GAP Activity

The structure of the RAS-RASGAP complex shows GAP-334 interacting predominantly with the switch regions of RAS [55]. Three regions (finger loop, FLR motif and helix α7/variable loop) constitute structural fingerprints of the RASGAP p120 and neurofibromin that form critical RAS binding sites in order to apply an arginine finger into the active center of RAS [67,68]. Amino acid sequence analysis of these RASGAPs with the three IQGAP paralogs showed that major parts of these fingerprints are different in IQGAPs (Figure 5A). Moreover, the catalytic arginine is missing and there is instead a threonine (T1045 in IQGAP1; Figure 5A). Thus, it is quite understandable why IQGAP1 did not display RASGAP activities towards HRAS [60]. It is, however, known that GAPs specific for other members of the RAS superfamily use other catalytic residues than an arginine (reviewed in [69,70]).

We set out to examine a possible GAP activity of IQGAP1 GRD towards different RAS family GTPases. Figure 5B shows that IQGAP1 GRD is a pseudo-RASGAP domain with no obvious catalytic ability (orange bars). Earlier studies have shown that the substitution of the arginine finger of the RASGAPs to other amino acids completely abolishes their GAP activity [67,68]. Therefore, threonine 1046 of IQGAP1 GRD was replaced by an arginine and the impact of T1046R on the GTP hydrolysis of the eight RAS proteins was measured. Data shown in Figure 5B revealed no apparent GAP activities of $IQGAP1\ GRD^{T1046R}$ (green bars)

as expected for a RASGAP. These data suggest that IQGAPs, besides lacking an arginine finger, do not contain critical RAS-binding residues of the a7/variable loop (Figure 5A).

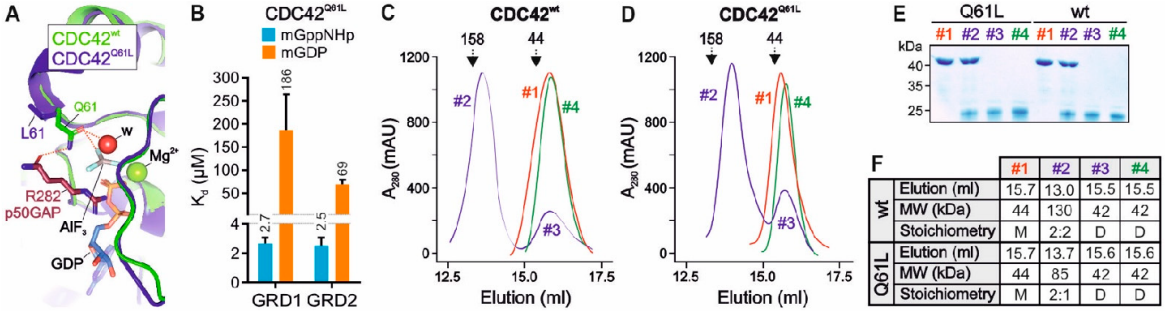

Figure 4. Comparative analysis of IQGAP1 GRD1 interaction with $CDC42^{Q61L}$ and $CDC42^{wt}$. (**A**) Structural overlay of $CDC42^{wt}$ GDP AlF_3 p50GAP (green; PDB: 1GRN) on $CDC42^{Q61L}$ GTP IQGAP2 (blue; PDB: 5CJP) with the focus on Q61 hydrogen bonds (red dashed lines). GDP AlF_3 mimics the transition state of the GTP hydrolysis reaction and is coordinated with the magnesium ion (Mg^{2+}) and the nucleophilic water molecule (w) and the arginine finger (R282) of p50GAP. Aluminum trifluoride (AlF_3) mimics the γ-phosphate of GTP in the transition state. In contrast to L61, Q61 is critical for the catalysis of the GTP hydrolysis reaction through three hydrogen bonds (see text). (**B**) Fluorescence polarization data of IQGAP GRD1 with CDC42 mGppNHp and CDC42 mGDP. (**C**–**F**) IQGAP GRD differently forms complexes with $CDC42^{WT}$ and $CDC42^{Q61L}$, respectively, when applied on an analytical SEC. For this purpose, $CDC42^{WT}$ GppNHp (**C**) or $CDC42^{Q61L}$ GppNHp (**D**) were mixed with IQGAP1 GRD1 and SEC was performed on a Superdex 200 10/300 column using an ÄKTA purifier (flow rate of 0.5 mL/min, fraction volume of 0.5 mL) and a buffer, containing 30 mM Tris/HCl, pH 7.5, 150 mM NaCl, and 5 mM $MgCl_2$. The elution profiles represented one peak for the respective CDC42 proteins (#1), two peaks for the respective mixtures of respective CDC42 proteins with GRD (#2 and #3) and one peak for the GRD1 (#4). (**E**) Coomassie brilliant blue staining of the corresponding elution volumes indicated that only peaks #2 contain GRD1 complexes with $CDC42^{WT}$ or $CDC42^{Q61L}$, respectively. Peaks #3 only contain the CDC42 proteins as compared to the peaks #1 and #4. (**F**) The SEC profiles of $CDC42^{WT}$ and $CDC42^{Q61L}$ are summarized for each peak regarding the elution volume, the molecular weight (MW) and the stoichiometry. M stands for monomeric and D for dimeric. The theoretical MWs of CDC42 (21.2 kDa) and GRD (43 kDa) were calculated using the Expasy Protparam tool. The presented MWs for each peak was calculated based on the calibration curve (aldolase 158 kDa and ovalbumin 44 kDa, respectively) and partition coefficient plot (Kav = Ve − V0/Vc − V0) versus the logarithm of MWs; Ve: elution volume number; V0: void volume (8 mL); Vc: geometric column volume (24 mL)). Accordingly, peaks #2 correspond to a heterotetrameric complex between $CDC42^{WT}$ GppNHp and GRD1 with a MW of 130 kDa, and a heterotrimeric complex of GRD and $CDC42^{Q61L}$ GppNHp with a MW of 85 kDa.

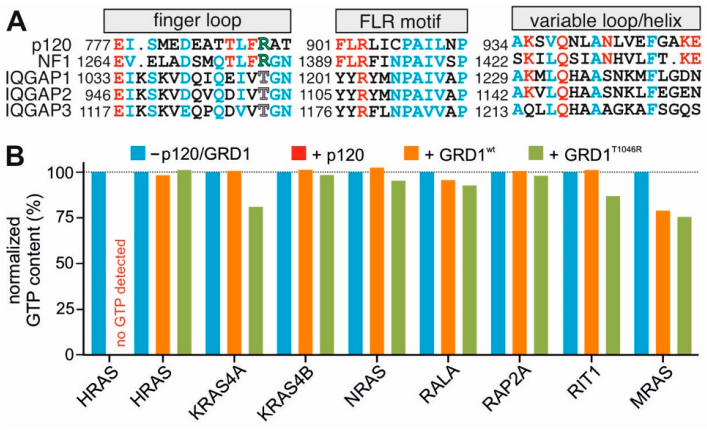

Figure 5. Deviation in RAS-binding residues in GRDs cause lack of RASGAP activity. (**A**) Sequence alignment of human RASGAPs p120, neurofibromin (NF1) and the three IQGAP paralogs highlights distinctive deviations in three signature motifs (grey boxes): the finger loop, FLR region and a7/variable loop. RAS-binding residues are shown in red and conserved residues in blue. The catalytic arginine (green) is substituted by threonine in IQGAPs. The numbers correspond to the amino acids of the respective proteins. (**B**) GTP hydrolysis of various RAS family GTPases was measured in the absence (blue) and in the presence of p120 GAP domain (red; positive control, where no GTP detected) or GRD1^{wt} (orange) and GRD1^{T1046R} (green). The GTP hydrolysis of the RAS proteins (10 μM) was measured via HPLC and the GTP content normalized to 100% before adding p120 or GRD1, respectively, at 100 μM concentrations and 1 min incubation time.

3. Material and Methods

3.1. Constructs

The pGEX4T1 encoding an N-terminal glutathione S-transferase (GST) fusion protein was used to overexpress human IQGAP1 (accession number P46940) GRD1 (aa 962–1345), C794 (aa 863–1657) and CT (aa 1576–1657); human IQGAP2 (accession number Q13576) GRD2 (aa 875–1246) and C795 (aa 780–1575); human IQGAP3 (accession number P60953) GRD3 (aa 942–1330); human CDC42 (accession number P60953; aa 1–178). All constructs and related variants are list in Supplementary Table S1. For purification of these proteins, pGEX-4T1 constructs were transformed in *Escherichia coli* and proteins were isolated via affinity chromatography using a glutathione Sepharose column on a ÄKTA start protein purification system (Cytiva, US) [71]. GST-cleavage was carried out by incubation with thrombin (#T6884-1KU, Sigma Aldrich, Taufkirchen, Germany) at 4 °C until full digestion of the fusion protein. Quality of the proteins were checked via SDS-PAGE and Coomassie staining. CDC42 variants were further verified for their activity in HPLC by determining the amount of bound nucleotide [71]. Nucleotide free proteins were prepared by incubating the proteins with alkaline phosphatase (#P0762-250UN, Sigma Aldrich, Germany) and phosphodiesterase (#P3243-1VL, Sigma Aldrich, Taufkirchen, Germany) at 4 °C [71]. CDC42 variants were labelled with either GDP (#51060, Sigma Aldrich, Taufkirchen, Germany), GppNHp (#NU-401, Jena Bioscience, Jena, Germany), mant-GDP (#NU-204, Jena Bioscience, Jena, Germany) or mant-GppNHp (#NU-207, Jena Bioscience, Jena, Germany).

3.2. Circular Dichroism (CD) Spectrometry

Far-UV-CD spectroscopy of protein samples were performed on a JASCO J-715 CD spectropolarimeter (Jasco, Gross-Umstadt, Germany) using quartz cuvettes (Helma, Mühlheim, Germany) with 1 mm path length. Spectra were recorded at protein concentrations of 20 μM CDC42 WT and variants in 1 mM NaPi buffer, pH 7.0 or 8 μM IQGAP WT and variants in 12.5 mM TRIS/HCl pH 7.4, 37.5 mM NaCl, 1.25 mM $MgCl_2$, at 22 °C with instrument settings as follows: 0.1 nm step size, 50 nm min^{-1} scan speed, 1 nm

band with. Signal-to-noise ratio was improved by accumulation of 10 scans per sample. The mean residue ellipticity $[\theta]_{mrw}$ in deg·cm^2·dmol^{-1} was calculated from the equation $[\theta]_{mrw} = (\theta_{obs} \times MRW)/(c \times d \times 10)$, with θ_{obs}, observed ellipticity (in degrees); c, concentration (in g/mL); d, cell path length (in cm); MRW (mean residue weight), molecular weight divided by number of peptide bonds.

3.3. Cell Culture and Lysis

HEK293 cells were cultured in Dulbecco's Modified Eagle's Medium (DMEM) (# 12320032, Thermo Fisher, Waltham, CA, USA) supplemented with 10 % FBS and 1% Penicillin/Streptomycin in an exponential growth phase at 37 °C with 5% CO_2 and 95% humidity. Lysis was performed by washing the cells with PBS$^{-/-}$ and scraping them down with FISH buffer (50 mM Tris/HCl pH 7.5, 100 mM NaCl, 2 mM $MgCl_2$, 10% glycerol, 20 mM β-glyerolphosphate, 1 mM Na_3VO_4, 1× protease inhibitor cocktail and 1% IGPAL). Cells were lysed for 10 min on ice and then centrifuged for 10 min at 15,000× g. Supernatant was used for affinity pull down measurements.

3.4. GST-Pull-Down

The pull-down of endogenously expressed proteins with purified GST-fused proteins was performed using glutathione agarose beads (#745500.10, Macherey-Nagel, Düren, Germany). Beads were coupled to the GST-fused protein for one hour at 4 °C while mixing and centrifuged for 5 min at 500× g. Excess protein was removed by three washing steps. Coupled beads were incubated with HEK293 lysate for one hour at 4 °C on a rotor and again washed 3 times. In the final step, beads were mixed with 1× Laemmli buffer and proteins were denatured at 95 °C for 5 min. Samples were evaluated via SDS-PAGE and western blotting using anti-GST (own antibody, mouse) and anti-IQGAP1 (NBP1-06529, Novus, Wiesbaden Nordenstadt, Germany, rabbit) primary antibodies and secondary antibodies: IRDye® 800 CW anti-Rabbit IgG and IRDye® 680 RD anti-Mouse IgG from LiCor. Values were analyzed by using multiple t test analysis in GraphPad Prism 6 (one unpaired t test per row, fewer assumptions by analyzing each row individually).

3.5. Fluorescence Stopped-Flow Spectrometry

All kinetic parameters (k_{obs}) evaluated in this study were analyzed using a previously described kinetic analysis protocol [72]. The kinetic parameters were monitored with a stopped-flow apparatus (HiTech Scientific, Applied Photophysics SX20, Leatherhead, UK). The excitation was set for mant at the wavelength of 362 nm, and emission was detected through a cutoff filter of 408 nm. The observed rate constants were calculated by fitting the data as single exponential decay using GraFit program.

3.6. Fluorescence Polarization

To determine the dissociation constant K_d of direct protein–protein interaction (including weak interactions) fluorescence polarization analysis was performed in a Fluoromax 4 fluorimeter (Horiba Scientific, Loos, France). Here, 1 µM mant-GDP or mant-GppNHp labelled CDC42 proteins were prepared in a total volume of 170 µL in a three directional cuvette. Measurement was performed in polarization mode versus time with an excitation wavelength of 360 nm (slit width: 8 µm) and an emission wavelength of 450 nm (slit width: 10 µm). K_d values were calculated in GraFit 5 by fitting the concentration-dependent binding curve using a quadratic ligand binding equation.

3.7. GTP Hydrolysis Measurements

GTP hydrolysis rates of a set of different GTPases in presence and absence of GRD1 and its T1046R mutant containing the arginine residue were measured by high-performance liquid chromatography (HPLC) analysis. GTP-bound HRAS in presence of p120 GAP was used as control. Then, 10 µM of each GTPase in the GTP bound state was injected into the HPLC mixing chamber after 1 min of incubation in absence (intrinsic) and presence

(GAP stimulated) of 100 µM of GRD1 WT and T1046R variant. The GTP content for each measurement was calculated by dividing the intensity of the GTP detection peak to the sum of the intensities of the GTP plus GDP peaks.

4. Conclusions

The exact binding site of the IQGAP GRD and CDC42 is still not completely clear to date. This article provides evidence that the IQGAP GRD does not act as the primary or leading effector binding domain of CDC42 and counterevidence the role of IQGAP GRD in CDC42 binding deduced from a crystal structure of an IQGAP2 GRD2-CDC42Q61L GTP complex. We could show that the GRD does not bind to CDC42 in a nucleotide-dependent manner and that even multiple mutations of the suggested main residues of interaction do not abolish the direct physical interaction in cells and under cell-free conditions. Our data support the binding model of Ozdemir et al. [54] and propose the CDC42 IH as a key binding site for GRD. Furthermore, we shed light once more into the interaction difference of $CDC42^{wt}$ and $CDC42^{Q61L}$ that might be one of the main reasons of the discrepancies in the published data as discussed above. By our comparative measurements of IQGAP1 and IQGAP2 variants, we found differences in their binding strength and specificity towards $CDC42^{wt}$ but also towards various CDC42 variants. Our efforts to investigate also IQGAP3 were so far not successful. The exact binding residues and interaction sites of IQGAP1 and IQGAP2 with the switch regions of CDC42 will still remain to be identified in the future.

Supplementary Materials: The following supporting information can be downloaded at: https://www.mdpi.com/article/10.3390/ijms23168842/s1.

Author Contributions: M.R.A. conceived and coordinated the study; N.M., S.P., F.B., N.S.K.J. and O.H.F.K. designed, performed and analyzed the experiments; N.M., L.G. and D.W. performed the CD experiments; R.D. performed structural analysis; N.M. and M.R.A. directed the experiments, analyzed the data and wrote the paper. All authors have read and agreed to the published version of the manuscript.

Funding: This study was supported by the European Network on Noonan Syndrome and Related Disorders (NSEuroNet, grant number: 01GM1621B to N.S.K.J. and M.R.A.), the German Research Foundation (Deutsche Forschungsgemeinschaft or DFG) through the International Research Training Group 'Intra- and interorgan communication of the cardiovascular system' (grant number: IRTG 1902-p6 701158241 to F.B. and M.R.A.), the German Federal Ministry of Education and Research (BMBF)—German Network of RASopathy Research (GeNeRARe, grant numbers: 01GM1902C to N.M. and M.R.A.), the Research Committee of the Medical Faculty of the Heinrich Heine University (grant number: 9772764 to S.P. and M.R.A) and the Operational Program Integrated Infrastructure ERDF: Open scientific community for modern interdisciplinary research in medicine (OPENMED; grant number: ITMS2014+: 313011V455 to R.D.).

Institutional Review Board Statement: Not applicable.

Informed Consent Statement: Not applicable.

Data Availability Statement: All the data are in the manuscript.

Acknowledgments: We thank Roland Piekorz and Kotsene Loumonvi for support and discussions.

Conflicts of Interest: The authors declare no conflict of interest.

References

1. Ahmadian, M.R.; Jaiswal, M.; Fansa, E.K.; Dvorsky, R. New insight into the molecular switch mechanism of human Rho family proteins: Shifting a paradigm. *Biol. Chem.* **2013**, *394*, 89–95. [CrossRef]
2. Mosaddeghzadeh, N.; Ahmadian, M.R. The RHO Family GTPases: Mechanisms of Regulation and Signaling. *Cells* **2021**, *10*, 1831. [CrossRef] [PubMed]
3. Abdul-Manan, N.; Aghazadeh, B.; Liu, G.A.; Majumdar, A.; Ouerfelli, O.; Simlnovitch, K.A.; Rosen, M.K. Structure of Cdc42 in complex with the GTPase-binding domain of the "Wiskott-Aldrich syndrome" protein. *Nature* **1999**, *399*, 379–383. [CrossRef] [PubMed]

4. Mott, H.R.; Owen, D.; Nietlispach, D.; Lowe, P.N.; Manser, E.; Lim, L.; Laue, E.D. Structure of the small G protein Cdc42 bound to the GTpasebinding domain of ACK. *Nature* **1999**, *399*, 384–388. [CrossRef]
5. Nouri, K.; Timson, D.J.; Ahmadian, M.R. New model for the interaction of IQGAP1 with CDC42 and RAC1. *Small GTPases* **2020**, *11*, 16–22. [CrossRef]
6. Morreale, A.; Venkatesan, M.; Mott, H.R.; Owen, D.; Nietlispach, D.; Lowe, P.N.; Laue, E.D. Structure of Cdc42 bound to the GTPase binding domain of PAK. *Nat. Struct. Biol.* **2000**, *7*, 384–388. [CrossRef]
7. Dvorsky, R.; Ahmadian, M.R. Always look on the bright site of Rho: Structural implications for a conserved intermolecular interface. *EMBO Rep.* **2004**, *5*, 1130–1136. [CrossRef]
8. Dvorsky, R.; Blumenstein, L.; Vetter, I.R.; Ahmadian, M.R. Structural Insights into the Interaction of ROCKI with the Switch Regions of RhoA. *J. Biol. Chem.* **2004**, *279*, 7098–7104. [CrossRef] [PubMed]
9. Hemsath, L.; Dvorsky, R.; Fiegen, D.; Carlier, M.F.; Ahmadian, M.R. An electrostatic steering mechanism of Cdc42 recognition by Wiskott-Aldrich syndrome proteins. *Mol. Cell* **2005**, *20*, 313–324. [CrossRef]
10. Rose, R.; Weyand, M.; Lammers, M.; Ishizaki, T.; Ahmadian, M.R.; Wittinghofer, A. Structural and mechanistic insights into the interaction between Rho and mammalian Dia. *Nature* **2005**, *435*, 513–518. [CrossRef]
11. Hall, A. Rho family GTPases. In *Biochemical Society Transactions*; Portland Press: London, UK, 2012; Volume 40, pp. 1378–1382.
12. LeCour, L.; Boyapati, V.K.; Liu, J.; Li, Z.; Sacks, D.B.; Worthylake, D.K. The Structural Basis for Cdc42-Induced Dimerization of IQGAPs. *Structure* **2016**, *24*, 1499–1508. [CrossRef] [PubMed]
13. Owen, D.; Mott, H.R. CRIB effector disorder: Exquisite function from chaos. *Biochem. Soc. Trans.* **2018**, *46*, 1289–1302. [CrossRef] [PubMed]
14. Mott, H.R.; Owen, D. Structures of Ras superfamily effector complexes: What have we learnt in two decades? *Crit. Rev. Biochem. Mol. Biol.* **2015**, *50*, 85–133. [CrossRef] [PubMed]
15. Thapar, R.; Karnoub, A.E.; Campbell, S.L. Structural and Biophysical Insights into the Role of the Insert Region in Rac1 Function. *Biochemistry* **2002**, *41*, 3875–3883. [CrossRef] [PubMed]
16. Haspel, N.; Jang, H.; Nussinov, R. Active and Inactive Cdc42 Differ in Their Insert Region Conformational Dynamics. *Biophys. J.* **2021**, *120*, 306. [CrossRef] [PubMed]
17. Wu, W.J.; Leonard, D.A.; Cerione, R.A.; Manor, D. Interaction between Cdc42Hs and RhoGDI Is Mediated through the Rho Insert Region. *J. Biol. Chem.* **1997**, *272*, 26153–26158. [CrossRef]
18. Nassar, N.; Hoffman, G.R.; Manor, D.; Clardy, J.C.; Cerione, R.A. Structures of Cdc42 bound to the active and catalytically compromised forms of Cdc42GAP. *Nat. Struct. Biol.* **1998**, *5*, 1047–1052. [CrossRef] [PubMed]
19. Lammers, M.; Meyer, S.; Kühlmann, D.; Wittinghofer, A. Specificity of Interactions between mDia Isoforms and Rho Proteins. *J. Biol. Chem.* **2008**, *283*, 35236–35246. [CrossRef] [PubMed]
20. Kühn, S.; Erdmann, C.; Kage, F.; Block, J.; Schwenkmezger, L.; Steffen, A.; Rottner, K.; Geyer, M. The structure of FMNL2–Cdc42 yields insights into the mechanism of lamellipodia and filopodia formation. *Nat. Commun.* **2015**, *6*, 7088. [CrossRef] [PubMed]
21. Walker, S.J.; Brown, H.A. Specificity of Rho insert-mediated activation of phospholipase D1. *J. Biol. Chem.* **2002**, *277*, 26260–26267. [CrossRef] [PubMed]
22. Karnoub, A.E.; Der, C.J.; Campbell, S.L. The Insert Region of Rac1 Is Essential for Membrane Ruffling but Not Cellular Transformation. *Mol. Cell. Biol.* **2001**, *21*, 2847–2857. [CrossRef] [PubMed]
23. Zong, H.; Kaibuchi, K.; Quilliam, L.A. The Insert Region of RhoA Is Essential for Rho Kinase Activation and Cellular Transformation. *Mol. Cell. Biol.* **2001**, *21*, 5287–5298. [CrossRef] [PubMed]
24. Fukata, M.; Watanabe, T.; Noritake, J.; Nakagawa, M.; Yamaga, M.; Kuroda, S.; Matsuura, Y.; Iwamatsu, A.; Perez, F.; Kaibuchi, K. Rac1 and Cdc42 capture microtubules through IQGAP1 and CLIP-170. *Cell* **2002**, *109*, 873–885. [CrossRef]
25. Watanabe, T.; Wang, S.; Noritake, J.; Sato, K.; Fukata, M.; Takefuji, M.; Nakagawa, M.; Izumi, N.; Akiyama, T.; Kaibuchi, K. Interaction with IQGAP1 links APC to Rac1, Cdc42, and actin filaments during cell polarization and migration. *Dev. Cell* **2004**, *7*, 871–883. [CrossRef] [PubMed]
26. Mosaddeghzadeh, N.; Nouri, K.; Krumbach, O.H.F.; Amin, E.; Dvorsky, R.; Ahmadian, M.R. Selectivity determinants of rho gtpase binding to iqgaps. *Int. J. Mol. Sci.* **2021**, *22*, 12596. [CrossRef] [PubMed]
27. Roy, M.; Li, Z.; Sacks, D.B. IQGAP1 Binds ERK2 and Modulates Its Activity. *J. Biol. Chem.* **2004**, *279*, 17329–17337. [CrossRef] [PubMed]
28. Roy, M.; Li, Z.; Sacks, D.B. IQGAP1 Is a Scaffold for Mitogen-Activated Protein Kinase Signaling. *Mol. Cell. Biol.* **2005**, *25*, 7940. [CrossRef] [PubMed]
29. Ren, J.G.; Li, Z.; Sacks, D.B. IQGAP1 modulates activation of B-Raf. *Proc. Natl. Acad. Sci. USA* **2007**, *104*, 10465–10469. [CrossRef] [PubMed]
30. Benseñor, L.B.; Kan, H.M.; Wang, N.; Wallrabe, H.; Davidson, L.A.; Cai, Y.; Schafer, D.A.; Bloom, G.S. IQGAP1 regulates cell motility by linking growth factor signaling to actin assembly. *J. Cell Sci.* **2007**, *120*, 658–669. [CrossRef] [PubMed]
31. Le Clainche, C.; Schlaepfer, D.; Ferrari, A.; Klingauf, M.; Grohmanova, K.; Veligodskiy, A.; Didry, D.; Le, D.; Egile, C.; Carlier, M.F.; et al. IQGAP1 stimulates actin assembly through the N-wasp-Arp2/3 pathway. *J. Biol. Chem.* **2007**, *282*, 426–435. [CrossRef]
32. Kaur, R.; Yuan, X.; Lu, M.L.; Balk, S.P. Increased PAK6 expression in prostate cancer and identification of PAK6 associated proteins. *Prostate* **2008**, *68*, 1510–1516. [CrossRef]

33. Usatyuk, P.V.; Gorshkova, I.A.; He, D.; Zhao, Y.; Kalari, S.K.; Garcia, J.G.N.; Natarajan, V. Phospholipase D-mediated Activation of IQGAP1 through Rac1 regulates hyperoxia-induced p47phox translocation and reactive oxygen species generation in lung endothelial cells. *J. Biol. Chem.* **2009**, *284*, 15339–15352. [CrossRef] [PubMed]
34. Pelikan-Conchaudron, A.; Le Clainche, C.; Didry, D.; Carlier, M.F. The IQGAP1 protein is a calmodulin-regulated barbed end capper of actin filaments: Possible implications in its function in cell migration. *J. Biol. Chem.* **2011**, *286*, 35119–35128. [CrossRef] [PubMed]
35. Pudewell, S.; Wittich, C.; Kazemein Jasemi, N.S.; Bazgir, F.; Ahmadian, M.R. Accessory proteins of the RAS-MAPK pathway: Moving from the side line to the front line. *Commun. Biol.* **2021**, *4*, 696. [CrossRef] [PubMed]
36. Watanabe, T.; Wang, S.; Kaibuchi, K. IQGAPs as Key Regulators of Actin-cytoskeleton Dynamics Mini-review and Review. *Cell Struct. Funct.* **2015**, *40*, 69–77. [CrossRef]
37. Abel, A.M.; Schuldt, K.M.; Rajasekaran, K.; Hwang, D.; Riese, M.J.; Rao, S.; Thakar, M.S.; Malarkannan, S. IQGAP1: Insights into the function of a molecular puppeteer. *Mol. Immunol.* **2015**, *65*, 336–349. [CrossRef] [PubMed]
38. Hedman, A.C.; Smith, J.M.; Sacks, D.B. The biology of IQGAP proteins: Beyond the cytoskeleton. *EMBO Rep.* **2015**, *16*, 427–446. [CrossRef] [PubMed]
39. Smith, J.M.; Hedman, A.C.; Sacks, D.B. IQGAPs choreograph cellular signaling from the membrane to the nucleus. *Trends Cell Biol.* **2015**, *25*, 171–184. [CrossRef]
40. Choi, S.; Anderson, R.A. IQGAP1 is a phosphoinositide effector and kinase scaffold. *Adv. Biol. Regul.* **2016**, *60*, 29–35. [CrossRef] [PubMed]
41. Tanos, B.E.; Yeaman, C.; Rodriguez-Boulan, E. An emerging role for IQGAP1 in tight junction control. *Small GTPases* **2018**, *9*, 375–383. [CrossRef] [PubMed]
42. Nussinov, R.; Zhang, M.; Tsai, C.J.; Jang, H. Calmodulin and IQGAP1 activation of PI3Kα and Akt in KRAS, HRAS and NRAS-driven cancers. *Biochim. Biophys. Acta Mol. Basis Dis.* **2018**, *1864*, 2304–2314. [CrossRef] [PubMed]
43. White, C.D.; Li, Z.; Dillon, D.A.; Sacks, D.B. IQGAP1 Protein Binds Human Epidermal Growth Factor Receptor 2 (HER2) and Modulates Trastuzumab Resistance. *J. Biol. Chem.* **2011**, *286*, 29734. [CrossRef] [PubMed]
44. Liu, C.; Billadeau, D.D.; Abdelhakim, H.; Leof, E.; Kaibuchi, K.; Bernabeu, C.; Bloom, G.S.; Yang, L.; Boardman, L.; Shah, V.H.; et al. IQGAP1 suppresses TβRII-mediated myofibroblastic activation and metastatic growth in liver. *J. Clin. Investig.* **2013**, *123*, 1138–1156. [CrossRef] [PubMed]
45. Jameson, K.L.; Mazur, P.K.; Zehnder, A.M.; Zhang, J.; Zarnegar, B.; Sage, J.; Khavari, P.A. IQGAP1 scaffold-kinase interaction blockade selectively targets RAS-MAP kinase–driven tumors. *Nat. Med.* **2013**, *19*, 626–630. [CrossRef] [PubMed]
46. Choi, S.; Hedman, A.C.; Sayedyahossein, S.; Thapa, N.; Sacks, D.B.; Anderson, R.A. Agonist-stimulated phosphatidylinositol-3,4,5-trisphosphate generation by scaffolded phosphoinositide kinases. *Nat. Cell Biol.* **2016**, *18*, 1324–1335. [CrossRef] [PubMed]
47. Peng, X.; Wang, T.; Gao, H.; Yue, X.; Bian, W.; Mei, J.; Zhang, Y. The interplay between IQGAP1 and small GTPases in cancer metastasis. *Biomed. Pharmacother.* **2021**, *135*, 111243. [CrossRef]
48. Wei, T.; Lambert, P.F. Role of IQGAP1 in Carcinogenesis. *Cancers* **2021**, *13*, 3940. [CrossRef]
49. Rotoli, D.; Díaz-Flores, L.; Gutiérrez, R.; Morales, M.; Ávila, J.; Martín-Vasallo, P. AmotL2, IQGAP1, and FKBP51 Scaffold Proteins in Glioblastoma Stem Cell Niches. *J. Histochem. Cytochem.* **2022**, *70*, 9–16. [CrossRef]
50. Elliott, S.F. Biochemical analysis of the interactions of IQGAP1 C-terminal domain with CDC42. *World J. Biol. Chem.* **2012**, *3*, 53. [CrossRef]
51. Nouri, K.; Fansa, E.K.; Amin, E.; Dvorsky, R.; Gremer, L.; Willbold, D.; Schmitt, L.; Timson, D.J.; Ahmadian, M.R. IQGAP1 interaction with RHO family proteins revisited kinetic and equilibrium evidence for multiple distinct binding sites. *J. Biol. Chem.* **2016**, *291*, 26364–26376. [CrossRef]
52. Swart-Mataraza, J.M.; Li, Z.; Sacks, D.B. IQGAP1 is a component of Cdc42 signaling to the cytoskeleton. *J. Biol. Chem.* **2002**, *277*, 24753–24763. [CrossRef] [PubMed]
53. Li, R.; Debreceni, B.; Jia, B.; Gao, Y.; Tigyi, G.; Zheng, Y. Localization of the PAK1-, WASP-, and IQGAP1-specifying regions of Cdc42. *J. Biol. Chem.* **1999**, *274*, 29648–29654. [CrossRef] [PubMed]
54. Sila Ozdemir, E.; Jang, H.; Gursoy, A.; Keskin, O.; Li, Z.; Sacks, D.B.; Nussinov, R. Unraveling the molecular mechanism of interactions of the Rho GTPases Cdc42 and Rac1 with the scaffolding protein IQGAP2. *J. Biol. Chem.* **2018**, *293*, 3685–3699. [CrossRef] [PubMed]
55. Scheffzek, K.; Ahmadian, M.R.; Kabsch, W.; Wiesmüller, L.; Lautwein, A.; Schmitz, F.; Wittinghofer, A. The Ras-RasGAP complex: Structural basis for GTPase activation and its loss in oncogenic ras mutants. *Science* **1997**, *277*, 333–338. [CrossRef] [PubMed]
56. Owen, D.; Campbell, L.J.; Littlefield, K.; Evetts, K.A.; Li, Z.; Sacks, D.B.; Lowe, P.N.; Mott, H.R. The IQGAP1-Rac1 and IQGAP1-Cdc42 interactions: Interfaces differ between the complexes. *J. Biol. Chem.* **2008**, *283*, 1692–1704. [CrossRef]
57. Kurella, V.B.; Richard, J.M.; Parke, C.L.; LeCour, L.F.; Bellamy, H.D.; Worthylake, D.K. Crystal structure of the GTPase-activating protein-related domain from IQGAP1. *J. Biol. Chem.* **2009**, *284*, 14857–14865. [CrossRef]
58. Gorisse, L.; Li, Z.; Wagner, C.D.; Worthylake, D.K.; Zappacosta, F.; Hedman, A.C.; Annan, R.S.; Sacks, D.B. Ubiquitination of the scaffold protein IQGAP1 diminishes its interaction with and activation of the Rho GTPase CDC42. *J. Biol. Chem.* **2020**, *295*, 4822–4835. [CrossRef]

59. McCallum, S.J.; Wu, W.J.; Cerione, R.A. Identification of a putative effector for Cdc42Hs with high sequence similarity to the RasGAP-related protein IQGAP1 and a Cdc42Hs binding partner with similarity to IQGAP2. *J. Biol. Chem.* **1996**, *271*, 21732–21737. [CrossRef]
60. Hart, M.J.; Callow, M.G.; Souza, B.; Polakis, P. IQGAP1, a calmodulin-binding protein with a rasGAP-related domain, is a potential effector for cdc42Hs. *EMBO J.* **1996**, *15*, 2997–3005. [CrossRef]
61. Zhang, B.; Chernoff, J.; Zheng, Y. Interaction of Rac1 with GTPase-activating proteins and putative effectors. A comparison with Cdc42 and RhoA. *J. Biol. Chem.* **1998**, *273*, 8776–8782. [CrossRef]
62. Kuroda, S.; Fukata, M.; Nakagawa, M.; Fujii, K.; Nakamura, T.; Ookubo, T.; Izawa, I.; Nagase, T.; Nomura, N.; Tani, H.; et al. Cdc42 and Rac1 Regulate the Interaction of IQGAP1 with $\hat{I}^2$-Catenin. *J. Biol. Chem.* **1999**, *274*, 26044–26050. [CrossRef]
63. Grohmanova, K.; Schlaepfer, D.; Hess, D.; Gutierrez, P.; Beck, M.; Kroschewski, R. Phosphorylation of IQGAP1 modulates its binding to Cdc42, revealing a new type of Rho-GTPase regulator. *J. Biol. Chem.* **2004**, *279*, 48495–48504. [CrossRef] [PubMed]
64. Mataraza, J.M.; Briggs, M.W.; Li, Z.; Frank, R.; Sacks, D.B. Identification and characterization of the Cdc42-binding site of IQGAP1. *Biochem. Biophys. Res. Commun.* **2003**, *305*, 315–321. [CrossRef]
65. Scheffzek, K.; Ahmadian, M.R.; Wittinghofer, A. GTPase-activating proteins: Helping hands to complement an active site. *Trends Biochem. Sci.* **1998**, *23*, 257–262. [CrossRef]
66. Chen, S.; Shu, L.; Zhao, R.; Zhao, Y. Molecular dynamics simulations reveal the activation mechanism of mutations G12V and Q61L of Cdc42. *Proteins Struct. Funct. Bioinform.* **2022**, *90*, 1376–1389. [CrossRef]
67. Ahmadian, M.R.; Stege, P.; Scheffzek, K.; Wittinghofer, A. Confirmation of the arginine-finger hypothesis for the GAP-stimulated GTP-hydrolysis reaction of Ras. *Nat. Struct. Biol.* **1997**, *4*, 686–689. [CrossRef] [PubMed]
68. Ahmadian, M.R.; Kiel, C.; Stege, P.; Scheffzek, K. Structural fingerprints of the Ras-GTPase activating proteins neurofibromin and p120GAP. *J. Mol. Biol.* **2003**, *329*, 699–710. [CrossRef]
69. Scheffzek, K.; Shivalingaiah, G. Ras-specific gtpase-activating proteins— structures, mechanisms, and interactions. *Cold Spring Harb. Perspect. Med.* **2019**, *9*, a031500. [CrossRef]
70. Scheffzek, K.; Ahmadian, M.R. GTPase activating proteins: Structural and functional insights 18 years after discovery. *Cell. Mol. Life Sci.* **2005**, *62*, 3014–3038. [CrossRef]
71. Jaiswal, M.; Dubey, B.N.; Koessmeier, K.T.; Gremer, L.; Ahmadian, M.R. Biochemical assays to characterize Rho GTPases. *Methods Mol. Biol.* **2012**, *827*, 37–58. [CrossRef]
72. Hemsath, L.; Ahmadian, M.R. Fluorescence approaches for monitoring interactions of Rho GTPases with nucleotides, regulators, and effectors. *Methods* **2005**, *37*, 173–182. [CrossRef] [PubMed]

7. NEW MECHANISTIC INSIGHTS INTO THE RAS-SIN1 INTERACTION AT THE MEMBRANE

Article

Silke Pudewell, Jana Lissy, Hossein Nakhaeizadeh, Niloufar Mosaddeghzadeh, Saeideh Nakhaei-Rad, Radovan Dvorsky, Mohammad R. Ahmadian

doi: 10.3389/fcell.2022.987754

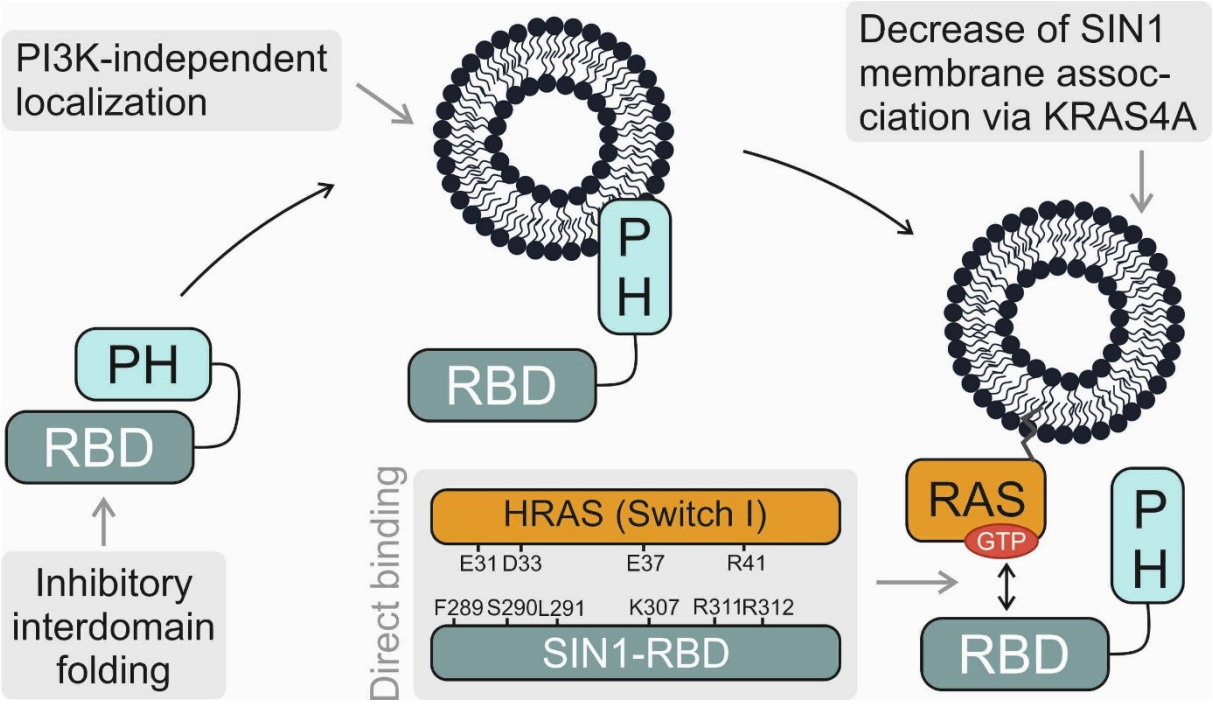

Journal:	Frontiers in Cell and Developmental Biology (accepted)
Published:	accepted on 20 September 2022
Impact factor:	6.081
Own contribution:	70%

Cloning, protein purification, fluorescence polarization, PIP-Strip assay, liposome sedimentation assay, flotation assay, western blotting, cell culture, insect cell culture, partial fractionation, preparation and illustration of figures, concept and preparation of the manuscript, reference management, discussion and conclusions

frontiers | Frontiers in Cell and Developmental Biology

TYPE Original Research
PUBLISHED XX XX 2022
DOI 10.3389/fcell.2022.987754

OPEN ACCESS

EDITED BY
M. Cecilia Caino,
University of Colorado Anschutz Medical Campus, United States

REVIEWED BY
Ignacio Rubio,
University Hospital Jena, Germany
Daniel Abankwa,
University of Luxembourg, Luxembourg
Enzo Martegani,
University of Milano-Bicocca, Italy

*CORRESPONDENCE
Mohammad R. Ahmadian,
reza.ahmadian@hhu.de

SPECIALTY SECTION
This article was submitted to Signaling, a section of the journal Frontiers in Cell and Developmental Biology

RECEIVED 06 July 2022
ACCEPTED 20 September 2022
PUBLISHED XX XX 2022

CITATION
Pudewell S, Lissy J, Nakhaeizadeh H, Mosaddeghzadeh N, Nakhaei-Rad S, Dvorsky R and Ahmadian MR (2022), New mechanistic insights into the RAS-SIN1 interaction at the membrane. *Front. Cell Dev. Biol.* 10:987754. doi: 10.3389/fcell.2022.987754

New mechanistic insights into the RAS-SIN1 interaction at the membrane

Silke Pudewell[1], Jana Lissy[1], Hossein Nakhaeizadeh[1], Niloufar Mosaddeghzadeh[1], Saeideh Nakhaei-Rad[1,2], Radovan Dvorsky[1,3] and Mohammad R. Ahmadian[1]*

[1]Institute of Biochemistry and Molecular Biology II, Medical Faculty and University Hospital Düsseldorf, Heinrich Heine University Düsseldorf, Düsseldorf, Germany, [2]Stem Cell Biology and Regenerative Medicine Research Group, Institute of Biotechnology, Ferdowsi University of Mashhad, Mashhad, Iran, [3]Center for Interdisciplinary Biosciences, P. J. Šafárik University, Košice, Slovakia

Stress-activated MAP kinase-interacting protein 1 (SIN1) is a central member of the mTORC2 complex that contains an N-terminal domain (NTD), a conserved region in the middle (CRIM), a RAS-binding domain (RBD), and a pleckstrin homology domain Recent studies provided valuable structural and functional insights into the interactions of SIN1 and RAS-binding domain with RAS proteins. However, the mechanism for a reciprocal interaction of the RBD-PH tandem with RAS proteins and membrane as upstream events to spatiotemporal mTORC2 regulation is not clear. The biochemical assays in this study led to the following results: 1) all classical RAS paralogs, including HRAS, KRAS4A, KRAS4B, and NRAS, can bind to SIN1-RBD in biophysical and SIN1 full-length (FL) in cell biology experiments; 2) the SIN1-PH domain modulates interactions with various types of membrane phosphoinositides and constantly maintains a pool of SIN1 at the membrane; and 3) a KRAS4A-dependent decrease in membrane binding of the SIN1-RBD-PH tandem was observed, suggesting for the first time a mechanistic influence of KRAS4A on SIN1 membrane association. Our study strengthens the current mechanistic understanding of SIN1-RAS interaction and suggests membrane interaction as a key event in the control of mTORC2-dependent and mTORC2-independent SIN1 function.

KEYWORDS

Ras, Ras family, Sin1, MAPKAP1, mTORC2, ras binding domain, PH domain, membrane binding

1 Introduction

Mammalian target of rapamycin complexes (mTORC) one and two are key regulators of many cellular processes in response to a broad spectrum of extracellular stimuli (Brown et al., 1994; Huang and Fingar, 2014; Saxton and Sabatini, 2017). mTORC1 mediates the control of cell growth through the activation of anabolic processes, whereas mTORC2 facilitates the spatial control of cell survival, cell growth, and actin cytoskeleton organization through the phosphorylation of AGC family protein kinases, including AKT, SGK, and PKC (Loewith et al., 2002; Jacinto et al., 2004;

Pearce, Komander and Alessi, 2010; Saxton and Sabatini, 2017). The catalytic subunit of both complexes is mTOR which contains a serine/threonine kinase domain.

The stress-activated MAP kinase-interacting protein 1 (SIN1) is one of the four conserved components of the mTORC2 complex, which consists of SIN1, mTOR, mLST8, RICTOR and can associate with the accessory proteins PROTOR and DEPTOR (Oh and Jacinto, 2011). Little is known about the upstream regulators of mTORC2 but it is shown that its regulation and activity depend on its subcellular localization and it is found in multiple pools in the cytosol, plasma membrane, early and late endosomes, and mitochondria (Ebner et al., 2017; Fu and Hall, 2020). The activity of the mTORC2 complex specifically depends on its components (Chen et al., 2018; Stuttfeld et al., 2018; Scaiola et al., 2020; Tafur, Kefauver and Loewith, 2020). MLST8 functions as a scaffold to maintain mTORC2 integrity and kinase activity (Hwang et al., 2019), whereas RICTOR acts as an essential core for mTORC2 complex formation (Gao et al., 2021). The role of PROTOR as a novel RICTOR-binding subunit of mTORC2 is yet unclear (Pearce et al., 2007). DEPTOR appears to block mTORC2 activity (Peterson et al., 2009), a process that is prevented by its tyrosine phosphorylation (Gagné et al., 2021). SIN1 is required for mTORC2 activity and may function by regulating mTOR association with membranes (Frias et al., 2006; Yang et al., 2006; Liu et al., 2013, 2014; Yuan et al., 2015; Yuan and Guan, 2015). SIN1-NTD interacts tightly with RICTOR and mLST8 in an extended conformation and links RICTOR to mLST8 (Scaiola et al., 2020). The increase in RICTOR ubiquitination prevented RICTOR and mSIN1 from interacting with mTOR while leaving the interaction between RICTOR and mSIN1 unaffected (Wrobel et al., 2020). In contrast to NTD and CRIM domains, RBD and PH domains of SIN1 remain flexibly disposed of this complex (Scaiola et al., 2020).

Phosphoinositide 3-kinase (PI3K)-dependent activation is partially executed at the plasma membrane in response to extracellular growth factors, which can trigger the recruitment of the effector AKT to the membrane. Insulin-PI3K signaling induces furthermore the association of mTORC2 with ribosomes, which activates the complex and may be part of the co-translational phosphorylation of AKT and PKC (Oh et al., 2010; Zinzalla et al., 2011). The role of SIN1 in the regulation and activation of mTORC2 is complex and predominantly involves the RAS-binding domain (RBD) and the pleckstrin homology (PH) domain. The other two domains, the N-terminal domain (NTD) and the conserved region in the middle (CRIM) domain, are responsible for interactions with RICTOR and mTORC2 substrate recognition, respectively (Tatebe et al., 2017). The PH domain of SIN1 binds to phosphatidylinositol (3,4,5)-triphosphate (PIP_3) and therefore relives the inhibitory binding of the PH domain on mTOR that initially masks the catalytic pocket of the complex (Liu et al., 2015; Yuan and Guan, 2015). The RBD of SIN1 raised many questions during the past years. SIN1 binding to HRAS and KRAS reduced RAS signaling toward ERK after its overexpression, while higher ERK activity was observed under SIN1 knockdown conditions (Schroder et al., 2007). Castel *et al.* characterized the SIN1-RBD/RAS interaction and demonstrated a critical interaction of the guanine nucleotide-binding (G) domain and the C-terminal hypervariable region (HVR) of KRAS4A with a region of SIN1 (amino acids: 364-390), which was called an alternative RBD or aRBD (Castel et al., 2021). However, deletion of the aRBD had no impact on cell signaling or animal development based on their observations. Zheng *et al.* recently provided further structural insights into the SIN1-RBD interaction with HRAS (Zheng et al., 2022). They remarkably proposed an insulin-induced reduction of ERK phosphorylation as a result of the RAS-SIN1 interaction (Zheng et al., 2022).

To gain more insights into the SIN1-RBD function, additional analyses are required to understand the inter-domain relationship of the SIN1-RBD-PH tandem in the interaction with RAS proteins, the membrane, and its mechanistic role in the regulation of mTORC2 in response to growth factor stimulation. Therefore, we have examined the direct binding of SIN1-RBD with various small GTPases and the effect of the PH domain on RAS and membrane binding. Furthermore, we monitored the impact of different SIN1 constructs on the mTORC2-AKT and MAPK pathways.

2 Materials and methods

2.1 Reagents

Dulbecco's modified Eagle's medium (DMEM), fetal bovine serum (FBS), and penicillin/streptomycin were obtained from Gibco® Life Technologies. The following antibodies were used: anti-α-tubulin (#ab52866, Abcam), anti-tAKT (#2920, Cell Signaling), anti-pAKT^{S473} (#4060, Cell Signaling), anti-pERK$^{T202/Y204}$ (#9106, Cell Signaling), anti-FLAG (#F3165, Sigma Aldrich), anti-GAPDH (#398600, Invitrogen), anti-GST (own antibody), anti-γ-tubulin (#T5326, Sigma Aldrich), anti-His (#MA5-33032, Thermo Fisher), anti-KRAS (#12063-1-AP, Proteintech), anti-NRAS (#EB08365, Erest Biotech) and anti-SIN1 (#2746272, Merck Millipore). The secondary antibodies IRDye® 800CW donkey anti-rabbit IgG and IRDye® 680RD donkey anti-mouse IgG were purchased from Li-Cor and analyzed in the Odyssey® XF Imaging System. The nucleotides mGDP (methylanthraniloyl- or mant-GDP), mGppNHp (mant-GppNHp) and GppNHp were obtained from Jena Bioscience GmbH. Human EGF and GDC-0941 were obtained from Merck (Darmstadt, Germany).

2.2 Constructs and proteins

Full-length genes of RAS and RHO GTPases (Table 1) were cloned into pGEX-4T1-N-Tev vectors and purified from

Q19 TABLE 1 SIN1-RBD interaction with proteins of the RAS superfamily.

Protein	K_d (μM)	Uniprot ID
HRAS	24 ± 2	P01112
NRAS	31 ± 2	P01111
KRAS4B	33 ± 2	P01116-2, P011118-1
KRAS4A	34 ± 1	P01116-1
RIT1	123 ± 15	Q92963
RRAS	123 ± 18	P10301
ERAS	171 ± 15	Q7Z444
RALA	331 ± 61	P11233
RHEB	358 ± 48	Q15382
RAP2A	483 ± 91	P10114
RHOA	535 ± 231	P61586
TC21	878 ± 472	P62070
CDC42	No binding observed	P60953
RAC1	No binding observed	P63000
RAC2	No binding observed	P15153

Values displayed are K_d ± SD, in μM.

Escherichia coli using glutathione-based affinity chromatography and size exclusion chromatography as described previously (Gremer et al., 2011). Full-length SIN1 (Q9BPZ7), SIN1 domains (RBD: aa 266-373; RBD-PH: aa 266-522; PH: aa 373-522), PI3Kα-RBD, RAF1-RBD and SIN1 mutants (RBD^{K307D}, $RBD^{RR311-312EE}$ and $RBD^{FSL289-291REE}$) were cloned and expressed in pGEX-4T1-N-Tev or pMal-c5X-His and purified by glutathione- or Ni-NTA-based affinity chromatography and size exclusion chromatography, as previously described (Hemsath and Ahmadian, 2005; Gremer et al., 2011). KRAS4A was further cloned into the pFAST-Bac vector for expression and purification from insect cells as described previously (Zhang et al., 2014). SIN1 FL, isoform 6 (Q9BPZ7-6), ΔaRBD (aa 363-390 missing), and the RAS GTPases HRAS (P01112), NRAS (P01111), KRAS4A (P01116-1), KRAS4B (P01116-2), RIT1 (Q92963) and ERAS (Q7Z444) were cloned into pcDNA-3.1-FLAG, pcDNA-3.1 (-) or pEYFP for eukaryotic expression. These vectors were provided by Alfred Wittinghofer of the Max Planck Institute Dortmund.

2.3 Cell culture, transfection and cell lysis

HEK293 and COS7 cells were cultured in DMEM supplemented with 10% FBS and 1% penicillin/streptomycin. Transfection was performed using TurboFect™ Transfection Reagent (Thermo Fisher Scientific) following the manufacturer's protocol. Cells were lysed in FISH buffer containing 50 mM Tris/HCl (pH 7.5), 100 mM NaCl, 2 mM $MgCl_2$, 10% glycerol, 20 mM β-glyerolphosphate, 1 mM Na_3VO_4, 1x protease inhibitor cocktail and 1% IGPAL on ice for 10 min and centrifuged for 10 min at 16,000 rpm.

2.4 CRISPR/Cas9 knock-out

CRISPR/Cas9 knockout was performed by incubating purified TrueCutTM Cas9 protein v2 (Thermo Fisher Scientific) with TrueGuideTM Synthetic sgRNA for human MAPKAP1 (Thermo Fisher Scientific, Assay ID: CRISPR1072864_SGM) in nucleofection solution SF (LONZA) for 30 min at room temperature. Then, $1*10^6$ HEK293 cells were resuspended in the solution and nucleofected in the 4D Nucleofector X-Unit (LONZA) using pulse CM-130. Cells were expanded for 1 week and then separated on 96-well plates to obtain single clones.

2.5 GST pull-down assay

Pull-down experiments were performed using purified GST-fused proteins coupled to glutathione agarose beads (Sigma Aldrich, Germany). Proteins were coupled for 1 h at 4°C on a rotor and centrifuged at 500 x g. The beads were washed 3 times with a cold buffer containing 50 mM Tris-HCl, 150 mM NaCl and 10 mM $MgCl_2$ and incubated with COS7 or HEK293 cell lysates with endogenous or overexpressed proteins for 1 hour. The beads were washed 3 times, and the proteins were mixed with 1x Laemmli buffer. Samples were analyzed using SDS-PAGE and immunoblotting.

2.6 Immunoprecipitation

EYFP-$HRAS^{G12V}$ was overexpressed in COS7 cells. Cell lysates were incubated overnight at 4°C with GFP nanobodies (GFP-binding domain of Lama single-chain antibody) covalently bound to Sepharose beads. The nanobody beads were washed three times, and the remaining protein was mixed with 1x Laemmli and analyzed by SDS-PAGE and immunoblotting as described previously (Rothbauer et al., 2008; Nakhaei-Rad et al., 2016). The nanobody beads were washed three times, and the remaining protein was mixed with 1x Laemmli and analyzed using SDS-PAGE and immunoblotting as described before.

2.7 Structural modeling of SIN1-RBD and its complex with HRAS

A structural model of the RBD from SIN1 was created with the computer program Modeler (https://www.ncbi.nlm.nih.gov/pmc/articles/PMC5031415/) using the automodel command. As a template, isolated SIN1-RBD and in complex with HRAS, the

structure of RAF kinase RBD in complex with HRAS•GppNHp (PDB: 4G0N) was used. Final structures were refined *via* a short minimization of complex energy with the program CHARMm (https://www.ncbi.nlm.nih.gov/pmc/articles/PMC2810661/) using default parameters.

2.8 Fluorescence polarization

Fluorescence polarization experiments were executed *via* the titration of increasing amounts of the effector (SIN1) proteins to 1 µM mGppNHp- and mGDP-bound GTPases as described before (Gremer et al., 2011; Nakhaeizadeh et al., 2016). Experiments were performed using a Fluoromax 4 fluorimeter in polarization mode vs. time (excitation wavelength: 360 nm, emission wavelength: 450 nm), at 21°C in a buffer, containing 30 mM Tris/HCl pH 7.5, 150 mM NaCl, 5 mM $MgCl_2$ and 3 mM dithiothreitol. The dissociation constants (K_d) were calculated using a quadratic ligand binding equation in GraFit 5.

2.9 Liposome assays

Liposomes were prepared by mixing 10% (w/w) phosphatidylethanolamine (PE) (for flotation assay: 5% (w/w) PE and 5% (w/w) fluorescently labeled NBD-PE), 50% (w/w) phosphatidylcholine (PC), 20% (w/w) phosphatidylserine (PS), 5% (w/w) phosphatidylserine, 5% (w/w./wt.) phosphatidylinositol-3-monophosphate (PIP), 5% (w/w) phosphatidylinositol-4,5-bisphosphate (PIP2), and 5% phosphatidylinositol-3,4,5-triphosphate (PIP3) from stock solutions dissolved in chloroform. Negative liposomes (Supplementary Figure S7) were prepared by mixing 90% (w/w) and 10% (w/w) PE. The final mixture (500 µg) was dried and rehydrated in 500 µl buffer containing 20 mM HEPES (pH 7.5), 50 mM NaCl, 5 mM MgCl2, and 3 mM DTT. The solution was sonicated 10 times under mild conditions (minimum power, 50% on and 50% off) and extruded 21 times through a membrane with a pore size of 0.2 µm.

PIP strips were purchased from Echelon Bioscience and treated according to the manufacturer's protocol. Briefly, the lipid-containing membrane was blocked for 1 hour with TBS containing 3% BSA (PanReac AppliChem GmbH). The SIN1-PH domain was incubated with the membrane at a concentration of 1 µg/ml in TBS +3% BSA for 1 hour. Three washing steps with TBS +0.1% Tween 20 were followed by a 1-h incubation with the appropriate primary antibody. The washing steps were repeated, and the membrane was incubated with the secondary antibody from Li-Cor for 1 hour. After three more washing steps, the membrane was evaluated in a Li-Cor Odyssey system.

Liposome sedimentation assays were performed by mixing 60 µl liposomes with 20 µl SIN1-PH (1-3 µM), incubating the sample for 30 min at 4°C while mixing followed by 30 min centrifugation at 20.000 *g* at 4°C. The supernatant and pellet were mixed or resuspended with 5x Laemmli to obtain a final volume of 92 µl. The samples were loaded on an SDS gel and analyzed using Coomassie staining or immunoblotting.

For the liposome flotation assay, 50 µl of liposomes (or negative liposomes; Supplementary Figure S8) containing 5% fluorescently labeled NBD-PE) were mixed with 50 µl of SIN1 proteins (25 µM) and incubated at 4°C for 30 min. The sample was mixed with 100 µl of 60% sucrose and pipetted into a small centrifuge tube (Beckman Coulter). On top of the first layer, 250 µl of 25% sucrose and 50 µl of PBS −/− were added without allowing the phases to mix. The samples were centrifuged for 1 hour at 50,000 rpm at 4°C. The fluorophore-containing liposome phase was detected using a UV lamp and taken in a 50 µl total volume. Samples were evaluated as described for the liposome sedimentation assay.

2.10 Partial fractionation

Partial fractionation was performed using the Mem-PER™ Plus Membrane Protein-Extraction Kit (Thermo Fisher Scientific) following the manufacturer's protocol. Briefly, cells were trypsinized and washed twice with a cell wash solution. The membrane was permeabilized with 375 µl permeabilization buffer for 10 min at 4°C and centrifuged for 15 min at 16,000 rpm. The cytosolic fraction was mixed with 5x Laemmli. The membrane pellet was resuspended in solubilization buffer and incubated for 30 min at 4°C while mixing. The sample was centrifuged for 15 min at 16,000 rpm, and the supernatant was mixed with 5x Laemmli. Samples were analyzed using SDS-PAGE and immunoblotting.

3 Results

To characterize the binding of SIN1 to RAS, we used several fragments of SIN1, including the full length (FL), isoform 6 (Iso6), ΔaRBD, which lacks amino acids 364-390 compared to the full length of SIN1, the RBD-PH tandem, and the isolated domains RBD and PH (Figure 1A). We investigated the physical interaction of different members of the RAS superfamily with the RBD *in vitro*, checked protein binding in cell-based experiments with SIN1-FL, and identified important amino acids for interaction based on a binding model of the RBD and HRAS. Moreover, we characterized the interaction of the RBD-PH tandem with the classical RAS proteins and analyzed the membrane binding of the PH and RBD-PH proteins. We also investigated the binding of the RBD-PH domain with liposomes in the presence or absence of RAS. A cell-based study analyzed the distribution of endogenous SIN1 FL in the cytosolic and membrane fractions of HEK293 cells. We checked the phosphorylation levels of pAKT S473 after overexpressing RAS or SIN1 ΔaRBD and isoform six to monitor the activity of the mTORC2.

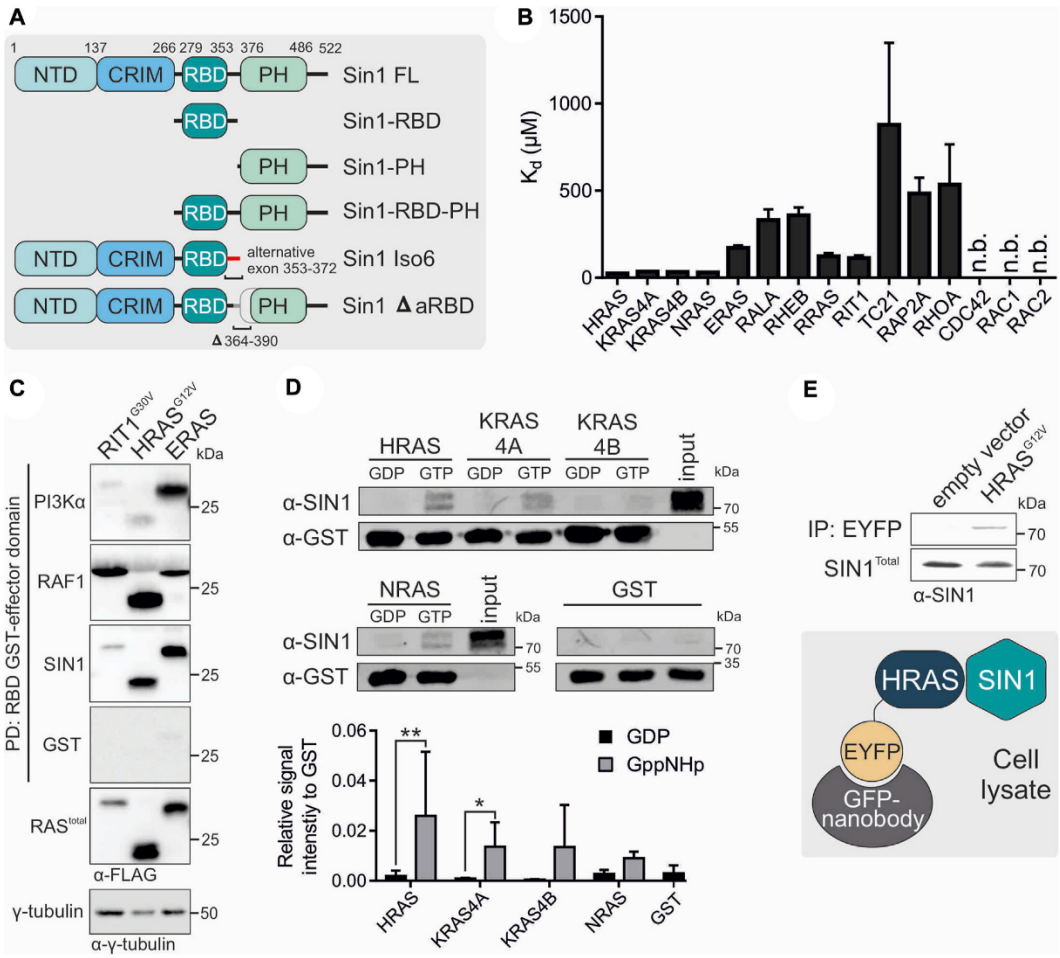

FIGURE 1
Interaction partners of SIN1. **(A)** Schematic domain organization of SIN1 and its generated fragments and variants. Numbers indicate amino acid numbering of isoform 1 (full length). **(B)** Fluorescence polarization analysis of SIN1-RBD with mGppNHp-labeled GTPases. N.b. indicates no binding observed. All K_d values are provided in Table 1. **(C)** Pull-down assay of the GST-bound RBDs of PI3Kα, RAF1 and SIN1 with overexpressed $RIT1^{G30V}$, $HRAS^{G12V}$ and ERAS containing a FLAG-Tag. γ-Tubulin served as a loading control, and GST alone served as the negative control. **(D)** Pull-down experiment with GST-bound HRAS, KRAS4A, KRAS4B or NRAS, labeled with GDP or GppNHp, and endogenous SIN1-FL in HEK293 lysates. GST alone served as a negative control. Bar charts were obtained from independent experiments. (HRAS, KRAS4A, NRAS n = 3; KRAS4B n = 2; GST n = 4). Data sets were evaluated in a two-tailed ratio paired *t* test using GraphPad Prism 6. HRAS GDP vs. GppNHp $p = 0.0010$, KRAS4A GDP vs. GppNHp $p = 0.0114$, KRAS4B and NRAS not significant. **(E)** Co-immunoprecipitation analysis of overexpressed EYFP-HRAS in COS7 cells. Proteins were immunoprecipitated using GFP nanobodies.

3.1 SIN1-RBD binds to all classical RAS proteins

The first aim of our study was to identify direct binding partners of SIN1-RBD (aa 279-353) within the RAS superfamily. Therefore, we investigated the binding of 15 different RAS and RHO proteins using fluorescence polarization measurements (Figure 1B; Table 1). In addition to the classical RAS proteins HRAS, NRAS, and the isoforms KRAS4A, and KRAS4B, we investigated RRAS1, RRAS2 (or TC21), ERAS, RIT1, RALA, RHEB, RAP2A, RHOA, CDC42, RAC1 and RAC2. The K_d values were determined *via* the titration of increasing concentrations of the SIN1-RBD to the mGppNHp-bound GTPases (Supplementary Figure S1). The classical RAS proteins

exhibited the highest affinities that ranged from 24 to 35 μM, followed by RIT1, RRAS, and ERAS, with K_d values of 112, 123, and 170 μM, respectively (Table 1). The other tested GTPases exhibited binding affinities greater than 300 μM, which are most likely not relevant in cell signaling. Among the RHO GTPases, RHOA was the only protein that showed very weak binding above 500 μM.

To compare the binding of the SIN1-RBD to the well-known RAS effectors RAF1 and PI3Kα, we performed pull-down analyses of the three GST-fused RBDs with the hyperactive GTPases $RIT1^{G30V}$, $HRAS^{G12V}$ and constitutively active ERAS (Nakhaei-Rad et al., 2015). GST alone served as the negative and γ-tubulin as the loading control (Figure 1C). ERAS, which had a low affinity for SIN1-RBD *in vitro*, can bind in cells as strong as $HRAS^{G12V}$, while $RIT1^{G30V}$ displayed weak binding to SIN1 and PI3Kα-RBD and strong binding to RAF1-RBD. $HRAS^{G12V}$ bound strongly to RAF1, moderately to SIN1 and weakly to PI3Kα. Notably, ERAS showed strong binding to all RBDs but the highest engagement to PI3Kα.

We examined whether binding of the SIN1-RBD was nucleotide dependent or independent and confirmed GTP-dependent binding in fluorescence polarization experiments using HRAS•mGDP vs. HRAS•mGppNHp (Supplementary Figure S2). Pull-down experiments of purified GST-fused HRAS, KRAS4A, KRAS4B and NRAS determined the binding of endogenous SIN1-FL with GDP- or GppNHp-bound RAS. The experiment clearly showed the binding of only GppNHp-bound RAS proteins (Figure 1D). The interaction of endogenous SIN1-FL with HRAS was confirmed by a co-immunoprecipitation experiment using overexpressed EYFP-$HRAS^{G12V}$ (GAP-insensitive and therefore mostly GTP-bound mutant; Figure 1E).

3.2 Identification of critical SIN1/HRAS interacting residues

To identify potential contact sites of SIN1-RBD on RAS, the SIN1-RBD structure in complex with HRAS was modeled based on sequence homology to the complex of RAF1-RBD with GppNHp-bound HRAS (PDB: 4G0N). We analyzed the interaction interface between HRAS and SIN1-RBD and selected several SIN1 residues in close proximity to HRAS that may be responsible for the direct interaction between RAS proteins and SIN1 (Figure 2A). Based on these identified interacting residues, three different mutants of SIN1-RBD were designed (Figure 2A): SIN1-RBD^{K307D}, SIN1-$RBD^{RR311\text{-}312EE}$, and SIN1-$RBD^{RSL289\text{-}291REE}$. Residues were substituted with amino acids with opposite charges to generate repulsion between the interacting residues.

The biophysical measurements revealed decreased binding of SIN1-RBD mutants with mGppNHp-bound HRAS, KRAS4A, KRAS4B and NRAS (Figure 2B and Supplementary Figure S3). The K_d of the single mutant was 5- to 15-fold higher than SIN1-RBD^{WT} (Tables 1 and 2). The double and triple mutants further decreased the binding affinity. All mutations abolished SIN1-RBD binding capability to KRAS4B but were still bound to KRAS4A with a low affinity. The recently published structure of KRAS binding with SIN1-RBD by Castel *et al.* (PDB: 7LC1 and 7LC2) and Zheng *et al.* (PDB: 7VVB) and HRAS binding of SIN1-RBD by Zheng et al. (PDB: 7VV9) confirmed that these residues are in close proximity to the switch I region of KRAS and are very likely involved in a physical interaction (Supplementary Figure S4) (Castel et al., 2021; Zheng et al., 2022). Notably, our SIN1 mutations were generated and characterized far before these structures of the SIN1-RAS complexes were published.

3.3 SIN1-RBD-PH tandem domain has much lower binding to RAS than RBD alone

We investigated the interaction of the tandem SIN1-RBD-PH domain with classical RAS proteins (HRAS, KRAS4A, KRAS4B and NRAS) using fluorescence polarization (Figure 2C and Supplementary Figure S5). Obtained K_d values were 5- to 10-fold higher than the SIN1-RBD interaction (Table 2), which strongly suggests a possible intermolecular interaction between the PH and RBD domains. To examine whether this RBD-PH interaction is due to direct binding of the individual domains or occurs only in the linked tandem domain, fluorescence polarization measurement of SIN1-RBD with HRAS•mGppNHp in the presence of 2x excess SIN1-PH was performed and resulted in a K_d of 27 ± 2 μM, which was similar to the K_d obtained for SIN1-RBD alone (24 ± 2 μM) (Figure 2D). The SIN1-PH domain alone showed no binding to HRAS (Supplementary Figure S6).

3.4 SIN1-PH and RBD-PH associate with the membrane

We further focused on the investigation of the membrane binding ability and lipid selectivity of SIN1-PH and SIN1-RBD-PH domains using PIP-Strips (Figure 3A), liposome sedimentation (Supplementary Figure S7), and liposome flotation assays (Figure 3B). PIP-Strip assays confirmed a similar selectivity and comparable intensity of the PH and RBD-PH domains toward all phosphoinositides. The strongest binding was detected for PI(3)P, PI(5)P, and PI(4,5)P. PH and RBD-PH bound to phosphatidic acid (PA) but no other lipids. Based on this assay, we used liposomes containing PC, PE, PS, PA, PI(3)P, PI(4,5)P, PI(3,4,5)P, and cholesterol for subsequent experiments to cover all possible binding modes.

We confirmed the binding of the GST-SIN1-PH domain to our synthetic liposomes compared to the GST control in a

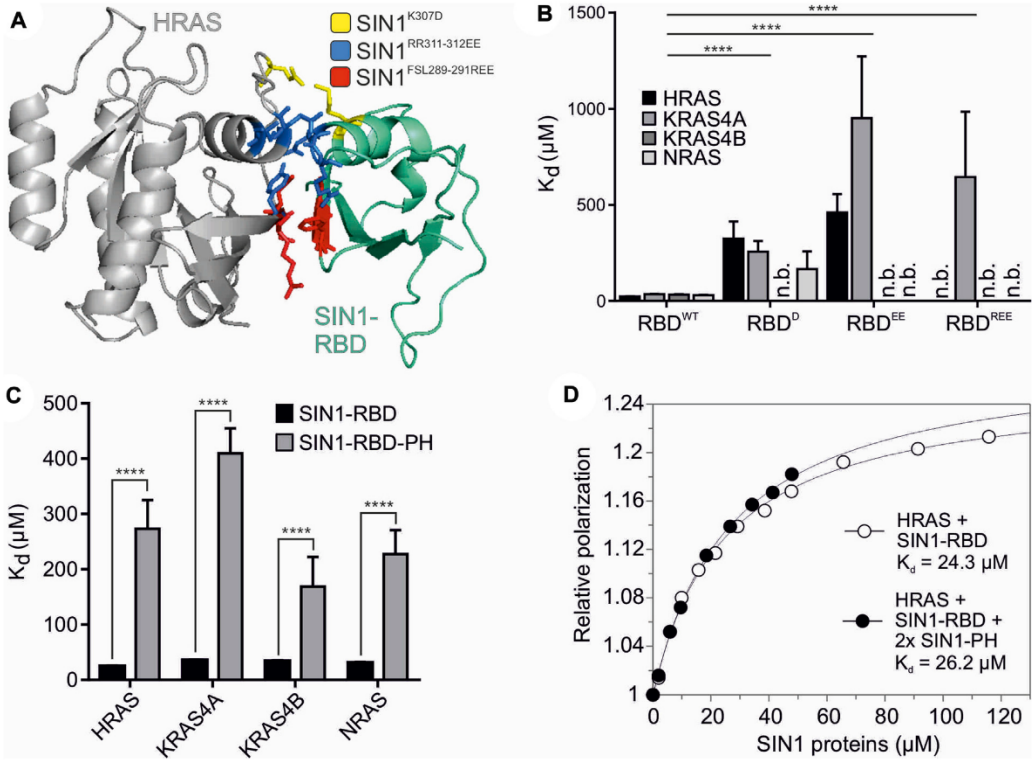

FIGURE 2
Structural analysis of SIN1-RBD and RBD-PH domains. **(A)** The interaction interface of HRAS (gray) and SIN1-RBD (teal) is highlighted in the model of their complex constructed based on the C-RAF RBD structure (PDB: 4G0N). Critical and mutated residues in the SIN1-RBD are colored as follows: $SIN1^{K307D}$ (yellow), $SIN1^{RR311-312EE}$ (blue), and $SIN1^{FSL289-291REE}$ (red). **(B)** Fluorescence polarization analysis of the RBD mutants compared to the WT SIN1-RBD with the mGppNHp-labeled classical RAS proteins HRAS, KRAS4A, KRAS4B, and NRAS. All K_d values are shown in Table 2. The difference in the binding affinity of WT SIN1-RBD in comparison to the three SIN1-RBD mutants was highly significant for all proteins (two-tailed unpaired *t* test, $p < 0.0001$). **(C)** Fluorescence polarization analysis of the SIN1-RBD-PH tandem construct with mGppNHp-labeled classical RAS proteins compared to SIN1-RBD binding alone. All K_d values are provided in Table 2. **(D)** Fluorescence polarization graphs of HRAS mGppNHp with SIN1-RBD (K_d = 24 ± 2 μM) and double the amount of SIN1-PH (K_d = 27 ± 2 μM). SIN1-RBD and SIN1-PH were premixed and pre-incubated before titration.

TABLE 2 The Interaction of SIN1-RBD mutants with RAS proteins.

Protein	HRAS	KRAS4A	KRAS4B	NRAS
SIN-RBD^{K307D}	324 ± 90	256 ± 56	No binding observed	166 ± 93
SIN-RBD ^{RR311,312EE}	461 ± 95	952 ± 321	No binding observed	No binding observed
SIN-RBD $^{FSL289-291REE}$	No binding observed	654 ± 339	No binding observed	No binding observed
SIN1-RBD-PH	273 ± 52	410 ± 45	168 ± 54	227 ± 43

Values displayed are K_d ± SD, in μM.

liposome sedimentation assay (Supplementary Figure S7). Most protein was detected in the liposome/pellet fraction. The GST control was only detectable in the supernatant. We checked the membrane binding ability of the MBP-SIN1-RBD-PH domain in a liposome flotation assay. Proteins were mixed and incubated with fluorescent-labeled synthetic liposomes and stacked in a

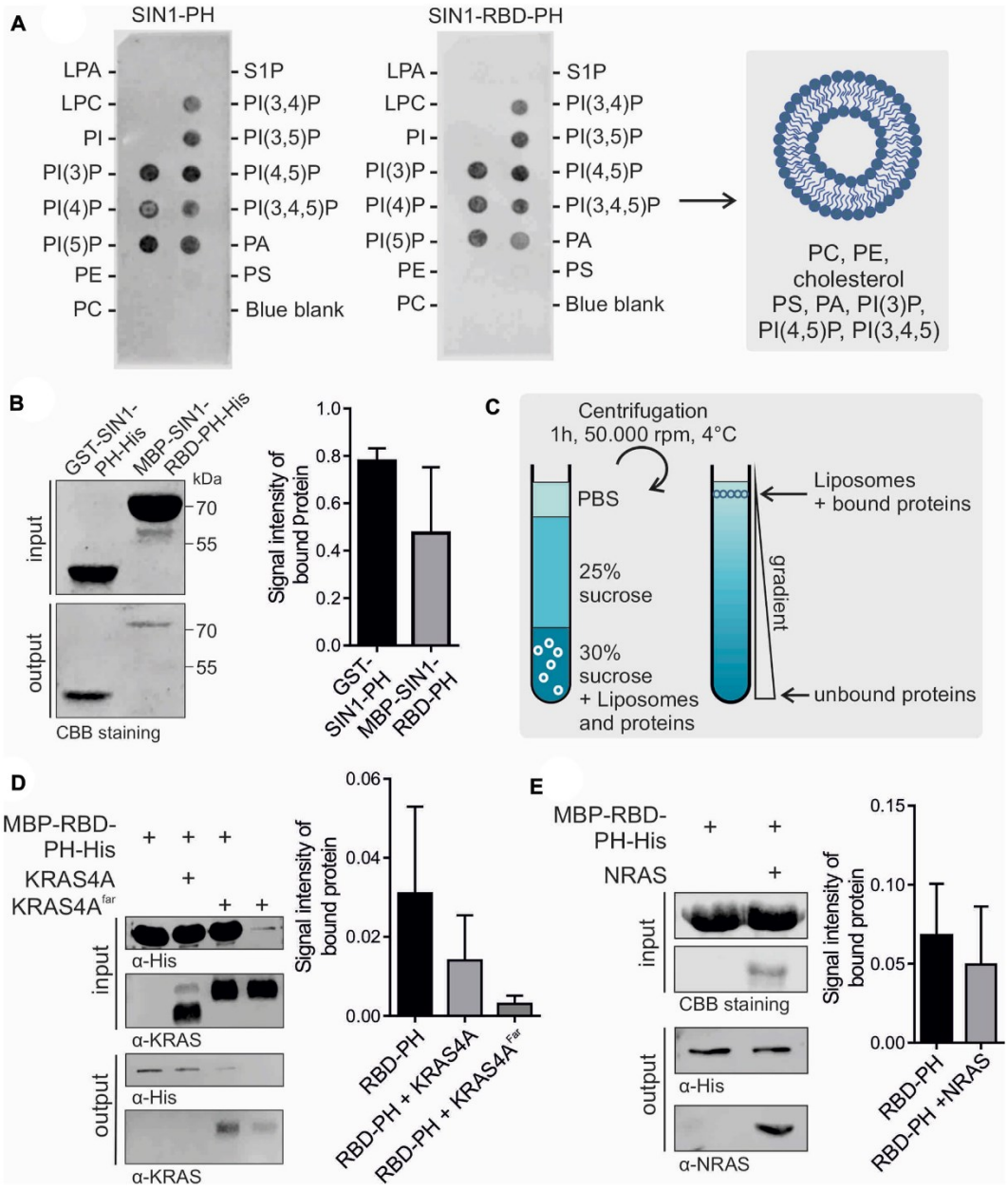

FIGURE 3
Membrane association of SIN1-PH and RBD-PH. **(A)** PIP-Strip assay of SIN1-PH (left) and SIN1-RBD-PH (right). The blue blank served as a negative control. CBB stands for Coomassie brilliant blue. **(B)** Flotation assay of SIN1-PH and SIN1-RBD-PH domains stained with Coomassie. (n = 3) Not significant. **(C)** Schematic principle of a liposome flotation assay using a sucrose gradient and ultracentrifugation. **(D)** Flotation assay of SIN1-RBD-PH in the presence of KRAS4A purified from *E. coli* and KRAS4A^{farnesylated} from insect cells (n = 3). **(E)** Flotation assay of SIN1-RBD-PH with NRAS purified from *E. coli*. (n = 3). Data sets were evaluated in a two-tailed unpaired *t* test using GraphPad Prism six and displayed no significance. CBB stands for Coomassie brilliant blue.

glucose gradient. After ultracentrifugation, liposomes, including bound proteins, were isolated and detected using Coomassie staining or Western blotting (Figures 3B,C). As a negative control, we used only purified MBP. In addition, we checked the lipid selectivity of the SIN1-PH domain by using negative liposomes containing only 90% PC and 10% PE, which showed no liposome association in the flotation assay (Supplementary Figure S8). Our results showed the binding of SIN1-PH and RBD-PH to the liposomes, with the binding of the latter being comparably weaker. This effect is most likely caused by interdomain interaction between the RBD and the PH domain discussed in Section 3.3. A remaining question is whether RAS binding to the RBD is supported by PH domain binding to the membrane or whether this PH-membrane interaction is regulated by RAS.

3.5 RAS weakens the membrane interaction of SIN1-RBD-PH

To determine the effect of RAS on the membrane binding of SIN1-RBD-PH, we performed liposome flotation assays using GppNHp-bound KRAS4A without and with posttranslational modifications, such as farnesylation in its CAAX box, that facilitates its binding to the membrane. The results indicated weaker binding of RBD-PH to the liposomes in the presence of non-farnesylated and farnesylated KRAS4A (Figure 3D) as well as in the presence of GppNHp-bound NRAS (Figure 3E). Both results suggest an influence of RAS on the localization of SIN1 and the mTORC2 complex within the cell.

3.6 SIN1-FL is always partially membrane associated

Different localizations of SIN1 within the cell have been reported in the past few years. We have now applied different approaches to study the translocation of endogenous SIN1 to the membrane. A first approach was to partially fractionate HEK293 cells and determine the ratio between cytosolic SIN1 and membrane fractions. Data from six independent experiments showed that most of the endogenous SIN1-FL protein was present in the cytosolic fraction, with a ratio of approximately 77:23 ($p \leq 0.0001$; Figure 4A). In a next step, we examined the effects of the PI3K-AKT pathway on the localization of SIN1 in the membrane. We used two opposing conditions, either inhibiting the pathway with GDC-0941, a small molecule PI3K inhibitor, or stimulating it with 10% FBS. The results presented in Figure 4B did not lead to an obvious shift of SIN1 between the cytosolic and membrane fractions compared to the serum-starved cells. Of note, the ratio of cytosolic to membrane immunodetectable SIN1 was quite similar among the three conditions (serum-starved 86:14; GDC-0941 treated 89:11; FBS stimulation 88:12). As a control for the cytosolic fraction, we used α-tubulin, which was present in the latter at approximately 96-98%, indicating only a very weak contamination of approximately 2-4% of the cytosolic fraction in the membrane fraction. The membrane fraction was checked using Na^+/K^+-ATPase as a marker protein (Supplementary Figure S9).

3.7 RAS overexpression does not alter AKT S473 phosphorylation

The RAS signaling pathway follows two canonical routes: one via RAF and MEK toward ERK, the other via PI3K activation toward AKT phosphorylation at T308 (Muñoz-Maldonado et al., 2019). As described before, the phosphorylation of AKT at S473 mostly depends on the mTORC2 complex and serves as a readout for its activity (Sarbassov et al., 2005; Castel et al., 2021). The PI3K inhibitor GDC-0941 blocks the conversion of PIP_2 to PIP_3 and many translocation events of PIP_3-dependent PH domain-containing proteins, such as AKT (Figure 4C). To investigate the influence of RAS on the phosphorylation of AKT, we overexpressed wild-type KRAS4A, HRAS, NRAS, and the hyperactive variants $HRAS^{G12V}$ and $NRAS^{G12V}$ in HEK293 cells (Figure 4D). Cells were serum starved and treated as indicated with EGF and/or GDC-0941. Stimulation with EGF led to strong AKT^{S473} phosphorylation in all cases (Figure 4D). The G12V mutation further promoted signaling, which was likely due to the constant activation of the PI3K pathway. The GDC-0941 inhibitor completely abolished AKT^{S473} phosphorylation. This could be further supported by stimulating HEK293 cells with EGF, insulin and 10% FBS in combination with the GDC-0941 inhibitor, which abolished the phosphorylation of AKT S473 in all cases (Supplementary Figure S10). This experiment strongly supports the need for PI3K activity for AKT phosphorylation. In order to better understand the role of the PH domain and eventually of the aRBD, as suggested by Castel *et al.*, on the activity of the mTORC2 complex toward AKT we overexpressed several SIN1 variants. SIN1-ΔaRBD lacks amino acids 364-390, and isoform 6 (Iso6) is missing the whole PH domain and contains an alternative exon 9a instead of the aRBD. Because endogenous SIN1 could interfere with the effect of transfected SIN1 variants, which could be caused by the formation of heterodimers (Stuttfeld et al., 2018; Scaiola et al., 2020), we performed a CRISPR/Cas9 knock-out of SIN1 in HEK293 cells and selected a single clone (clone 2A) for further overexpression experiments. The single clone showed no signal for either SIN1 antibody or phosphorylated AKT at S473 (Supplementary Figure S11). All overexpressed SIN1 proteins were able to rescue

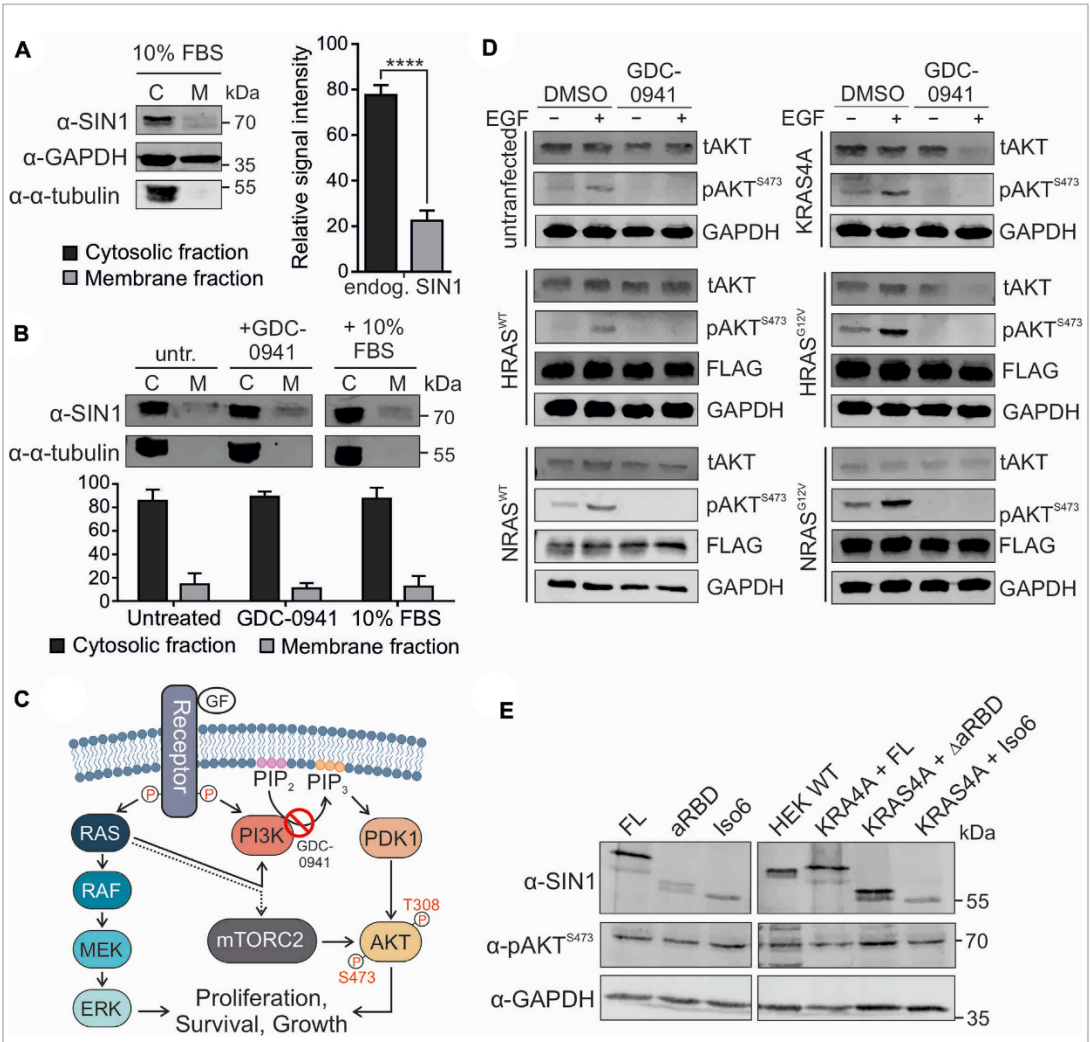

FIGURE 4
Localization and signaling of SIN1. **(A)** Partial fractionation of HEK293 cells into cytosolic and membrane fractions (n = 6, two-tailed paired *t* test $p < 0.0001$). GAPDH served as a loading control and α-tubulin as a control for the cytosolic fraction. **(B)** Partial fractionation of 16 h serum staved HEK293 cells under untreated, 1 μM GDC-0941 inhibited or 10% FBS-stimulated conditions (1 h each) (not significant, two-tailed unpaired *t* test). α-Tubulin served as a control for the cytoplasmic fraction (98:2). **(C)** Illustration of the RAS-MAPK and PI3K-AKT pathways induced by EGF. The dotted line indicates an unknown effect of RAS on the mTORC2 complex. **(D)** Stimulation experiment with untransfected or EYFP-KRAS4A-, $HRAS^{WT}$-, $HRAS^{G12V}$-, $NRAS^{WT}$- or $NRAS^{G12V}$-transfected HEK293 cells. For KRAS4A, green fluorescence was used as an expression control. The other constructs carried an N-terminal FLAG-tag and were detected using an α-FLAG antibody. GAPDH served as a loading control. tAKT and $pAKT^{S473}$ levels were estimated after serum starvation, followed by treatment with DMSO or 1 μM GDC-0941 for 1 h and stimulation with 100 ng/ml EGF for 20 min as indicated. **(E)** Western blot analysis of overexpressed SIN1 constructs (FL, ΔaRBD, and Iso6) or co-expressed SIN1 variants with EYFP-KRAS4A in HEK293-SIN1 knock-out cells, clone 2A, under normal culture conditions (10% FBS). For KRAS4A, green fluorescence was used as an expression control. SIN1 antibody indicates the overexpressed variants and indicates knock-out compared to wild-type (WT) cells. The pAKTS473 levels were analyzed with a specific antibody. GAPDH served as a loading control.

phosphorylation of AKTS473 and did not dramatically increase or decrease AKT phosphorylation when co-expressed with KRAS4A (Figure 4E).

Overall, our cell biological results suggest PI3K-dependent phosphorylation of AKT^{S473}, likely through recruitment of AKT to the membrane, but not through alteration of SIN1 and thus

mTORC2 localization within the cell, as a small fraction appears to be constantly localized to the membrane. In addition, we failed to demonstrate a RAS-dependent increase in AKT-S473 phosphorylation after GDC-0941 treatment, as well as the ability of SIN1-FL, ΔaRBD, and isoform six to rescue pAKTS473 levels in SIN1 knockout cells. It seems that some specific issues related to AKT regulation and feedback mechanisms still need to be clarified.

4 Discussion

The role of the SIN1-RBD and the interaction of RAS and SIN1 raised more questions than answers during the past years. Zheng et al. (Zheng et al., 2022), Castel et al. (Castel et al., 2021) and Liu et al. (Liu et al., 2015) added new interesting concepts for the function of the RBD and the PH-domain of SIN1 in the complex regulatory network of mTORC2. Our study adds the influence of RAS on the membrane binding of SIN1 as another functional factor.

Schroder *et al.* (2007) described the RAS binding domain of SIN1 and showed the association of $HRAS^{G12V}$ and $KRAS4B^{G12V}$ with SIN1 (Schroder et al., 2007). Castel *et al.* revised this study and introduced KRAS4A•GTP as the ultimate binding partner for SIN1. Consistent with Zheng *et al.*, who showed an association with HRAS, KRAS, and NRAS, we identified the four classical RAS proteins (HRAS, KRAS4A, KRAS4B, and NRAS) as the strongest binders of SIN1-RBD and confirmed the GTP-dependent binding of these proteins with FL SIN1 in cells. We have added ERAS, RRAS, and RIT1 to the list of potential binding partners based on fluorescence polarization which serves as a sensitive biophysical method for the identification of protein complexes with lower binding affinities. RIT1-SIN1 interaction has also been shown previously to be required for oxidative stress survival (Cai, Andres and Reiner, 2014). Pull-down assays confirmed the binding of ERAS and RIT1 with SIN1-RBD and further confirmed the preferable binding of $HRAS^{G12V}$ with RAF1, SIN1, and PI3Kα RBDs, which is exactly the order shown by Zheng *et al.*

Our structural analysis identified a few residues for the interaction of SIN1-RBD with the switch region of HRAS. The residues R311, R312, F289, S290 and L291, which showed a much lower or complete loss of binding after mutation, were also identified by Castel *et al.* and Zheng *et al.*, and collectively highlight these residues as the main interaction sites of SIN1 and RAS, although this binding site may not be exclusive (Castel et al., 2021; Zheng et al., 2022). Interestingly, the F289L, S290F, and R311Q mutations were found to be SIN1 cancer mutations (COSMIC database, 2022), suggesting their critical role in SIN1 function. The RBD-PH construct showed much weaker binding to RAS than RBD alone, which was also reported by Castel *et al.*, Zheng *et al.*, and by this study. Contrary to these results, we did not detect a direct interaction of the free PH domain with the RBD but proposed a low-affinity RBD-PH tandem interdomain interaction.

The PH domain of SIN1 was examined by Liu *et al.* (2015), who reported the binding of the PH domain to mTOR in an inhibitory manner and to PIP_3 to activate the complex by opening the mTORC2 binding pocket. Their study concluded that the activity of the mTORC2 complex was PI3K dependent, which produced PIP_3 in response to growth factors. Ebner *et al.* (2017) investigated the localization and activity of the mTORC2 complex in the cell using a new reporter system called LocaTOR2 (localization of mTOR complex 2), based on its effector AKT2. The study identified different pools of the mTORC2 complex at the plasma membrane, mitochondria, and endosomal vesicles. This finding highlighted that mTORC2 activity at the plasma membrane was PI3K independent and activated the reporter upon PI3K inhibition with GDC-0941. Nevertheless, the substrate AKT was not recruited to the PM under PI3K inhibition, which indicates that the phosphorylation of AKT is PI3K dependent based on its localization, but mTORC2 activity does not need PI3K for its activity. Our study also shows stimulation-independent SIN1 localization at the plasma membrane, which was supported by the binding of the SIN1-PH domain to phosphoinositides other than only PIP_3. Other members of the mTORC2 complex may also trigger membrane localization. The domain organization of RICTOR is not completely defined, and two possible PH domains (including one split PH domain), in addition to HEAT and WD repeats, were identified based on sequence and structural similarities (Zhou et al., 2015).

Taken together, our study shows for the first time the membrane association of SIN1-RBD-PH compared to the PH domain alone and additionally analyzed this interaction in the presence of farnesylated and non-farnesylated RAS. We showed that RAS interfered with the binding of SIN1-RBD-PH to liposomes. Mechanistically, it is tempting to hypothesize that RAS association with the membrane-bound SIN1 results in spatial rearrangement of the RBD-PH tandem followed by SIN1 dissociation from the membrane and then subsequently from RAS. The RAS-SIN1 interaction is consequently accompanied by crosstalk and feedback mechanisms of the RAS-MAPK and PI3K-AKT signaling pathways (Figure 5). The binding of RAS to SIN1 rather than PI3K may reduce the activity of the PI3K-AKT pathway and AKT phosphorylation by mTORC2, which is alternatively followed by the disassembly of the mTORC2 complex. This assumption is based on our observation that some mTORC2 continuously resides at the membrane. It suggests that the spatiotemporal control of AKT, its recruitment and clustering to lipid rafts is the key to switching the AKT signaling pathway on and off.

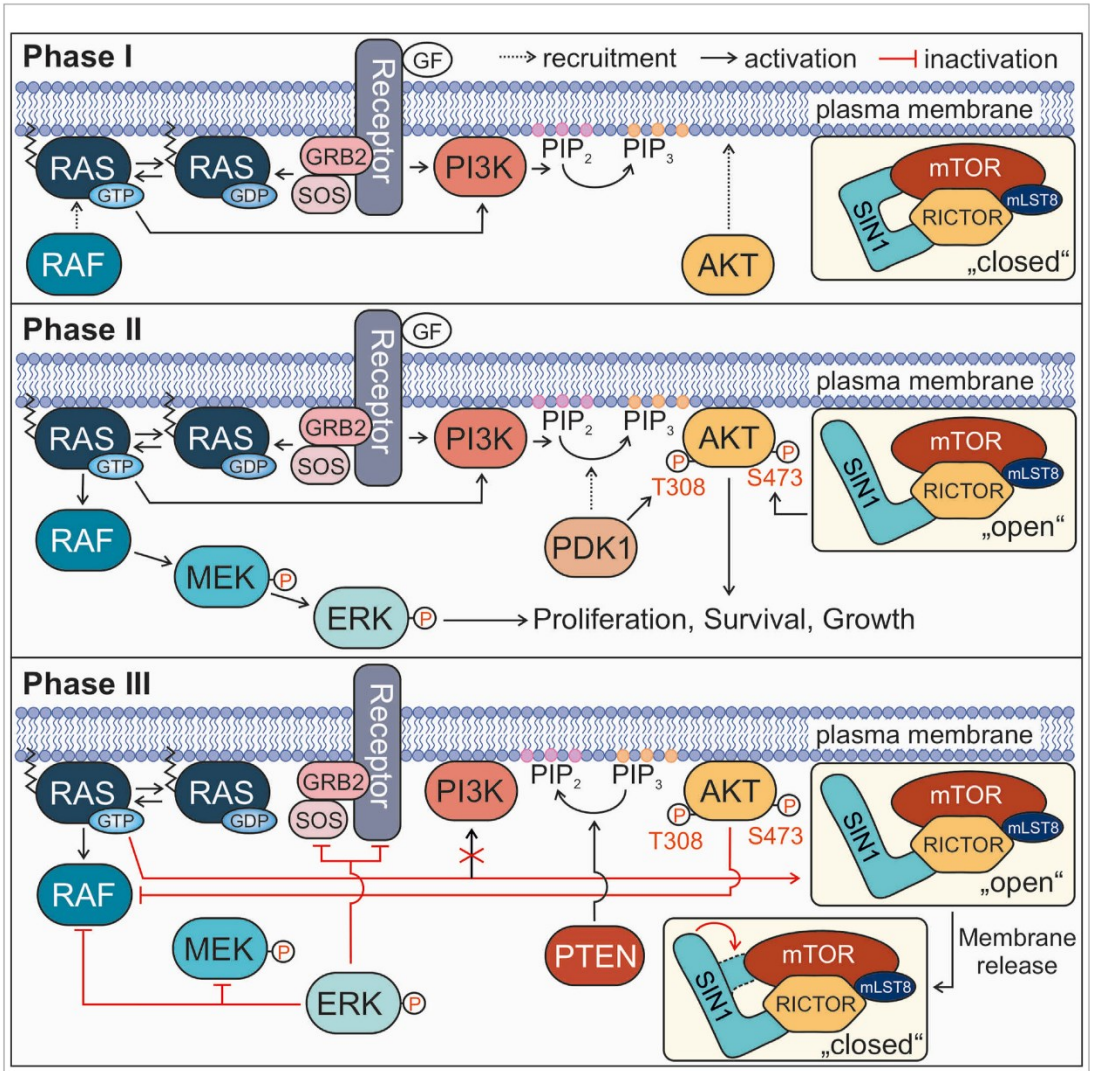

FIGURE 5
Proposed model for the involvement of the RAS-SIN1 interaction in signal termination. Phases I, II, and III describe the signaling process from growth factor binding to signal termination. For more details see text.

All in all, the results of the present study and the previous work by other groups led to the following model proposing the role of SIN1-RAS interaction in the negative feedback loop of RAS-RAF-MEK-ERK and PI3K-AKT signaling pathways. Our model divides the activation of RAS and its downstream effectors into three phases until the termination of signal transduction (Figure 5). In phase I (the initiation phase), RAS activation through a GDP/GTP exchange by the RTK-GRB2-SOS axis (Kazemein Jasemi and Reza Ahmadian, 2022) transmits the extracellular signals (*e.g.*, EGF) towards both RAF and PI3K. This recruits RAF to the plasma membrane, and activates PI3K to catalyze the conversion of PIP_2 to PIP_3, followed by membrane recruitment of AKT. In this phase, the mTORC2 complex with SIN1 is present in a partially "closed" conformation at the membrane and therefore, inaccessible for RAS. The inhibitory binding of the PH domain to mTOR blocks the catalytic binding

pocket of the complex (Liu et al., 2015). In phase II (maximum signaling phase) the two canonical RAS signaling pathways are fully activated. RAF is activated by several dephosphorylation, conformational change and homo- or heterodimerization events and transmits the signal to MEK and ERK (Lavoie and Therrien, 2022). PDK1 recruitment to PIP_3-rich clusters results in T308 phosphorylation and activation of AKT. At the same time, SIN1 switches into an open conformation, which may be triggered by the association of the PH domain with the membrane accompanied with mTORC2 substrate recognition, which seems to be different for AKT and SGK1 (Yu et al., 2022). The mTORC2 complex phosphorylates AKT at S473, leading to its complete activation. Both phosphorylated ERK and AKT now stimulate cell responses, such as proliferation, survival and cell growth. In the following phase III (the signal termination), several feedback loops lead to the shutdown of the signaling processes, including: 1) RAS•GTP binding to SIN1 in its open conformation, dissociating the SIN1-PH domain from the membrane back to its closed conformation, disrupting the positive feedback loop to PI3K and interfering with the activation of AKT by mTORC2; 2) activated ERK inhibits its own signaling cascade by phosphorylating RTKs, SOS, RAF and MEK; 3) activated AKT re-phosphorylates RAF at S259 (CRAF numbering), the critical inhibitory phosphorylation site (Zimmermann and Moelling, 1999; Dhillon et al., 2002; Lake, Corrêa and Müller, 2016); 4) PTEN dephosphorylates PIP_3 to PIP_2 (Lee, Chen and Pandolfi, 2018). Notably, there are more negative feedback processes known, like the ubiquitination and internalization of receptors (Tomas, Futter and Eden, 2014), the inactivation of RAS by GAPs (Lorenzo and McCormick, 2020), and the negative feedback of ERK towards other signaling proteins, *e.g.*, sprouty or FRS2α (Lake, Corrêa and Müller, 2016), that were not included in the model.

Data availability statement

The original contributions presented in the study are included in the article/Supplementary Material, further Q11 inquiries can be directed to the corresponding author.

Author contributions

MA conceived and coordinated the study; SP, JL, HN, NM and SR designed, performed, and analyzed the experiments; RD performed structural analyses; SP and MA wrote the paper. All authors have read and agreed to the published version of the manuscript. Q12

Funding

This study was supported by the Deutsche Forschungsgemeinschaft through Collaborative Research Center 974 (SFB 974 to SP, JL, HN, SR, and MA), the European Network on Noonan Syndrome and Related Disorders (NSEuroNet, grant number: 01GM1621B to NM and MA), and the Operational Program Integrated Infrastructure ERDF: Open scientific community for modern interdisciplinary research in medicine (OPENMED; grant number: ITMS 2014+: 313011V455 to RD). Q13

Acknowledgments

We thank the group members at the Institute of Biochemistry and Molecular Biology II of the Heinrich Heine University, particularly Petra Oprée and Kotsene Loumonvi, for supports.

Conflict of interest

The authors declare that the research was conducted in the absence of any commercial or financial relationships that could be construed as a potential conflict of interest. Q14

Publisher's note

All claims expressed in this article are solely those of the authors and do not necessarily represent those of their affiliated organizations, or those of the publisher, the editors and the reviewers. Any product that may be evaluated in this article, or claim that may be made by its manufacturer, is not guaranteed or endorsed by the publisher.

Supplementary material

The Supplementary Material for this article can be found online at: https://www.frontiersin.org/articles/10.3389/fcell.2022.987754/full#supplementary-material Q15

References

Brown, E. J., Albers, M. W., Shin, T. B., IchiKawa, K., Keith, C. T., Lane, W. S., et al. (1994). A mammalian protein targeted by G1-arresting rapamycin-receptor Q16 complex', *Nature. Nature* 369 (6483), 756–758. doi:10.1038/369756A0

Cai, W., Andres, D. A., and Reiner, D. J. (2014). MTORC2 Is required for rit-mediated oxidative stress resistance', *PLoS ONE. PLoS One* 9 (12), e115602. doi:10.1371/journal.pone.0115602

Castel, P., Dharmaiah, S., Sale, M. J., Messing, S., Rizzuto, G., Cuevas-Navarro, A., et al. (2021). RAS interaction with Sin1 is dispensable for mTORC2 assembly and activity. *Proc. Natl. Acad. Sci. U. S. A.* 118 (33), 2103261118. doi:10.1073/pnas.2103261118

Chen, X., Liu, M., Tian, Y., Li, J., Qi, Y., Zhao, D., et al. (2018). Cryo-EM structure of human mTOR complex 2', *Cell Research. Cell Res.* 28 (5), 518–528. doi:10.1038/S41422-018-0029-3

Dhillon, A. S., Pollock, C., Steen, H., Shaw, P. E., Mischak, H., and Kolch, W. (2002). Cyclic AMP-dependent kinase regulates Raf-1 kinase mainly by phosphorylation of serine 259', *Molecular and cellular biology. Mol. Cell. Biol.* 22 (10), 3237–3246. doi:10.1128/MCB.22.10.3237-3246.2002

Ebner, M., Sinkovics, Benjamin, Szczygieł, Magdalena, Wolfschoon Ribeiro, Daniela, Yudushkin, Ivan, et al. (2017). Localization of mTORC2 activity inside cells. *J. Cell Biol.* 216 (2), 343–353. doi:10.1083/JCB.201610060

Frias, M. A., Thoreen, C. C., Jaffe, J. D., Schroder, W., Sculley, T., Carr, S. A., et al. (2006). mSin1 is necessary for akt/PKB phosphorylation, and its isoforms define three distinct mTORC2s', *current biology. Curr. Biol.* 16 (18), 1865–1870. doi:10.1016/j.cub.2006.08.001

Fu, W., and Hall, M. N. (2020). Regulation of MTORC2 signaling. *Genes* 11, Q17 10455–E1119. doi:10.3390/genes11091045

Gagné, L. M., Morin, N., Lavoie, N., Bisson, N., Lambert, J. P., Mallette, F. A., et al. (2021). Tyrosine phosphorylation of DEPTOR functions as a molecular switch to activate mTOR signaling', *Journal of Biological Chemistry. J. Biol. Chem.* 297 (5), 101291. doi:10.1016/j.jbc.2021.101291

Gao, Q., Hou, Y., Li, Z., Hu, J., Huo, D., Zheng, H., et al. (2021). mTORC2 regulates hierarchical micro/nano topography-induced osteogenic differentiation via promoting cell adhesion and cytoskeletal polymerization', *Journal of Cellular and Molecular Medicine. J. Cell. Mol. Med.* 25 (14), 6695–6708. doi:10.1111/jcmm.16672

Gremer, L., Merbitz-Zahradnik, T., Dvorsky, R., Cirstea, I. C., Kratz, C. P., Zenker, M., et al. (2011). Germline KRAS mutations cause aberrant biochemical and physical properties leading to developmental disorders', *Human Mutation. Hum. Mutat.* 32 (1), 33–43. doi:10.1002/humu.21377

Hemsath, L., and Ahmadian, M. R. (2005). Fluorescence approaches for monitoring interactions of Rho GTPases with nucleotides, regulators, and effectors', *Methods. Methods* 37 (2), 173–182. doi:10.1016/j.ymeth.2005.05.014

Huang, K., and Fingar, D. C. (2014). Growing knowledge of the mTOR signaling network. *Semin. Cell Dev. Biol.* 36, 79–90. doi:10.1016/j.semcdb.2014.09.011

Hwang, Y., Kim, L. C., Song, W., Edwards, D. N., Cook, R. S., and Chen, J. (2019). Disruption of the scaffolding function of mLST8 selectively inhibits mTORC2 assembly and function and suppresses mTORC2-dependent tumor growth *in vivo*', *Cancer Research. Cancer Res.* 79 (13), 3178–3184. doi:10.1158/0008-5472.CAN-18-3658

Jacinto, E., Loewith, R., Schmidt, A., Lin, S., Ruegg, M. A., Hall, A., et al. (2004). Mammalian TOR complex 2 controls the actin cytoskeleton and is rapamycin insensitive. *Nat. Cell Biol.* 6, 1122–1128. doi:10.1038/ncb1183

Kazemein Jasemi, N. S., and Reza Ahmadian, M. (2022). Allosteric regulation of GRB2 modulates RAS activation. *Small GTPases* 13 (1), 282–286. doi:10.1080/21541248.2022.2089001

Lake, D., Corrêa, S. A. L., and Müller, J. (2016). Negative feedback regulation of the ERK1/2 MAPK pathway. *Cell. Mol. Life Sci.* 73 (23), 4397–4413. doi:10.1007/S00018-016-2297-8

Lavoie, H., and Therrien, M. (2022). Structural keys unlock RAS-MAPK cellular signalling pathway. *Nature* 609, 248–249. doi:10.1038/D41586-022-02189-7

Lee, Y. R., Chen, M., and Pandolfi, P. P. (2018). The functions and regulation of the PTEN tumour suppressor: New modes and prospects', *Nature reviews. Molecular cell biology. Nat. Rev. Mol. Cell Biol.* 19 (9), 547–562. doi:10.1038/S41580-018-0015-0

Liu, P., Asara, John M., Manning, Brendan D., Blenis, John, Su, Bing, Wei, Wenyi, et al. (2013). Sin1 phosphorylation impairs mTORC2 complex integrity and inhibits downstream Akt signalling to suppress tumorigenesis. *Nat. Cell Biol.* 15 (11), 1340–1350. doi:10.1038/ncb2860

Liu, P., Gan, W., Chin, Y. R., Ogura, K., Guo, J., Zhang, J., et al. (2015). Ptdins(3, 4, 5) P3 -dependent activation of the mTORC2 kinase complex. *Cancer Discov.* 5 (11), 1194–1209. doi:10.1158/2159-8290.CD-15-0460

Liu, P., Guo, J., Gan, W., and Wei, W. (2014). Dual phosphorylation of Sin1 at T86 and T398 negatively regulates mTORC2 complex integrity and activity. *Protein Cell* 5 (3), 171–177. doi:10.1007/s13238-014-0021-8

Loewith, R., Crespo, José L., Bonenfant, Débora, Oppliger, Wolfgang, Jenoe, Paul, Hall, Michael N., et al. (2002). Two TOR complexes, only one of which is rapamycin sensitive, have distinct roles in cell growth control. *Mol. Cell* 10 (3), 457–468. doi:10.1016/S1097-2765(02)00636-6

Lorenzo, C., and McCormick, F. (2020). SPRED proteins and their roles in signal transduction, development, and malignancy', *Genes & development. Genes Dev.* 34 (21–22), 1410–1421. doi:10.1101/GAD.341222.120

Muñoz-Maldonado, C., Zimmer, Y., and Medová, M. (2019). A comparative analysis of individual ras mutations in cancer biology. *Front. Oncol.* 9, 1088. doi:10.3389/fonc.2019.01088

Nakhaei-Rad, S., et al. (2016). The role of embryonic stem cell-expressed RAS (ERAS) in the maintenance of quiescent hepatic stellate cells.', *the Journal of biological chemistry. Am. Soc. Biochem. Mol. Biol.* 291 (16), 8399–8413. doi:10.1074/jbc.M115.700088

Nakhaei-Rad, S., Nakhaeizadeh, H., Kordes, C., Cirstea, I. C., Schmick, M., Dvorsky, R., et al. (2015). The function of embryonic stem cell-expressed RAS (E-RAS), a unique RAS family member, correlates with its additional motifs and its structural properties. *J. Biol. Chem.* 290 (25), 15892–15903. doi:10.1074/jbc.M115.640607

Nakhaeizadeh, H., Amin, E., Nakhaei-Rad, S., Dvorsky, R., and Ahmadian, M. R. (2016). The RAS-effector interface: Isoform-specific differences in the effector binding regions', *PLoS ONE. PLoS One* 11 (12), e0167145. doi:10.1371/JOURNAL.PONE.0167145

Oh, W. J., and Jacinto, E. (2011). mTOR complex 2 signaling and functions', *Cell Cycle. Cell Cycle* 10 (14), 2305–2316. doi:10.4161/CC.10.14.16586

Oh, W. J., Wu, C. c., Kim, S. J., Facchinetti, V., Julien, L. A., Finlan, M., et al. (2010). MTORC2 can associate with ribosomes to promote cotranslational phosphorylation and stability of nascent Akt polypeptide. *EMBO J. EMBO J* 29 (23), 3939–3951. doi:10.1038/emboj.2010.271

Pearce, L. R., Huang, X., Boudeau, J., Pawlowski, R., Wullschleger, S., Deak, M., et al. (2007). Identification of protor as a novel rictor-binding component of mTOR complex-2', *biochemical journal. Biochem. J.* 405 (3), 513–522. doi:10.1042/BJ20070540

Pearce, L. R., Komander, D., and Alessi, D. R. (2010). The nuts and bolts of AGC protein kinases. *Nat. Rev. Mol. Cell Biol.* 11 (1), 19–22. doi:10.1038/nrm2822

Peterson, T. R., Laplante, M., Thoreen, C. C., Sancak, Y., Kang, S. A., Kuehl, W. M., et al. (2009). DEPTOR is an mTOR inhibitor frequently overexpressed in multiple myeloma cells and required for their survival', *cell. Cell* 137 (5), 873–886. doi:10.1016/j.cell.2009.03.046

Rothbauer, U., Zolghadr, K., Muyldermans, S., Schepers, A., Cardoso, M. C., and Leonhardt, H. (2008). A versatile nanotrap for biochemical and functional studies with fluorescent fusion proteins. *Mol. Cell. Proteomics* 7 (2), 282–289. doi:10.1074/MCP.M700342-MCP200

Sarbassov, D. D., Guertin, D. A., Ali, S. M., and Sabatini, D. M. (2005). Phosphorylation and regulation of Akt/PKB by the rictor-mTOR complex', *Science (New York, N.Y.). Science* 307 (5712), 1098–1101. doi:10.1126/SCIENCE.1106148

Saxton, R. A., and Sabatini, D. M. (2017). mTOR signaling in growth, metabolism, and disease', *cell. Cell* 168 (6), 960–976. doi:10.1016/J.CELL.2017.02.004

Scaiola, A., Mangia, F., Imseng, S., Boehringer, D., Berneiser, K., Shimobayashi, M., et al. (2020). The 3.2-Å resolution structure of human mTORC2', *Science Advances. Sci. Adv.* 6 (45), 2020. doi:10.1126/SCIADV.ABC1251

Schroder, W. A., Buck, M., Cloonan, N., Hancock, J. F., Suhrbier, A., Sculley, T., et al. (2007). Human Sin1 contains Ras-binding and pleckstrin homology domains and suppresses Ras signalling. *Cell. Signal.* 19 (6), 1279–1289. doi:10.1016/j.cellsig.2007.01.013

Stuttfeld, E., Scaiola, Alain, Sauer, Evelyn, Hall, Michael N., Maier, Timm, Ban, Nenad, et al. (2018). 7. eLife. doi:10.7554/eLife.33101Architecture of the human mTORC2 core complex

Tafur, L., Kefauver, J., and Loewith, R. (2020). Structural insights into TOR signaling. *Genes* 11 (8), 8855–E924. doi:10.3390/genes11080885 Q18

Tatebe, H., et al. (2017). Substrate specificity of tor complex 2 is determined by a ubiquitin-fold domain of the sin1 subunit', eLife. *eLife Sci. Publ. Ltd.* 6. doi:10.7554/eLife.19594.001

Tomas, A., Futter, C. E., and Eden, E. R. (2014). EGF receptor trafficking: Consequences for signaling and cancer', *Trends in cell biology. Trends Cell Biol.* 24 (1), 26–34. doi:10.1016/J.TCB.2013.11.002

Wrobel, L., Siddiqi, F. H., Hill, S. M., Son, S. M., Karabiyik, C., Kim, H., et al. (2020). mTORC2 assembly is regulated by USP9X-mediated deubiquitination of RICTOR', *cell reports. Cell Rep.* 33 (13), 108564. doi:10.1016/j.celrep.2020.108564

Yang, Q., Inoki, K., Ikenoue, T., and Guan, K. L. (2006). Identification of Sin1 as an essential TORC2 component required for complex formation and kinase activity. *Genes Dev.* 20 (20), 2820–2832. doi:10.1101/GAD.1461206

Yu, Z., Chen, J., Takagi, E., Wang, F., Saha, B., Liu, X., et al. (2022). Interactions between mTORC2 core subunits Rictor and mSin1 dictate selective and context-dependent phosphorylation of substrate kinases SGK1 and Akt. *J. Biol. Chem.* 298, 102288. doi:10.1016/j.jbc.2022.102288

Yuan, H. X., and Guan, K. L. (2015). The SIN1-PH domain connects mTORC2 to PI3K', *Cancer Discovery. Cancer Discov.* 5 (11), 1127–1129. doi:10.1158/2159-8290.CD-15-1125

Yuan, Y., Pan, B., Sun, H., Chen, G., Su, B., and Huang, Y. (2015). Characterization of Sin1 isoforms reveals an mTOR-dependent and independent function of Sin1γ', *PLoS ONE. PLoS One* 10 (8), e0135017. doi:10.1371/JOURNAL.PONE.0135017

Zhang, S.-C., et al. (2014). in *'Liposome reconstitution and modulation of recombinant prenylated human rac1 by GEFs, GDI1 and Pak1'*, PLoS ONE. Editor E. Manser, 9, e102425. doi:10.1371/journal.pone.0102425*Public Libr. Sci.*7

Zheng, Y., Ding, L., Meng, X., Potter, M., Kearney, A. L., Zhang, J., et al. (2022). Structural insights into Ras regulation by SIN1. *Proc. Natl. Acad. Sci. U. S. A.* 119 (19), e2119990119. doi:10.1073/pnas.2119990119

Zhou, P., Zhang, N., Nussinov, R., and Ma, B. (2015). Defining the domain arrangement of the mammalian target of rapamycin complex component rictor protein. *J. Comput. Biol.* 22 (9), 876–886. doi:10.1089/CMB.2015.0103

Zimmermann, S., and Moelling, K. (1999). Phosphorylation and regulation of raf by akt (protein kinase B)', *science. Science* 286 (5445), 1741–1744. doi:10.1126/science.286.5445.1741

Zinzalla, V., Stracka, D., Oppliger, W., and Hall, M. N. (2011). Activation of mTORC2 by association with the ribosome', *Cell. Cell* 144 (5), 757–768. doi:10.1016/j.cell.2011.02.014

8. DISCUSSION

The RAS signaling pathways are central in the response to growth factors and other ligand stimulations and are not only involved in cell survival and proliferation but also the formation and progression of various diseases [143]. These diseases are based on the hyperactivation of the RAS signaling cascade towards RAF-MEK-ERK and PI3K-AKT. Mutations in the classical RAS genes can be found in over 25% of human cancers and are mostly located in the hotspot amino acids G12, G13 and Q61 [144], which lead to GAP-insensitivity (G12V) or drastically increased nucleotide exchange (G13D and Q61L) [145]. Additionally, common cancer mutations can be found in accessory proteins, like SPRED1, KSR1 or SHP2, that modulate and regulate the RAS signaling pathways [15]. Gain- or loss-of-function mutations in accessory proteins play a major role in RASopathies. This group of syndromes comprises germline mutations that cause a mild gain-of-function of the RAS signaling cascade and lead to phenotypes, including neurocognitive impairment, cardiac and facial anomalies, and an increased risk of cancer development [146,147].

Direct treatment of RAS-driven cancers or diseases is still incredibly difficult as the intracellular signaling pathways are connected via fine-tuned cross-talks, auto-inhibition and feedback loops, and often develop drug resistance or major side effects upon protein inhibition. Basic research is needed to understand the relationship between signaling cascades and the regulation of enzymatic activities, but also to identify new interaction partners and binding sites to predict and estimate new therapeutic strategies. Different approaches were used to inhibit hyperactive RAS, which includes: (i) targeting franesyltransferases to avert RAS membrane localization [148], (ii) using small molecules to specifically target G12C mutated RAS [149], (iii) target RAS dimerization events at the membrane [150] or (iv) target activators, inactivators or effectors of RAS signaling pathways [151]. Even though some of these approaches already provided promising results, the read out of those studies mostly focuses on ERK or AKT phosphorylation and tumor progression. Other cascades that might be affected by RAS inhibition, the non-canonical signaling pathways, are usually overlooked.

Chapters 3 and 4 of this thesis summarize the role of accessory proteins in the RTK-RAS-MAPK-signaling pathway and highlight them as possible therapeutic targets. This way, the attenuation of a signaling pathway, instead of inhibition (total abolishment) via directly targeting the main components, may bring the signaling to a physiological level and lead to less toxicity and unpredictable events towards other signaling cascades. In this context, Chapter 6 describes and focuses on the detailed binding of the scaffold protein IQGAP, in this case not towards RAS signaling members, but towards another member of the RAS superfamily: CDC42, and highlights the importance of accurate binding models. In Chapters 5 and 7, two non-canonical RAS signaling pathways are investigated, which, in the case of arginase, opens a whole new downstream pathway regarding the production of polyamines, and in the case of SIN1, might be part of the fine-tuned feedback mechanisms to terminate the intracellular signaling cascade. Their interaction with RAS and their role in the cells will be further discussed below.

8.1 THE INTERACTION OF ARG1 AND ERAS

In our study, we could identify arginase 1 as a new, direct interaction partner of ERAS using mass spectroscopy, various biophysical and biochemical methods as well as cell biological approaches and confocal imaging. Furthermore, we could monitor the role of ARG1 in the context of hepatic stellate cell quiescence and activation by using selective inhibitors. The direct consequence of ERAS and ARG1 interaction is still unanswered but our results open up room for discussion.

Previously, it was shown that ERAS is located on the plasma and endo-membranes as well as in the nucleus [10]. In our study, we could additionally show that ARG1 can associate with the membrane and further co-localizes with ERAS on the PM of quiescent HSCs. It is tempting to speculate that the functional relationship of ERAS and ARG1 either takes place at the membrane or is all about the localization itself. The formation of microdomains is important for several different signaling pathways and could be shown for EGFR signaling towards RAS [152] but also for eNOS activity, which co-localizes with caveolin-1 and is negatively regulated in caveolae in erythrocytes [153]. In red blood cells, which contain a high amount of ARG1 as well, the activity of ARG1 was found to be approximately 100 times higher in membrane fraction than cytoplasmic fraction [154]. Additionally, it was proposed that ARG1 interacts with flotillin-1, which might coordinate membrane localization and also increases ARG1 activity. Even though we could not confirm an influence of the membrane or ERAS on ARG1 activity, the interaction with other proteins, like flotillin-1, which is also a scaffold protein of the RAS-MAPK pathway [15,155] and known to be part of lipid microdomains [156], could increase the K_m of ARG1 and/or determine a microdomain which optimizes its enzymatic activity. In this context, the interaction of ARG1 and ERAS could be important to orchestrate the localization of both proteins in the same microdomain and increase the dwell time of ARG1 on the membrane where it could localize close to L-arginine transporters. An important class of L-arginine transporters is the cationic amino acid transporter with the isoforms CAT1, 2A, 2B and 3. The CAT isoforms differ in their affinity and specificity for CAAs (CAT1: 0.10-0.16 mM, CAT2B and CAT3: 0.25-0.70 mM and CAT2A 2-5 mM) [157]. The affinity of CAT2A for CAAs is comparatively low but squares with the affinity of ARG1 to L-arginine. Both proteins are furthermore following the same expression pattern in HSCs during activation, showing a strong peak in quiescent cells at day 0. iNOS is co-expressed with CAT1 and CAT2B mRNA. Interestingly, CAT1 expressing cells can be L-arginine depleted by other ARG1 containing cells due to their preferred exchange function and quite slow L-arginine uptake [157]. The CAT isoform 2B is the inducible isoform and has a higher transportation capacity than CAT1. CAT2B and iNOS are often co-expressed or even control the other's expression like it was shown in astrocytes [157,158]. In a proximal protein interaction landscape of HRAS, KRAS and NRAS, hundreds of potential RAS interaction partners were collected, comprising 14 different amino acid transporters, including CAT1 and CAT2(A/B) [47]. If CATs are also interacting with ERAS and form a microdomain together with ARG1, needs to be investigated in the future.

The role of ARG1 in the maintenance of HSC quiescence could be studied using the arginase inhibitor nor-NOHA. After the addition of nor-NOHA, accelerated HSC differentiation was observed, which included an early loss of lipid droplets and a fast switch of the cell phenotype into myofibroblast-like cells. The same observations could be monitored while treatment with the ODC1 inhibitor DFMO (α-difluoromethylornithine),

leading to the hypothesis that polyamines exert influence on HSC quiescence and therefore take part in controlling HSC fate decisions. Polyamines are well known for their effect on proliferation [159] and autophagy modulation [101,102,160,161]. Additionally, polyamines are strongly regulated during liver regeneration caused by partial hepatectomy [162–165] but also exhibit a protective effect against liver fibrosis [166–168]. Direct downstream effectors of polyamines are hardly identified. In the context of HSC quiescence and maintenance of stemness, two pathways that are controlled by polyamines are of particular interest. One important function of polyamines is the hypusination of the transcription initiation factor 5A (eIF5A), a unique post-translational modification, which is needed to proceed with the translation of proteins with proline-rich sequences and other motifs [169,170]. The post-translational modification of eIF5A is tightly regulated by the two enzymes deoxyhypusine synthase and deoxyhypusine hydroxylase, which transfer the hypusine residue from spermidine to eIF5A. Until now, eIF5A is the only known substrate of these enzymes and the hypusination is highly conserved in all eukaryotes [171,172]. One target of hypusinated eIF5A is the autophagy-related protein 3 (ATG3), which is part of the complex for LC3 (Microtubule-associated proteins 1A/1B light chain 3) lipidation (converting LC3-I to LC3-II) and therefore central for the autophagosome assembly [170]. Additionally, it was shown, that polyamines have a promoting effect on ATG5 (autophagy protein 5) levels facilitating autophagy while liver damage [168]. Another effector of polyamines is Mindy-1, a deubiquitinase that was shown to maintain stemness by sustaining OCT4 protein levels and inducing self-renewal in ESCs [173]. HSCs are considered liver resident mesenchymal stem cells, which are able to differentiate into diverse cell types in response to liver damage [137]. Furthermore, it was reported that the stem cell marker OCT4 is expressed in quiescent HSCs [134], but disappears quickly after isolation and cultivation of these cells *in vitro*. Even though, low expression of OCT4 mRNA levels could also be detected in our experiments, the existence of this stem cell marker in HSCs is highly controversial and extensively debated [174]. However, Mindy-1 could be one of the many polyamine effectors that participate in the maintenance of HSC quiescence. The third point of ARG1 expression in HSCs may cover the counteraction of iNOS activity. As explained earlier, arginase and NO synthases are competing for the same substrate L-arginine. While simultaneous expression of both proteins, high arginase levels inhibit the production of NO [111]. Especially in endothelial cells, red blood cells as well as smooth muscle cells, the counteraction of eNOS or iNOS respectively and ARG1 fulfills an important regulatory function for the vascular system [113,175]. In the case of HSCs, ARG1 and iNOS are not counteracting and stealing away each other's substrate, but are reciprocally regulated on transcriptional level by each other. This switch can also be observed in immune cells in response to inflammation [176]. ARG1 activity is promoting cell homeostasis and repair, while iNOS is inducing acute inflammatory events in response to cytokines and dramatic environmental changes like the isolation of these cells from their stem cell niche. The inhibition of iNOS activity with the molecule L-NIO could decelerate HSC differentiation in our experiments and underlined the need for an ARG1-iNOS switch while HSC activation.

Taken together, the reason for direct ERAS-ARG1 interaction still needs more research and should focus of the formation and isolation of microdomains on the plasma membrane. Furthermore, it would be interesting to investigate, whether it is possible to interfere with the bidirectional control of ARG1 and iNOS to prevent rapid iNOS activation by sustaining ARG1 levels to decelerate early liver fibrosis. Strategies that maintain HSC quiescence or

even induce HSC reversion would be a great tool for the treatment of liver fibrosis and need basic research to unravel signaling pathways of HSC activation and quiescence.

8.2 THE INTERACTION OF RAS AND SIN1

SIN1 is an indispensable member of the mTORC2 complex. The importance of the NTD and the CRIM domain for complex integrity and substrate recognition, respectively, is well studied and reported multiple times [54,56,179]. The interest in the PH domain in facilitating membrane localization as well as the RBD and its ability to associate with RAS proteins increased a lot, seeking answers to understand mTORC2 regulation.

TABEL 3: CANCER MUTATIONS OF SIN1 (MAPKAP1)

Mutation		Mutation		Mutation	
V30I	NTD	D188N	CRIM	D360G	
L31V/F	NTD	M193V	CRIM	G361V	
D37G	NTD	T194I	CRIM	F363L	aRBD
P44H	NTD	V196A	CRIM	S367L	aRBD
S45L	NTD	A201T	CRIM	H381Q	aRBD
G51W	NTD	G208R/W	CRIM	R395Q	PH
Q55H	NTD	Q213R	CRIM	L402P	PH
N58T	NTD	T215I	CRIM	E410Q	PH
G59C	NTD	S216I	CRIM	D412H/G	PH
Q62H	NTD	R219Q	CRIM	P413L	PH
G63S	NTD	E220K	CRIM	T415M	PH
D71N	NTD	P221L	CRIM	N416H	PH
D77Y	NTD	N224D/S	CRIM	I425N	PH
G79V	NTD	S228N	CRIM	P429L	PH
R81T	NTD	A229V	CRIM	I432V	PH
R82K	NTD	H233Y/L	CRIM	S434F	PH
R83C/L	NTD	E240K	CRIM	A439V	PH
S84L	NTD	D242N	CRIM	S449I	PH
T86K	NTD	T243I	CRIM	H450R	PH
R89T/I	NTD	N251S	CRIM	A451T/E	PH
E91K	NTD	K256Q	CRIM	T456M	PH
R92Q	NTD	F257S	CRIM	S459N	PH
R94Q/L	NTD	S260N	CRIM	N460K	PH
N99T	NTD	E266K	CRIM	D462N	PH
I101M	NTD	R282Q	RBD	Y467N	PH
N105S	NTD	F289L	RBD	E469K	PH
Q107R	NTD	S290F	RBD	S470L	PH
S113Y	NTD	V294A	RBD	A472T	PH
F124I	NTD	A308V	RBD	T474N	PH
G137A	NTD	R311Q	RBD	E477K	PH
Q139P	CRIM	S315F	RBD	L480P	PH
R145C/H	CRIM	Q316K	RBD	R494W/Q/L	PH
P150H	CRIM	R324H	RBD	D496Y	PH
L151V	CRIM	A334V	RBD	K501E	PH
P156S	CRIM	V335I	RBD	R503T	PH
S161C	CRIM	D338Y	RBD	R508C/H	PH
H168R	CRIM	R353H	RBD	T509M	PH
D178N	CRIM	E354Q	RBD	K517N	PH
Y180H/C	CRIM	D360G		S519F	PH
P182S	CRIM	G361V		Q522K	PH

Data from COSMIC data base [177,178]

Several cancer mutations in SIN1 were yet identified, leading to increased mTORC2 activity and therefore AKT-mediated cell growth and proliferation (Table 3). As explained earlier, the double phosphorylation of SIN1 on T86 and T398 dissociates the protein from its complex and terminates its activity [80]. Known kinases executing these phosphorylations are S6K and AKT. Both AGC kinases detect the recognition motif RXRXXS/T [180,181] and therefore recognize SIN1 by the sequences ^{81}RRRSNT^{86} and ^{393}RLRFTT^{398}. On this note, it is not surprising that cancer mutations occur within the first N-terminal motif (Table 3; marked in orange), which impairs T86 phosphorylation and sustains mTORC2 integrity. Interestingly, only one mutation has been detected in the second motif (Table 3; marked in red). It was reported, that the phosphorylation of T398 disrupts the binding towards mTOR [80] and may take part in releasing the inhibitory binding of the SIN1-PH domain that masks the catalytic pocket. As in general, the single phosphorylation of SIN1 seems to be favorable, the preservation of the T398 might be beneficial for cancer cell signaling. More mutations were observed and characterized by Liu et al. in 2015, which are located within the PH domain (Table 3; marked in blue) [59]. Those four mutations released the direct, inhibitory binding of SIN1 to mTOR, therefore opening the catalytic pocket of the complex that resulted in increased AKT phosphorylation. Cancer mutations in the CRIM domain are not characterized yet. As deletion of the CRIM domain abolishes the mTORC2

activity, pro-tumorigenic mutations, in contrast, might increase the interaction with the substrate or are not from major effect but occur as a result of genomic instability. A particular focus is on the mutations located in the RBD of SIN1. In our study, we could identify F289, S290, L291, K307, R311 and R312 as critical binding residues of SIN1-RBD to the classical RAS proteins. Interestingly, three of these six residues were also found as cancer mutations (Table 3; marked in green) and would therefore abolish SIN1-RAS interaction. Additionally, the newly assigned aRBD, which spans from aa 364 to 390, comprises two more cancer mutations at F363 and H381 (Table 3; marked in yellow) that were specifically considered as interaction sites with KRAS4A and contribute to their direct binding [62]. These mutational circumstances suggest that the abolishment of RAS-SIN1 interaction leads to cancerogenic cell signaling that is most likely executed by either hyperactive mTORC2-AKT or RAS-MAPK pathway.

In our study of SIN1-RAS interaction, we observed for the first time that the association of SIN1 with the membrane was reduced in the presence of RAS. Furthermore, we confirmed that SIN1, and most likely the mTORC2 complex, exists in different pools and is always partly membrane localized [73]. Additionally, we again showed that the binding preference of $HRAS^{G12V}$ is the strongest towards C-RAF-RBD, followed by SIN1-RBD and lastly PI3K-RBD and that the RBD-PH tandem domain folds into an auto-inhibited state [63]. Combining all that information into one process, leads us to the model displayed in Figures 8 and 9.

Upon growth factor binding, RAS gets activated via adaptor proteins in complex with RAS GEFs and switches from its GDP- into a GTP-bound state [182]. Several receptors can, additionally to RAS, activate PI3K and enable the conversion of PIP_2 to PIP_3. Upon initial activation, RAS•GTP recruits the RAF paralogues to the membrane, which get further activated by dephosphorylation events, including the conserved inhibitory site at S259 (for C-RAF), and subsequently hetero- or homo-dimerization of the RAF paralogues. Furthermore, RAS•GTP potentiates PI3K activity by directly binding the p110 subunit [28]. From this point, the signaling towards PI3K could be initiated without former interaction of the latter with the receptor. As a response, AKT translocates towards the PIP_3 containing cluster and is available for upcoming activations of the corresponding kinases. In Phase I of our model (initiation of the signaling cascade), the mTORC2 complex is already partly membrane localized, independent of PI3K activity (Figure 8; upper panel). In our experiments, we noted the ability of the SIN1-PH domain to associate with a variety of lipids, not only PIP_3. Ebner et al. have furthermore shown, that the phosphorylation of AKT was only dependent on its translocation to the membrane, but not on PI3K activity itself [73]. This leads to the suggestion, that the SIN1-PH domain, or even another component of the mTORC2 complex, contributes to persistent membrane localization of the complex that might lead to the release of the inhibitory binding from SIN1-PH domain to mTOR. The “closed” conformation of the mTORC2 complex could be existent as the cytosolic form, or a state that allows no immediate RAS interaction with the RBD. Phase II (Figure 8; lower panel) resembles the active signaling state. Here, RAF activation leads to MEK and ultimately ERK phosphorylation, which can induce cell responses resulting in proliferation and cell survival. On the other side, membrane associated AKT gets phosphorylated by PDK1, which is also recruited to the membrane by PIP_3-rich clusters and is finally phosphorylated by mTORC2 on S473. The double phosphorylation fully activates AKT and regulates cell growth, proliferation, and survival. In this state, the mTORC2 complex is in an

“open” conformation, that may be caused by PIP_3 binding of the SIN1-PH domain, or simply by the co-localization in the same signaling cluster as AKT.

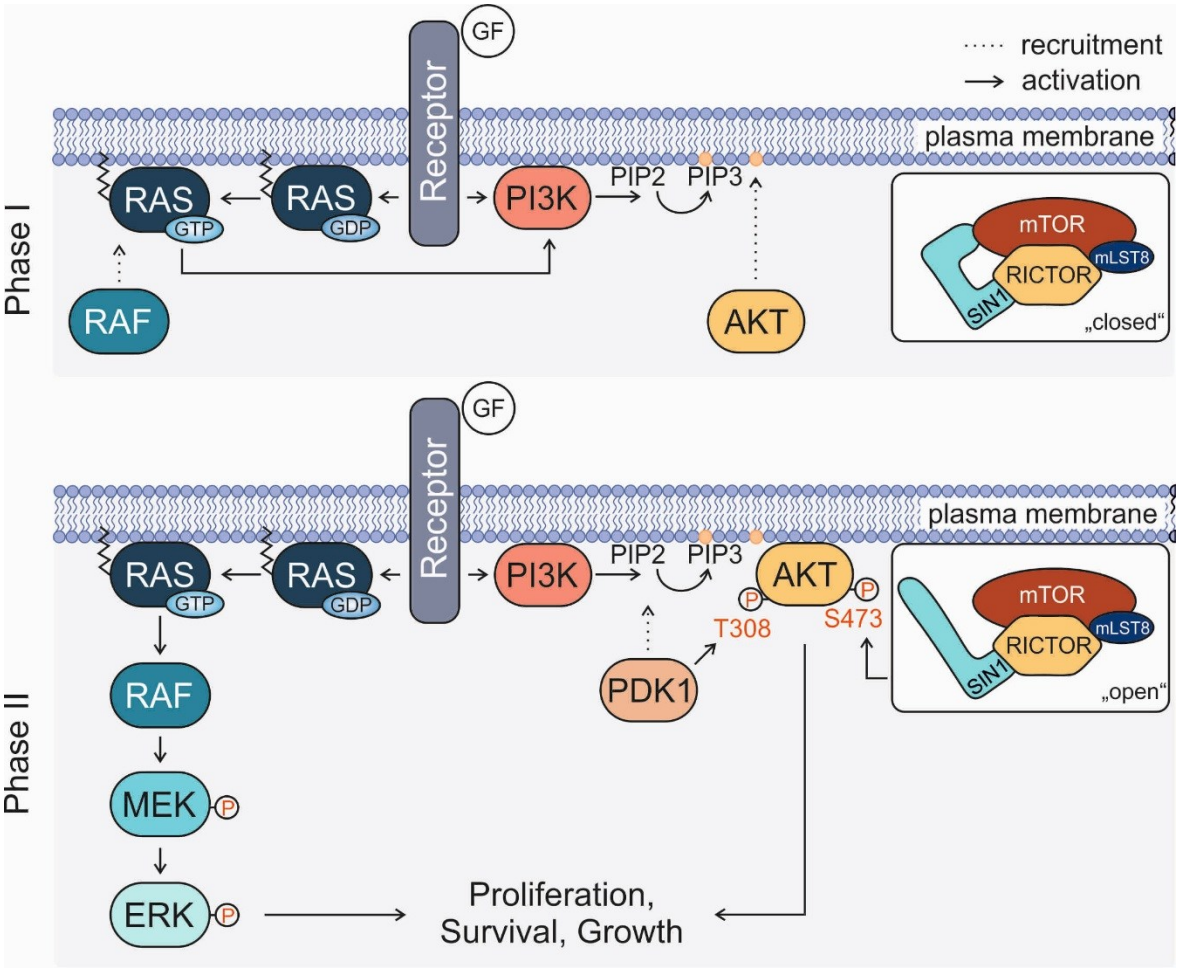

FIGURE 8. Phase I and II – Initiation and activation of the RAS-MAPK and PI3K-AKT signaling cascade. The activation process of the canonical RAS-signaling pathway can be divided into Phase I, the early initial activation, and Phase II, the downstream activation of mediators, like ERK and AKT, that regulate proliferation, survival, and cell growth. In the first Phase, recruitment of signaling components to the site of action as well as positive cross-talks are essential to initiate and potentiate the signaling cascade in response to growth factor binding. In Phase II, the actual signal transmission takes place by multiple phosphorylation and dephosphorylation events. Dotted lines resemble recruitment; arrows stand for positive interactions or transformations.

In Phase III, negative feedback mechanisms shut down the signaling cascades and terminate growth factor induced stimulation (Figure 9). The model only displays a few feedback loops, as the whole network includes many more steps and interactions but would exceed the scope of this scheme, like the inactivation of RAS, the ubiquitination and endocytosis of the receptors, the dephosphorylation of PIP_3 by PTEN and more [183–185]. Phosphorylated ERK can, among other members, directly inactivate RAF kinase by interfering with RAF-RAS interaction and RAF dimerization. Furthermore, fully activated AKT re-phosphorylates the critical S259 of C-RAF thereby, returning RAF to its inactive cytosolic state [186,187]. Simultaneously, GTP-bound RAS is now able to bind to the accessible “open” conformation of SIN1 that either opened due to specific lipid or even substrate interaction. Since at least HRAS has a higher affinity towards SIN1-RBD, rather

than PI3K-RBD, the activation events of the latter signaling pathway will be abolished. On top of that, RAS-SIN1 interaction now interferes with the membrane binding of the SIN1-PH domain and releases the complex to the cytosol. The mTORC2 complex now either dissociates or returns to a closed, auto-inhibited conformation (Figure 9). In this model, RAS-SIN1 interaction thus fulfills an important role in the inhibitory self-regulation of the pathway by shutting down the PI3K-AKT pathway upon RAS activation. The effect of RAS-SIN1 association towards ERK signaling or other effectors is not included here but would be interesting to add in the future. The abolishment of this natural feedback loop by mutation of the SIN1-RBD, for example in the residues mentioned in Table 3, would disrupt the natural crosstalk of RAS-MAPK and PI3K-AKT cascade and could lead to sustained downstream signaling.

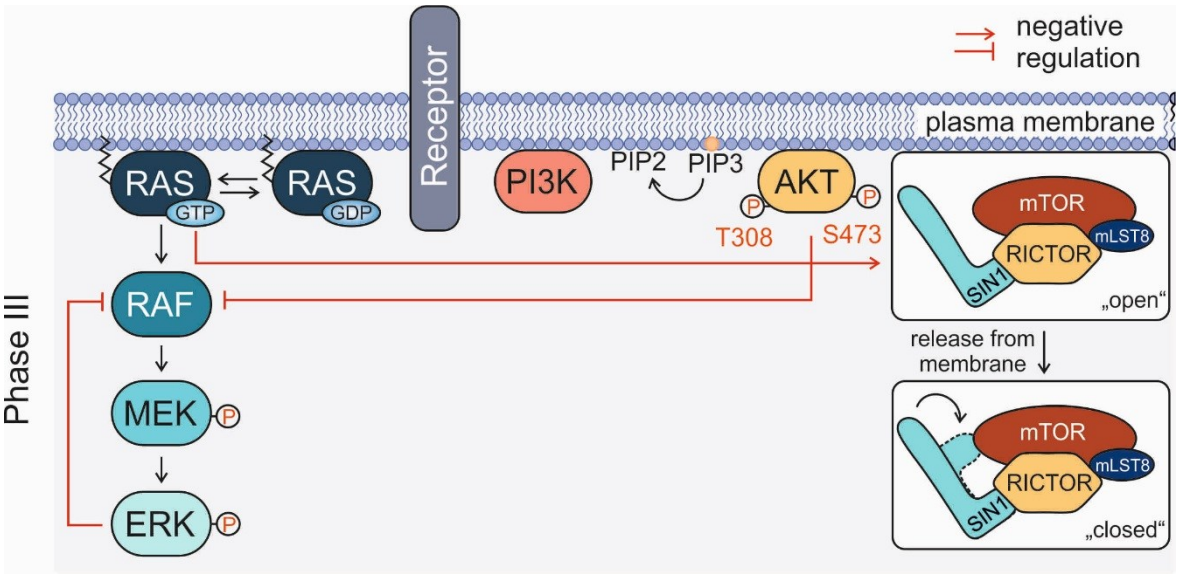

FIGURE 9. Phase III – Negative feedback regulation of RAS-MAPK and PI3K-AKT pathway. In Phase III, negative feedback mechanisms terminate ERK and AKT activation pathways by (i) re-phosphorylation of C-RAF by p-ERK and p-AKT, (ii) competitive binding of RAS•GTP to SIN1-RBD instead of PI3K-RBD, (iii) dissociation of SIN1-PH domain from the membrane and return to its auto-inhibited state in response to RAS binding. Red lines resemble negative regulations.

The model presented in Figures 8 and 9, was formed out of the observations made from the interaction of classical RAS proteins and the domains of SIN1 isoform 1. Other SIN1 isoforms lack parts of the RBD or the PH domain (see Table 1) and may undergo different types of regulation in their respective mTORC2 complex. Other members of the RAS family, like ERAS and RIT1, exhibit dissimilar affinities towards the RBDs of RAF, SIN1, and PI3K than HRAS, which suggests another involvement of their interaction in signaling regulation.

In the future, it would be of major interest to include and distinguish the involvement of different upstream stimulations, like EGF, insulin and others, as well as the modulation of other downstream effectors to the regulatory system of the mTORC2 complex. SIN1 needs to be understood as a critical regulator of mTORC2 activity that is not only irreplaceable for the complex integrity and activity, but the central negative gatekeeper of the complex by (i) phosphorylation (T86 and T398), (ii) inhibitory binding of mTOR, (iii) membrane association, (iv) subcellular localization, and (v) conformation-depended RAS binding.

9. REFERENCES

1. Wennerberg, K.; Rossman, K.L.; Der, C.J. The Ras superfamily at a glance. *J. Cell Sci.* **2005**, *118*, 843–846, doi:10.1242/jcs.01660.
2. Wittinghofer, A.; Vetter, I.R. Structure-function relationships of the G domain, a canonical switch motif. *Annu. Rev. Biochem.* **2011**, *80*, 943–971, doi:10.1146/annurev-biochem-062708-134043.
3. Vetter, I.R.; Wittinghofer, A. The guanine nucleotide-binding switch in three dimensions. *Science (80-.).* **2001**, *294*, 1299–1304, doi:10.1126/science.1062023.
4. Casey, P.J.; Seabra, M.C. Protein Prenyltransferases. *J. Biol. Chem.* **1996**, *271*, 5289–5292, doi:10.1074/JBC.271.10.5289.
5. Levental, I.; Lingwood, D.; Grzybek, M.; Coskun, Ü.; Simons, K. Palmitoylation regulates raft affinity for the majority of integral raft proteins. *Proc. Natl. Acad. Sci. U. S. A.* **2010**, *107*, 22050–22054, doi:10.1073/pnas.1016184107.
6. Jang, H.; Abraham, S.J.; Chavan, T.S.; Hitchinson, B.; Khavrutskii, L.; Tarasova, N.I.; Nussinov, R.; Gaponenko, V. Mechanisms of membrane binding of small GTPase K-Ras4B farnesylated hypervariable region. *J. Biol. Chem.* **2015**, *290*, 9465–9477, doi:10.1074/JBC.M114.620724.
7. Takahashi, K.; Mitsui, K.; Yamanaka, S. Role of ERas in promoting tumour-like properties in mouse embryonic stem cells. *Nature* **2003**, *423*, 541–545, doi:10.1038/nature01646.
8. Nakhaei-Rad, S.; Nakhaeizadeh, H.; Kordes, C.; Cirstea, I.C.; Schmick, M.; Dvorsky, R.; Bastiaens, P.I.H.; Häussinger, D.; Ahmadian, M.R. The function of embryonic stem cell-expressed RAS (E-RAS), a unique RAS family member, correlates with its additional motifs and its structural properties. *J. Biol. Chem.* **2015**, *290*, 15892–15903, doi:10.1074/jbc.M115.640607.
9. Kubota, E.; Kataoka, H.; Aoyama, M.; Mizoshita, T.; Mori, Y.; Shimura, T.; Tanaka, M.; Sasaki, M.; Takahashi, S.; Asai, K.; et al. Role of ES cell-expressed Ras (ERas) in tumorigenicity of gastric cancer. *Am. J. Pathol.* **2010**, *177*, 955–963, doi:10.2353/ajpath.2010.091056.
10. Nakhaei-Rad, S.; Nakhaeizadeh, H.; Götze, S.; Kordes, C.; Sawitza, I.; Hoffmann, M.J.; Franke, M.; Schulz, W.A.; Scheller, J.; Piekorz, R.P.; et al. The Role of Embryonic Stem Cell-expressed RAS (ERAS) in the Maintenance of Quiescent Hepatic Stellate Cells. *J. Biol. Chem.* **2016**, *291*, 8399–413, doi:10.1074/jbc.M115.700088.
11. Muñoz-Maldonado, C.; Zimmer, Y.; Medová, M. A comparative analysis of individual ras mutations in cancer biology. *Front. Oncol.* **2019**, *9*, 1088, doi:10.3389/FONC.2019.01088/BIBTEX.
12. Schlessinger, J. Signal transduction by allosteric receptor oligomerization. *Trends Biochem. Sci.* **1988**, *13*, 443–447, doi:10.1016/0968-0004(88)90219-8.
13. Schlessinger, J. Cell Signaling by Receptor Tyrosine Kinases. *Cell* **2000**, *103*, 211–225, doi:10.1016/S0092-8674(00)00114-8.
14. Kuriyan, J.; Cowburn, D. Modular peptide recognition domains in eukaryotic signaling. *Annu. Rev. Biophys. Biomol. Struct.* **1997**, *26*, 259–288, doi:10.1146/annurev.biophys.26.1.259.
15. Pudewell, S.; Wittich, C.; Kazemein Jasemi, N.S.; Bazgir, F.; Ahmadian, M.R. Accessory proteins of the RAS-MAPK pathway: moving from the side line to the front line. *Commun. Biol.* **2021**, *4*, 696, doi:10.1038/s42003-021-02149-3.
16. Jasemi, N.S.K.; Herrmann, C.; Estirado, E.M.; Gremer, L.; Willbold, D.; Brunsveld, L.; Dvorsky, R.; Ahmadian, M.R. The intramolecular allostery of GRB2 governing its interaction with SOS1 is modulated by phosphotyrosine ligands. *Biochem. J.* **2021**, *478*, 2793–2809, doi:10.1042/BCJ20210105.
17. Giubellino, A.; Burke, T.R.; Bottaro, D.P. Grb2 signaling in cell motility and cancer. *http://dx.doi.org/10.1517/14728222.12.8.1021* **2008**, *12*, 1021–1033, doi:10.1517/14728222.12.8.1021.

18. Lowenstein, E.J.; Daly, R.J.; Batzer, A.G.; Li, W.; Margolis, B.; Lammers, R.; Ullrich, A.; Skolnik, E.Y.; Bar-Sagi, D.; Schlessinger, J. The SH2 and SH3 domain-containing protein GRB2 links receptor tyrosine kinases to ras signaling. *Cell* **1992**, *70*, 431–442, doi:10.1016/0092-8674(92)90167-B.

19. Adariani, S.R.; Buchholzer, M.; Akbarzadeh, M.; Nakhaei-Rad, S.; Dvorsky, R.; Ahmadian, M.R. Structural snapshots of RAF kinase interactions. *Biochem. Soc. Trans.* **2018**, *46*, 1393–1406, doi:10.1042/BST20170528.

20. Terrell, E.M.; Morrison, D.K. Ras-mediated activation of the Raf family kinases. *Cold Spring Harb. Perspect. Med.* **2019**, *9*, doi:10.1101/cshperspect.a033746.

21. Vojtek, A.B.; Hollenberg, S.M.; Cooper, J.A. Mammalian Ras interacts directly with the serine/threonine kinase Raf. *Cell* **1993**, *74*, 205–214, doi:10.1016/0092-8674(93)90307-C.

22. Cseh, B.; Doma, E.; Baccarini, M. "RAF" neighborhood: Protein–protein interaction in the Raf/Mek/Erk pathway. *Febs Lett.* **2014**, *588*, 2398, doi:10.1016/J.FEBSLET.2014.06.025.

23. Zhao, Q.; Lee, F.S. Mitogen-activated protein kinase/ERK kinase kinases 2 and 3 activate nuclear factor-κB through IκB kinase-α and IκB kinase-β. *J. Biol. Chem.* **1999**, *274*, 8355–8358, doi:10.1074/JBC.274.13.8355.

24. Gonzalez, F.A.; Seth, A.; Raden, D.L.; Bowman, D.S.; Fay, F.S.; Davis, R.J. Serum-induced translocation of mitogen-activated protein kinase to the cell surface ruffling membrane and the nucleus. *J. Cell Biol.* **1993**, *122*, 1089–1101, doi:10.1083/JCB.122.5.1089.

25. Mendoza, M.C.; Er, E.E.; Blenis, J. ERK-MAP Kinase Signaling in the Cytoplasm. *Methods Mol. Biol.* **2010**, *661*, 185–203, doi:10.1007/978-1-60761-795-2_11.

26. Wortzel, I.; Seger, R. The ERK cascade: Distinct functions within various subcellular organelles. *Genes and Cancer* **2011**, *2*, 195–209, doi:10.1177/1947601911407328.

27. Vivanco, I.; Sawyers, C.L. The phosphatidylinositol 3-Kinase AKT pathway in human cancer. *Nat. Rev. Cancer* **2002**, *2*, 489–501, doi:10.1038/NRC839.

28. Castellano, E.; Downward, J. RAS Interaction with PI3K: More Than Just Another Effector Pathway. *Genes Cancer* **2011**, *2*, 261, doi:10.1177/1947601911408079.

29. Stokoe, D.; Stephens, L.R.; Copeland, T.; Gaffney, P.R.J.; Reese, C.B.; Painter, G.F.; Holmes, A.B.; McCormick, F.; Hawkins, P.T. Dual role of phosphatidylinositol-3,4,5-trisphosphate in the activation of protein kinase B. *Science* **1997**, *277*, 567–570, doi:10.1126/SCIENCE.277.5325.567.

30. Tzivion, G.; Dobson, M.; Ramakrishnan, G. FoxO transcription factors; Regulation by AKT and 14-3-3 proteins. *Biochim. Biophys. Acta - Mol. Cell Res.* **2011**, *1813*, 1938–1945, doi:10.1016/J.BBAMCR.2011.06.002.

31. Romorini, L.; Garate, X.; Neiman, G.; Luzzani, C.; Furmento, V.A.; Guberman, A.S.; Sevlever, G.E.; Scassa, M.E.; Miriuka, S.G. AKT/GSK3β signaling pathway is critically involved in human pluripotent stem cell survival. *Sci. Reports 2016 61* **2016**, *6*, 1–15, doi:10.1038/srep35660.

32. Berwick, D.C.; Hers, I.; Heesom, K.J.; Kelly Moule, S.; Tavaré, J.M. The Identification of ATP-citrate Lyase as a Protein Kinase B (Akt) Substrate in Primary Adipocytes. *J. Biol. Chem.* **2002**, *277*, 33895–33900, doi:10.1074/JBC.M204681200.

33. Navé, B.T.; Ouwens, D.M.; Withers, D.J.; Alessi, D.R.; Shepherd, P.R. Mammalian target of rapamycin is a direct target for protein kinase B: identification of a convergence point for opposing effects of insulin and amino-acid deficiency on protein translation. *Biochem. J.* **1999**, *344*, 427, doi:10.1042/0264-6021:3440427.

34. Hedman, A.C.; Smith, J.M.; Sacks, D.B. The biology of IQGAP proteins: beyond the cytoskeleton. *EMBO Rep.* **2015**, *16*, 427–446, doi:10.15252/embr.201439834.

35. Roy, M.; Li, Z.; Sacks, D.B. IQGAP1 Is a Scaffold for Mitogen-Activated Protein Kinase Signaling. *Mol. Cell. Biol.* **2005**, *25*, 7940, doi:10.1128/MCB.25.18.7940-7952.2005.

36. Choi, S.; Hedman, A.C.; Sayedyahossein, S.; Thapa, N.; Sacks, D.B.; Anderson, R.A. Agonist-stimulated phosphatidylinositol-3,4,5-trisphosphate generation by scaffolded

phosphoinositide kinases. *Nat. Cell Biol.* **2016**, *18*, 1324–1335, doi:10.1038/ncb3441.

37. Chen, M.; Choi, S.; Jung, O.; Wen, T.; Baum, C.; Thapa, N.; Lambert, P.F.; Rapraeger, A.C.; Anderson, R.A. The Specificity of EGF-Stimulated IQGAP1 Scaffold Towards the PI3K-Akt Pathway is Defined by the IQ3 motif. *Sci. Reports 2019 91* **2019**, *9*, 1–15, doi:10.1038/s41598-019-45671-5.

38. Nouri, K.; Fansa, E.K.; Amin, E.; Dvorsky, R.; Gremer, L.; Willbold, D.; Schmitt, L.; Timson, D.J.; Ahmadian, M.R. IQGAP1 interaction with RHO family proteins revisited kinetic and equilibrium evidence for multiple distinct binding sites. *J. Biol. Chem.* **2016**, *291*, 26364–26376, doi:10.1074/jbc.M116.752121.

39. Abel, A.M.; Schuldt, K.M.; Rajasekaran, K.; Hwang, D.; Riese, M.J.; Rao, S.; Thakar, M.S.; Malarkannan, S. IQGAP1: insights into the function of a molecular puppeteer. *Mol. Immunol.* **2015**, *65*, 336–349, doi:10.1016/J.MOLIMM.2015.02.012.

40. Watanabe, T.; Wang, S.; Kaibuchi, K. IQGAPs as Key Regulators of Actin-cytoskeleton Dynamics. *Cell Struct. Funct.* **2015**, *40*, 69–77, doi:10.1247/CSF.15003.

41. Mosaddeghzadeh, N.; Nouri, K.; Krumbach, O.H.F.; Amin, E.; Dvorsky, R.; Ahmadian, M.R. Selectivity determinants of rho gtpase binding to iqgaps. *Int. J. Mol. Sci.* **2021**, *22*, doi:10.3390/ijms222212596.

42. McKay, M.M.; Morrison, D.K. Integrating signals from RTKs to ERK/MAPK. *Oncogene* **2007**, *26*, 3113–3121, doi:10.1038/sj.onc.1210394.

43. Yamauchi, J.; Miyamoto, Y.; Tanoue, A.; Shooter, E.M.; Chan, J.R. Ras activation of a Rac1 exchange factor, Tiam1, mediates neurotrophin-3-induced Schwann cell migration. *Proc. Natl. Acad. Sci. U. S. A.* **2005**, *102*, 14889–14894, doi:10.1073/pnas.0507125102.

44. Huang, L.; Hofer, F.; Martin, G.S.; Kim, S.H. Structural basis for the interaction of Ras with RalGDS. *Nat. Struct. Biol.* **1998**, *5*, 422–426, doi:10.1038/NSB0698-422.

45. Gentry, L.R.; Martin, T.D.; Reiner, D.J.; Der, C.J. Ral small GTPase signaling and oncogenesis: more than just 15 minutes of fame. *Biochim. Biophys. Acta* **2014**, *1843*, 2976, doi:10.1016/J.BBAMCR.2014.09.004.

46. Adariani, S.R.; Kazemein Jasemi, N.S.; Bazgir, F.; Wittich, C.; min, E.; Seidel, C.A.M.; Dvorsky, R.; Ahmadian, M.R. A comprehensive analysis of RAS-effector interactions reveals interaction hotspots and new binding partners. *J. Biol. Chem.* **2021**, *296*, doi:10.1016/j.jbc.2021.100626.

47. Béganton, B.; Coyaud, E.; Laurent, E.M.N.; Mangé, A.; Jacquemetton, J.; Romancer, M. Le; Raught, B.; Solassol, J. Proximal protein interaction landscape of RAS paralogs. *Cancers (Basel).* **2020**, *12*, 1–21, doi:10.3390/cancers12113326.

48. Heitman, J.; Movva, N.R.; Hall, M.N. Targets for Cell Cycle Arrest by the Immunosuppressant Rapamycin in Yeast. *Science (80-.).* **1991**, *253*, 905–909, doi:10.1126/SCIENCE.1715094.

49. Baretić, D.; Berndt, A.; Ohashi, Y.; Johnson, C.M.; Williams, R.L. Tor forms a dimer through an N-terminal helical solenoid with a complex topology. *Nat. Commun. 2016 71* **2016**, *7*, 1–9, doi:10.1038/ncomms11016.

50. Wang, T.; Blumhagen, R.; Lao, U.; Kuo, Y.; Edgar, B.A. LST8 regulates cell growth via target-of-rapamycin complex 2 (TORC2). *Mol. Cell. Biol.* **2012**, *32*, 2203–2213, doi:10.1128/MCB.06474-11.

51. Hwang, Y.; Kim, L.C.; Song, W.; Edwards, D.N.; Cook, R.S.; Chen, J. Disruption of the scaffolding function of mLST8 selectively inhibits mTORC2 assembly and function and suppresses mTORC2-dependent tumor growth in vivo. *Cancer Res.* **2019**, *79*, 3178–3184, doi:10.1158/0008-5472.CAN-18-3658.

52. Jacinto, E.; Facchinetti, V.; Liu, D.; Soto, N.; Wei, S.; Jung, S.Y.; Huang, Q.; Qin, J.; Su, B. SIN1/MIP1 maintains rictor-mTOR complex integrity and regulates Akt phosphorylation and substrate specificity. *Cell* **2006**, *127*, 125–137, doi:10.1016/J.CELL.2006.08.033.

53. Yang, Q.; Inoki, K.; Ikenoue, T.; Guan, K.L. Identification of Sin1 as an essential TORC2 component required for complex formation and kinase activity. *Genes Dev.* **2006**, *20*, 2820,

doi:10.1101/GAD.1461206.

54. Scaiola, A.; Mangia, F.; Imseng, S.; Boehringer, D.; Berneiser, K.; Shimobayashi, M.; Stuttfeld, E.; Hall, M.N.; Ban, N.; Maier, T. The 3.2-Å resolution structure of human mTORC2. *Sci. Adv.* **2020**, *6*, 2020.04.10.029835, doi:10.1126/SCIADV.ABC1251.

55. Chen, X.; Liu, M.; Tian, Y.; Li, J.; Qi, Y.; Zhao, D.; Wu, Z.; Huang, M.; Wong, C.C.L.; Wang, H.W.; et al. Cryo-EM structure of human mTOR complex 2. *Cell Res.* **2018**, *28*, 518, doi:10.1038/S41422-018-0029-3.

56. Tatebe, H.; Murayama, S.; Yonekura, T.; Hatano, T.; Richter, D.; Furuya, T.; Kataoka, S.; Furuita, K.; Kojima, C.; Shiozaki, K. Substrate specificity of tor complex 2 is determined by a ubiquitin-fold domain of the sin1 subunit. *Elife* **2017**, *6*, doi:10.7554/eLife.19594.001.

57. Cameron, A.J.M.; Linch, M.D.; Saurin, A.T.; Escribano, C.; Parker, P.J. mTORC2 targets AGC kinases through Sin1-dependent recruitment. *Biochem. J.* **2011**, *439*, 287–297, doi:10.1042/BJ20110678.

58. Pan, D.; Matsuura, Y. Structures of the pleckstrin homology domain of Saccharomyces cerevisiae Avo1 and its human orthologue Sin1, an essential subunit of TOR complex 2. *Acta Crystallogr. Sect. F. Struct. Biol. Cryst. Commun.* **2012**, *68*, 386–392, doi:10.1107/S1744309112007178.

59. Liu, P.; Gan, W.; Chin, Y.R.; Ogura, K.; Guo, J.; Zhang, J.; Wang, B.; Blenis, J.; Cantley, L.C.; Toker, A.; et al. PtdIns(3,4,5)P3-dependent Activation of the mTORC2 Kinase Complex. *Cancer Discov.* **2015**, *5*, 1194, doi:10.1158/2159-8290.CD-15-0460.

60. Liu, P.; Gan, W.; Chin, Y.R.; Ogura, K.; Guo, J.; Zhang, J.; Wang, B.; Blenis, J.; Cantley, L.C.; Toker, A.; et al. Ptdins(3,4,5) P3 -dependent activation of the mTORC2 kinase complex. *Cancer Discov.* **2015**, *5*, 1194–11209, doi:10.1158/2159-8290.CD-15-0460.

61. Yuan, H.X.; Guan, K.L. The SIN1-PH domain connects mTORC2 to PI3K. *Cancer Discov.* **2015**, *5*, 1127–1129, doi:10.1158/2159-8290.CD-15-1125.

62. Castel, P.; Dharmaiah, S.; Sale, M.J.; Messing, S.; Rizzuto, G.; Cuevas-Navarro, A.; Cheng, A.; Trnka, M.J.; Urisman, A.; Esposito, D.; et al. RAS interaction with Sin1 is dispensable for mTORC2 assembly and activity. *Proc. Natl. Acad. Sci. U. S. A.* **2021**, *118*, 2103261118, doi:10.1073/pnas.2103261118.

63. Zheng, Y.; Ding, L.; Meng, X.; Potter, M.; Kearney, A.L.; Zhang, J.; Sun, J.; James, D.E.; Yang, G.; Zhou, C. Structural insights into Ras regulation by SIN1. *Proc. Natl. Acad. Sci. U. S. A.* **2022**, *119*, doi:10.1073/pnas.2119990119.

64. Schroder, W.A.; Buck, M.; Cloonan, N.; Hancock, J.F.; Suhrbier, A.; Sculley, T.; Bushell, G. Human Sin1 contains Ras-binding and pleckstrin homology domains and suppresses Ras signalling. *Cell. Signal.* **2007**, *19*, 1279–1289, doi:10.1016/j.cellsig.2007.01.013.

65. Lone, M.U.D.; Miyan, J.; Asif, M.; Malik, S.A.; Dubey, P.; Singh, V.; Singh, K.; Mitra, K.; Pandey, D.; Haq, W.; et al. Direct physical interaction of active Ras with mSIN1 regulates mTORC2 signaling. *BMC Cancer* **2019**, *19*, 1–16, doi:10.1186/S12885-019-6422-6/FIGURES/5.

66. Yuan, Y.; Pan, B.; Sun, H.; Chen, G.; Su, B.; Huang, Y. Characterization of Sin1 Isoforms Reveals an mTOR-Dependent and Independent Function of Sin1γ. *PLoS One* **2015**, *10*, doi:10.1371/JOURNAL.PONE.0135017.

67. Sengupta, S.; Peterson, T.R.; Sabatini, D.M. Regulation of the mTOR complex 1 pathway by nutrients, growth factors, and stress. *Mol. Cell* **2010**, *40*, 310, doi:10.1016/J.MOLCEL.2010.09.026.

68. Sarbassov, D.D.; Guertin, D.A.; Ali, S.M.; Sabatini, D.M. Phosphorylation and regulation of Akt/PKB by the rictor-mTOR complex. *Science* **2005**, *307*, 1098–1101, doi:10.1126/SCIENCE.1106148.

69. Pearce, L.R.; Komander, D.; Alessi, D.R. The nuts and bolts of AGC protein kinases. *Nat. Rev. Mol. Cell Biol. 2010 111* **2010**, *11*, 9–22, doi:10.1038/nrm2822.

70. Jacinto, E. AGC Kinases in mTOR Signaling. *Enzymes* **2010**, *27*, 101–128,

doi:10.1016/S1874-6047(10)27007-5.

71. Lang, F.; Shumilina, E. Regulation of ion channels by the serum- and glucocorticoid-inducible kinase SGK1. *FASEB J.* **2013**, *27*, 3–12, doi:10.1096/FJ.12-218230.

72. Li, X.; Gao, T. mTORC2 phosphorylates protein kinase Cζ to regulate its stability and activity. *EMBO Rep.* **2014**, *15*, 191–198, doi:10.1002/EMBR.201338119.

73. Ebner, M.; Sinkovics, B.; Szczygieł, M.; Ribeiro, D.W.; Yudushkin, I. Localization of mTORC2 activity inside cells. *J. Cell Biol.* **2017**, *216*, 343–353, doi:10.1083/JCB.201610060.

74. Saci, A.; Cantley, L.C.; Carpenter, C.L. Rac1 regulates the activity of mTORC1 and mTORC2 and controls cellular size. *Mol. Cell* **2011**, *42*, 50–61, doi:10.1016/J.MOLCEL.2011.03.017.

75. Zinzalla, V.; Stracka, D.; Oppliger, W.; Hall, M.N. Activation of mTORC2 by association with the ribosome. *Cell* **2011**, *144*, 757–768, doi:10.1016/j.cell.2011.02.014.

76. VanHook, A.M. mTORC2 Akt-ing at the Ribosome. *Sci. Signal.* **2010**, *3*, doi:10.1126/SCISIGNAL.3151EC369.

77. Oh, W.J.; Wu, C.C.; Kim, S.J.; Facchinetti, V.; Julien, L.A.; Finlan, M.; Roux, P.P.; Su, B.; Jacinto, E. MTORC2 can associate with ribosomes to promote cotranslational phosphorylation and stability of nascent Akt polypeptide. *EMBO J.* **2010**, *29*, 3939–3951, doi:10.1038/emboj.2010.271.

78. Gleason, C.E.; Oses-Prieto, J.A.; Li, K.H.; Saha, B.; Situ, G.; Burlingame, A.L.; Pearce, D. Phosphorylation at distinct subcellular locations underlies specificity in mTORC2-mediated activation of SGK1 and Akt. *J. Cell Sci.* **2019**, *132*, doi:10.1242/JCS.224931.

79. Yang, G.; Murashige, D.S.S.; Humphrey, S.J.J.; James, D.E.E. A Positive Feedback Loop between Akt and mTORC2 via SIN1 Phosphorylation. *Cell Rep.* **2015**, *12*, 937–943.

80. Liu, P.; Gan, W.; Inuzuka, H.; Lazorchak, A.S.; Gao, D.; Arojo, O.; Liu, D.; Wan, L.; Zhai, B.; Yu, Y.; et al. Sin1 phosphorylation impairs mTORC2 complex integrity and inhibits downstream Akt signalling to suppress tumorigenesis. *Nat. Cell Biol. 2013 1511* **2013**, *15*, 1340–1350, doi:10.1038/ncb2860.

81. Liu, P.; Guo, J.; Gan, W.; Wei, W. Dual phosphorylation of Sin1 at T86 and T398 negatively regulates mTORC2 complex integrity and activity. *Protein Cell* **2014**, *5*, 171–177, doi:10.1007/s13238-014-0021-8.

82. Hay, N.; Sonenberg, N. Upstream and downstream of mTOR. *Genes Dev.* **2004**, *18*, 1926–1945, doi:10.1101/GAD.1212704.

83. Jhanwar-Uniyal, M.; Amin, A.G.; Cooper, J.B.; Das, K.; Schmidt, M.H.; Murali, R. Discrete signaling mechanisms of mTORC1 and mTORC2: Connected yet apart in cellular and molecular aspects. *Adv. Biol. Regul.* **2017**, *64*, 39–48, doi:10.1016/j.jbior.2016.12.001.

84. Pudewell, S.; Lissy, J.; Nakhaeizadeh, H.; Taha, M.S.; Akbarzadeh, M.; Adariani, S.R.; Nakhaei-Rad, S.; Li, J.; Kordes, C.; Häussinger, D.; et al. Physical Interaction between Embryonic Stem Cell-Expressed Ras (ERas) and Arginase-1 in Quiescent Hepatic Stellate Cells. *Cells* **2022**, *11*, 508, doi:10.3390/cells11030508.

85. Holmes, F.L. Hans Krebs and the discovery of the ornithine cycle. *Fed. Proc.* **1980**, *39*, 216–225.

86. Hirsch-Kolb, H.; Heine, J.P.; Kolb, H.J.; Greenberg, D.M. Comparative physical-chemical studies of mammalian arginases. *Comp. Biochem. Physiol.* **1970**, *37*, 345–359, doi:10.1016/0010-406X(70)90563-3.

87. Type, S.C. Single cell type - PIK3CB - The Human Protein Atlas Available online: https://www.proteinatlas.org/ENSG00000051382-PIK3CB/single+cell+type (accessed on Apr 21, 2022).

88. MacParland, S.A.; Liu, J.C.; Ma, X.Z.; Innes, B.T.; Bartczak, A.M.; Gage, B.K.; Manuel, J.; Khuu, N.; Echeverri, J.; Linares, I.; et al. Single cell RNA sequencing of human liver reveals distinct intrahepatic macrophage populations. *Nat. Commun.* **2018**, *9*, doi:10.1038/S41467-018-06318-7.

89. He, S.; Wang, L.H.; Liu, Y.; Li, Y.Q.; Chen, H.T.; Xu, J.H.; Peng, W.; Lin, G.W.; Wei, P.P.; Li, B.; et al. Single-cell transcriptome profiling of an adult human cell atlas of 15 major organs. *Genome Biol.* **2020**, *21*, doi:10.1186/S13059-020-02210-0.

90. Hildreth, A.D.; Ma, F.; Wong, Y.Y.; Sun, R.; Pellegrini, M.; O'Sullivan, T.E. Single-cell sequencing of human white adipose tissue identifies new cell states in health and obesity. *Nat. Immunol.* **2021**, *22*, 639–653, doi:10.1038/S41590-021-00922-4.

91. Bhat-Nakshatri, P.; Gao, H.; Sheng, L.; McGuire, P.C.; Xuei, X.; Wan, J.; Liu, Y.; Althouse, S.K.; Colter, A.; Sandusky, G.; et al. A single-cell atlas of the healthy breast tissues reveals clinically relevant clusters of breast epithelial cells. *Cell reports. Med.* **2021**, *2*, doi:10.1016/J.XCRM.2021.100219.

92. Parikh, K.; Antanaviciute, A.; Fawkner-Corbett, D.; Jagielowicz, M.; Aulicino, A.; Lagerholm, C.; Davis, S.; Kinchen, J.; Chen, H.H.; Alham, N.K.; et al. Colonic epithelial cell diversity in health and inflammatory bowel disease. *Nature* **2019**, *567*, 49–55, doi:10.1038/S41586-019-0992-Y.

93. Wang, W.; Vilella, F.; Alama, P.; Moreno, I.; Mignardi, M.; Isakova, A.; Pan, W.; Simon, C.; Quake, S.R. Single-cell transcriptomic atlas of the human endometrium during the menstrual cycle. *Nat. Med.* **2020**, *26*, 1644–1653, doi:10.1038/S41591-020-1040-Z.

94. Vento-Tormo, R.; Efremova, M.; Botting, R.A.; Turco, M.Y.; Vento-Tormo, M.; Meyer, K.B.; Park, J.E.; Stephenson, E.; Polański, K.; Goncalves, A.; et al. Single-cell reconstruction of the early maternal-fetal interface in humans. *Nature* **2018**, *563*, 347–353, doi:10.1038/S41586-018-0698-6.

95. De Micheli, A.J.; Spector, J.A.; Elemento, O.; Cosgrove, B.D. A reference single-cell transcriptomic atlas of human skeletal muscle tissue reveals bifurcated muscle stem cell populations. *Skelet. Muscle* **2020**, *10*, doi:10.1186/S13395-020-00236-3.

96. Guo, J.; Grow, E.J.; Mlcochova, H.; Maher, G.J.; Lindskog, C.; Nie, X.; Guo, Y.; Takei, Y.; Yun, J.; Cai, L.; et al. The adult human testis transcriptional cell atlas. *Cell Res.* **2018**, *28*, 1141–1157, doi:10.1038/S41422-018-0099-2.

97. Brain-map.org, H.M. 10x- Allen Brain Map Available online: https://portal.brain-map.org/atlases-and-data/rnaseq/human-m1-10x (accessed on Apr 14, 2022).

98. Caldwell, R.W.; Rodriguez, P.C.; Toque, H.A.; Priya Narayanan, S.; Caldwell, R.B. Arginase: A multifaceted enzyme important in health and disease. *Physiol. Rev.* **2018**, *98*, 641–665, doi:10.1152/physrev.00037.2016.

99. Kitowska, K.; Zakrzewicz, D.; Königshoff, M.; Chrobak, I.; Grimminger, F.; Seeger, W.; Bulau, P.; Eickelberg, O. Functional role and species-specific contribution of arginases in pulmonary fibrosis. *Am. J. Physiol. - Lung Cell. Mol. Physiol.* **2008**, *294*, 34–45, doi:10.1152/ajplung.00007.2007.

100. Pegg, A.E. The function of spermine. *IUBMB Life* **2014**, *66*, 8–18, doi:10.1002/iub.1237.

101. Eisenberg, T.; Knauer, H.; Schauer, A.; Büttner, S.; Ruckenstuhl, C.; Carmona-Gutierrez, D.; Ring, J.; Schroeder, S.; Magnes, C.; Antonacci, L.; et al. Induction of autophagy by spermidine promotes longevity. *Nat. Cell Biol.* **2009**, *11*, 1305–1314, doi:10.1038/ncb1975.

102. Ghosh, I.; Sankhe, R.; Mudgal, J.; Arora, D.; Nampoothiri, M. Spermidine, an autophagy inducer, as a therapeutic strategy in neurological disorders. *Neuropeptides* **2020**, *83*, 102083, doi:10.1016/j.npep.2020.102083.

103. Hesterberg, R.; Cleveland, J.; Epling-Burnette, P. Role of Polyamines in Immune Cell Functions. *Med. Sci.* **2018**, *6*, 22, doi:10.3390/medsci6010022.

104. Zhao, T.; Goh, K.J.; Ng, H.H.; Vardy, L.A. A role for polyamine regulators in ESC self-renewal. *Cell Cycle* **2012**, *11*, 4517–4523, doi:10.4161/cc.22772.

105. Xie, Q.W.; Kashiwabara, Y.; Nathan, C. Role of transcription factor NF-kappa B/Rel in induction of nitric oxide synthase. *J. Biol. Chem.* **1994**, *269*, 4705–4708, doi:10.1016/S0021-9258(17)37600-7.

106. Griffith, O.W.; Stuehr, D.J. Nitric oxide synthases: Properties and catalytic mechanism. *Annu.*

Rev. Physiol. **1995**, *57*, 707–736, doi:10.1146/annurev.physiol.57.1.707.

107. Lucas, R.; Fulton, D.; Caldwell, R.W.; Romero, M.J. Arginase in the Vascular Endothelium: Friend or Foe? *Front. Immunol.* **2014**, *5*, doi:10.3389/FIMMU.2014.00589.

108. Grody, W.W.; Dizikes, G.J.; Cederbaum, S.D. Human arginase isozymes. *Isozymes Curr Top Biol Med Res.* **1987**, *13*, 181–214.

109. Reczkowski, R.S.; Ash, D.E. Rat liver arginase: kinetic mechanism, alternate substrates, and inhibitors. *Arch. Biochem. Biophys.* **1994**, *312*, 31–37, doi:10.1006/ABBI.1994.1276.

110. Dioguardi, F.S. To Give or Not to Give? Lessons from the Arginine Paradox. *J. Nutrigenet. Nutrigenomics* **2011**, *4*, 90–98, doi:10.1159/000327777.

111. Durante, W.; Johnson, F.K.; Johnson, R.A. Arginase: a critical regulator of nitric oxide synthesis and vascular function. *Clin. Exp. Pharmacol. Physiol.* **2007**, *34*, 906–911, doi:10.1111/j.1440-1681.2007.04638.x.

112. Kim, P.S.; Iyer, R.K.; Lu, K. V.; Yu, H.; Karimi, A.; Kern, R.M.; Tai, D.K.; Cederbaum, S.D.; Grody, W.W. Expression of the liver form of arginase in erythrocytes. *Mol. Genet. Metab.* **2002**, *76*, 100–110, doi:10.1016/S1096-7192(02)00034-3.

113. Yang, J.; Gonon, A.T.; Sjöquist, P.O.; Lundberg, J.O.; Pernow, J. Arginase regulates red blood cell nitric oxide synthase and export of cardioprotective nitric oxide bioactivity. *Proc. Natl. Acad. Sci. U. S. A.* **2013**, *110*, 15049–15054, doi:10.1073/pnas.1307058110.

114. Leo, F.; Suvorava, T.; Heuser, S.K.; Li, J.; Lobue, A.; Barbarino, F.; Piragine, E.; Schneckmann, R.; Hutzler, B.; Good, M.E.; et al. Red Blood Cell and Endothelial eNOS Independently Regulate Circulating Nitric Oxide Metabolites and Blood Pressure. *Circulation* **2021**, *144*, 870–889, doi:10.1161/CIRCULATIONAHA.120.049606.

115. Rath, M.; Müller, I.; Kropf, P.; Closs, E.I.; Munder, M. Metabolism via arginase or nitric oxide synthase: Two competing arginine pathways in macrophages. *Front. Immunol.* **2014**, *5*, 532.

116. Hecker, M.; Nematollahi, H.; Hey, C.; Busse, R.; Racké, K. Inhibition of arginase by in alveolar macrophages: implications for the utilization of l-arginine for nitric oxide synthesis. *FEBS Lett.* **1995**, *359*, 251–254, doi:10.1016/0014-5793(95)00039-C.

117. Bauer, P.M.; Fukuto, J.M.; Buga, G.M.; Pegg, A.E.; Ignarro, L.J. Nitric Oxide Inhibits Ornithine Decarboxylase by S-Nitrosylation. *Biochem. Biophys. Res. Commun.* **1999**, *262*, 355–358, doi:10.1006/BBRC.1999.1210.

118. Mössner, J.; Hammermann, R.; Racké, K. Concomitant Down-regulation of L-arginine Transport and Nitric Oxide (NO) Synthesis in Rat Alveolar Macrophages by the Polyamine Spermine. *Pulm. Pharmacol. Ther.* **2001**, *14*, 297–305, doi:10.1006/PUPT.2001.0297.

119. Lee, J.; Ryu, H.; Ferrante, R.J.; Morris, S.M.; Ratan, R.R. Translational control of inducible nitric oxide synthase expression by arginine can explain the arginine paradox. *Proc. Natl. Acad. Sci. U. S. A.* **2003**, *100*, 4843–4848, doi:10.1073/pnas.0735876100.

120. Schachtrup, C.; Le Moan, N.; Passino, M.A.; Akassoglou, K. Hepatic stellate cells and astrocytes: Stars of scar formation and tissue repair. *Cell Cycle* **2011**, *10*, 1764–1771, doi:10.4161/cc.10.11.15828.

121. Saxena, R.; Theise, N.D.; Crawford, J.M. Microanatomy of the human liver—exploring the hidden interfaces. *Hepatology* **1999**, *30*, 1339–1346, doi:10.1002/HEP.510300607.

122. Chen, Y.; Tian, Z. Innate lymphocytes: pathogenesis and therapeutic targets of liver diseases and cancer. *Cell. Mol. Immunol. 2020 181* **2020**, *18*, 57–72, doi:10.1038/s41423-020-00561-z.

123. Racanelli, V.; Rehermann, B. The liver as an immunological organ. *Hepatology* **2006**, *43*, S54–S62, doi:10.1002/HEP.21060.

124. Bogdanos, D.P.; Gao, B.; Gershwin, M.E. Liver Immunology. *Compr. Physiol.* **2013**, *3*, 567, doi:10.1002/CPHY.C120011.

125. Michalopoulos, G.K. Liver Regeneration. *J. Cell. Physiol.* **2007**, *213*, 286, doi:10.1002/JCP.21172.

126. Nishikawa, H.; Osaki, Y. Liver Cirrhosis: Evaluation, Nutritional Status, and Prognosis. *Mediators Inflamm.* **2015**, *2015*, doi:10.1155/2015/872152.

127. Kalra, A.; Yetiskul, E.; Wehrle, C.J.; Tuma, F. *Physiology, Liver*; StatPearls Publishing, 2022;

128. Fujita, T.; Narumiya, S. Roles of hepatic stellate cells in liver inflammation: A new perspective. *Inflamm. Regen.* **2016**, *36*, 1–6, doi:10.1186/S41232-016-0005-6/FIGURES/1.

129. Kupffer, K. Uber Sternzellen der Leber. Briefliche Mitteilung an Professor Waldeyer. *Arch Mikr Anat* **1876**, *12*, 353–358.

130. Ito, T.; Nemoto, M. Uber die Kupfferschen Sternzellen und die ``Fettspeicherungszellen'' (fat storing cells) in der Blutkapillarenwand der menschlichen Leber. *Okajima Folia Anat Jpn* **1952**, *24*, 243–258.

131. Wake, K. ``Sternzellen'' in the liver: perisinusoidal cells with special reference to storage of vitamin A. *Am J Anat* **1971**, *132*, 429–462.

132. Balmer, J.E.; Blomhoff, R. Gene expression regulation by retinoic acid. *J. Lipid Res.* **2002**, *43*, 1773–1808, doi:10.1194/JLR.R100015-JLR200.

133. Khomich, O.; Ivanov, A. V.; Bartosch, B. Metabolic Hallmarks of Hepatic Stellate Cells in Liver Fibrosis. *Cells* **2020**, *9*, doi:10.3390/CELLS9010024.

134. Kordes, C.; Sawitza, I.; Müller-Marbach, A.; Ale-Agha, N.; Keitel, V.; Klonowski-Stumpe, H.; Häussinger, D. CD133+ hepatic stellate cells are progenitor cells. *Biochem. Biophys. Res. Commun.* **2007**, *352*, 410–417, doi:10.1016/J.BBRC.2006.11.029.

135. Kordes, C.; Bock, H.H.; Reichert, D.; May, P.; Häussinger, D. Hepatic stellate cells: current state and open questions. *Biol. Chem.* **2021**, *402*, 1021–1032, doi:10.1515/HSZ-2021-0180.

136. Geerts, A. History, heterogeneity, developmental biology, and functions of quiescent hepatic stellate cells. *Semin. Liver Dis.* **2001**, *21*, 311–335, doi:10.1055/S-2001-17550/ID/46.

137. Kordes, C.; Sawitza, I.; Götze, S.; Häussinger, D. Hepatic Stellate Cells Support Hematopoiesis and are Liver-Resident Mesenchymal Stem Cells. *Cell. Physiol. Biochem.* **2013**, *31*, 290–304, doi:10.1159/000343368.

138. Kordes, C.; Sawitza, I.; Götze, S.; Herebian, D.; Häussinger, D. Hepatic stellate cells contribute to progenitor cells and liver regeneration. *J. Clin. Invest.* **2014**, *124*, 5503–5515, doi:10.1172/JCI74119.

139. Lee, Y.A.; Wallace, M.C.; Friedman, S.L. Pathobiology of liver fibrosis: a translational success story. *Gut* **2015**, *64*, 830–841, doi:10.1136/GUTJNL-2014-306842.

140. Tsuchida, T.; Friedman, S.L. Mechanisms of hepatic stellate cell activation. **2017**, *14*, 397–411, doi:10.1038/NRGASTRO.2017.38.

141. Kisseleva, T.; Cong, M.; Paik, Y.H.; Scholten, D.; Jiang, C.; Benner, C.; Iwaisako, K.; Moore-Morris, T.; Scott, B.; Tsukamoto, H.; et al. Myofibroblasts revert to an inactive phenotype during regression of liver fibrosis. *Proc. Natl. Acad. Sci. U. S. A.* **2012**, *109*, 9448–9453, doi:10.1073/pnas.1201840109.

142. Troeger, J.S.; Mederacke, I.; Gwak, G.Y.; Dapito, D.H.; Mu, X.; Hsu, C.C.; Pradere, J.P.; Friedman, R.A.; Schwabe, R.F. Deactivation of hepatic stellate cells during liver fibrosis resolution in mice. *Gastroenterology* **2012**, *143*, doi:10.1053/J.GASTRO.2012.06.036.

143. Simanshu, D.K.; Nissley, D. V.; McCormick, F. RAS Proteins and Their Regulators in Human Disease. *Cell* **2017**, *170*, 17–33, doi:10.1016/j.cell.2017.06.009.

144. Hobbs, G.A.; Der, C.J.; Rossman, K.L. RAS isoforms and mutations in cancer at a glance. *J. Cell Sci.* **2016**, *129*, 1287–1292, doi:10.1242/jcs.182873.

145. Smith, M.J.; Neel, B.G.; Ikura, M. NMR-based functional profiling of RASopathies and oncogenic RAS mutations. *Proc. Natl. Acad. Sci. U. S. A.* **2013**, *110*, 4574–4579, doi:10.1073/pnas.1218173110.

146. Rauen, K.A. The RASopathies. *Annu. Rev. Genomics Hum. Genet.* **2013**, *14*, 355–369, doi:10.1146/annurev-genom-091212-153523.

147. Niemeyer, C.M. RAS diseases in children. *Haematologica* **2014**, *99*, 1653–1662, doi:10.3324/haematol.2014.114595.

148. Berndt, N.; Hamilton, A.D.; Sebti, S.M. Targeting protein prenylation for cancer therapy. *Nat. Rev. Cancer 2011 1111* **2011**, *11*, 775–791, doi:10.1038/nrc3151.

149. Ostrem, J.M.; Peters, U.; Sos, M.L.; Wells, J.A.; Shokat, K.M. K-Ras(G12C) inhibitors allosterically control GTP affinity and effector interactions. *Nature* **2013**, *503*, 548–551.

150. O'Bryan, J.P. Pharmacological targeting of RAS: Recent success with direct inhibitors. *Pharmacol. Res.* **2019**, *139*, 503–511, doi:10.1016/j.phrs.2018.10.021.

151. Chappell, W.H.; Steelman, L.S.; Long, J.M.; Kempf, R.C.; Abrams, S.L.; Franklin, R.A.; Bäsecke, J.; Stivala, F.; Donia, M.; Fagone, P.; et al. Ras/Raf/MEK/ERK and PI3K/PTEN/Akt/mTOR inhibitors: Rationale and importance to inhibiting these pathways in human health. *Oncotarget* **2011**, *2*, 135–164, doi:10.18632/oncotarget.240.

152. Laude, A.J.; Prior, I.A. Plasma membrane microdomains: organisation, function and trafficking. *Mol. Membr. Biol.* **2004**, *21*, 193, doi:10.1080/09687680410001700517.

153. Leo, F.; Hutzler, B.; Ruddiman, C.A.; Isakson, B.E.; Cortese-Krott, M.M. Cellular microdomains for nitric oxide signaling in endothelium and red blood cells. *Nitric Oxide - Biol. Chem.* **2020**, *96*, 44–53, doi:10.1016/j.niox.2020.01.002.

154. Jiang, M.; Ding, Y.; Su, Y.; Hu, X.; Li, J.; Zhang, Z. Arginase-flotillin interaction brings arginase to red blood cell membrane. *FEBS Lett.* **2006**, *580*, 6561–6564, doi:10.1016/j.febslet.2006.11.003.

155. Amaddii, M.; Meister, M.; Banning, A.; Tomasovic, A.; Mooz, J.; Rajalingam, K.; Tikkanen, R. Flotillin-1/Reggie-2 protein plays dual role in activation of receptor-tyrosine kinase/mitogen-activated protein kinase signaling. *J. Biol. Chem.* **2012**, *287*, 7265–7278, doi:10.1074/jbc.M111.287599.

156. Langhorst, M.F.; Reuter, A.; Stuermer, C.A.O. Scaffolding microdomains and beyond: The function of reggie/flotillin proteins. *Cell. Mol. Life Sci.* **2005**, *62*, 2228–2240, doi:10.1007/s00018-005-5166-4.

157. Closs, E.I.; Simon, A.; Vékony, N.; Rotmann, A. Plasma membrane transporters for arginine. *J. Nutr.* **2004**, *134*, 2752S-2759S, doi:10.1093/jn/134.10.2752s.

158. Stevens, B.R.; Kakuda, D.K.; Yu, K.; Waters, M.; Vo, C.B.; Raizada, M.K. Induced nitric oxide synthesis is dependent on induced alternatively spliced CAT-2 encoding L-arginine transport in brain astrocytes. *J. Biol. Chem.* **1996**, *271*, 24017–24022, doi:10.1074/jbc.271.39.24017.

159. Bae, D.-H.; Lane, D.J.R.; Jansson, P.J.; Richardson, D.R. The old and new biochemistry of polyamines. *Biochim. Biophys. Acta - Gen. Subj.* **2018**, *1862*, 2053–2068, doi:10.1016/j.bbagen.2018.06.004.

160. Minois, N. Molecular Basis of the "Anti-Aging" Effect of Spermidine and Other Natural Polyamines - A Mini-Review. *Gerontology* **2014**, *60*, 319–326, doi:10.1159/000356748.

161. Madeo, F.; Eisenberg, T.; Büttner, S.; Ruckenstuhl, C.; Kroemer, G. Spermidine: A novel autophagy inducer and longevity elixir. *Autophagy* **2010**, *6*, 160–162, doi:10.4161/auto.6.1.10600.

162. Dayoub, R.; Thasler, W.E.; Bosserhoff, A.K.; Singer, T.; Jauch, K.W.; Schlitt, H.J.; Weiss, T.S. Regulation of polyamine synthesis in human hepatocytes by hepatotrophic factor augmenter of liver regeneration. *Biochem. Biophys. Res. Commun.* **2006**, *345*, 181–187, doi:10.1016/J.BBRC.2006.04.040.

163. Marchesini, G.; Checchia, G.A.; Stefanelli, C.; Bianchi, G.; Fabbri, A.; Zoli, M.; Caldarera, C.M.; Pisi, E. Polyamine plasma levels and liver regeneration following partial hepatic resection in man. *J. Hepatol.* **1992**, *16*, 159–164, doi:10.1016/S0168-8278(05)80109-6.

164. Luk, G.D. Essential role of polyamine metabolism in hepatic regeneration: Inhibition of deoxyribonucleic acid and protein synthesis and tissue regeneration by difluoromethylornithine in the rat. *Gastroenterology* **1986**, *90*, 1261–1267, doi:10.1016/0016-5085(86)90394-X.

165. Ogiso, S.; Matsumoto, T.; Nimura, Y. The role of polyamines in liver regeneration after hepatectomy with ischemic injury. *Surg. Today* **1997**, *27*, 833–839, doi:10.1007/BF02385274.

166. Liu, P.; de la Vega, M.R.; Dodson, M.; Yue, F.; Shi, B.; Fang, D.; Chapman, E.; Liu, L.; Zhang, D.D. Spermidine Confers Liver Protection by Enhancing NRF2 Signaling Through a MAP1S-Mediated Noncanonical Mechanism. *Hepatology* **2019**, *70*, 372–388, doi:10.1002/hep.30616.

167. Yue, F.; Li, W.; Zou, J.; Jiang, X.; Xu, G.; Huang, H.; Liu, L. Spermidine prolongs lifespan and prevents liver fibrosis and hepatocellular carcinoma by activating MAP1S-mediated autophagy. *Cancer Res.* **2017**, *77*, 2938–2951, doi:10.1158/0008-5472.CAN-16-3462.

168. Zhou, S.; Gu, J.; Liu, R.; Wei, S.; Wang, Q.; Shen, H.; Dai, Y.; Zhou, H.; Zhang, F.; Lu, L. Spermine alleviates acute liver injury by inhibiting liver-resident macrophage pro-inflammatory response through ATG5-dependent autophagy. *Front. Immunol.* **2018**, *9*, 948, doi:10.3389/fimmu.2018.00948.

169. Gutierrez, E.; Shin, B.S.; Woolstenhulme, C.J.; Kim, J.R.; Saini, P.; Buskirk, A.R.; Dever, T.E. eif5A promotes translation of polyproline motifs. *Mol. Cell* **2013**, *51*, 35–45, doi:10.1016/j.molcel.2013.04.021.

170. Lubas, M.; Harder, L.M.; Kumsta, C.; Tiessen, I.; Hansen, M.; Andersen, J.S.; Lund, A.H.; Frankel, L.B. eIF 5A is required for autophagy by mediating ATG 3 translation . *EMBO Rep.* **2018**, *19*, doi:10.15252/embr.201846072.

171. Park, M.H.; Nishimura, K.; Zanelli, C.F.; Valentini, S.R. Functional significance of eIF5A and its hypusine modification in eukaryotes. *Amino Acids* **2010**, *38*, 491–500, doi:10.1007/s00726-009-0408-7.

172. Chen, K.Y.; Liu, A.Y.C. Biochemistry and function of hypusine formation on eukaryotic initiation factor 5A. *NeuroSignals* **1997**, *6*, 105–109, doi:10.1159/000109115.

173. James, C.; Zhao, T.Y.; Rahim, A.; Saxena, P.; Muthalif, N.A.; Uemura, T.; Tsuneyoshi, N.; Ong, S.; Igarashi, K.; Lim, C.Y.; et al. MINDY1 Is a Downstream Target of the Polyamines and Promotes Embryonic Stem Cell Self-Renewal. *Stem Cells* **2018**, *36*, 1170–1178, doi:10.1002/stem.2830.

174. Coll, M.; Perea, L.; Boon, R.; Leite, S.B.; Vallverdú, J.; Mannaerts, I.; Smout, A.; El Taghdouini, A.; Blaya, D.; Rodrigo-Torres, D.; et al. Generation of Hepatic Stellate Cells from Human Pluripotent Stem Cells Enables In Vitro Modeling of Liver Fibrosis. *Cell Stem Cell* **2018**, *23*, 101-113.e7, doi:10.1016/j.stem.2018.05.027.

175. Cortese-Krott, M.M.; Kelm, M. Endothelial nitric oxide synthase in red blood cells: Key to a new erythrocrine function? *Redox Biol.* **2014**, *2*, 251–258, doi:10.1016/j.redox.2013.12.027.

176. Satriano, J. Arginine pathways and the inflammatory responses: Interregulation of nitric oxide and polyamines. Review article. *Amino Acids* **2004**, *26*, 321–329, doi:10.1007/s00726-004-0078-4.

177. Forbes, S.A.; Beare, D.; Boutselakis, H.; Bamford, S.; Bindal, N.; Tate, J.; Cole, C.G.; Ward, S.; Dawson, E.; Ponting, L.; et al. COSMIC: Somatic cancer genetics at high-resolution. *Nucleic Acids Res.* **2017**, *45*, D777–D783, doi:10.1093/NAR/GKW1121.

178. COSMIC data base MAPKAP1 Gene - Somatic Mutations in Cancer Available online: https://cancer.sanger.ac.uk/cosmic/gene/analysis?all_data=&coords=AA%3AAA&dr=&gd=&id=331372&ln=MAPKAP1&res_type=AA&seqlen=523&export=html&start=29&end=undefined (accessed on Aug 19, 2022).

179. Stuttfeld, E.; Imseng, S.; Maier, T. A central role for a region in the middle: A domain called the 'Conserved region in the middle' is responsible for target recognition in the TORC2 complex in fission yeast and the mTORC2 complex in mammals. *Elife* **2017**, *6*, doi:10.7554/eLife.25700.

180. Tavares, M.R.; Pavan, I.C.B.; Amaral, C.L.; Meneguello, L.; Luchessi, A.D.; Simabuco, F.M. The S6K protein family in health and disease. *Life Sci.* **2015**, *131*, 1–10, doi:10.1016/j.lfs.2015.03.001.

181. Bradley, D.; Beltrao, P. Evolution of protein kinase substrate recognition at the active site. *PLOS Biol.* **2019**, *17*, e3000341, doi:10.1371/JOURNAL.PBIO.3000341.

182. Kazemein Jasemi, N.S.; Reza Ahmadian, M. Allosteric regulation of GRB2 modulates RAS activation. *https://doi.org/10.1080/21541248.2022.2089001* **2022**, *13*, 282–286, doi:10.1080/21541248.2022.2089001.

183. Kochańczyk, M.; Kocieniewski, P.; Kozłowska, E.; Jaruszewicz-Błońska, J.; Sparta, B.; Pargett, M.; Albeck, J.G.; Hlavacek, W.S.; Lipniacki, T. Relaxation oscillations and hierarchy of feedbacks in MAPK signaling. *Sci. Reports 2017 71* **2017**, *7*, 1–15, doi:10.1038/srep38244.

184. Shin, S.Y.; Rath, O.; Choo, S.M.; Fee, F.; McFerran, B.; Kolch, W.; Cho, K.H. Positive- and negative-feedback regulations coordinate the dynamic behavior of the Ras-Raf-MEK-ERK signal transduction pathway. *J. Cell Sci.* **2009**, *122*, 425–435, doi:10.1242/JCS.036319.

185. Georgescu, M.M. PTEN Tumor Suppressor Network in PI3K-Akt Pathway Control. *Genes Cancer* **2010**, *1*, 1170, doi:10.1177/1947601911407325.

186. Zimmermann, S.; Moelling, K. Phosphorylation and regulation of Raf by Akt (protein kinase B). *Science (80-.).* **1999**, *286*, 1741–1744, doi:10.1126/science.286.5445.1741.

187. Dhillon, A.S.; Pollock, C.; Steen, H.; Shaw, P.E.; Mischak, H.; Kolch, W. Cyclic AMP-dependent kinase regulates Raf-1 kinase mainly by phosphorylation of serine 259. *Mol. Cell. Biol.* **2002**, *22*, 3237–3246, doi:10.1128/MCB.22.10.3237-3246.2002.

ACKNOWLEDGMENT

There are many people to whom I am extremely grateful and who have supported and guided me on my journey.

Reza, thank you so much for the chance to be a part of your lab, to develop myself and to follow my ideas. I learned so much in these past years, about science, about consistency and what it means to think outside the box and became a researcher that I would not be without you.

I want to thank all members of our institute for being great colleagues and supportive whenever it was needed. Especially, Petra and Feri, thank you for being caring, funny and always on our side; Roland and Doreen, for lots of help and support; Marci and Olli, for being the best tutors, advisors and coffee fellows I could have ever asked for as a first year PhD, and of course all my old and new group members, for just making work feel a little less like work.

Niloufar, you are simply amazing and I am so, so, so happy that we met each other during this time. You always had my back no matter what and I am beyond grateful for you being my colleague, office buddy, partner in crime and most of all my friend.

Jetzt möchte ich mich noch bei allen bedanken, die vielleicht nicht im Labor, aber in allen anderen Lebenslagen stets für mich da waren, allen voran meinen Eltern: Danke, dass ihr mein Fels in der Brandung seid, immer ein offenes Ohr für mich habt und mich auf meinem ganzen Weg bedingungslos unterstützt. Ich habe euch sehr, sehr lieb!

Und nicht zu vergessen den Rest meiner Familie, meine Schwester, meine Freunde: Ihr wart immer für mich da, wenn ich den Kopf frei bekommen musste, habt so viel Verständnis gezeigt, wenn es um Laborkram ging, und standet mir mit Rat und Tat zur Seite. Ich könnte nicht nach tolleren Menschen in meinem Leben fragen und bin so unendlich glücklich jeden einzelnen von euch darin zu haben. Danke, dass ihr so seid, wie ihr seid!

EIDESSTATTLICHE ERKLÄRUNG

Ich versichere an Eides Statt, dass die Dissertation von mir selbständig und ohne unzulässige fremde Hilfe unter Beachtung der „Grundsätze zur Sicherung guter wissenschaftlicher Praxis an der Heinrich-Heine-Universität Düsseldorf“ erstellt worden ist. Diese Dissertation wurde in der vorgelegten oder einer ähnlichen Form noch bei keiner anderen Institution eingereicht und es wurden bisher keine erfolglosen Promotionsversuche von mir unternommen.

Düsseldorf, den

_____

Silke Pudewell